# THE ROLE OF THALAMIC STATE IN DYNAMIC TACTILE ENCODING

A Thesis

Presented to

The Academic Faculty

by

Clarissa J Whitmire

In Partial Fulfillment

of the Requirements for the Degree

Doctor of Philosophy in the

Wallace H. Coulter Department of Biomedical Engineering

Georgia Institute of Technology

Emory University

December 2017

**THE ROLE OF THALAMIC STATE IN DYNAMIC TACTILE ENCODING**

Approved by:


Dr. Garrett Stanley, Advisor
Department of Biomedical Engineering
*Georgia Institute of Technology*

Dr. Dieter Jaeger
Department of Biology
*Emory University*

Dr. Christopher Rozell
Department of Electrical and Computer Engineering
*Georgia Institute of Technology*

Dr. Robert Liu
Department of Biology
*Emory University*

Dr. Cornelius Schwarz
Department of Cognitive Neurology
*University of Tübingen*


Date Approved: October 24, 2017

To Lucas

## ACKNOWLEDGEMENTS

Throughout my time in graduate school, I have been extremely fortunate to work with an incredible research community that shaped my development as a scientist. I am perhaps most indebted to my advisor, Dr. Garrett Stanley, who guided my technical, professional, and personal development over the last six years and has continued to be a champion for my career as I move beyond my graduate studies. I am also extremely grateful to have received significant mentoring and guidance on the untaught topics in graduate school from my committee member and collaborator, Dr. Chris Rozell. Furthermore, I have also had the opportunity to work with a number of faculty members through lab rotations (Dr. Robert Liu, Dr. Robert Butera), the computational neuroscience training program (Dr. Dieter Jaeger, Dr. Lena Ting), and established collaborations with the Stanley lab (Dr. Cornelius Schwarz, Dr. Steve Potter). Despite the increasingly busy schedules of these professors, I would like to thank each of them for finding the time to interact with me and help me to push my work to the next level.

Within the Stanley lab, I received significant support from two generations of the lab including Dr. Daniel Millard, Dr. Doug Ollerenshaw, Dr. Clare Gollnick, Dr. He Zheng, Dr. Sean Kelly, Dr. Qi Wang, Dr. Christian Waiblinger, Dr. Aurélie Pala, Dr. Audrey Sederberg, Dr. Caleb Wright, Peter Borden, Yi Juin Liew, Michael Bolus, and Adam Willats. Each of these lab members helped me develop my skills as a researcher, a scientist, a teacher, a student, a mentor, and a mentee.

Outside of my scientific interactions, there were a number of people within the Georgia Tech and Emory umbrella that really influenced my trajectory. I would first like

to recognize Shannon Sullivan, who has been an incredible source of guidance, support, and enthusiasm throughout my time in the program. Next, I would like to thank the Physiology Research Lab members who enabled my research project through their hard work and expertise in animal care and handling. I also found teaching to be a very rewarding experience in graduate school, so I would like to thank James Rains for allowing me to be a continuing presence in his classroom over the last few years.

Beyond the graduate program itself, I received (what felt like) unprecedented support from my husband, Lucas. Whether he was picking me up at midnight after a long experiment day or waking up at 4AM to listen to one more practice talk, he has been a part of this thesis every step of the way. I am deeply indebted to him for his unending support, which empowered me to pursue my academic curiosities without barriers.

Finally, I found graduate school to be a very individual journey that was embedded in the framework of my life. There were times for celebrating, times for easing frustration, and times for overcoming losses. I would like to thank my friends (Chelsea Biggs, Kelly Davey, Sara Hardin, Jessie Oldham) and my family (Dan, Melissa, Cole, Wade, Jess, and Clay Shephard) for joining me in the ups and the downs of the last six years. Your support made this possible.

## TABLE OF CONTENTS

## LIST OF FIGURES

## LIST OF SYMBOLS AND ABBREVIATIONS

| | |
|---|---|
| VPm | Ventral posteromedial nucleus of the thalamus |
| POm | Posterior nucleus of the thalamus |
| S1 | Primary somatosensory nucleus |
| nRT | Reticular nucleus of the thalamus |
| STA | Spike triggered average |
| STC | Spike triggered covariance |
| LNP | Linear-nonlinear Poisson |

## SUMMARY

Sensory pathways extract information about the local environment to guide our actions and behaviors. The internal representation of the outside world is built on patterns of neural activity, commonly referred to as the 'neural code'. While we often model the neural code as a linear mapping from stimulus to spikes, it is actually extremely complicated and nonlinear even very early in the sensory pathway. In particular, the neural code explodes in complexity at the thalamocortical circuit where it has been hypothesized that the thalamus gates information flow to the cortex through dynamic transitions in thalamic state. Mechanistically, the baseline membrane potential of an individual thalamic neuron controls its state, or firing mode. Here, we have found that the thalamic state, and presumably the subthreshold membrane potential, can be externally modulated by sensory stimulation, identifying a role for sensory driven state manipulations. Furthermore, we have found that manipulation of thalamic state affects stimulus-evoked cortical dynamics, consistent with the view that the thalamus can gate information flow to cortex. Finally, we linked thalamic state transitions to shifts in the precise stimulus encoding from thalamus to cortex. Through this work, we provide evidence that the state of the thalamus determines what types of information are transmitted to cortex through modulations to thalamic spike timing. Dynamic shifts in thalamic state set the stage for an intricate control strategy upon which cortical computation is built.

# CHAPTER 1 INTRODUCTION

Understanding how the brain encodes and processes information has become one of the grand challenges of the 21st century. However, we face a daunting task when we simply consider the sheer number of neurons available for neural processing. For reference, the human brain has an estimated 86 billion neurons while the rat model system used in this thesis has an estimated 200 million neurons (Azevedo et al., 2009). Instead of considering each neuron as an independent entity, we can begin to look for commonalities in function to identify general principles of neural processing. Arguably, there are a few neural computations that have been identified as canonical neural computations including linear filtering (Schwartz et al., 2006), divisive normalization (M Carandini and Heeger, 2012), and adaptation (Whitmire and Stanley, 2016). As we develop an understanding of these 'building blocks' of neural processing and how they are implemented across different neural circuits, we will begin to develop comprehensive yet tractable models of neural function. In this thesis, I have studied the role of thalamic state in dynamically encoding tactile stimuli. Given the commonality of the thalamocortical circuitry for sensory processing across species, I believe this work could be widely applicable as general principles of neural coding in the thalamocortical circuit. In the next section, I will outline the relevant introductory material to describe the neural coding of state-dependent properties in the thalamocortical circuit of the rodent vibrissa pathway.

## 1.1 Thalamocortical processing in sensory pathways

Sensory perception builds the foundation for interacting with the external world. Without the ability to sense external cues such as visual scenes or auditory stimuli, we would be unable to recognize the presence of these stimuli and react. While humans are often viewed as relying heavily on visual cues to navigate daily environments, all sensory pathways are precisely tuned to provide relevant information about external stimuli. In each sensory pathway, the encoding of sensory information becomes increasingly

complicated as information travels from the periphery to sensory cortex. In the rodent vibrissa pathway, sensations are encoded in a fairly linear and reliable fashion at the mechanoreceptors (i.e. firing rate is proportional to the intensity of the stimulus) (Arabzadeh et al., 2005; Lottem and Azouz, 2011), but the encoding becomes incredibly complex as the information reaches the highly interconnected thalamocortical circuit (Adams et al., 1997). Nearly every sensation, excluding olfaction, travels from the periphery through thalamus before reaching cortex such that each sensory region of thalamus has a corresponding cortical projection. Rather than acting as a relay from the periphery to cortex, the thalamus is capable of fundamentally shaping the information that reaches primary sensory cortex by dynamically gating the sensory information it receives (Crick, 1984; Poulet et al., 2012; Sherman, 2001a; Sherman and Guillery, 2002, 1996; Sherman and Koch, 1986). Furthermore, the cortex alters encoding in the thalamus through direct corticothalamic feedback and indirect corticothalamic feedback via reticular thalamus (nRT) (Figure 1-1). The ubiquity of the thalamocortical circuitry across sensory modalities and across species suggests that this represents a critical stage of processing and may represent a canonical circuit motif. The strongly interconnected thalamocortical circuit has been chosen as the focus of the project because it plays a fundamental role in sensory perception yet the mechanistic understanding of how information is transformed in this circuit in a state-dependent manner remains unclear.

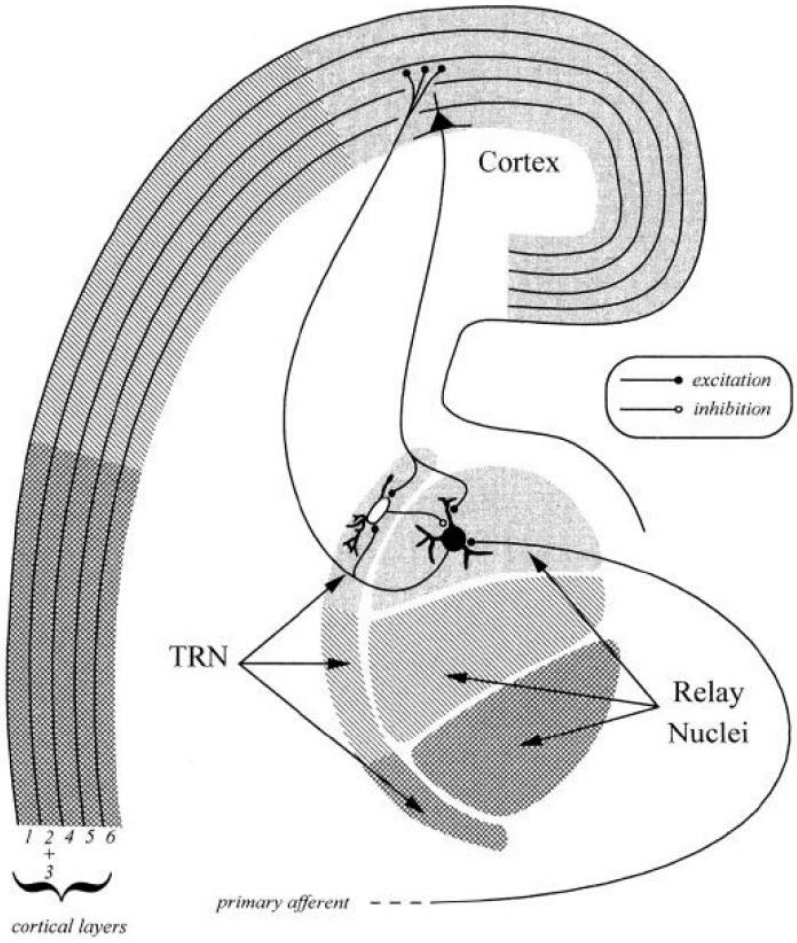


**Figure 1-1. Functional organization of the thalamocortical circuitry.** Figure adapted from (Sherman and Guillery, 1996). Driving inputs from the primary afferents synapse onto thalamocortical neurons within the relay nuclei. These neurons project to layer IV of primary sensory cortex and the reticular nucleus of the thalamus (nRT). Thalamocortical neurons receive inhibitory feedback from nRT and excitatory feedback from layer VI of primary sensory cortex.

### 1.1.1 Cortex

Studies of the macroscopic properties of brain anatomy across mammalian species revealed a striking trend – larger brains tended to have greater cortical folding and therefore a larger cortical surface area (Hofman, 1985). The disproportionate scaling of cortical surface area relative to brain weight in mammalian species (Prothero and Sundsten, 1984) has led many to hypothesize that cortical circuitry is the neural correlate of intelligence

(Hofman, 2014). While the true computational role of cortical circuitry in neural processing remains unknown, it has become the subject of extensive research due to an impressive collection of tools, such as imaging techniques, which have made it possible to record functionally from cortex in an unprecedented manner.

Similarities in the anatomical and physiological properties of cortical circuits across sensory regions as well as across mammalian species support commonality of function such that information learned in one sensory modality or species could be applicable to another. For example, mammalian neocortical circuitry is subdivided into a six-layer laminar structure with distinctive populations of neurons and anatomical connectivity (Shipp, 2007) (for an excellent review of the neocortical circuit, see (Harris and Shepherd, 2015)). Although the thickness of each cortical layer varies as a function of the cortical circuit engaged, the commonality of the laminar structure across the functional neocortical circuits suggests some common circuit motifs that may allow extrapolation of theories developed in one cortical region to another. In the somatosensory pathway, this common circuit motif was identified as a cortical column (Mountcastle, 1997, 1957). The cortical column has since been described as the functional computational unit of cortex. That concept will permeate the work presented here, specifically in the context of the rodent vibrissa pathway.

### 1.1.2 Thalamus

Nearly every sensory modality is processed in thalamus before projecting to the corresponding cortical area (Figure 1-1), leading to the hypothesis that the thalamus gates information flow to cortex. One mechanism for gating information flow could be the distinct firing modes of the thalamic neurons known as burst and tonic firing (see 1.4.3) that are mediated by the T-type calcium channels. While burst and tonic firing are related to the generation of rhythmic activity in the thalamocortical circuit (Steriade et al., 1993), both firing modes are also important for encoding sensory information (Bezdudnaya et al.,

2006; Lesica and Stanley, 2004; Wang et al., 2007). Furthermore, physiological characteristics of thalamic neurons such as the ability to fire both tonically and in bursts appears to be conserved across different vertebrates (Llinas and Steriade, 2006). The commonality of these physiological characteristics suggests that burst and tonic firing play an important role in neural processing.

Although we often discuss the thalamus as a feedforward processing station where sensory information is processed in the primary sensory thalamus (lemniscal pathway) before it is propagated to the cortex, it actually receives multiple feedback projections in addition to the feedforward input from the periphery including inhibitory feedback from the reticular nucleus of the thalamus (nRT) and modulatory feedback from the cortex (Figure 1-2). Comparative anatomy studies in the evolution of the thalamus have shown many of the common features of the thalamocortical processing in mammals, including dorsal and ventral nuclei that project to cortex or a cortical analogue as well as an inhibitory thalamic reticular nucleus, might be conserved across all jawed vertebrates (Butler, 2008). The commonality of the thalamocortical anatomy and the thalamic firing modes suggest that knowledge from studies performed in non-human model species could be transferrable as common computations in similar circuit motifs.

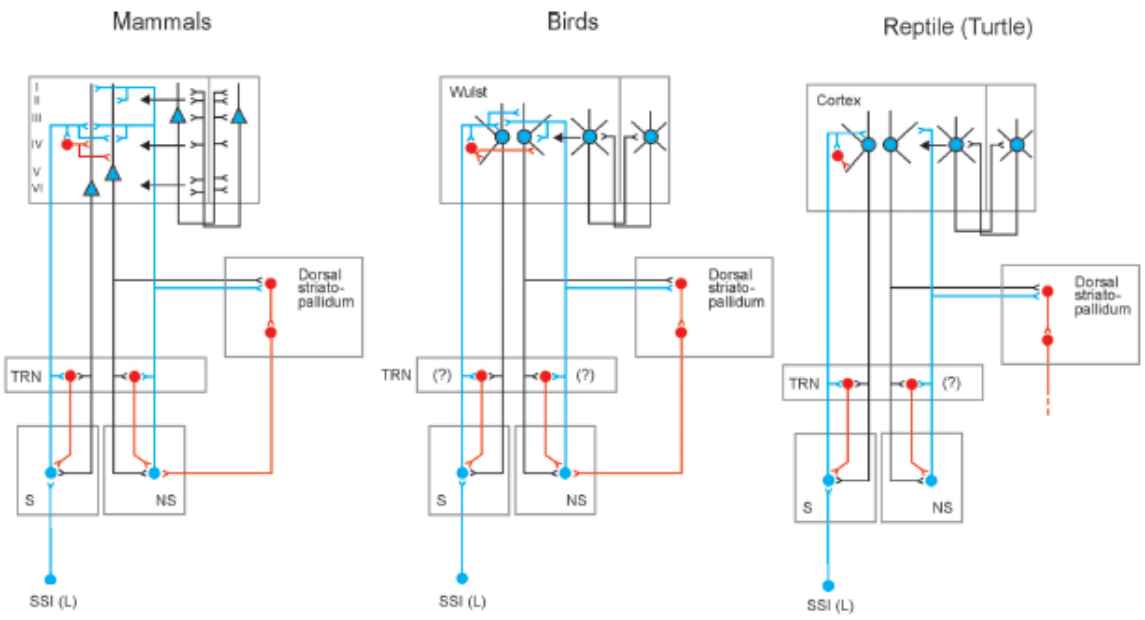


**Figure 1-2. Conserved Thalamocortical Circuitry Across Species.** Figure adapted from (Butler, 2008) shows commonality in the thalamocortical connectivity across species including mammals, reptiles, and birds. Partial original caption: "Glutamate-containing neurons are indicated by blue cell bodies, with blue axons for thalamic neurons and black dendrites and axons for pallial neurons; GABA-containing neurons are indicated by red cell bodies and axons. … specific, lemnothalamic sensory input [SSI (L)] is shown to the specific nuclei (S) …, and ascending thalamocortical projections are shown for both the specific and nonspecific (NS) nuclei to … neocortex".

## 1.2 Rodent vibrissa pathway as a model of somatosensation

Somatosensation, which represents multiple modalities such as touch, pain, proprioception, and temperature, encodes information about stimuli presented to the body surface as well as deeper tissues. In humans, the highest tactile acuity is collocated in regions with the highest density of mechanoreceptors such as the fingertips or the lips (Mancini et al., 2014; Sathian and Zangaladze, 1996). These high acuity regions are ideal for discriminating complex tactile stimuli. In rodents, the whisker pathway provides an excellent model system of high acuity tactile sensing due to the stereotyped, discretized representation of the whisker pad at each stage of sensory processing.

### 1.2.1 Somatosensation

Somatosensation encompasses multiple sensations that are sensed peripherally including touch, temperature, proprioception, and pain. While each of these sensations is experienced locally, they are encoded by distinct receptors. Here, we will focus specifically on the sense of touch. While the sense of touch is one of several senses available to interact with the external world, unlike vision or audition, touch requires local interaction with the explored object. As an object comes into contact with the body, sensory receptors in the skin respond to the mechanical deformations and transduce the physical stimulus into an electrical signal that can be transmitted to the brain. The specialized sensory receptors that perform this process for touch are called mechanoreceptors (Gardner, 2010). There are multiple types of mechanoreceptors found within mammalian skin that encode different properties of the stimulus (Johansson and Vallbo, 1979b). As described above, the human hand is densely innervated with these mechanoreceptors (Johansson and Vallbo, 1983) with fingertips showing the highest tactile acuity (Johansson and Vallbo, 1979a).

Once the tactile signal has been transduced by the mechanoreceptors, it must be transmitted to the central nervous system. Touch information travels along peripheral nerves with other somatosensory modalities from the same regional area (such as temperature, proprioception, and pain) to the spinal cord. In humans, these impulses will travel up the dorsal columns of the spinal cord to synapse in the brainstem. From there, axons will cross the midline and travel to the somatosensory nuclei of the thalamus before projecting to somatosensory cortex (Goodwin, 2005). From here, the sensory signals will continue to be processed by higher order cortical areas before ultimately reaching conscious perception of the tactile stimulus.

### 1.2.2 Vibrissa pathway

Humans are often described as visual creatures due to the strong reliance on visual information to navigate through complex environments. There is psychophysical evidence

to support this claim showing that humans will weight visual information more strongly than other sensory inputs, such as auditory information for example (MacDonald and McGurk, 1978; McGurk and Macdonald, 1976). Unlike humans, rats are not typically considered visual creatures due to their nocturnal behavior and generally poor visual acuity. Instead, rats have developed their sense of touch, particularly through the whisker pad, and olfaction to navigate their sensory environment. This highly developed vibrissa system was first noticed anatomically due to the obvious columnar structure in the somatosensory cortex of the rodent (Woolsey and Van der Loos, 1970). These cortical columns found within rodent primary somatosensory cortex (S1), or more specifically barrel cortex, are discrete 'barrel'-shaped whisker representations in layer IV (For extensive review of barrel cortex, see (Diamond et al., 2008a; Petersen, 2007)). The discretized topographical alignment between these cortical barrels and the whisker pad that is stereotyped across animals provides a repeatable model system to study the encoding of touch information.

Although there are obvious differences between the sense of touch in the rodent vibrissa and the human fingertip, there are important similarities. As described for human touch, mechanical deformations of the rodent whisker are also transduced by mechanoreceptors located within the whisker follicle (Ebara et al., 2002). Also similar to human touch is the neural pathway from the mechanoreceptors to the sensory cortex. From the whisker follicle, the transduced touch signal is transmitted along the facial nerve to the trigeminal nuclei of the brainstem. From here, the touch information travels to whisker nuclei of the thalamus (lemniscal station: Ventral Posteromedial (VPm), paralemniscal station: posterior nucleus (POm)) before reaching somatosensory cortex. This commonality in the pathway from the brainstem to the thalamus to the cortex for the rodent vibrissa pathway provides the potential for neural processing theories developed in the thalamocortical circuitry of the rodent to be translated into human models of sensation.

The columnar organization of the barrel cortex, as well as other cortical areas, has received considerable attention as a potential modular organization of cortical circuitry

(Mountcastle, 1997). In the rodent vibrissa pathway, S1 receives feedforward input from the thalamus (Bruno and Sakmann, 2006), lateral inputs from other cortical regions (Feldmeyer et al., 2013), and neuromodulatory inputs from the reticular formation (Castro-alamancos and Gulati, 2014). While our knowledge of the exact computations performed in S1 are still developing, previous work has shown that primary sensory cortex is required for perception of sensory stimulation (O'Connor et al., 2010). Importantly, sensory cortex receives sensory information from thalamus. Within the rodent vibrissa pathway, the thalamus also has a modular topographic organization such that the lemniscal thalamic station (VPm) is subdivided into discrete regions of tissue, termed 'barreloids', that are primarily sensitive to a single whisker (termed the 'primary whisker'). Projections from thalamus to cortex are highly ordered such that a barreloid with a primary whisker of A1, for example, will primarily project to a barrel with primary whisker A1. This one-to-one mapping from thalamus to cortex provides a strong advantage for mapping the transformation of a sensory signal from one brain region to the next. Furthermore, this mapping is also maintained in the brainstem where these single-whisker sensitive regions of tissue are referred to as 'barrelettes'. This discretized representation of the whiskers at each stage of sensory processing is in contrast to human touch where the representation is far more continuous (albeit with definite boundaries between distinct tissue regions such as different digits), making it more difficult to follow sensory signal transmission.

In summary, the rodent vibrissa pathway exhibits a discrete topographic map of the whisker pad at each stage of sensory processing in the lemniscal pathway. This topographic map is stereotyped across animals and encompasses a large volume of tissue, making it easier to target for neural recording and stimulation. These advantages of the rodent vibrissa pathway paired with the commonalities to other mammalian sensory modalities make this an excellent model system to study sensory encoding properties.

## 1.3 Neural coding

Neural coding describes the relationship between sensory stimuli and the corresponding complex patterns of neural activity that underlie our internal representation of the outside world (Stanley, 2013). Sensory encoding represents the transformation from sensory stimulus to neural firing activity while sensory decoding describes methods to infer the sensory stimulus from the neural activity. Using both encoding and decoding techniques, we can build a framework for quantifying information representation and transmission in neural pathways that we hope can be applicable across sensory modalities and species.

### 1.3.1 Sensory encoding

Sensory encoding describes the process of transforming physical properties of the world (light, sound, proximal forces, etc.) into electrical activity that can be processed by the brain (Hart and Sengupta, 2001). The transformation from sensory stimulation into neural activity begins with transduction at the periphery. For example, vision begins with phototransduction at the retina. Light photons are absorbed by the light-sensitive cells (rods/cones) and transformed into electrical activity in the retina. The output of the retina, or retinal ganglion cells, is action potentials (or spikes) (Hooser, 2005). Spikes act as messengers that can then transmit information from one brain region to the next for further processing. Beyond the peripheral receptors, the information about a stimulus are only contained in the electrical activity of the brain. Therefore, there are sensory-specific receptors that transduce information for each sensory modality into electrical activity the brain can interpret. In audition, sound waves are transformed into mechanical vibrations that are encoded by hair cells in the inner ear (Forsythe, 2002). Mechanoreceptors are used to encode mechanical deformations of the skin (touch) (Gardner, 2010). Chemical senses such as olfaction and taste are encoded by diverse receptor-ligand binding (Scott, 2007; Wilson et al., 2010). Although the process of sensory transduction differs for each sensory

modality, the central processing of spiking activity within the brain shows some commonality (DiCarlo, 2001). Therefore, we can develop decoding techniques to begin to infer which features of the sensory stimulus drive firing in an individual neuron and extrapolate findings from one sensory modality to the next.

### 1.3.2 Sensory decoding

Sensory decoding describes the process of deciphering which features of a sensory stimulus are represented by the spiking activity of an individual neuron. In the visual pathway, seminal work by Hubel and Wiesel found that the neural responses, or the presence or absence of spiking activity, to simple flashes of light were not random. Instead, they were highly structured with each neuron responding to a particular feature of the visual stimulus such as spatial location (Figure 1-3), stimulus orientation, and stimulus size (Hubel and Wiesel, 1959). The features of the visual space that elicit the maximal response of the neuron, known as the feature selectivity or stimulus tuning of that neuron, can then be used to describe the sensory encoding properties of the neuron.

In this example, the spatial receptive field represents the region of visual space that maximally excites a neuron in the visual pathway (Figure 1-3). When light is shone along the y-axis of this stimulus coordinate system, the neuron is inhibited (Figure 1-3a,b,d). However, when the light stimulus is targeted outside of the y-axis, the neuron responds with an increased firing rate (Figure 1-3c,e). These spiking responses were then categorized as inhibited (reduced spiking activity; triangles) or excited (increased spiking activity; crosses) and plotted on a physical map of visual space (Figure 1-3, right). From this representation of the data, the spatial stimulus selectivity of the stimulus becomes evident. These experimental characterizations of neural firing patterns with respect to stimulus parameters built the foundation for the field of neural coding.

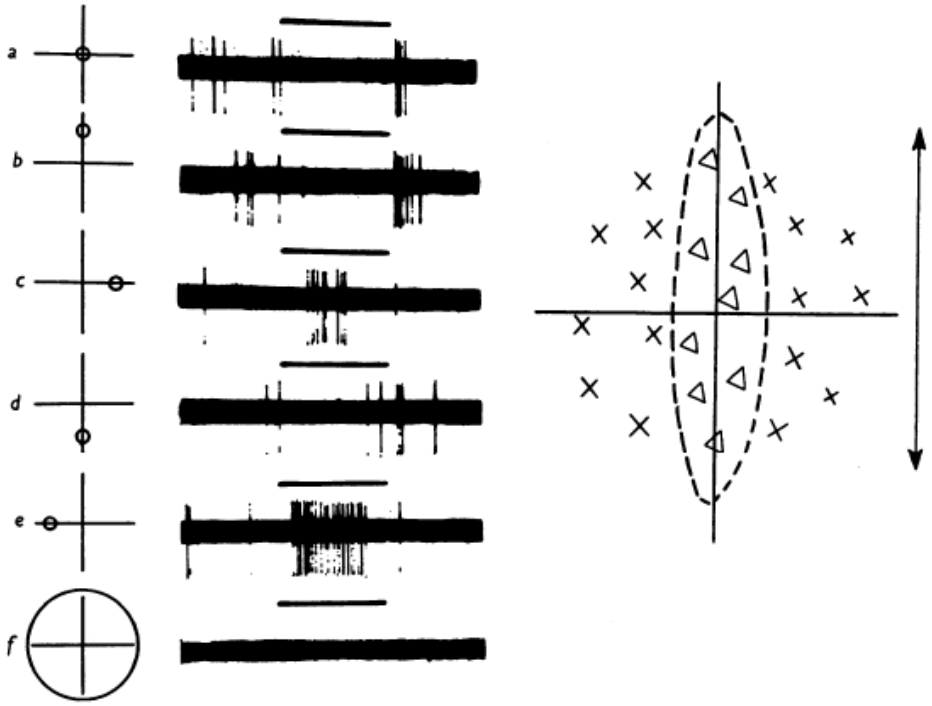


Fig. 1. Responses of a cell in the cat's striate cortex to a 1° spot of light. Receptive field located in the eye contralateral to the hemisphere from which the unit was recorded, close to and below the area centralis, just nasal to the horizontal meridian. No response evoked from the ipsilateral eye. The complete map of the receptive field is shown to the right. ×, areas giving excitation; △, areas giving inhibitory effects. Scale, 4°. Axes of this diagram are reproduced on left of each record. *a*, 1° (0·25 mm) spot shone in the centre of the field; *b–e*, 1° spot shone on four points equidistant from centre; *f*, 5° spot covering the entire field. Background illumination 0·17 log. m.c. Stimulus intensity 1·65 log. m.c. Duration of each stimulus 1 sec. Positive deflexions upward.

**Figure 1-3. Receptive field mapping in cat visual cortex demonstrates clear stimulus tuning in individual neurons.** In these seminal studies, Hubel and Wiesel flashed circles of light (left column) and recorded the spiking activity during the stimulation period (middle column, light duration indicated by the horizontal bars) to map the spatial selectivity of this neuron (right). Figure from: Hubel D, Wiesel T. Receptive fields of single neurones in the cat's striate cortex. J Physiol 1959:574–91.

The pioneering work of Hubel and Wiesel identified sensory neurons as feature selective through rigorous experimental trial-and-error style testing (Hubel and Wiesel, 1962, 1959). Since then, experimental stimulus design has developed to incorporate unbiased sampling of the sensory space and computational techniques have developed to quantify feature selectivity estimation through reverse correlation/spike triggered analysis (Figure 1-4) (Schwartz et al., 2006). With this analytic technique, the neural pathway is

driven with an uncorrelated sensory stimulus (sensory white noise; here shown as temporally uncorrelated whisker position stimulus). The representation of spiking activity as the presence or absence of a spike within a short time window led to a binary representation of the elicited patterns of temporal spiking. The stimulus immediately preceding a spike in the response train is then extracted for each spike (spike triggered ensemble, STE) and averaged together to generate the spike-triggered average (STA). In this example, the STA represents the temporal feature selectivity of the recorded neuron. However, this framework can be extended to any dimension of the sensory stimulus space such as spatial (Ramirez et al., 2014) and temporal selectivity (Petersen et al., 2008) as well as any sensory modality including visual (Pillow and Simoncelli, 2006), auditory (Theunissen et al., 2000), and tactile (Estebanez et al., 2012) stimuli.

After estimating the feature selectivity of an individual neuron, the predictive capabilities of that stimulus selectivity can be estimated using statistical techniques to model the response of the neuron to a novel stimulus. A simple encoding model, known as the linear-nonlinear-Poisson (LNP) model, consists of two stages. The first is the feature selectivity of the neuron, quantified as the STA, and the second is the point nonlinearity, which is representative of the spiking threshold of the neuron. Using a series of analytical and experimental techniques such as these, we aim to determine what information is represented by a single neuron and how this is integrated across neuronal populations to represent a stimulus. Ultimately, these techniques provide a framework for interpreting the encoding properties of individual neurons and making principled comparisons across neurons, circuits, and species.

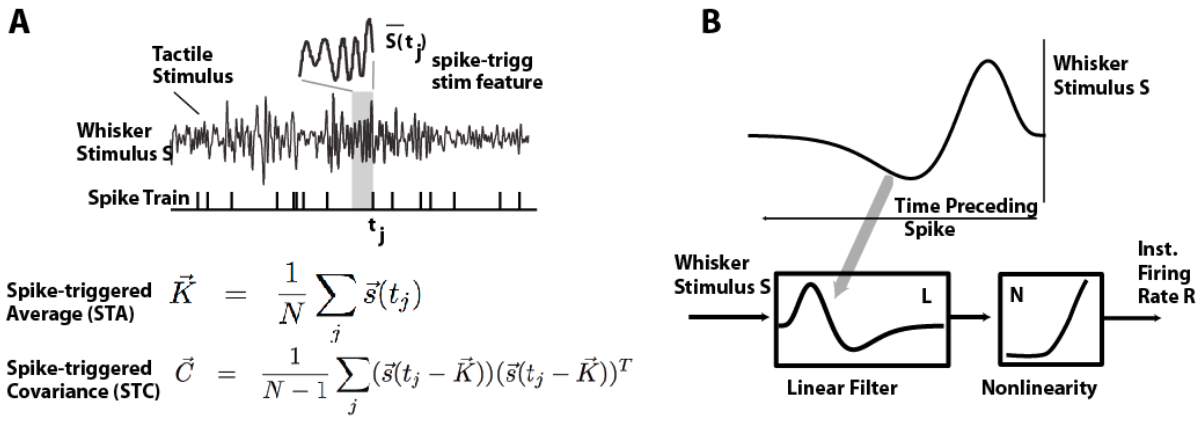


**Figure 1-4. Spike Triggered Analysis (STA) to Build Linear-Nonlinear Model.** A. STA methodology. B. Schematic of Linear-Nonlinear model built from linear filter recovered using STA method.

### 1.4 State-dependent neural processing

Although encoding properties are described as static descriptors of an individual cell, there is actually significant variability in the neural response properties. This variability leads to flexible encoding properties that are dynamic on a moment-by-moment basis. Furthermore, the variability or complexity of the signal is intensified at each stage of the sensory pathway such that cortical responses are far more variable than primary sensory afferent responses, for example (Arabzadeh et al., 2005). It has been proposed that one source of the variability in cortical responses is largely due to variations in spontaneous activity or brain state (Petersen et al., 2003b; Poulet and Petersen, 2008). In the normal functioning brain, the state is constantly changing due to both intrinsic and extrinsic mechanisms and these state fluctuations lead to extensive alterations in sensory encoding. This suggests that neurons are not fixed in their information capacity, but instead can flexibly adjust based on a variety of factors.

Multiple mechanisms have been implicated in the control of brain state. While we understand that these constant fluctuations in state are ongoing, we know very little about the role these state changes play in neural computation. Within the context of this work,

we quantified how brain state modulates information in the thalamus, a critical structure for the transmission of information to and from cortex. Although we have some knowledge of the firing modes induced by thalamic state, we do not have a clear understanding of how these firing modes affect the transmission of sensory information. One major limitation to our understanding of the effect of thalamic state on sensory coding is our ability to experimentally control it.

### 1.4.1 Mechanisms of state modulation

The evoked response to a sensory stimulus is dynamic both over time in response to a static stimulus and over trials in response to repeated presentations of an identical stimulus. This variability in the neural response has been at least partially attributed to shifts in the internal state of the brain interacting with the external stimulus (Buonomano and Maass, 2009). Dynamic internal brain states are influenced by many factors including sensory drive, network activity, neuromodulatory effects, and intrinsic properties of the neurons (Castro-alamancos and Gulati, 2014; Castro-Alamancos, 2004a; Halassa et al., 2011; Poulet et al., 2012). Each of these mechanisms can shift the state of the brain and therefore the evoked response to sensory stimulation.

### 1.4.2 Cortical State

Network activity within and across brain regions will shape, if not define, the intrinsic state of the brain. For example, the highly interconnected cortical neurons can rapidly adjust the functional state of the network to meet varying task demands (Haider and McCormick, 2009). Within the cortex, state is typically classified by the frequency content in the local field potential. A high ratio of low-frequency power is indicative of the synchronized state while a high ratio of high-frequency power is indicative of the desynchronized state. Within the synchronized state, there are sub-classifications of up and down states. The presence or absence of network activity in cortex has been classically described by up and down states, respectively. These cortical states display fundamentally

different spontaneous neural activity that strongly impacts the encoding of sensory stimuli (Haider et al., 2007; Pachitariu et al., 2015; Petersen et al., 2003b). The network activation at the time of stimulus arrival represents one mechanism to fundamentally alter sensory encoding.

### 1.4.3 Thalamic State

Often, brain state is described in the context of cortical state. However, thalamic activity, and ultimately cortical processing, is also strongly affected by fluctuating subthreshold membrane potential levels in the thalamus, or the thalamic state. Throughout this thesis, I focus extensively on how thalamic state can be manipulated by sensory drive and how manipulation of thalamic state impacts thalamocortical encoding properties.

Shifts in thalamic state are known to induce shifts in firing modes, specifically burst and tonic firing (Sherman, 2001a). Although the thalamic membrane potential is constantly fluctuating as incoming signals transiently excite or inhibit a cell, it is a net depolarization of the cell membrane that transitions the cell between different operating points, or thalamic states. The burst mode is characterized by a net hyperpolarization of the baseline membrane potential of the thalamic neuron that de-inactivates the T-type calcium channels. When the thalamic neuron is in this hyperpolarized state, an incoming depolarizing signal will activate the T-type calcium channels to allow an influx of calcium, which transiently depolarizes the neuron and permits burst firing. By contrast, a net depolarization of the baseline membrane potential of the thalamic neuron inactivates the T-type calcium channel such that an incoming excitatory signal will not elicit an influx of calcium. In this tonic mode, the thalamic cells are believed to maintain a more linear relationship between stimulus intensity and elicited response. Burst spikes can be identified in intracellular recordings by the slow wave calcium depolarization, but this is not visible in extracellular recordings. Extracellularly, burst spikes are classically defined as two or more spikes with an interspike interval of less than 4 milliseconds with the first spike preceded by 100

milliseconds while tonic spikes are identified as any spikes not classified as part of a burst (Sherman, 2001a). These two firing modes suggest that the thalamus is capable of sending fundamentally different signals in response to the same stimulus due to differences in the state of the thalamus prior to stimulus presentation.

Although firing mode presents one mechanism of dynamic or state-dependent encoding, the thalamus can also achieve dynamic gating by varying the number of spikes elicited in response to a given stimulus, the temporal properties of those spikes, and the synchrony of firing across thalamic neurons. Alterations to thalamic gating have been demonstrated in response to sensory adaptation (Q. Wang et al., 2010), thalamic depolarization in vitro (Sherman, 2001a) and in vivo (Whitmire et al., 2016), reticular thalamus stimulation (Halassa et al., 2011), and reticular formation stimulation (M. a Castro-Alamancos, 2002). This extremely interconnected circuitry combined with a large number of state-altering mechanisms creates a framework for highly dynamic encoding of sensory information.

## 1.5 Thesis Organization

There is a significant body of work focused on the role of spontaneous cortical state in modulated evoked sensory responses as well as the role of thalamic firing modes in spontaneous synaptic efficacy. However, the link between thalamic state and sensory driven responses in the thalamocortical circuit remains unclear. Here, I use the rodent vibrissa pathway as a model system to investigate the role of thalamic state in dynamic thalamocortical information transmission. First, in Chapter 2, I discuss the role of sensory adaptation as one mechanism by which sensory encoding is dynamically modulated on a moment-by-moment basis. In Chapter 3, I link sensory adaptation with shifts in thalamic firing mode and quantify the implications using an ideal observer analysis of extracellular electrophysiology with optogenetic modulation. In Chapter 4, I expand upon this method of optogenetic modulation to quantify the role of thalamic state in information transmission

from thalamus to cortex using a paired pulse paradigm. In Chapter 5, I perform high-resolution sampling of the feature selectivity in the thalamocortical circuit as a function of imposed thalamic state manipulations. Finally, in Chapter 6, I discuss the implications of this work and outline some of the remaining gaps in knowledge that need to be addressed next.

# CHAPTER 2 BACKGROUND

*This chapter was originally published as a Perspective article in* Neuron *and is presented with only minor stylistic changes*[1]

Adaptation is fundamental to life. All organisms adapt over timescales that span from evolution to generations and lifetimes to moment-by-moment interactions. The nervous system is particularly adept at rapidly adapting to change, and this in fact may be one of its fundamental principles of organization and function. Rapid forms of sensory adaptation have been well-documented across all sensory modalities in a wide range of organisms, yet we do not have a comprehensive understanding of the adaptive cellular mechanisms that ultimately give rise to the corresponding percepts due in part to the complexity of the circuitry. In this Perspective, we aim to build links between adaptation at multiple scales of neural circuitry by investigating the differential adaptation across brain regions and sub-regions and across specific cell-types, for which the explosion of modern tools has just begun to enable. This investigation points to a set of challenges for the field to link functional observations to adaptive properties of the neural circuit that ultimately underlie percepts.

## 2.1 Introduction

To live is to adapt to the world around us. This is a notion so embedded in our way of thinking and our language, that even though we all know it when we see it, it remains difficult to define precisely what adaptation means. On long time scales, species evolve to

---

[1] Whitmire CJ, Stanley GB. Rapid sensory adaptation redux: A circuit perspective. Neuron 2016;92:298–315. doi:10.1016/j.neuron.2016.09.046.

adapt characteristics that are favorable for survival. Adapt or die! On shorter time scales, individual organisms adapt behaviorally in response to changes in their environment, as, for example, an animal adapts their scavenging behavior to take advantage of a new food source as the previous one is suddenly no longer available. On even faster time scales, we are all familiar with our eyes adapting as we move from the bright sunlight to a dark room, or as we become accustomed to the sensation of clothing on our bodies, or as we quickly adapt our gait in response to a new pair of shoes. The binding agent between all of these different phenomena seems to be time – adaptation is a change in function that takes time to develop (be it fast or slow) and time to dissipate. Although it is certainly the case that these different notions of adaptation at disparate time scales arise from different mechanisms and engage different systems within our bodies, they collectively embody something profound that connects them – the ability of organisms to respond to changes in the environment.

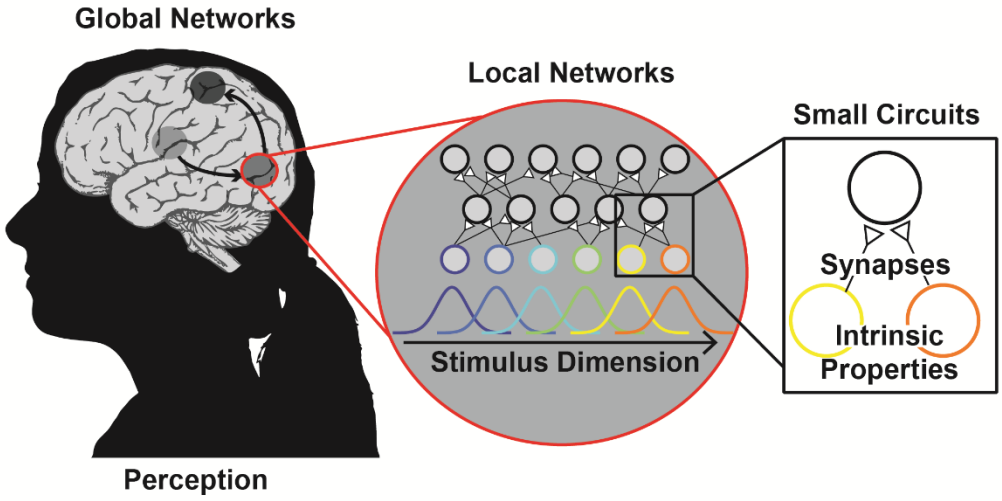


**Figure 2-1: Concepts of adaptation span from intrinsic currents in a single neuron to the perception of a sensory stimulus.** In this perspective, we aim to expand our neurophysiological understanding of adaptation at the single neuron level to a circuit level representation of adaptation as a method of determining the underlying neural correlates of the perceptual effects of adaptation. Brain image edited from Livingstone, BIODIDAC.

On the time scale relevant for an individual organism, there are still many forms of adaptation, but none perhaps as well studied as rapid sensory adaptation of the nervous system, a ubiquitous property of all sensory pathways that has profound effects both perceptually and neurophysiologically (Figure 2-1). From a historical perspective, there is documented evidence of the perceptual effects of rapid sensory adaptation going back several centuries. For example, Aristotle observed in 350 B.C. a phenomenon that later came to be referred to as the visual "waterfall" illusion, with perceived visual motion of stationary objects following a fixed gaze on moving objects for just a few seconds. Over the last few decades, adaptation paradigms have been implemented in psychophysical studies to more precisely determine the extent to which persistent exposure to a sensory input affects our perception. For example, fundamental properties of the visual pathway include adaptation to visual contrast (Georgeson and Harris, 1984; Greenlee and Heitger, 1988), visual orientation (Blakemore and Campbell, 1969a, 1969b), visual motion (Anstis et al., 1998; Sekuler and Ganz, 1963; Wohlgemuth, 1911), and even complex visual features such as faces (Webster and MacLeod, 2011). For review of visual adaptation, see (Clifford et al., 2007; Kohn, 2007). Although a very wide range of adaptive phenomena has been observed both psychophysically and neurophysiologically at the single neuron level across different sensory pathways, until now we have not been in a position to pose questions in the context of circuits and networks to ultimately enable us to link these to behavior for a more holistic view on rapid sensory adaptation.

In this Perspective, we revisit this classical issue in sensory neuroscience and consider multiple levels of investigation into rapid sensory adaptation to build from intrinsic adaptive properties of a single neuron to adaptive properties within common circuit motifs (Figure 2-1). Specifically, we will ask 1) How do we disambiguate adaptation effects occurring within a single neuron from those inherited presynaptically or generated locally in the context of the highly interconnected and detailed anatomy of our sensory pathways? And 2) how does differential adaptation of neurons by synapse type, cell type,

or stimulus tuning develop the adaptive circuit properties observed and is this generalized across circuit motifs? Here, we seek to open these questions up in the context of the modern tools that are making it possible to dissect the function of complex circuits relevant for behavior, and to pose some questions related to how we as organisms navigate the dynamics of the world in which we live.

## 2.2 Encoding Framework

While there is significant evidence that changes in neural function occur on longer timescales in response to changes in sensory environment and peripheral modification of the sensory organ (Buonomano and Merzenich, 1998; Gilbert, 1998; Karmarkar and Dan, 2006; Suga and Ma, 2003), our focus in this Perspective is the rapid sensory adaptation that occurs on the timescale of milliseconds to seconds which represents the ability of the pathway to dynamically adjust to the recent sensory environment. Despite extensive psychophysical investigation of many different rapid sensory adaptation phenomena, the underlying neural basis for most of these observations remains elusive even though neural signatures of the corresponding perceptual phenomena have been observed at multiple stages of processing across different sensory pathways.

Here we consider how the neural circuitry gives rise to these rapid adaptation effects in the context of a sensory encoding framework that relates the firing activity of individual neurons to the sensory stimulus driving them. Perhaps the simplest form of this encoding framework is a class of models that maps sensory inputs to observed neuronal activity, whose basic form has been widely applied in capturing coding properties of sensory pathways since the 1960's (de Boer and Kuyper, 1968; Eggermont et al., 1983), known as linear-nonlinear models (Schwartz et al., 2006; Simoncelli et al., 2004). In this two-stage model framework, the first stage can be envisioned to represent the aggregate synaptic input to the neuron in question while the second stage represents the overall gain of the input-output relationship combined with some elements of spike generation. We

might thus think of the first stage as representative of the synaptically driven feature selectivity or filtering of the neuron, and the second stage as an intrinsic property of the neuron (Figure 2-2A). Throughout this perspective, we will use this model as a framework for describing how adaptation reshapes the encoding properties of the pathway. It is important to note that, within the context of this framework, we define adaptation as a change in functional properties, be it through changes in synaptic feature selectivity and/or intrinsic neuronal properties. But this naturally begs the question as to what properties that we observe, if any, are static, instantaneous properties (e.g. tuning properties such as contrast sensitivity in the visual pathway), and which are dynamic due to adaptation (e.g. contrast adaptation in the visual pathway), as the tools we use to measure functional properties often require time-averaging which would obscure any adaptive process, and likely change the very properties that we are attempting to measure.

### 2.3 Intrinsic adaptation in a single neuron

What is the role of the individual neuron in adaptation? On timescales of tens of milliseconds, individual neurons exhibit intrinsic properties of rapid adaptation, such as spike frequency adaptation, that are independent of any network level phenomenon. Spike frequency adaptation is a well-described component of neural activity that is present in nearly every neuron type, whereby the rate of spiking will decrease in response to constant synaptic input. There are multiple somatic currents that have been implicated in mediating spike frequency adaptation (Benda and Herz, 2003) including M-currents (Constanti and Brown, 1981), calcium activated and sodium activated potassium currents (Bhattacharjee and Kaczmarek, 2005; Lancaster and Nicoll, 1987; Sanchez-Vives et al., 2000), and slow recovery from the inactivation of sodium channels (Fleidervish et al., 1996) as well as dendritic activity dependent effects such as reduced efficacy of distal inputs due to slow sodium channel de-inactivation (Häusser et al., 2015; Jung et al., 1997). An increase in the spiking threshold, possibly due to the slow recovery of sodium channels (Azouz and Gray,

2000; Toib et al., 1998), has also been identified as an intrinsic activity-dependent mechanism to induce spike frequency adaptation (Henze and Buzsáki, 2001; Pozzorini et al., 2013; Wilent and Contreras, 2005a). Each of these mechanisms allows a single neuron to modulate its firing rate in an activity- and cell type-dependent manner (Mensi et al., 2012) and the effect is not subtle (for review of biophysical mechanisms that enable single neuron computation see (Silver, 2010). These intrinsic adaptation properties have been observed across many different pathways and cell types.

A tantalizing hypothesis was asserted by Barlow in the 1960's that proposed that sensory pathways evolve and adapt to efficiently process information (Barlow, 1961). Without the ability to adapt to constant input, neurons would be fundamentally limited in the dynamic range of encoding that could be achieved. If the neuron did not display intrinsic adaptation, it would faithfully encode information in a fairly straightforward way as the neural response would be unchanged regardless of stimulus input. However, because of the fixed gain, the stimulus intensity would be encoded only at a very coarse resolution, as quantified by the range of inputs captured by the input-output relationship. If we consider the information to be captured in the spike count or firing rate of the individual neurons over a short time window, each neuron is limited in the total number of inputs that it can differentially encode across the full input range (Figure 2-2B). If, however, the recent input range is restricted such that only a subset of potential stimuli is likely to be encountered, these non-adapting neurons cannot adjust and will continue to act as rigid look-up tables that are only able to encode a finite number of stimuli, across a limited fixed range of firing rates (Figure 2-2C, left). In contrast, the ability of an individual neuron to adapt to constant input represents a fundamental capability of the neuron to dynamically shift its operating point and expand the dynamic range to accommodate a finer resolution of encoding over the relevant range (Figure 2-2C, right). This method of remapping the nonlinearity to match the input distribution, known as histogram equalization, maximizes

the response entropy to optimize the encoding (Dayan and Abbott, 2001; Laughlin and Hardie, 1978).

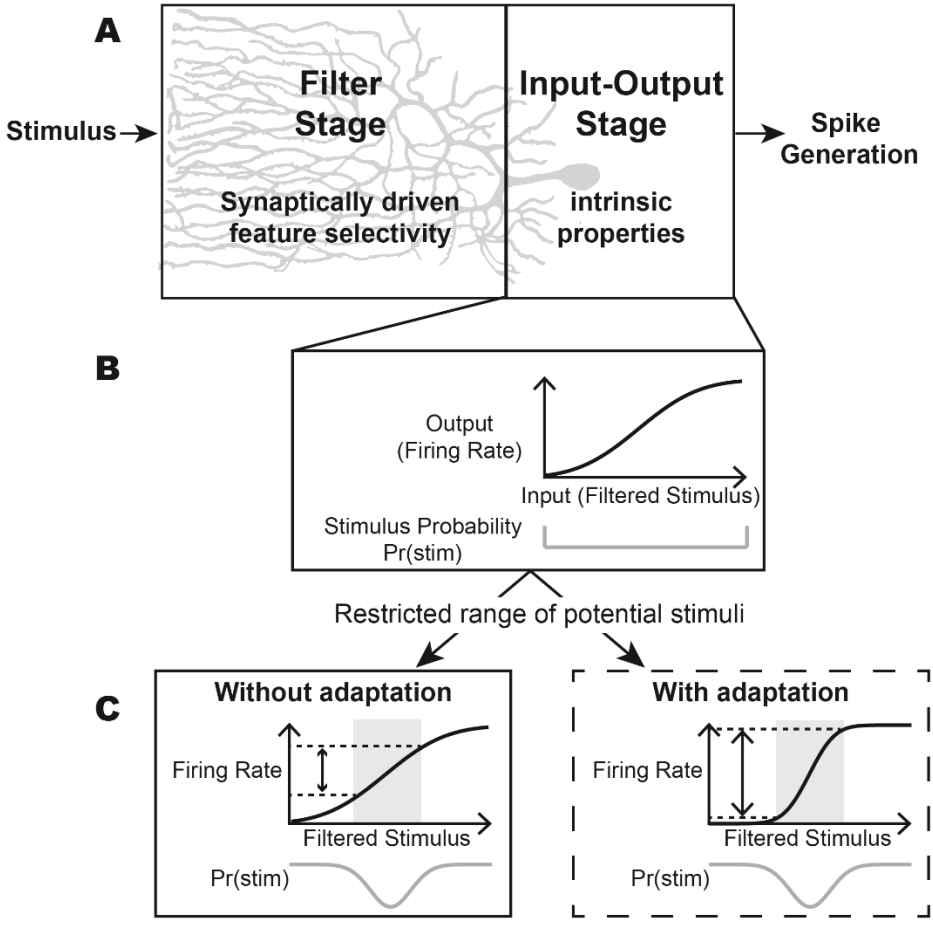


**Figure 2-2: Intrinsic adaptation allows rescaling of the input-output function.** A) Sensory encoding models have classically described two stages of transformation from the sensory stimulus to the spike output. The first stage can be envisioned as a filter stage where the sensory stimulus is filtered by the feature selectivity of a given neuron. The second stage can be described as an input-output stage that transforms the filtered stimulus input into a firing rate output. B) A neuron has a finite amount of spikes that can be elicited in a given time window. If a neuron is tuned to encode a finite number of potential stimuli, the neuron could encode each input linearly such that there is a one-to-one mapping between the input and the output. C. Realistically, a neuron will not encounter every possible stimulus in a short time window so the range of potential stimuli is likely restricted. Without adaptation, the input-output function for the neuron would not rescale which would limit the dynamic range of the outputs (left, grey shading). With adaptation, the input-output function can be rescaled to shift the dynamic firing range of the neuron to

the stimulus range that is likely (right, grey shading). Neuron image adapted from Ramon y Cajal (1889).

Adaptive gain rescaling, or the dynamic rescaling of the input-output function to match the statistics of the input, has been demonstrated at multiple stages of processing across several sensory modalities (Fairhall et al., 2001; Maravall et al., 2013, 2007). Using in vitro recordings, adaptive gain rescaling can also be generated in response to current injection using only intrinsic properties of the neurons (Díaz-Quesada and Maravall, 2008; Mease et al., 2013). Furthermore, this rescaling is not instantaneous; the time course of gain rescaling is dependent on the duration of the stimulus (Fairhall et al., 2001). Intrinsic adaptation currents occur on multiple timescales (La Camera et al., 2006) that may serve to tune the timescale of adaptation to the input statistics (Lundstrom et al., 2008). In fact, it has been proposed that spike frequency adaptation employs temporal whitening whereby the output spikes of an individual neuron are decorrelated to improve information transmission within a single neuron (Huang et al., 2016; Pozzorini et al., 2013). While the intrinsic adaptation can account for many of the adaptive properties described here, neurons obviously do not act in isolation but instead are embedded in a network. In highly interconnected neural circuitry, intrinsic adaptation properties of a single neuron will elicit widespread changes in information processing when interpreted in the context of network activity (Gjorgjieva et al., 2014). Observations of the coding properties associated with any individual recorded neuron indicate a potential compounding of the intrinsic cell properties of all cells feeding into the neuron in question combined with the adaptation effects occurring at the synapse between them.

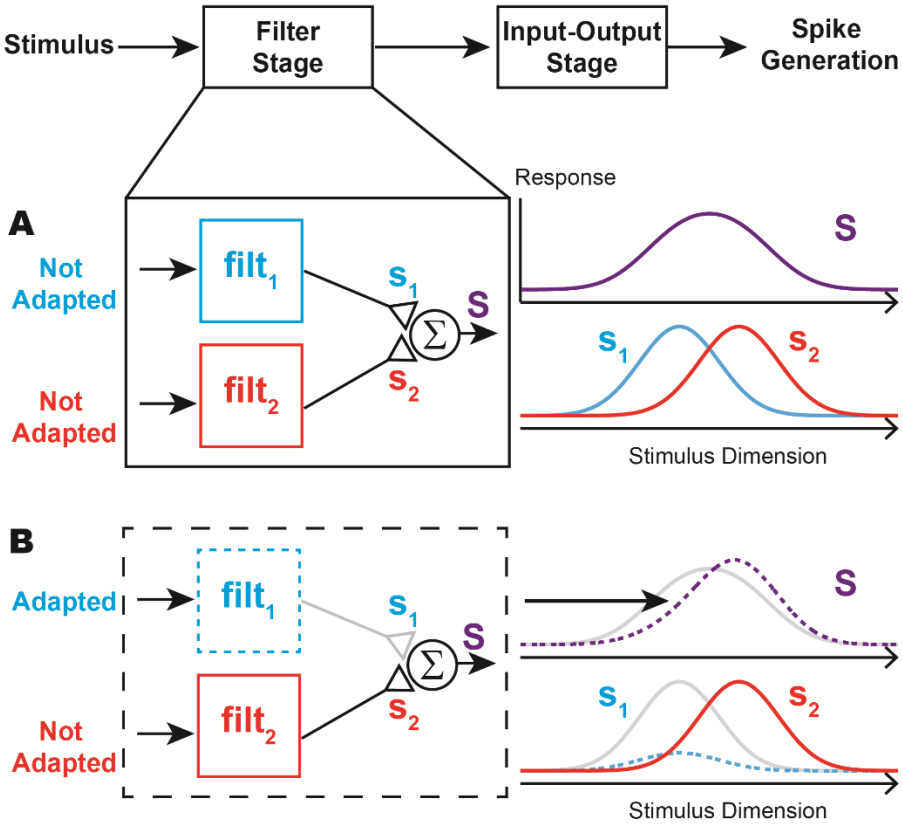


**Figure 2-3: Synaptic plasticity dynamically alters feature selectivity in an input-specific manner.** A) The feature selectivity of a neuron is determined by its presynaptic inputs. In a simplistic scenario, the feature selectivity of a neuron (S, purple) could be the sum of the feature selectivity of its presynaptic inputs ($s_1$, $s_2$; blue, red respectively). B) When the synaptic drive from one presynaptic population ($s_1$, dashed) is adapted, the synapse projecting downstream may become depressed (grey). The reduced drive from one synaptic input will cause the feature selectivity of the downstream cortical neuron to momentarily shift away from the adapted population (purple, dashed).

## 2.4 Adaptation at the chemical synapse

Beyond the intrinsic properties of a single neuron, rapid adaptation has also been described in the context of a modulation of the synaptic inputs to a measured neuron, captured as synaptic efficacy (Sen et al., 1996). Similar to intrinsic adaptation properties, rapid synaptic plasticity has been proposed as a potential neural mechanism to implement gain control (Abbott et al., 1997) as well as to decorrelate spike sequences (Goldman et al.,

1999). However in contrast to intrinsic adaptation effects of a single neuron that are indifferent to the input, rapid synaptic plasticity represents an input-specific change in the synaptic drive to a postsynaptic neuron (Chance and Abbott, 2001). Repeated spiking activity from a pre-synaptic neuron can lead to reduced or enhanced post-synaptic potentials depending on whether the synapse is depressing or facilitating. Paired-pulse studies have revealed that rapid synaptic depression, where increased pre-synaptic activity reduces the synaptic efficacy, persists for hundreds of milliseconds to seconds, while sustained stimulation can produce even longer lasting effects (Regehr, 2012). Short-term facilitation, where increased pre-synaptic activity enhances the synaptic efficacy, occurs on the timescale of tens to hundreds of milliseconds (Zucker and Regehr, 2002). In addition to chemical synaptic transmission, electrical synapses also show activity-dependent plasticity (Haas et al., 2016). In terms of nomenclature, note that changes in synaptic transmission have been described as a form of short term plasticity, but it occurs on the same time scale as the activity-dependent adaptation effects we consider here, and thus is functionally tangled. Activity-dependent synaptic adaptation compounds the adaptive effects described for single neuron input-output models by providing a mechanism to fundamentally alter the feature selectivity of neurons.

As information is transmitted from one neuron to the next, adaptive changes in synaptic transmission will directly impact the encoding in downstream neurons through modulation to the overall amplitude of the synaptic drive. Depression at the thalamocortical synapse has been implicated as a major contributing factor underlying the reduction in firing activity seen for cortical adaptation in the somatosensory pathway (Chung et al., 2002; Lundstrom et al., 2010), although certainly not the only contributing factor (Ganmor et al., 2010). In a simple hypothetical scenario, we can consider the effects of adaptive changes in the amplitude of sensory drive on the feature selectivity of a neuron that receives input from two distinct populations of pre-synaptic neurons (Figure 2-3A). If the sensory drive adapts only one population of these neurons such that the neurons are fatigued and

the synapses are sufficiently depressed, the feature selectivity of the post synaptic neuron will dynamically shift away from the tuning of the adapted pre-synaptic population (Figure 2-3B). With constantly ongoing and fluctuating sensory environments, the feature selectivity of neurons will rapidly shift in an activity-dependent manner. In the context of our simplified model framework introduced previously, even moderate selectivity in plasticity could fundamentally change the feature selectivity embodied in the first filtering stage. Indeed, rapid stimulus dependent changes in the filter properties have been demonstrated in the visual (Lesica et al., 2007; Sharpee et al., 2006), auditory (Theunissen et al., 2000) and somatosensory (Ramirez et al., 2014) pathways.

In addition to modulating the amplitude of the synaptic response, adaptation also shifts the temporal dynamics of the synaptic drive (Chance et al., 1998). Repetitive stimulation has been shown to increase the latency of the evoked response in sensory neurons (Ahissar et al., 2000) as well as decrease the trial-to-trial timing precision in the onset of the neural response (Desbordes et al., 2008; Higley and Contreras, 2006). However, at intermediate adaptation levels, repetitive stimulation can improve temporal precision (Eggermont, 1991; Garabedian et al., 2003), suggesting that adaptation effects are non-monotonic, and likely reflect more subtle schemes. In addition to altering the temporal precision of the evoked response of a single neuron, adaptation has also been shown to alter the synchrony of spiking across neurons (Q. Wang et al., 2010). In many neural pathways, coordinated pre-synaptic spike timing is important as synchronous population activity is hypothesized to play a major role in the successful transmission of information (Abeles, 1982), perhaps best exemplified in the thalamocortical circuit in the gating of information flow to cortex (Bruno, 2011; Jones, 2002; Tiesinga et al., 2008; H.-P. Wang et al., 2010). Due to synaptic integration in cortical neurons, for example, the change in temporal dynamics with sensory adaptation has been identified as a key role-player underlying the synchrony-mediated trade-off between signals that are well-suited

for detection and those that allow fine discrimination between different inputs (Ollerenshaw et al., 2014; Q. Wang et al., 2010).

While these studies provide general principles about the adaptive effects of ongoing sensory stimulation on synaptic transmission, there are also substantial differences in the adaptation of the synaptic efficacy as a function of cell type. In the thalamocortical pathway, synaptic efficacy varies as a function of both the pre- and post-synaptic neuron properties. Recordings from cortical neurons have demonstrated thalamocortical synapses are more effective than corticocortical synapses (Gil et al., 1999), but they also depress to a greater extent (Gil et al., 1997). Furthermore, by separating cortical responses into regular spiking and fast spiking populations, it has been shown that thalamocortical axons make stronger connections onto fast spiking inhibitory interneurons (Cruikshank et al., 2007) that also depress more (Beierlein et al., 2003) than thalamocortical connections onto regular spiking excitatory neurons. The variability of synaptic properties based on both pre- and post-synaptic neuron properties presents a fairly complicated interaction that is difficult to interpret (Reyes et al., 1998). However, recent work taking advantage of advances in genetic cell type labeling and stimulation techniques have begun to articulate these cell-type specific synaptic properties in controlled experimental conditions that do not rely on imperfect classification of cell-type based on waveform characteristics (Crandall et al., 2015b; Jouhanneau et al., 2015; Pala and Petersen, 2015). As we begin to pull together the synaptic properties between different cell-types and anatomical regions, these experimental advances will uncover the role of individual cell types in the development of adaptive synaptic properties within functional circuits to develop generalized principles of neural coding.

Importantly, much of our knowledge of the neurophysiological underpinnings of rapid sensory adaptation was developed in the anesthetized animal, while all of our knowledge of the perceptual effects of sensory adaptation was reported from the awake subject. Brain state plays an important role in shaping spontaneous neural activity as well

as sensory evoked responses (Anderson et al., 2000; Buonomano and Maass, 2009; McCormick et al., 2015; Petersen et al., 2003b; Poulet and Petersen, 2008; Zagha and McCormick, 2014) and therefore will impact encoding properties in the sensory pathways. Given that the state of the synapse is a function of activity levels, it follows that reduced synaptic efficacy will be present in thalamocortical neurons during states of arousal or with ongoing neural activity (Boudreau and Ferster, 2005; Castro-Alamancos and Oldford, 2002). In awake sensing conditions, organisms are constantly bombarded with a continuous stream of sensory information. The continuity of sensation has led some to hypothesize that depressing synapses, such as those found in feedforward sensory information transmission, are always in some state of depression during natural sensing (Borst, 2010; Reinhold et al., 2015). The difference between the state of the brain during most neurophysiological recordings and the state of the brain during conscious perception of adaptation may suggest potential differences in encoding (Castro-Alamancos, 2004b). While the absolute neural responses likely vary with state, there is significant evidence to suggest that many of the neural adaptation effects, such as reductions in neural activity levels (Ollerenshaw et al., 2014; Stoelzel et al., 2015), shifts in encoding states (Whitmire et al., 2016), and changes in population coding (Gutnisky and Dragoi, 2008), seen in the anesthetized animal are also present in the awake animal. The qualitative ability to rapidly adapt neural properties appears to be a conserved mechanism across brain states. While extrapolating additional results from the anesthetized animal to the awake preparation will require significant validation, we can begin to make clear and testable predictions about how the neural activity may change in the awake state and the implications for adaptive sensory encoding.

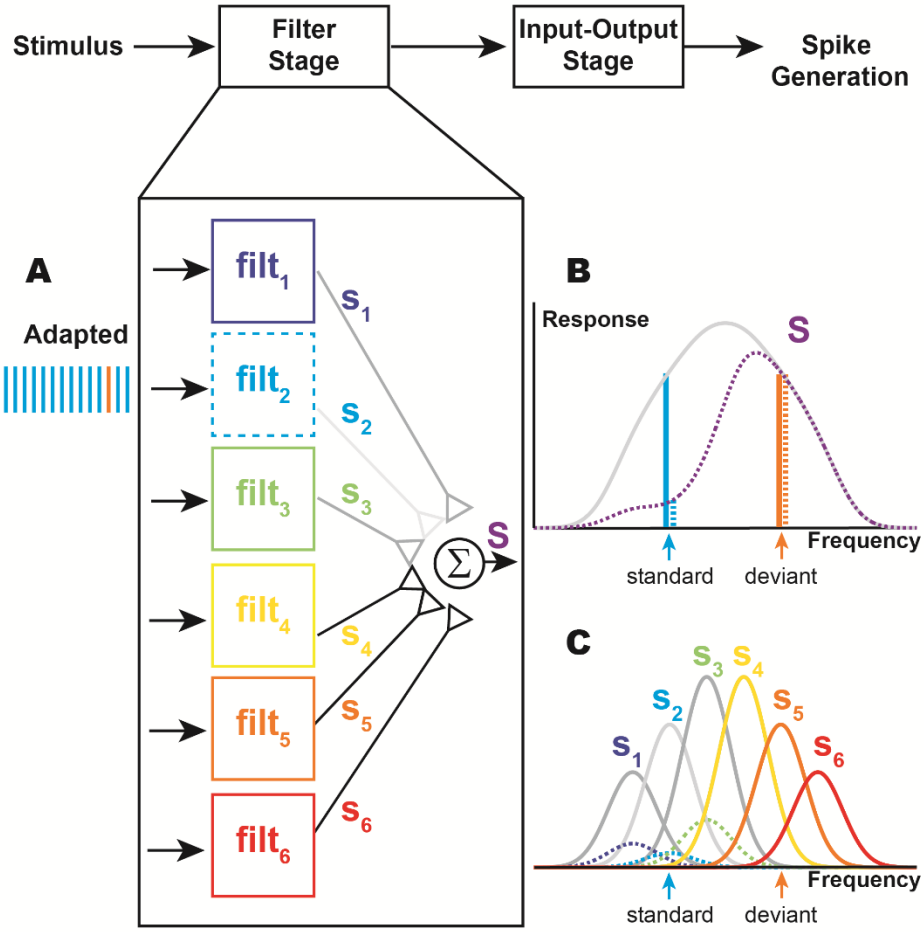


**Figure 2-4: Stimulus specific adaptation can be partially explained by the adaptation in narrow frequency model.** A) The frequency tuning of a neuron in primary auditory cortex (A1) could be inherited from the frequency tuning of its presynaptic inputs. In an SSA paradigm, one off-peak frequency for the A1 is used as the 'standard' stimulus that is presented frequently (blue) while a second off-peak frequency is used as the infrequently presented 'deviant' stimulus (orange). Repetitive 'standard' stimulation will depress the feedforward synapses (grey). B) The evoked responses to the 'deviant' and 'standard' stimuli are approximately equal without adaptation (solid vertical lines). The evoked response to the 'standard' stimulus is greatly reduced when adapted, while the 'deviant' stimulus is largely unaffected (dashed vertical lines). C) It has been proposed that differential adaptation of the presynaptic populations that are tuned to the 'standard' stimulus will reduce the inputs from those neurons (dashed frequency tuning curves) and shift the frequency tuning of the A1 neuron (B, purple dashed line).

## 2.5 Differential adaptation of specific populations of tuned neurons

Moving from adaptation between pairs of neurons to adaptation across circuits, there is evidence that the properties of the ongoing sensory stimulation will differentially activate distinct populations of tuned neurons. In the auditory pathway, "oddball" paradigms that reduce the dimensionality of the stimulus space to a single dimension, such as frequency, have been used extensively to study this phenomenon known in the auditory field as stimulus specific adaptation (Ulanovsky et al., 2003). Stimulus specific adaptation (SSA) is defined by a reduced response to a frequent stimulus (standard) that does not affect, or minimally affects, the response to a rare stimulus (deviant) on a trial-by-trial basis (Pérez-González and Malmierca, 2014). SSA has been identified in the non-lemniscal stations of the inferior colliculus (Ayala and Malmierca, 2015; Malmierca et al., 2009) and the thalamus (Anderson et al., 2009; Antunes et al., 2010), while primary auditory cortex (A1) is the first lemniscal station that shows strong SSA (Taaseh et al., 2011). SSA has also been identified in these brain regions in the awake animal (Duque and Malmierca, 2014; Richardson et al., 2013; von der Behrens et al., 2009), further underscoring the ubiquity of neural adaptation across brain states.

While the origin of SSA in the auditory pathway is debated, it is generally accepted to be generated from a network phenomenon because it cannot be explained from the intrinsic properties of the neurons alone (Malmierca, 2015). Instead, a model of adaptation in narrow frequency channels has been proposed that suggests SSA is due to the differential adaptation of tuned populations of pre-synaptic neurons (Figure 2-4A). As discussed previously in the context of synaptic plasticity, presynaptic neurons tuned to the standard stimulus (Figure 2-4, blue) will experience synaptic depression in response to the standard stimulus presentation and therefore will elicit reduced sensory drive in the postsynaptic neurons (Figure 2-4C, dashed lines). In a separate population of presynaptic neurons that are tuned to the deviant stimulus (Figure 4, orange), the standard stimulus will not evoke a response and therefore the synapses in this population will not be depressed (Mill et al.,

2011; Taaseh et al., 2011) (Figure 2-4C, solid lines, warm colors). When these differentially tuned populations of neurons drive a common downstream brain region, the postsynaptic population integrating their inputs will demonstrate stimulus specific adaptation simply due to differential adaptation of the stimulus selective neurons (Figure 2-4B, dashed line). Recent evidence further supports this model by demonstrating that SSA is not present for intensity oddball paradigms where presumably the same population of neurons would be activated by the standard and the deviant (Duque et al., 2016). This simple theoretical model provides a framework for a network level adaptation whereby information is differentially processed by complementary populations of neurons to generate an adaptation effect not necessarily present in the presynaptic populations.

Although the adaptation in narrow frequency channels model presents a simple feedforward mechanism for the generation of SSA from the upstream driving inputs, it has been shown that the model is insufficient to fully account for the properties of SSA seen in primary auditory cortex (A1) (Hershenhoren et al., 2014; Yaron et al., 2012), suggesting that there are also locally generated mechanisms of SSA. In A1, there are a variety of cell types classified broadly into excitatory and inhibitory neurons that form complex cortical circuits which are proposed to enhance SSA (Taaseh et al., 2011). These functionally distinct classes of neurons likely contribute differentially to the function of the cortical circuit, and in this case, to the generation or enhancement of SSA locally within A1. Using traditional electrophysiological techniques it is incredibly difficult to deconstruct the role of each cell type in cortical function. However, the advent of genetic tools has made it possible to perform cell-type specific circuit dissection (Luo et al., 2008). In the auditory pathway, the implementation of these genetic tools has demonstrated that SSA is evident in both excitatory neurons and inhibitory neurons in A1 (specifically somatostatin-positive (SOM) and parvalbumin-positive (PV) GABAergic interneurons) (Chen et al., 2015; Natan et al., 2015). Systematic investigation of the role of SOM and PV interneurons suggests that the two inhibitory cell types are actually playing complementary roles in the

enhancement of SSA in excitatory cortical neurons (Natan et al., 2015). In this work, Natan et al. found that PV interneurons amplify SSA through non-specific inhibition while SOM interneurons amplify SSA by selectively suppressing excitatory responses to the standard tone. These cell-type specific adaptation effects demonstrate that all interneurons are not equal in the context of adaptation and information coding (Moore et al., 2010), but questions still remain about how these cell types work together within and across brain regions to generate functional percepts. It is possible that the adaptation in narrow frequency channels model represents an inherited mechanism of adaptation in A1 while the differential adaptation of cell types within A1 represents a locally generated mechanism to enhance SSA. However, understanding the mechanisms underlying SSA is significantly more complex than this. These sensory pathways are highly interconnected and receive a significant number of top-down influences in addition to the bottom-up and local influences described here (Malmierca, 2015). However, only recently have the tools been available to perform circuit level assessments of functional properties using fast and reversible control of discrete cell-types to enable answers to these fundamental questions of adaptation. Using these techniques, we will be able to quantify the adaptive properties across neuron populations that may differ genetically but function together as one efficient unit. Only by understanding the role each population plays in information processing will we be able to understand the true function of the circuitry.

The SSA paradigm has become an excellent tool to probe the neural response along a single dimension of the sensory stimulus space. There have also been demonstrations of a similar phenomenon to auditory SSA, although likely a different neural correlate, in human event related potentials known as mismatch negativity in response to auditory stimuli (Escera and Malmierca, 2014; Farley et al., 2010; Grimm and Escera, 2012; Khouri and Nelken, 2015). Although neural signatures of SSA has been most widely studied in the context of frequency in the auditory pathway, it has also been demonstrated in the context of a range of tuning property dimensions in the visual pathway (Baylis and Rolls, 1987;

Miller et al., 1991; Ringo, 1996; Sawamura et al., 2006) and in slice recordings in response to spatially separated electrical stimuli (Eytan et al., 2003). Many forms of adaptation have been identified in the visual pathway, but adaptation of orientation tuning is one dimension of the visual space that has been investigated most extensively. As shown for frequency-specific adaptation in the auditory pathway, orientation-specific adaptation can shift the orientation tuning of primary visual cortex (V1) neurons away from the adapting orientation (Benucci et al., 2013; Dragoi et al., 2000; Felsen et al., 2002; Jin et al., 2005). The adaptation of orientation tuning is stronger with longer adaptation stimulation (Patterson et al., 2013) and more prominent for neurons at the center of orientation pinwheels where there is the most access to multiple orientation directions (Dragoi et al., 2001) (but see (Sengpiel and Bonhoeffer, 2002)). Interestingly, orientation responses are also quickly adapted by simultaneous presentation of a stimulus at a different orientation (Mrsic-Flogel and Hübener, 2002).

What might be the perceptual consequences of such phenomena? While not completely understood in terms of the electrophysiology, perhaps because of the distributed nature of the activity, the perceptual "waterfall" illusion described previously is also thought to arise from a differential adaptation of visual neurons tuned for specific directions of motion (Anstis et al., 1998). Prolonged exposure to motion in one direction preferentially adapts neurons tuned to that direction, resulting in biased population codes (Zavitz et al., 2016) and ultimately a biased percept of subsequent stimuli (Levinson, E., Sekular, 1976). Until we are truly able to identify the neural basis of perception, it will be extremely difficult to directly link the perceptual effects to the underlying neural correlates. However, the commonality of this phenomenon across sensory modalities, brain regions, and species, suggests that differential adaptation of distinct neuronal populations is a conserved adaptive response where the response properties of neurons, and ultimately perception, are adaptive on a moment-by-moment basis.

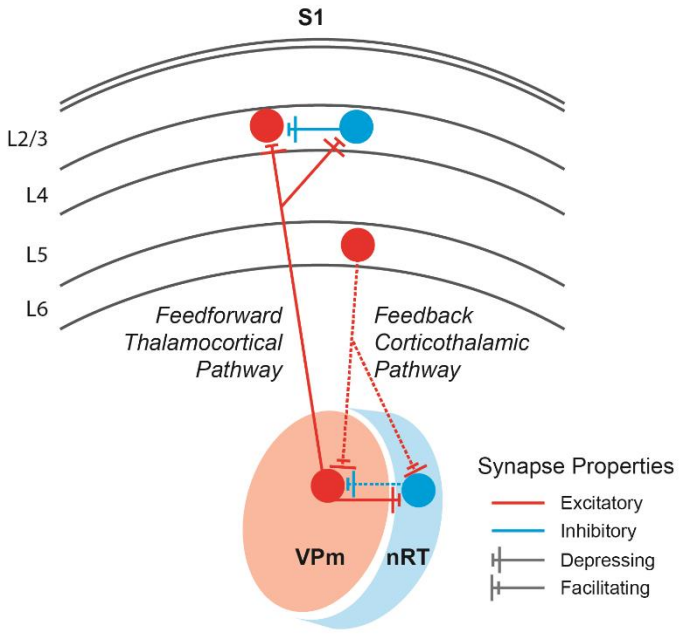


**Figure 2-5: Feedforward inhibition in the thalamocortical and corticothalamic pathways of the rodent vibrissa system.** The feedforward thalamocortical inputs from the ventral posteromedial (VPm) thalamus project to both excitatory and inhibitory neurons in layer 4 of primary sensory cortex (S1L4; solid lines). The corticothalamic feedback inputs from S1 L6 provide direct excitation to VPm and feedforward inhibition to VPm mediated through the reticular nucleus of the thalamus (nRT; dashed lines). While the exact properties of these feedforward and feedback pathways differ in detail, the similar feedforward inhibition motif leads to common adaptive properties.

## 2.6 Differential adaptation of excitatory and inhibitory neurons

Given that the differential adaptation of sub-populations of neurons could profoundly shape neural activity, to what extent does the anatomical wiring influence these effects? Throughout all neural pathways, there are a number of common circuit motifs that are believed to perform canonical functions for neural processing (Miller, 2016). In sensory pathways, disynaptic feedforward inhibition is a common motif, exemplified in the thalamocortical projection where sensory information transmitted from the thalamus will elicit a stereotyped pattern of excitation followed by inhibition at the level of the primary sensory cortex (Isaacson and Scanziani, 2011) (Figure 2-5; solid lines). The rapid onset of

the inhibition that follows excitation is likely due to feedforward inhibition from thalamocortical inputs that synapse onto both excitatory and inhibitory cortical neurons (Cruikshank et al., 2007; Miller et al., 2001; Wilent and Contreras, 2005b; Wu et al., 2006). Disynaptic feedforward inhibition has been proposed as a mechanism to enable cortical neurons to be particularly sensitive to the timing of their inputs within a window of integration (Wehr and Zador, 2003). Furthermore, the sequence of excitation followed by inhibition that generates precise timing sensitivity appears to represent a common circuit motif for neural processing within brain regions that receive excitatory projections and contain interneurons including primary sensory cortex (Gabernet et al., 2005; Higley and Contreras, 2006; Wehr and Zador, 2003), hippocampus (Buzsáki, 1984; Finch et al., 1988; Pouille and Scanziani, 2001), amygdala (Bissière et al., 2003), and visual thalamus (Blitz and Regehr, 2005). While this conserved circuit motif leads to a repeatable E-I activation pattern, the temporal aspects of the dynamic interaction between the excitatory and inhibitory conductances are also variable as a function of the input. In the presence of adaptation, the onset of inhibition relative to excitation shifts such that the cortical window of integration can lengthen to allow integration over longer time windows (Gabernet et al., 2005; Higley and Contreras, 2006). While the absolute duration of the cortical integration window is debated, it is believed to be on the order of milliseconds when the pathway is not adapted and on the order of tens of milliseconds in the presence of adaptation (Gabernet et al., 2005). Elongation of the excitability period of cortical neurons is paired with shifts in thalamic synchrony which ultimately controls the gating of signals to cortex (Q. Wang et al., 2010).

In our simplified modeling framework, the summed output across filters can now be separated by the sign of interaction to generate both excitatory and inhibitory filters (Figure 2-6). In the visual pathway, the filter component of a thalamic encoding model can be described as a combination of an excitatory filter with a temporally lagging inhibitory filter (Butts et al., 2011), which is consistent with disynaptic feedforward inhibition (Figure

2-6A). Because the excitatory and inhibitory inputs interact in a complex manner, adaptation of these two components will have profound effects on the temporal feature selectivity and timing of responses. Contrast adaptation, for example, has been linked to changes in temporal dynamics and gain in the visual system (Shapley and Victor, 1979; Solomon et al., 2004). Contrast is obviously an important parameter for visual processing, and contrast sensitivity is considered one of the fundamental instantaneous/static properties of visual neurons. Interestingly, however, contrast-sensitivity is typically measured with the presumption that it is a static property of the pathway, obscuring any adaptive process that may be going on. In the context of adaptation, with an increase in contrast in a switching paradigm, the adapted linear filters for LGN neurons show faster temporal dynamics and a decrease in the gain of the input-output function relative to a low contrast condition (Figure 2-6B) (Lesica et al., 2007; Mante et al., 2005). However, it is difficult to estimate dynamic feature selectivity to robustly capture adaptive behaviors across stimulus conditions (Lesica and Stanley, 2006, 2005; Stanley, 2002) because the feature selectivity of a neuron (Fritz et al., 2003; Lesica et al., 2007; Sharpee et al., 2006; Ulanovsky et al., 2003) can change rapidly with only a short adapting stimulus. This suggests that the fundamental features of a stimulus that drive a neuron to fire are flexible on rapid timescales such that adaptation can reshape what information is transmitted through the sensory pathway, which has even more profound effects if there is differential adaptation across excitatory and inhibitory inputs.

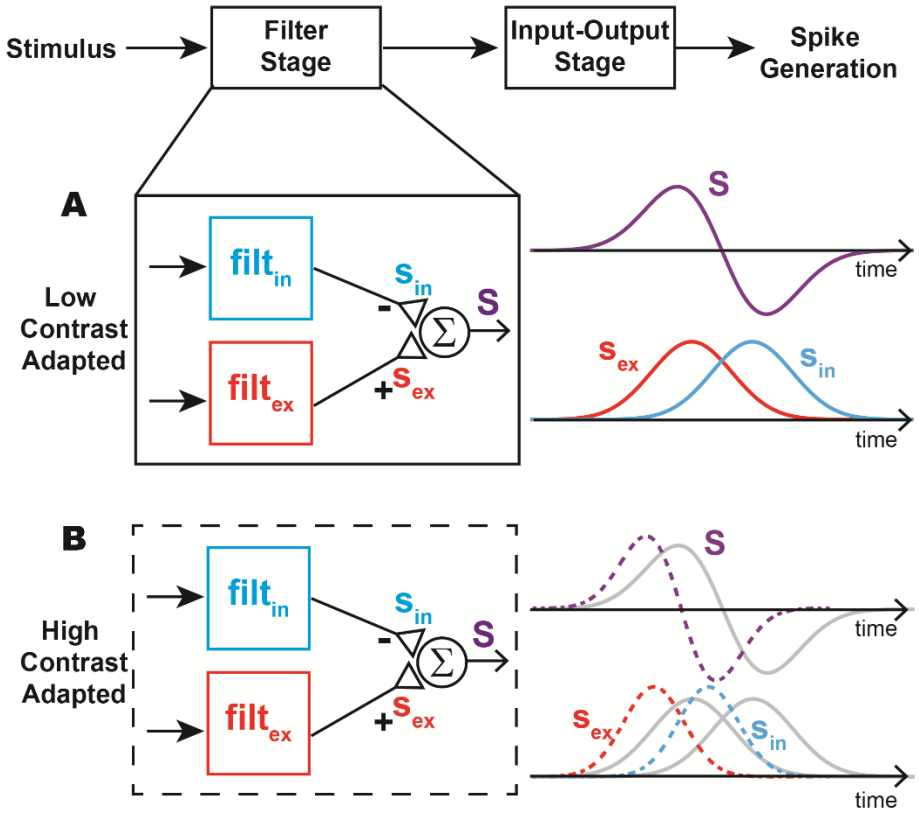


**Figure 2-6: Shifts in contrast adaptation can sharpen temporal dynamics of receptive fields.** The feature selectivity of a neuron will incorporate both excitatory and inhibitory inputs. In this example, the inhibitory input is simply a temporally shifted version of the excitatory input (right, bottom). The subtraction of these two temporal features results in a biphasic feature selectivity (right, top). B) In the high contrast adapted condition, the excitatory and inhibitory filters are more temporally precise (right, bottom) leading to a temporally sharpened component of the receptive field (right, top).

In addition to differentially modulating the timing of the excitatory and inhibitory inputs in response to punctate stimuli, adaptation has also been shown to differentially modulate the overall amount of the excitatory and inhibitory synaptic drive onto a L4 excitatory cortical neuron (Heiss et al., 2008). The thalamocortical synapses onto both excitatory and inhibitory neurons will depress with ongoing sensory drive leading to an overall reduction in the absolute amount of excitation and inhibition (Chung et al., 2002; Reinhold et al., 2015). However, the effect of adaptation is greater for inhibition than for

excitation (Gabernet et al., 2005) such that the E-I balance is transiently shifted toward excitation (Cohen-Kashi Malina et al., 2013; Heiss et al., 2008). While extracellular recordings have shown that spiking activity in fast-spiking inhibitory neurons can sustain higher firing frequencies than excitatory neurons during sustained stimulation (Khatri et al., 2004), both the input synapse from the thalamus and the output synapse to the regular spiking neuron show substantial depression (Beierlein et al., 2003; Gabernet et al., 2005). Furthermore, the recovery of inhibition from adaptation is slower than the recovery of excitation, which can provide a period of facilitation immediately following adaptation (Cohen-Kashi Malina et al., 2013). At first glance, it may seem contradictory that adaptation of cortical L4 neurons results in both a transient shift towards excitation and a reduced suprathreshold spiking response to ongoing stimulation. However, the marked reduction in excitation due to depression of the thalamocortical synapse prevents the cortical neurons from reaching spiking threshold. Consistent with this view, recent work in the rodent whisker pathway found a net depolarization of the membrane potential was elicited in the barrel cortex in response to an adaptation stimulus, but the depolarization was paired with a reduction in the excitatory PSP amplitude (Ramirez et al., 2014). Note that there is also recent evidence of thalamic projections to other layers of cortex (Constantinople and Bruno, 2013), but the role of these connections in adaptive gating is current unknown.

While this has been well studied in the feedforward thalamocortical pathway, disynaptic feedforward inhibition is also a circuit motif in the corticothalamic pathway from primary sensory cortex to the lemniscal nucleus of the thalamus mediated through the reticular nucleus (nRT) (Figure 2-5; dashed lines, rodent vibrissa pathway). The results described here have been investigated in the context of the rodent vibrissa pathway, but likely apply more broadly. In contrast to the feedforward processing of the thalamocortical pathway where thalamocortical synapses depress, corticothalamic synapses show short-term facilitation (Cruikshank et al., 2010; Deschênes and Hu, 1990; Landisman and

Connors, 2007). Yet similar to the thalamocortical circuit of the rodent vibrissa pathway, repeated activation of the corticothalamic feedback (S1L6) to whisker thalamus (VPm) also results in decreased inhibition in the VPm (Crandall et al., 2015b). Given that the reticular thalamus (nRT) is the only known source of inhibitory input to VPm (Pinault, 2004), this suggests that nRT must be exhibiting greater adaptation than the excitatory feedback input from S1L6. As demonstrated for inhibitory neurons in cortex, inhibitory neurons in thalamus (nRT) can also maintain high tonic firing rates during repetitive whisker (Hartings et al., 2003) or S1L6 stimulation, but with reduced levels of inhibition in the postsynaptic excitatory neurons (VPm) due to robust short-term synaptic depression at the nRT-VPm synapse (Crandall et al., 2015b). Furthermore, sustained activation of S1L6 will lead to a net depolarization of the membrane potentials in VPm (Mease et al., 2014), as was seen in both thalamus (Jubran et al., 2016) and cortex (Ramirez et al., 2014) in response to repetitive stimulation of the whiskers. Finally, nRT responses also recover much more slowly than VPm responses (Ganmor et al., 2010), as was demonstrated for the level of inhibitory synaptic drive in cortex (Cohen-Kashi Malina et al., 2013).

The parallels between these highly interconnected feedforward and feedback pathways of the thalamocortical system present what may be a fundamental component of dynamic neural encoding. Differential adaptation of excitatory and inhibitory neural populations provides a mechanism to shift the properties of synaptic integration and therefore the function of the circuit, specifically in the context of timing. Timing in sensory circuits play an important role in stimulus representation (Desbordes et al., 2008; Montemurro et al., 2007), and work in the visual system has shown how the temporal precision of the pathway is matched to the statistics of the input (Butts et al., 2007). Adaptation modulates not only temporal precision within neurons, but also synchronous firing across neurons (Q. Wang et al., 2010). Furthermore, transitions in the coding properties of the pathway in response to adaptation also extend to state-related firing such as burst-tonic firing in the thalamus (Lesica et al., 2006; Lesica and Stanley, 2004;

Whitmire et al., 2016), that could underlie the shift in information processing modes (Ollerenshaw et al., 2014).

## 2.7 Pooled population effects

While adaptation has cell-type specific effects, there are also large-scale properties of adaptation due to pooled population effects. Normalization has been proposed as a canonical computation of neural circuits whereby a neuron's response is normalized by the pooled neural activity of the local circuitry (Matteo Carandini and Heeger, 2012). Normalization was originally proposed to explain responses in primary visual cortex (Heeger, 1992), but the principles have since been demonstrated in a wide range of studies, including processing in visual thalamus (Bonin et al., 2005) and inferior temporal cortex (Kaliukhovich and Vogels, 2016), olfactory processing (Olsen et al., 2010), multisensory integration (Ohshiro et al., 2011), visual attention (Reynolds and Heeger, 2009), and context-dependent decision making (Louie et al., 2013). While the exact biophysical mechanism underlying this computation depends upon the neural architecture (Sato et al., 2016), this activity-dependent computation has a common theme: normalization of the neural response.

Although the relationship between normalization and adaptation is not clear, the normalization computation occurs on time scales relevant for the rapid adaptation discussed here. As such, normalization could represent an added layer of population level adaptation effects to modulate sensory responses. Normalization can be visualized as a form of gain control whereby the activity of the circuit serves as negative feedback for the input-output function. In the context of the model framework described here, the response of any given neuron is still a cascade of its feature selectivity that is shaped by synaptic inputs and a second nonlinearity stage associated with intrinsic properties and some elements of spike generation, but this second stage input-output function is now modulated by the population activity (Figure 2-7). Whereas we previously discussed shifts in the

nonlinearity due to intrinsic adaptation currents, normalization presents an additional modulation due to pooled neural activity. Depending on the mechanism of action, normalization can scale the input to the nonlinearity (Figure 7A) or the output of the nonlinearity (Figure 2-7B). In the olfactory processing of drosophila, Olsen et al. implemented a sensory paradigm to investigate the role of lateral inhibition in generating normalization that takes advantage of the highly structured odorant tuning to independently stimulate the neuronal population of interest and the surrounding neuronal populations (Olsen et al., 2010). In this work, inclusion of lateral inhibition (through a non-specific odorant stimulus) led to input scaling as the normalization effect in this pathway (Figure 2-7A). In visual processing of macaque V1, Cavanaugh et al. implemented a spatial integration paradigm to investigate divisive normalization in the context of response gain (Cavanaugh et al., 2002). In this work, a receptive field model identified output scaling as the best fit to the experimental data (Figure 2-7B). Importantly, while both input and output rescaling have been demonstrated in olfactory and visual processing, the underlying neural correlates of normalization vary based on the circuitry. Normalization described for the olfactory pathway of drosophila is likely mediated through increased inhibition while divisive normalization in visual cortex may actually result from a decrease in synaptic excitation rather than an increase in inhibition (Sato et al., 2016). Yet despite these varying mechanisms, the normalization computation appears conserved across different pathways and brain structures (Matteo Carandini and Heeger, 2012). Note that much of the existing literature providing empirical support for the normalization computation does not explicitly include time as an element (time to develop, time to dissipate). However, given that the normalization is activity dependent, it is very likely that the effects fit within our definition of adaptation as requiring time to manifest.

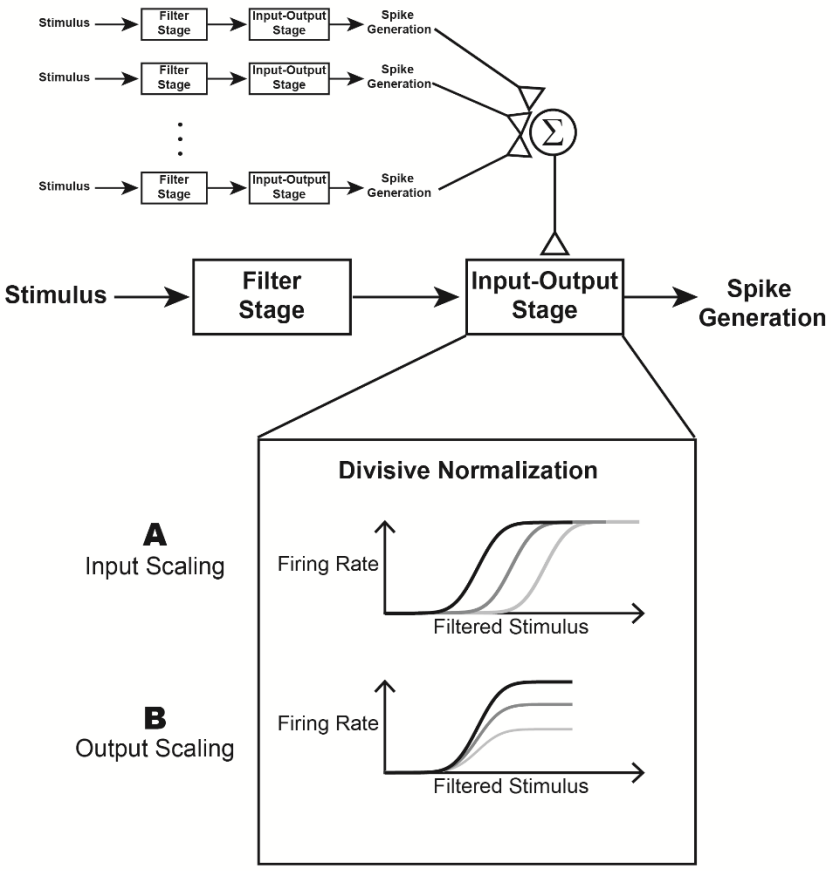


**Figure 2-7: Divisive normalization modulates the input-output tuning function.** Although not typically described in conjunction with sensory adaptation, divisive normalization could also be considered a pooled adaptation effect where the firing activity across neurons can reshape the input-output function of an individual cell in an activity dependent manner. There are two methods of input-output scaling that have been proposed and demonstrated in different sensory pathways. A) Input scaling refers to shifting the input-output curve laterally while B) output scaling refers to scaling the input-output curve vertically. Both scaling mechanisms represent an activity dependent network mechanism to shift the encoding of sensory neurons.

Given the prevalence of normalization computations in the brain, we might ask how this compares to other rapid adaptation mechanisms described thus far. Previously, we discussed mechanisms to drive changes in the feature selectivity of sensory-driven neurons such as stimulus specific adaptation or changes in E-I conductances. The role of normalization is not necessarily to drive changes in the feature selectivity of the neuron,

but instead to modulate the neural response in more subtle ways. In the visual pathway for example, normalization has been used to describe the role of the non-classical receptive field in modulating cortical responses. The classical receptive field is defined by the region of visual space that elicits firing from the sensory neuron (Hubel and Wiesel, 1959) while the non-classical receptive field is the visual space that extends beyond the classical receptive field (Allman et al., 1985). Simultaneous activation of the classical and non-classical receptive fields will reduce the evoked response relative to stimulation of the classical receptive field alone (Jones et al., 2001) giving non-classical receptive field the description of a suppressive field (Bonin et al., 2005). The suppressive field normalizes the neural response relative to the stimulus intensity in the non-classical receptive field (Matteo Carandini and Heeger, 2012), but not without purpose. Visual stimulation with natural movies has shown that stimulation of the non-classical receptive field increases the efficiency of information transmission (Vinje and Gallant, 2002), as expected for sensory adaptation, through intracortical network interactions (Haider et al., 2010). Building on the complexity of the adaptive modulation of feature selectivity, normalization represents the ability of the neural circuitry to pool information across neurons to fundamentally alter the input-output relationship. There is still much to learn, however, about how these mechanisms might operate dynamically in a transient environment, and about the time-scales over which the normalization takes place.

### 2.8 Implications of highly interconnected circuitry in adaptive coding

As described throughout this Perspective, adaptation effects will build and compound from a single neuron to a single synapse to a small circuit to a local network before eventually forming adaptive percepts. In order to interpret network activity in the context of highly interconnected circuitry, we must consider the detailed anatomy of our sensory pathways and how these canonical microcircuits might give rise to the adaptive neural responses discussed here.

### 2.8.1 Disentangling inherited and locally generated adaptation effects

Thus far, we have primarily discussed adaptation within the thalamocortical circuit. But things become increasingly complex as we consider how adaptation shapes encoding across entire pathways in which the fundamental properties of a given neuron can be rapidly altered by recent sensory drive. In the rodent vibrissa pathway, somatosensory information is transduced by the primary sensory neurons in the whisker follicle and then transmitted from the vibrissa to the brainstem and then to the thalamus before reaching primary somatosensory cortex (Diamond et al., 2008b). If we consider the cortical response to repetitive whisker stimulation, we can ask how much of the rapid adaptation seen in cortex is generated locally compared to how much is inherited from rapid adaptation at earlier stages of the pathway. Rapid adaptation has been quantified in the most basic sense as the change in the spike counts (firing rate) in response to repetitive stimulation. In the vibrissa pathway, the amount of spike count adaptation increases at each stage of the processing pathway from the brainstem to the thalamus to cortex (Ganmor et al., 2010). This would suggest, perhaps unsurprisingly, that at least some basic components of adaptation are inherited from one brain region to the next. However, as we have discussed, there are also mechanisms of adaptation that are generated locally rather than inherited only from presynaptic adaptation effects. Locally generated adaptation effects have been described perceptually by 'higher order' adaptation whereby a subject adapts to higher order stimulus features, such as face adaptation, that cannot be entirely inherited from non-face selective regions (Strobach and Carbon, 2013; Webster et al., 2004) in the absence of complex scenarios that seem exceedingly unlikely. While the effects of face adaptation can be seen perceptually, it is difficult to identify the neural correlates of higher order adaptation (Fox and Barton, 2007). However, this dichotomy between inherited and locally generated adaptive processes likely exists at each stage of sensory processing for even very simple sensory stimuli. In the visual pathway, the inheritance of adaptation has been studied from LGN to V1 (Dhruv and Carandini, 2014; King et al., 2016) and from V1 to

MT (Patterson et al., 2014). For example, by silencing V1 optogenetically, King et al. were able to dissociate local cortical processing from the feedforward adapted thalamic input to determine the relative weights of inherited versus locally generated contrast adaptation effects. If we begin to consider the commonality of neural processing between excitatory and inhibitory neurons or differential adaptation of tuned populations of neurons, we can begin to extrapolate the effects on information processing as each stage of processing inherits earlier adaptation effects and locally generates additional encoding shifts.

### 2.8.2 Adaptation effects in highly interconnected circuitry

It is also important to consider that sensory information is not only being processed in a feedforward manner from the periphery to the cortex, but instead there are an immense number of feedback projections that suggest information is processed in a highly complex way. A particularly salient example is the thalamocortical circuit. While we traditionally study the feedforward projections from thalamus to cortex, it is well documented that the vast majority of synapses onto a thalamic neuron are actually cortical in origin (Varela, 2014). While these synapses are more modulatory in nature than the sensory drive (Sherman and Guillery, 1998), the sheer volume suggests an important role of corticothalamic feedback in information transmission. Furthermore, the feedback circuit motifs share anatomical and functional properties with the feedforward circuit, such as disynaptic feedforward inhibition and common adaptation responses for excitatory and inhibitory neurons at each stage of processing, as described above in the context of the rodent vibrissa pathway. Recent evidence from the stimulus specific adaptation (SSA) literature that has sought to disentangle the role of feedforward SSA generation from feedback SSA modulation suggests that while SSA can be inherited in a feedforward manner, it is refined subcortically through cortical feedback (Malmierca, 2015). Similar to the roles of specific cell-types in the enhancement of SSA in cortex, the ability of cortical feedback to modulate information transmission presents a complementary role for

modulatory feedback in rapid sensory encoding. Disentangling the role of any given neuron in inducing or demonstrating sensory adaptation will likely require a more sophisticated understanding of artificial stimulation techniques (Millard et al., 2015) that can be implemented in conjunction with cell-type specificity and real-time feedback control of neural activity to functionally decouple causally related variables (Grosenick et al., 2015; Newman et al., 2015). By understanding the part each neural component plays in building the network level response, we can begin to understand the functional role of the circuitry in dynamic encoding.

## 2.9 Implications of adaptation paradigms for natural sensing and behavior

While significant progress in the field has demonstrated various adaptive properties across neural circuits, the experimental paradigms employed are still restricted in their scope due to practical limitations of experimental preparations. How do we bridge the electrophysiological findings developed under reduced sensory stimulus adaptation paradigms to natural sensing environments? And further, what are the implications of these dynamic encoding properties demonstrated in neurophysiological studies on information encoding and ultimately sensory perception? While the answers to these questions remain abstract, we can begin to piece together prior experimental results to propose a few open questions for the field.

### 2.9.1 Extrapolating adaptation effects from simplified experimental paradigms to natural sensing

In probing the dynamics of neural pathways, a simple paired-pulse paradigm has been widely utilized to capture the dynamics in the simplest possible manner. This paired pulse paradigm has built the foundation for our understanding of synaptic facilitation and depression dynamics (Stevens and Wang, 1995) and sensory evoked cortical dynamics (Simons, 1985). Although experimentally and analytically attractive, these kinds of pairs of probes separated in time only capture second-order interactions. The immediate question

becomes whether or not second order dynamics are sufficient to explain the neural dynamics observed in more realistic regimes. More specifically, does this kind of characterization make accurate predictions when extended to even just a triplet of stimuli, or more importantly, to complex temporal patterns? In the rodent vibrissa pathway, pairs of punctate whisker stimuli have been commonly employed to quantify neural dynamics (Simons, 1985). However, models built from the cortical response to a pair of whisker stimuli alone are insufficient to fully predict even the cortical response to just a triplet of whisker stimuli (Webber and Stanley, 2004). As the patterns of whisker stimuli become increasingly complex, the encoding must expanded to incorporate the temporal interactions across stimuli that capture the interplay between excitatory and inhibitory circuitry (Boloori et al., 2010). Similar findings from the crustacean neuromuscular junction demonstrate that the dynamic synaptic response to temporally random stimuli has a temporal dependence on recent spiking history that cannot be predicted by the response to a single stimulus alone (Sen et al., 1996). Even in spike-timing dependent plasticity experiments where the stimulation occurs over a longer time period, the depression/potentiation dynamics are dependent on these more complex spiking patterns within neurons as opposed to simply the single pair of pre- and post-synaptic spikes (Froemke and Dan, 2002). The addition of more complicated, yet more realistic, spiking patterns did not refute earlier findings developed using paired pulse paradigms but instead added another layer of interaction in the spike trains. As we consider how to scale our adaptation principles developed from studies of a single dimension of the sensory space to a naturalistic scene, existing models from simpler stimulation paradigms should be used as the foundation of these neural interactions that can be expanded to identify the appropriate stimulus interactions to incorporate under more complex stimulation paradigms.

Returning to the more general modeling framework discussed here, we might ask to what extent an adaptation effect such as SSA identified along a single stimulus dimension maps to the adaptation of the full feature selectivity of a neuron. Within this

context lies a Catch-22 – the timeframe over which these adaptive changes in feature selectivity occur is fairly fast, yet the ability to capture the feature selectivity through approaches such as reverse correlation requires sufficient measurement time (and spikes) to robustly capture the dynamics. By restricting the stimulus space when using an SSA paradigm, the overall data requirement is reduced and the adaptive modulation to the tuning function can be measured. Connecting general descriptions of feature selectivity to the tuning properties associated with a reduced dimension stimulus space is therefore difficult, particularly in the context of rapid adaptation that exists on the timescale of milliseconds to seconds. Multiple layers of interaction between the sensory stimulus and the evoked neural response paired with limited sampling capabilities may seem like an intractable problem. However, there is evidence that rapid modulation of feature selectivity is present in the spectrotemporal receptive fields of A1 neurons (Fritz et al., 2003) as well as the spatiotemporal receptive fields of V1 neurons (Debanne et al., 1998; Lesica et al., 2007). Future work should be aimed at bridging the gap between tuning results from a limited stimulus space and tractable assessments of more general feature selectivity.

### 2.9.2 Perceptual implications of sensory adaptation

Despite a long history of scientific investigation, the link between neural adaptation and perceptual adaptation remains unknown. However, in a few cases, this link has become more salient due to the pairing of new experimental techniques with creative experimental design. One particularly valuable example aimed at linking cortical adaptation with behavioral perception using optogenetic techniques provided a clear relationship between the adaptation of evoked cortical responses and the perceptually-based response of the rodent (Musall et al., 2014). While there are a limited number of studies making this link, significant work has been done to bridge the gap using estimates of information from the neural spiking data to predict task performance using encoder-decoder frameworks. From an information-theoretic perspective, the differential adaptation of different populations of

neurons based on tuning, cell type, circuit dynamics, and so on presents a very interesting coding problem. In a complex sequence of encoding through a pathway, it would seem imperative to understand the degree of adaptation that occurs at each point in the chain and whether decoding of the signals ultimately requires knowledge of the adaptation (Seriès et al., 2009).

Recent evidence has linked the effects of sensory adaptation to the specific information processing tasks of detection and discrimination. The efficient coding hypothesis put forth by Barlow proposed optimization of sensory encoding, but without explicit consideration for varying task demands. The flexibility of organisms to perform a variety of behaviors, such as dynamically shifting between detection and discrimination modes, may require a more expansive view of optimization than that reflected in our classical framework. In the somatosensory pathway, spatial discrimination tasks have been well studied due to the distributed nature of the sensation. More than half a century ago, von Békésy noted that the perceived size of a tactile stimulus decreased with increasing frequency of a repetitive sensory stimulus (von Békésy, 1957). Perceptual studies in human tactile sensing further suggested that somatosensory adaptation enhanced spatial discrimination between stimuli through vibrotactile input to the fingertip (Goble and Hollins, 1994, 1993; Tannan et al., 2006; Vierck and Jones, 1970) and subsequent studies have investigated the spatial sharpening of representations in somatosensory cortex in response to repetitive, ongoing sensory inputs (Lee and Whitsel, 1992; Moore et al., 1999; Sheth et al., 1998; Simons et al., 2005; Tommerdahl et al., 2002), posited as a potential explanation for enhanced spatial acuity (Lee and Whitsel, 1992; Moore et al., 1999; Vierck and Jones, 1970). These results have been expanded to investigate the underlying neural correlates of spatial discrimination in multiple animals models of somatosensation including the monkey fingertip (Simons et al., 2005) and the rodent vibrissa pathway (Ollerenshaw et al., 2014).

More importantly, however, is the assertion that the adaptation mediates a trade-off between detectability and discriminability (Moore, 2004) that has been linked behaviorally and electrophysiologically (Ollerenshaw et al., 2014; Q. Wang et al., 2010; Zheng et al., 2015), controlling the nature of the utility of the sensory representation in a dynamically changing environment. Importantly, the adaptive switch from a detection to a discrimination mode is highly stimulus dependent. Adaptation of a particular stimulus dimension will only enhance discrimination performance when the test stimulus is similar to the adapting stimulus (Blakemore and Campbell, 1969b; Sekuler and Ganz, 1963; Tommerdahl and Hollins, 2005). In a sensory environment that is filled with rich stimuli that are continuously changing, dynamic changes to sensory encoding on fast timescales presents a mechanism to rapidly shift information processing states with respect to the current state of the world and therefore the perceptual capabilities of an organism.

## 2.10 Conclusions

As we stated at the onset, we all know what adaptation is, but in the nervous system, it is hard to define and harder still to identify what it is not. Words like evolution, development, plasticity, and adaptation may be bound together philosophically as a way organisms face a changing environment, but are implemented through wildly different mechanisms on entirely different spatial and temporal scales. Focusing on rapid sensory adaptation over timescales of milliseconds to seconds, we have laid out a wide range of biophysical mechanisms that can contribute to, and compound, effects within and across networks. While the perceptual effects of adaptation are sometimes dramatic, the neural signatures that we think are related can be subtle, and likely distributed and hard to interpret. The rapid adaptation effects described here vary as a function of cell-type, synapse-type, feature selectivity, and anatomical connectivity. Due to the complexity of neural recordings, most experimental adaptation evidence is analyzed with respect to only a single region of the brain. However, this becomes increasingly difficult to interpret when

we consider the inherited effects of adaptation as information is transmitted from one processing stage to the next as well as the highly interconnected circuitry that is constantly providing feedback between processing centers. The set of tools that are emerging in the field enable, for the first time, the ability to dissect the potential neural underpinnings of complex phenomena like adaptation. Importantly, at key stages of processing, the nervous system is exquisitely organized, and the anatomical connectivity is likely to play a major role in determining the link between the perceptual effect and the underlying neural activity that drives it.

# CHAPTER 3 ADAPTIVE THALAMIC GATING

*This chapter was originally published as an article in* Cell Reports *and is presented with only minor stylistic changes*[2].

It has been posited that the regulation of burst/tonic firing in the thalamus could function as a mechanism for controlling not only how much, but what kind of information is conveyed to downstream cortical targets. Yet how this gating mechanism is adaptively modulated on fast time scales by ongoing sensory inputs in rich sensory environments remains unknown. Using single unit recordings in the rat vibrissa thalamus (VPm), we found that the degree of bottom-up adaptation modulated thalamic burst/tonic firing as well as the synchronization of bursting across the thalamic population along a continuum for which the extremes facilitate detection or discrimination of sensory inputs. Optogenetic control of baseline membrane potential in thalamus further suggests that this regulation may result from an interplay between adaptive changes in thalamic membrane potential and synaptic drive from inputs to thalamus, setting the stage for an intricate control strategy upon which cortical computation is built.

## 3.1 Introduction

The majority of our sensations travel from the periphery through the thalamus before reaching cortex, such that each sensory region of thalamus has a corresponding cortical projection. Despite the strategic positioning of this brain structure, surprisingly little is known about its ultimate function. While it is clear that the various nuclei of the

---

[2] Whitmire CJ, Waiblinger C, Schwarz C, Stanley GB. Information Coding through Adaptive Gating of Synchronized Thalamic Bursting. Cell Reports 2016; 14:1–13. doi:10.1016/j.celrep.2015.12.068.

thalamus play a vital role in high level functions such as attention, perception, and consciousness, as evidenced by lesioning of the thalamus (Schmahmann, 2003; Van Der Werf et al., 2000), it is unclear as to what active role it plays. Due to a preponderance of T-type calcium channels in this region, thalamic neurons are particularly prone to vacillate between burst and tonic firing modes in a state-dependent manner (Suzuki and Rogawski, 1989). Although thalamic bursting was originally associated with a disconnection between the cortex and the periphery (Steriade et al., 1993), it has been posited that regulation of burst firing in the thalamus may serve as a dynamic gating mechanism for controlling information flow to cortex (Crick, 1984; Lesica et al., 2006; Lesica and Stanley, 2004; Sherman, 1996; Wang et al., 2007). It has been established that the continuous transition between burst and tonic firing is determined by both the subthreshold membrane potential of the neuron as well as the ongoing synaptic activity (Mukherjee and Kaplan, 1995; Wolfart et al., 2005). However, what is not at all understood is how the transition between burst and tonic firing modes is modulated in a dynamic sensory environment, how this is coordinated across the neuronal population, and how this thalamic state transition affects information transmission.

The rapid adaptation of functional properties in response to changes in sensory stimulation, over a range of temporal and spatial scales, is common to all sensory modalities (Wark et al., 2007). For example, a simple change in statistics of a sensory signal, such as the stimulus contrast, can lead to a cascade of changes in sensory encoding, from gain rescaling (Fairhall et al., 2001; Shapley and Victor, 1979) to fundamental alterations to the feature selectivity of sensory neurons (Lesica et al., 2007), which are even more pronounced when considering differential adaptation across neuronal populations. This has led to the proposal that this form of adaptation serves to enhance information transmission in the dynamic sensory environments (Sharpee et al., 2006). In the thalamocortical pathway, the functional role of adaptation in modulating the spike timing of sensory-evoked activity within and across thalamic neurons has a particularly strong

impact on the activation of their downstream cortical targets that rely on weak, but highly convergent inputs from the thalamus (Bruno and Sakmann, 2006). We have recently shown that adaptation serves to desynchronize the firing activity of thalamic neurons (Ollerenshaw et al., 2014; Q. Wang et al., 2010), but the interaction between adaptive mechanisms and the regulation of synchronized bursting across thalamic inputs to cortex is not at all understood, yet could serve as a robust mechanism for gating information flow as a function of bottom up and top down influences.

Here, we demonstrate a direct link between ongoing bottom-up sensory adaptation and the modulation of feature-evoked bursting in the ventral posterior medial (VPm) region of the thalamus in the vibrissa pathway of the rat. Baseline recordings were obtained under fentanyl anesthesia, corresponding to a relatively hyperpolarized thalamic state, such that adaptation transitioned the thalamus from a burst to a tonic firing mode. Using optogenetic depolarization to directly modulate thalamus, we identified a graded, sustained depolarization of thalamic neurons as the likely mechanism by which adapting stimuli modulate evoked bursting activity, working in concert with changes in synaptic drive, to gate thalamic activity. From the perspective of timing-based ideal observer analysis of thalamic spiking activity, sensory adaptation led to reduced detectability, but enhanced discriminability at an intermediate level of adaptation. Furthermore, paired recordings demonstrated a reduction in not only synchronous firing, but synchronous burst firing with more profound adaptation. Therefore, the regulation of stimulus-driven synchronized bursting may be a critical mechanism for gating peripheral inputs that form sensory cortical representations.

## 3.2 Methods

### 3.2.1 Experimental Procedures

#### 3.2.1.1 Acute Surgery

All procedures were approved by the Georgia Institute of Technology Institutional Animal Care and Use Committee and were in agreement with guidelines established by the National Institutes of Health. 19 female albino rats (Sprague-Dawley, 250-300g) were used for these experiments (n = 14 naïve animals, n = 5 optogenetically modified animals). Animals were initially anesthetized using 4-5% isoflurane and maintained at 2-3% until the tail vein was inserted. The anesthesia was then switched to a fentanyl cocktail (fentanyl (5 μg/kg), midazolam (2 mg/kg), dexmedetomidine (150 μg/kg)) continuously administered intravenously using a drug pump throughout the duration of the experiment. Anesthesia depth was monitored by heart rate, respiratory rate, and toe pinch reflex. Body temperature was maintained using a feedback controlled heating pad (FHC, Inc.). The animal was secured in a stereotaxic device (Kopf Instruments) using penetrating ear bars on a vibration isolation table in an electromagnetically shielded surgery suite. A craniotomy was performed (2-4 mm caudal to bregma, 1.5-3.5 mm lateral to the midline) to permit access to the left ventral posteromedial nucleus (VPm) of thalamus. The craniotomy was filled with saline to prevent drying of the cortex. At the termination of the experiment, the animal was euthanized with an overdose of sodium pentobarbital (euthasol, 0.5 mL at 390 mg/mL).

#### 3.2.1.2 Electrophysiology

Tungsten microelectrodes (70 μm diameter, 2MΩ impedance, FHC, Inc.) or quartz-insulated platinum/tungsten microelectrodes (95%/5%, 2MΩ impedance, Thomas Recording) were lowered into the brain (depth: 4.5-6 mm) using a hydraulic micropositioner (Kopf) to record extracellularly from VPm neurons. Multiple single unit

recordings were performed using independently controllable electrodes (Mini Matrix Drive, Thomas Recordings). Recordings were made using a 32 channel Plexon data acquisition system (Plexon, Inc.) or a 64-channel TDT data acquisition system (Tucker Davis Technologies). The topographic location of the electrode was identified through manual stimulation of the whisker pad. Upon identification of a whisker sensitive single unit, the primary whisker was threaded into the galvo motor to permit stimulation of a single whisker.

3.2.1.3 Sensory Stimulus

Mechanical whisker stimulation was delivered using a precisely controlled galvo motor (Cambridge Technologies). The galvo motor was controlled using custom software (Matlab, Mathworks) to provide millisecond precision. The mechanical stimulus applied to the whisker in the rostral-caudal direction consisted of features (5 ms rise time, amplitude of the feature (AF) = 0.25, 0.5, 1, 2, 4, 8, 16°) embedded in two conditions: without background noise and with white noise background (low pass filtered at 200 Hz due to mechanical limitations of the galvo motor, standard deviation of the noise (AN) = 0, 0.025, 0.07, 0.172, 0.343, 0.6854, 2.7432, 5.485°). The feature was designed as a Gaussian waveform (10 ms duration). To generate different velocity stimuli, the amplitude of the feature was changed while the temporal duration remained fixed. The noise was silenced at the feature locations. Each noise epoch had a catch trial with silenced noise, but no feature (negative control). Different noise amplitudes were interleaved to avoid long-term adaptation effects.

3.2.1.4 Optogenetic Injection Surgeries

All surgical procedures followed sterile protocol. Animals were initially anesthetized using 4-5% isoflurane and were maintained at 2-3%. A small craniotomy was made above VPm (3 mm lateral, 3 mm caudal to bregma). A 10 µL syringe (Neuros Syringe, Hamilton, Inc) filled with the virus (rAAV5/CamKIIa-hchR2(H134R)-mcherry-

WPRE-pA, UNC Vector Core Services) was lowered to depth of 5 mm before injecting 1 µL of virus at a rate of 0.2 µL/min (iSi system, Stoelting). The syringe was left in place for five minutes after the injection was complete to allow the virus to diffuse. After the syringe had been removed, the hole in the skull was filled with bone wax and the skin was closed using wound clips. The animal was given buprenorphine for pain management (0.03 mg/kg). Animals were monitored daily following injection surgery. Wound clips were removed at 10-13 days post-surgery. Further experimentation resumed following full recovery and full opsin expression (2-3 weeks post-surgery).

#### 3.2.1.5 Optogenetic Stimulus

Optical manipulation was administered with a controlled pulse of light from a blue LED through a custom optrode consisting of an optical fiber (200µm diameter; Thorlabs) and an electrode (Tungsten microelectrode; FHC) that was lowered into the VPm. Upon identifying a whisker sensitive cell, light sensitivity was assessed using a train of 10 Hz light pulses ($\lambda$ = 470nm). The optical & whisker stimulus consisted of a feature (AF = 1°, 8°) embedded in 750 ms square light pulses (0, 0.36, 0.6, 1.2, 1.8mW/mm2).

#### 3.2.1.6 Awake Electrophysiology

A subset of experiments was performed in the awake behaving animals by our collaborator Christian Waiblinger in the lab of Cornelius Schwarz. Data are included here as the work was collaborative, but all awake recordings were performed by Christian Waiblinger. All experimental and surgical procedures were carried out in accordance with standards of the Society of Neuroscience and the German Law for the Protection of Animals. Awake electrophysiological recordings were obtained from two female albino rats (Sprague-Dawley). The basic procedures for head-cap surgery, habituation to head-fixation, and behavioral training followed previously published methods (Schwarz et al., 2010). Electrophysiological recordings were obtained while the rats were performing a detection of change task (Waiblinger et al., 2015b).

### 3.2.2 Analytical Methods

#### 3.2.2.1 Spike Response Metrics

Data was recorded on multiple electrophysiology systems including Plexon and Tucker Davis Technologies data acquisition systems. Spike sorting was performed online using negative threshold crossing at least two standard deviations above the noise and online sorting of the recorded waveforms. The sorting results performed online were validated offline using Waveclus (Quiroga et al., 2004). Isolation of the unit was confirmed by the waveform amplitude (absolute and relative to the background noise) and the interspike-interval distributions. The whisker sensitivity was quantified by the magnitude and latency of the evoked response. The extended neural response window to the feature was defined as the thirty millisecond window immediately following the stimulus feature presentation. First spike latency was defined as the first spike fired during the neural response window on each trial. First spike latency jitter was defined as the standard deviation of the first spike latencies for each stimulus condition. The amplitude of the response to the sensory feature was defined as the maximum neural response in a ten millisecond sliding window (narrow response window) within the neural response window, normalized by the number of trials. The narrow response window (10 ms) was chosen to match the duration of the cortical integration window in the adapted state (Gabernet et al., 2005). Although it has been shown that the cortical integration window changes with the adaptation condition, we used a constant window duration of 10 ms for simplicity. We allowed the exact temporal onset of this window to vary within the extended response window (30 ms) period following stimulus presentation to account for increases in first spike latency jitter with adaptation. The amplitude of the sensory response and the first spike latency were analyzed across all noise and feature amplitude conditions as well as across cells.

3.2.2.2 Synchrony Metrics

A cross correlogram of firing between two neurons was computed for spikes fired within the neural response window (feature-evoked synchrony) and outside of the neural response window (noise-evoked synchrony). The synchrony strength was defined as the total number of spikes within a 10 ms window ($N_{cc}$) normalized by the number of spikes from each neuron ($N_1$, $N_2$) included in the analysis (Temereanca et al., 2008).

$$strength = \frac{N_{cc}}{\sqrt{\frac{N_1^2 + N_2^2}{2}}}$$

3.2.2.3 Burst Analysis

All spikes were classified as burst or tonic spikes by the classical bursting definition of two or more spikes with an interspike interval ($t_{isi}$) of less than four milliseconds with the first spike preceded by 100 milliseconds of silence ($t_{silence}$) (Reinagel et al., 1999). Burst ratio was quantified as the total number of burst spikes divided by the total number of spikes in the narrow neural response window. The presentation of a sensory feature typically evokes a large increase in the firing rate of a thalamic neuron. This increase in firing rate will increase the probability of multiple spikes occurring within the $t_{isi}$ window and therefore could increase the probability of a burst classification due only to the increase in firing activity from the neuron. To estimate the amount of bursting activity expected by chance given the increase in firing rate with stimulus feature presentation, an inhomogeneous Poisson model was generated. The firing rate of the inhomogeneous Poisson model was determined by the mean firing rate (peristimulus time histogram) from each experimental condition. The spiking activity of the model (n = 1000 simulated trials) was then classified according to the experimental bursting criteria to estimate the probability of eliciting a burst with a simple change in firing rate.

#### 3.2.2.4 Ideal Observer Analysis

The responses to sensory features ($R_F$) and noise ($R_N$) were quantified as the response within a ten millisecond sliding window. The probability distributions of the number of spikes elicited in response to sensory features (p(r|f)) and sensory noise (p(r|n)) were estimated from the observed spike counts within a ten millisecond bin. A parameterized gamma distribution was used to estimate these probability distributions. Using classical signal detection theory, receiver operator characteristic (ROC) curves were generated. ROC curves plot the false alarm rate versus the hit rate to quantify the detectability of a given stimulus distribution from the noise distribution. Detectability was defined as the area under the ROC curve (AUROC). Discriminability between two feature amplitudes ($A_F$ = 2, 16°) was quantified from the parameterized distributions by using maximum likelihood estimation (MLE) to determine the threshold such that an observer would infer which stimulus was presented by selecting the stimulus for which the likelihood $p(r|f_i)$ is maximized. The performance of an observer was quantified using a performance matrix whereby the accuracy of the observer is compared to the correct stimulus classification. In this analysis, burst trials were defined as all trials that had a burst within the narrow 10 ms window. Any stimulus conditions with less than 6 trials were excluded from the analysis due to the difficulty in estimating the probability distributions.

#### 3.2.2.5 Computational Model

An integrate and fire model with a bursting mechanism (IFB Model) was developed using previously published models in vision (Lesica et al., 2006). An additional spike history component was added to simulate the effect of ongoing stimulation (IFBS Model) (Ladenbauer et al., 2012). The model is described by the following equations:

$$C\frac{dV}{dt} = I_{stim} - I_L - I_T - I_S$$

$$I_L = g_L(V - V_L)$$

$$I_T = g_T m_\infty h(V - V_T)$$

$$\frac{dh}{dt} = \begin{cases} -h/\tau_h^-, & V > V_h \\ (1-h)/\tau_h^+, & V < V_h \end{cases}$$

$$\tau_{I_S}\frac{dI_S}{dt} = a(V - V_L) - I_S$$

$$if\ V > V_{thres}, \begin{cases} V = V_{reset} \\ I_s = I_s + b \end{cases}$$

Where the IFBS model included all model components and the IFB model did not include the $I_S$ current. Model parameters were identical to those used previously (Ladenbauer et al., 2012; Lesica and Stanley, 2004): $V_L$ = -65 mV, C = 2μF/cm$^2$, $g_L$ = 0.035 mS/cm$^2$, $V_{reset}$ = -50 mV, $V_h$ = -60 mV, $V_T$ = 120 mV, $\tau_h^-$ = 20 ms, $\tau_h^+$ = 100 ms, $g_T$ = 0.07 mS/cm$^2$, a = 0.1 mS/cm$^2$, b = 0.2 μA/cm$^2$, $\tau_{IS}$ = 100 ms. Simulated sensory stimuli ($I_{stim}$) were passed through a linear filter and point nonlinearity to become input currents to the model (Lesica and Stanley, 2004). The simulated sensory stimulus was composed of a feature (10 millisecond duration) embedded in a noisy context (low pass filtered at 200 Hz, varying amplitude). Simulated neural responses were analyzed using the same techniques described for experimental data.

## 3.3 Results

### 3.3.1 Adaptation shifts thalamus from burst to tonic firing

We recorded single unit activity in the ventral posteromedial (VPm) nucleus of the rat vibrissal lemniscal pathway in response to single whisker stimuli with or without optogenetic modulation of the thalamic membrane potential under fentanyl-cocktail anesthesia (Fig 1A). The sensory stimulus consisted of an ethologically relevant feature embedded in an ongoing adapting background stimulus (Fig 1B; Whisker Angle, see Methods). The shape of the feature was designed to mimic high velocity deflections, or stick-slip events, that match the feature selectivity of thalamic neurons in this pathway (Petersen et al., 2008; Ritt et al., 2008; Wolfe et al., 2008), while the amplitudes of the feature were chosen to span the behavioral range of feature detectability from ongoing sensory stimulation (Stüttgen et al., 2006) ($A_F$ = 0, 1, 2, 4, 8, 16°; rise time = 5 ms). The frequency content of the adapting noise stimulus spanned 0-200Hz to sample relevant whisker stimulation frequencies (Lottem and Azouz, 2008) within the physical limitations of the whisker stimulator, while the amplitude of the noise were set at levels perceptible to the animal ($A_N$ = 0, 0.07, 0.17, 0.34, 0.68, 2.75, 5.5°), as ascertained in a separate study (Waiblinger et al., 2015b). Note that we have demonstrated that this form of rapid adaptation is very similar in the presence of repetitive/periodic whisker stimulation and "white noise" stimulation, depending primarily on the overall power in the adapting stimulus (Zheng et al., 2015), and is distinctly different from forms of stimulus-specific adaptation. While sensory adaptation has many definitions/meanings within specific sensory modalities, the universal ability of the pathway to adapt to ongoing changes in the stimulus statistics has been demonstrated in auditory (Dean et al., 2005), visual (Fairhall et al., 2001), and somatosensory (Maravall et al., 2007) pathways. Here, the statistics of the adapting stimulus were systematically varied to investigate the

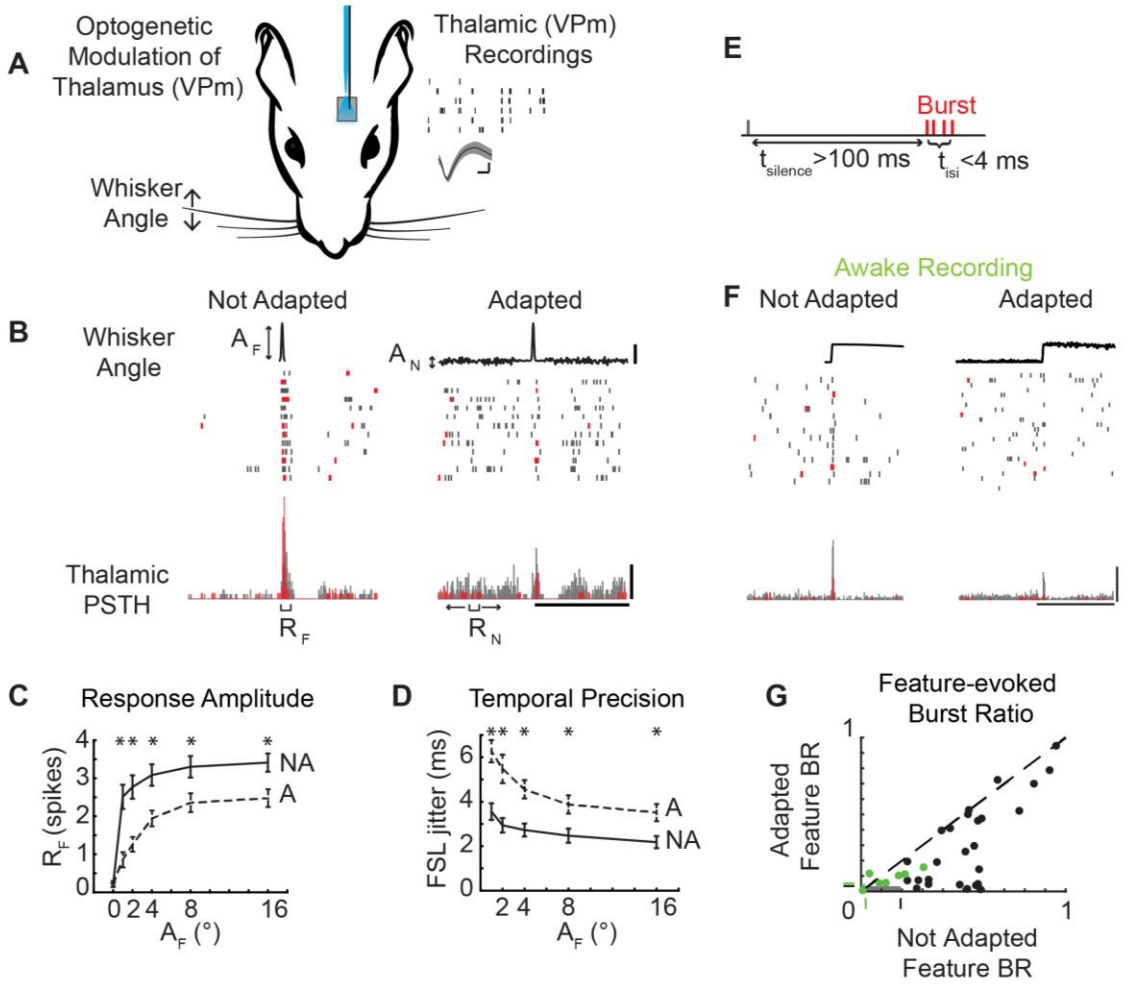


**Figure 3-1: Sensory adaptation modulates burst/tonic firing.** A. Extracellular recordings from the ventral posteromedial (VPm) nucleus of the thalamus during sensory stimulation and, in a subset of animals transfected with channelrhodopsin, light modulation applied via an optic fiber. Waveform scale bars: 200μV, 200 μs. B. Example neural response to a sensory feature ($A_F$ = 8°) presented in isolation ($A_N$ = 0°) and with adaptation ($A_N$ = 0.168°, 125°/s) with burst spikes colored red and tonic spikes colored gray. $A_F$: Amplitude of stick-slip feature (°); $A_N$: Standard deviation of adapting noise (°); $R_F$: Feature-evoked response; $R_N$: Adapting noise-evoked response. Scale bars: 4°, 250 ms, 100 Hz. C. Mean evoked response to Not Adapted features responses (black; $A_N$ = 0°) and Adapted feature responses (grey; $A_N$ :0.168°) across cells (n = 26 cells; mean ± SEM, *p<0.05, paired Wilcoxon signed-rank test with Bonferroni-Holm correction). D. First spike latency jitter in response to Adapted features (grey) and Not Adapted features (black) (n = 26 cells; mean ± SEM, *p<0.05, paired Wilcoxon signed-rank test with Bonferroni-Holm correction). E. A burst is defined as two or more spikes with an interspike interval of four milliseconds or less ($t_{isi}$) with the first spike preceded by at least 100 milliseconds

of silence ($t_{inhib}$). F. Example neuron recording from the awake behaving animal in response to sensory features with and without noise ($A_F$ = 9°, $A_N$ = 0.48°). Scale bars: 4°, 100 Hz, 250 ms. G. Feature burst ratio in Adapted and Not Adapted condition across cells (n = 33 cells (26 cells from anesthetized preparation, black; 7 cells from awake preparation, green) , p = 4.99e-6, paired Wilcoxon signed-rank test).

changes in feature selectivity in the presence of varying statistical properties of the adapting stimulus.

Thalamic neurons responded strongly when stimulus features were presented in isolation (Not Adapted condition), but the stimulus feature elicited fewer spikes when surrounded by an adapting noise stimulus (Adapted condition), even when the amplitude of the adaptive noise stimulus was relatively small compared to the amplitude of the feature (shown for an example neuron in Figure 3-1B; $A_F$ = 8°, $A_N$ = 0.32°). In this example neuron, the Not Adapted feature response was strong (as defined by the number of elicited spikes) and temporally precise (as defined by the first spike latency jitter) on nearly every trial (Figure 3-1B; Not Adapted). In contrast, the Adapted neural response for this example neuron showed greater background firing due to the evoked response from the adapting stimulation and reduced feature-evoked activity (Figure 3-1B; Adapted). Across cells, the background firing activity due to the evoked response from the adapting stimulus was increased relative to the spontaneous firing in the Not Adapted condition (p = 1.18e-5, paired Wilcoxon signed-rank test, data not shown). The response to the stimulus feature ($R_F$), defined as the number of spikes in a 10 millisecond window following feature presentation (see Methods), increased with increasing feature amplitude across cells (Figure 3-1C solid, Not Adapted; n = 26 cells), but was significantly attenuated in the Adapted condition (Figure 3-1C dashed, Adapted; n = 26 cells, *p<0.05, paired Wilcoxon signed-rank test with Bonferroni-Holm correction). The first spike latency (FSL) in response to the features in the Not Adapted condition was consistent with the latencies expected for VPm neurons ($A_F$ = 16°, FSL = 5.7 ± 0.7 ms, n = 26 cells). As expected for

sensory adaptation, the FSL increased in the Adapted condition ($A_F$ = 16°, FSL = 8.2 ± 0.8 ms, n = 26 cells, p = 3.67e-5, paired Wilcoxon signed-rank test). Note that the degree of adaptation observed in these thalamic neurons was consistent with that observed for more simple, periodic whisker stimulation (Temereanca et al., 2008; Q. Wang et al., 2010), and that the amplitude of the increased latency with adaptation was consistent with VPm neurons as opposed to neurons located in the nearby posteromedial (POm) complex of the thalamus (Ahissar et al., 2000). The first spike latency jitter, a metric of temporal precision, was also higher in the Adapted condition than in the Not Adapted condition (Figure 3-1D, n = 26 cells, *p<0.05, paired Wilcoxon signed-rank test with Bonferroni-Holm correction).

Shifts in thalamic state are known to induce shifts in firing modes, specifically in the context of burst and tonic firing (Sherman, 2001a). What is not well understood is how adaptation changes thalamic state, and in turn modulates tonic and burst firing. To isolate bursts likely originating from T-type calcium channels, burst spikes were defined as two or more spikes with an inter-spike interval ($t_{isi}$) of less than four milliseconds with the first spike in the burst preceded by silence ($t_{silence}$) of 100 milliseconds or more (Figure 3-1E), consistent with classical definitions (Lesica et al., 2006; Lu et al., 1992; Reinagel et al., 1999). Burst and tonic spikes are color-coded for a typical thalamic neuron in Figure 3-1B (red & grey, respectively). In addition to the reduction in the feature-evoked spiking activity, this example neuron displays a disproportionate loss of burst spikes in the Adapted condition (Figure 3-1B). Consistent with this example neuron, the presence of the adapting noise stimulus led to a decrease in the total number of feature-evoked spikes across cells (Figure 3-1C, n = 26 cells), but an even larger reduction in the number of burst spikes in response to the feature as captured by the burst ratio (BR), defined as the number of burst spikes in the feature response window divided by the total number of spikes in the feature response window (Figure 3-1G; n = 26 cells, p = 2.63e-5, Wilcoxon signed-rank test).

Furthermore, a limited number of single unit recordings were performed in the awake behaving, head-fixed rat in a similar adaptation paradigm (n = 7 cells, 2 rats).

Although the embedded feature was different in detail from that used in the anesthetized recordings, the rise time and feature amplitude were matched to those described above (rise time = 5ms, $A_F$ = 9°, $A_N$ = 0.48°). In an example cell recorded in the awake animal, there was a higher spontaneous firing rate than in the anesthetized animal, but spontaneous bursting prior to feature presentation was present (Figure 3-1F, Not Adapted). In the Adapted condition, this neuron showed a reduction in number of feature-evoked spikes as well as a reduction in the feature-evoked bursting (Figure 3-1F, Adapted). Consistent with the anesthetized findings, sensory adaptation in the awake rat led to a reduction in the overall number feature-evoked spikes (data not shown). Comparing the bursting in the Not Adapted and Adapted conditions in single unit neurons recorded in the awake animal also revealed the same basic trend of a reduction in bursting with adaptation as seen in the larger dataset of the anesthetized animal (Figure 3-1G, green; n = 7 cells). However, the absolute level of bursting in the awake animal was reduced relative to the anesthetized animal. Importantly, the level of bursting seen in both the anesthetized and the awake animal was significantly greater than that expected by chance from a Poisson model neuron with an inhomogeneous firing rate that matches the evoked peristimulus time histogram measured experimentally (Figure 3-1G, green and black shaded regions with boundaries shown as tick marks on axes; see Methods).

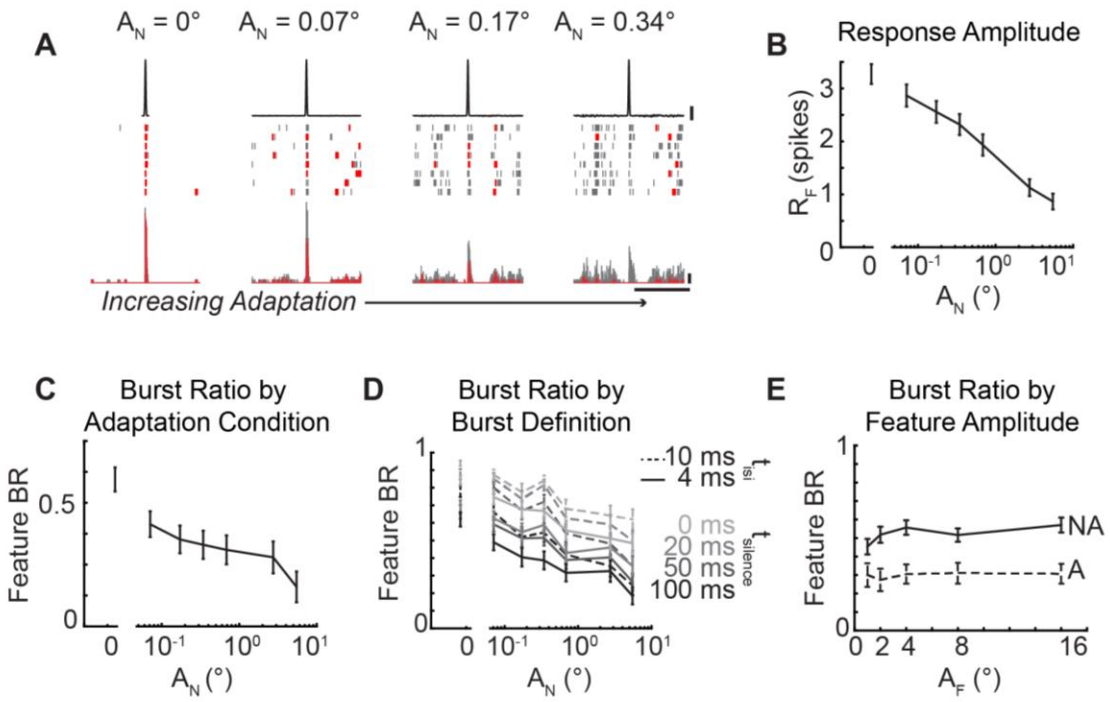


**Figure 3-2: Thalamic bursting is continuously modulated by sensory adaptation.** A. Example neural response to increasing adapting noise amplitudes ($A_F$ = 16°, $A_N$ = 0, 0.17, 0.34, 0.7°). Scale bars: 4°, 100 Hz, 250 ms. B. Feature-evoked response across adaptation conditions ($A_F$ = 16°, n = 44 cells; mean ± SEM). C. Feature burst ratio across adaptation conditions ($A_F$ = 16°, n = 44 cells; mean ± SEM). D. Feature burst ratio across adaptation conditions defined using alternate burst definitions ($t_{inhib}$: 0, 20, 50, 100 ms; $t_{isi}$: 4, 10 ms; n = 44 cells; mean ± SEM). E. Feature burst ratio in single adaptation condition across feature amplitudes (n = 26; mean ± SEM).

### 3.3.2 Adaptation modulates burst/tonic firing on a continuum

While the dichotomy of burst/tonic firing in neural coding has often been described as a switch between thalamic states (Steriade et al., 1993), it has been shown that the thalamus actually operates in a graded fashion (Mukherjee and Kaplan, 1995). However, how this transition between the burst and tonic firing modes is influenced by external stimulation has not been explored. To systematically investigate the role of the adapting noise stimulus on the feature-evoked bursting activity, we systematically varied the

amplitude of the adapting noise (Figure 3-2A, example neuron). In the Not Adapted condition, the feature elicited burst firing from this neuron (Figure 3-2A, $A_F$ = 16°, $A_N$ = 0°). As the amplitude of the adapting noise stimulus increased, the amplitude of the feature-evoked response and the amount of burst firing decreased for this example neuron (Figure 3-2A, $A_N$ = 0.07, 0.17, 0.34°). Across cells, the response to the feature ($R_F$) decreased monotonically with increasing adapting noise stimulus amplitudes, consistent with increasing noise amplitudes leading to increasing degrees of adaptation (Figure 3-2B; $A_F$ = 16°, n = 44 cells). However, the continuous decrease in the burst ratio with increasing adaptation intensity across cells (Figure 3-2C; n = 44 cells) quantified the reduced number of burst spikes in the feature-evoked relative to the overall reduction in the total number of evoked spikes. This continuum confirms that the thalamus can indeed operate in a graded fashion between burst and tonic firing, rather than in two discrete states of burst or tonic firing, and that this continuum can be modulated through sensory adaptation.

With increasing levels of adaptation, thalamic neurons were driven more strongly prior to feature presentation (example cell, Figure 3-2A). It is possible that the increase in firing rate due to ongoing stimulation during adaptation simply induced spiking activity in the 100 ms period of silence prior to the first spike of a burst ($t_{silence}$, Figure 3-1E) and therefore precluded classification as a burst in this context. To investigate whether the trend of reduced bursting with increasing adapting noise amplitude was simply due to increased noise-driven spiking, we systematically varied the definition of a burst to reduce the duration of silence prior to the first spike ($t_{silence}$ = 0, 20, 50, 100 ms) used to classify a series of spikes with short interspike intervals ($t_{isi}$ = 4 ms) as a burst. While reducing the duration of $t_{silence}$ led to a larger number of spikes being classified as burst spikes (and therefore quantitatively larger mean burst ratios across 44 cells), there were continuous reductions in the burst ratio regardless of the burst definition (Figure 3-2D; solid lines, n = 44 cells). We further altered our burst definition to allow the interspike interval for spikes within a burst to occur within 10 ms ($t_{isi}$ = 10 ms, $t_{silence}$ = 0, 20, 50, 100 ms) and again

found that the burst ratio decreased with increasing noise amplitude (Figure 3-2D; dashed lines, n = 44 cells). This control analysis demonstrates that the modulation of burst ratio was not dependent on the specific burst definition. However, the underlying mechanisms of the channel suggest that a prolonged period of hyperpolarization is critical to the function of burst spikes because it primes T-type calcium channels to open and allows depressing synapses to recover from previous spiking activity (Sherman, 2001a).

It is also possible that the amount of elicited bursting could actually be a function of the sensory feature used to probe the pathway rather than the state of the thalamus. By holding the statistics of the adapting noise stimulus constant and varying the feature, we found that the burst ratio was approximately constant across feature amplitudes. Importantly, this suggests that the bursting activity is a function of the ongoing sensory stimulation rather than the feature itself (Figure 3-2E; n = 26 cells).

### 3.3.3 Depolarization as an adaptive mechanism to modulate bursting

When a thalamic neuron is in a hyperpolarized state, an incoming depolarizing signal will activate the T-type calcium channels to allow an influx of calcium, which transiently depolarizes the neuron and permits burst firing (Perez-Reyes, 2003). By contrast, a net depolarization of the baseline membrane potential of the thalamic neuron inactivates the T-type calcium channel such that an incoming excitatory signal will not elicit the Ca-based wave of depolarization. Although the thalamic membrane potential is constantly fluctuating on a millisecond by millisecond timeframe as incoming signals transiently excite or inhibit a cell, it is the slower fluctuations of the cell membrane on the order of tens or hundreds of milliseconds that transitions the cell between different operating regimes. Thus, the reduction in feature-evoked burst firing with adaptation observed here suggests that the adapting stimulus may be inducing a sustained depolarization of the thalamic neurons and that this depolarization is sufficient to inactivate the T-type calcium channels.

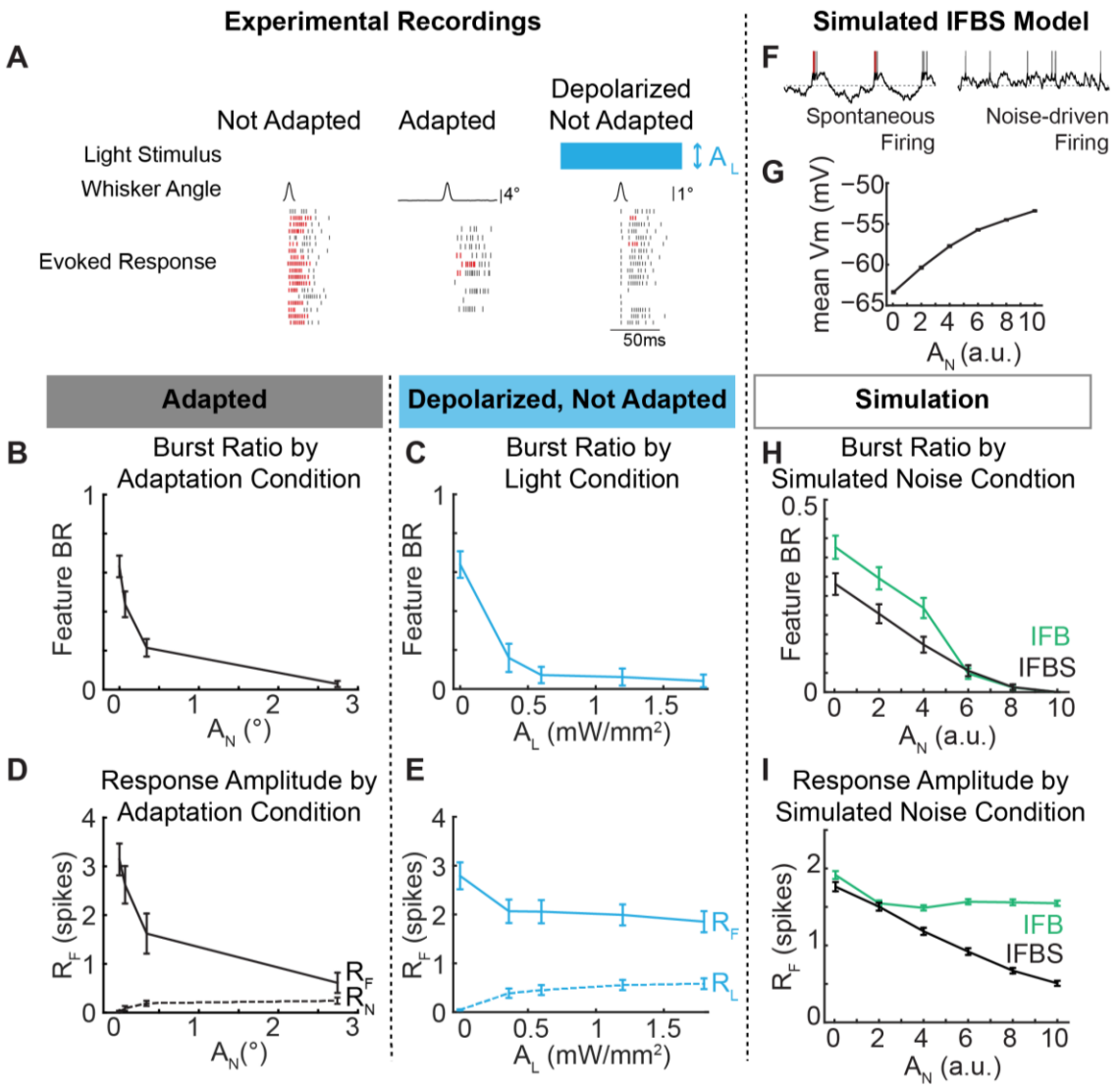


**Figure 3-3: Direct depolarization of thalamic neurons shifts the burst ratio, but not the feature encoding.** A. Example neuron response to the Not Adapted feature, the Not Adapted feature with modulating depolarization, and the Adapted feature. B-E. Comparison of the feature burst ratio (B-C) and evoked feature response (D-E) to Adapted sensory features ($A_F$ = 8°) presented in sensory noise (black; n = 12) and Not Adapted sensory features (2°) presented while directly depolarizing thalamic neurons using ChR2 (blue; n = 12). Responses to the noise ($R_N$) and light stimulation ($R_L$) prior to feature presentation are shown as dotted lines in D,E. Error bars are standard error. F. Example simulated membrane potentials from an IFBS model with and without simulated sensory input. E. Mean simulated membrane potential across simulated noise amplitudes in an IFBS model (n = 250 trials). E, F. Comparison of the burst ratio (H) and feature response

(I) to simulated sensory features presented in sensory noise with an IFBS model (black; n = 250 trials) and an IFB model (green; n = 250 trials). Error bars are standard error.

To test this more directly, we transfected VPm neurons with a depolarizing opsin (ChR2(H134R)) and directly manipulated the baseline membrane potential using continuous blue light stimulation administered through an optic fiber lowered directly into VPm ($\lambda$=470nm, 0.5 mW/mm$^2$). We recorded sensory feature-evoked activity in three conditions: in the absence of any adapting stimulus or optogenetic manipulation (Not Adapted), in the presence of an adapting stimulus but absence of optogenetic manipulation (Adapted), and in the presence of an optogenetic depolarization but absence of adapting stimulus (Depolarized Not Adapted). Note that the ChR2 is being utilized as a modulating input, as compared to a driving input. As with the onset of the adapting noise stimulus, the onset of the optical stimulus would strongly drive neural activity initially, but the firing rate reached steady state within approximately 500 ms, after which we performed our measures.

In an example cell, both artificial depolarization and sensory adaptation reduced the bursting in response to the feature (Figure 3-3A; Depolarized Not Adapted, Adapted; red: burst, grey: tonic) compared to the evoked response the absence of the depolarizing optical input or the sensory adaption (Figure 3-3A; Not Adapted). Across cells, direct control of the baseline membrane potential of the thalamic neurons was sufficient to shift the feature-evoked thalamic firing along the burst/tonic continuum (Figure 3-3C; n = 12 cells) in a very similar manner to the burst/tonic transition for a range of adaptation levels (Figure 3-3B; n = 12 cells). Although the firing rate prior to feature presentation ($R_{N,L}$) remained low across the adaptation and light conditions (Figure 3-3D, E, dashed lines, n = 12 cells), we performed an additional control analysis to confirm the reduction of bursting activity with increasing light and adaptation conditions regardless of firing activity prior to feature presentation.

Although the shift in bursting activity aligned well between the adaptation and light conditions, the evoked response to the feature did not. Consistent with the sensory adaption results in Figure 3-2B, increasing the amplitude of the adapting sensory noise stimulus led to a dramatic reduction in the feature-evoked neural response (Figure 3-3D). In contrast, increasing the depolarizing light input did not significantly reduce the feature-evoked thalamic responses (Figure 3-3E). This suggests that a net depolarization is sufficient to explain the decrease in bursting, but that there may be a secondary mechanism by which the adapting sensory stimulus reduced the amplitude of the feature-evoked response. Specifically, the optogenetic depolarization of the thalamic neurons will not directly impact activity at the presynaptic terminals. Given the potential for depression of the trigemino-thalamic synapse (Deschênes et al., 2003), we hypothesize that the reduction in the evoked neural response seen for adaptation, but not optogenetic modulation, could be due to reduced sensory drive/synaptic input.

To further probe these mechanistic issues, a biophysically inspired integrate-and-fire model was constructed (see Methods). The IFBS model was an integrate-and-fire (IF) model neuron with an incorporated bursting mechanism (B) to represent a T-type calcium channel current (Lesica et al., 2006) and a subthreshold and spike dependent history component (S) to represent activity dependent effects (Ladenbauer et al., 2012). The simulated spiking activity of the IFBS model without simulated sensory drive consisted primarily of burst spikes, whereas the inclusion of the simulated noise stimulus induced more depolarized conditions and tonic firing (Figure 3-3F). Increasing amplitudes of adapting sensory noise led to monotonically increasing levels of depolarization of the subthreshold membrane potential in the IFBS model (Figure 3-3G). Consistent with the experimental adaptation data (Figure 3-2C), the IFBS model showed a continuous decrease in feature-evoked burst ratio and the evoked feature response with increasing adapting noise amplitude (Figure 3-3H, 3I; black).

However, the development of the IFB model through the removal of the subthreshold and spike dependent history component (S) more closely mimicked the experimental optogenetics results. Similar to the IFBS model, the IFB model experienced increasing levels of depolarization with increasing noise amplitudes (data not shown) and was able to recreate a continuous modulation of bursting activity with increasing simulated noise amplitudes (Figure 3-3H; green). In contrast to the adaptation data and in agreement with the optogenetic data, the IFB model actually maintained the evoked feature response due to the lack of any spiking history dependence (Figure 3-3I, green).

Taken together, these experimental and simulated results suggest that sensory noise adaptation may be affecting bursting activity by depolarizing the thalamic neurons and inactivating the T-type calcium channels. However, the inability of depolarization through optogenetic modulation and the IFB model to mimic the reduction in the evoked feature response seen with increasing noise amplitudes suggests that depolarization of the cell membrane alone is insufficient to fully explain the mechanism underlying sensory adaptation. Given the qualitative alignment of the burst ratio and feature-evoked response of the IFBS simulations and the experimental sensory adaptation data, we suggest that one combination of mechanisms by which sensory adaptation could be acting is through thalamic membrane depolarization to modulate bursting paired with reduced efficacy of the sensory drive due to activity-dependent synaptic effects to modulate evoked feature responses.

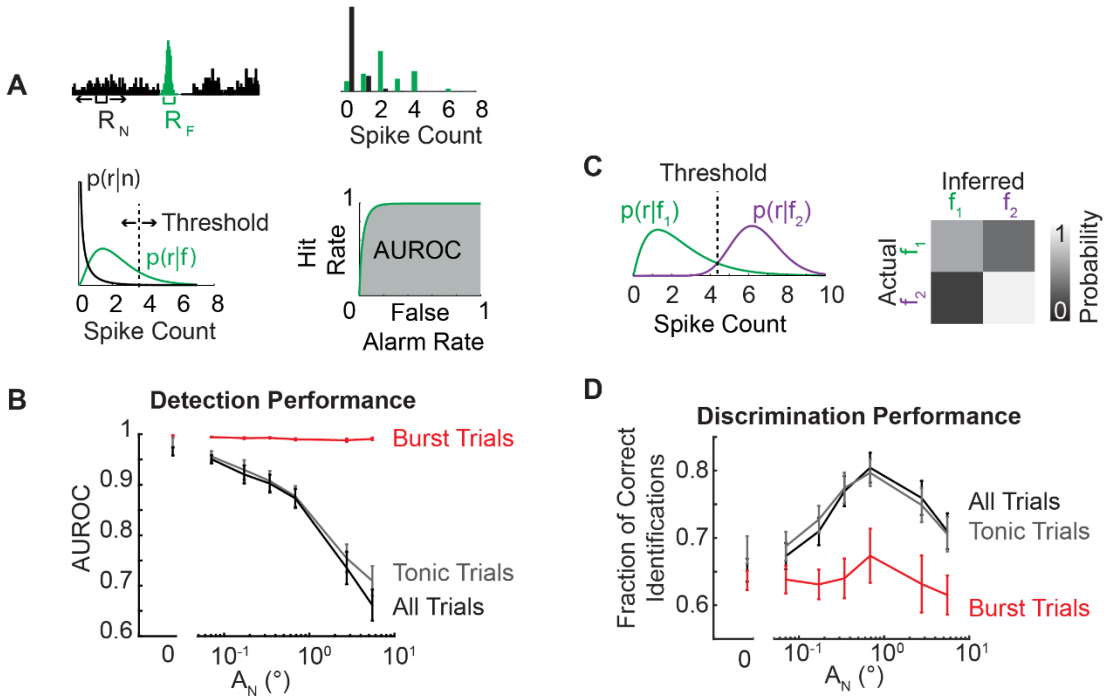


**Figure** 3-4**: Adaptation shifts encoding from detection to discrimination mode.** A. Schematic depicting the quantification of the evoked response to the noise ($R_N$) and the feature ($R_F$) and the estimation of a probability distribution that can be parameterized. Detectability was quantified as the area under the receiver operator characteristic's curve (AUROC). B. Detectability (AUROC) across adaptation conditions for all trials, burst trials, and tonic trials (black, red, and grey lines respectively; n = 44 cells, $A_F$ = 16°; mean ± SEM). C. Schematic depicting the probability distributions for two different features ($A_F$ = 2, 16°) and the threshold set using a maximum likelihood estimator. The performance matrix estimated the fraction of correct identifications. D. The discriminability (fraction of correct identifications) across adaptation conditions for all trials, burst trials, and tonic trials (black, red, and grey lines respectively; n = 44 cells, $A_F$ = 16°; mean ± SEM).

### 3.3.4 Functional consequences of shifts in burst/tonic firing

Thalamic firing modes have profound implications for the transmission of information from the thalamus to cortex. Burst spikes have shown enhanced, but highly nonlinear probability of eliciting a spike in a monosynaptically connected downstream cortical neuron (Swadlow and Gusev, 2001), whereas tonic spikes are believed to maintain a more linear relationship between stimulus intensity and elicited response (Sherman,

2001a). As such, adaptive gating of thalamic firing modes represents a potentially profound mechanism of modulating information transmission.

Using an ideal observer of thalamic spiking activity, we quantified the effect of increasing adapting noise levels on the detectability of a single feature or the discriminability between two features from the thalamic spiking. Thalamic responses were quantified as the number of spikes elicited in response to the feature ($R_F$) and to the adapting noise ($R_N$) in a 10 ms window (Figure **3-4**A; top left). Spike count probability distributions were estimated from the observed thalamic spike counts (Figure **3-4**A; top right). Using parameterized distributions (Figure **3-4**A; bottom left, see Methods), a sliding threshold was used to compute a Receiver Operator Characteristics (ROC) curve (Figure **3-4**A; bottom right). The ROC curve represents the probability of a false alarm versus the probability of a correct detection (hit). The area under the ROC curve (AUROC) was used as a metric of detectability where an AUROC value of 1 corresponds to a perfect detector and an AUROC value of 0.5 corresponds to complete overlap of the feature and noise distributions (p(r|f) and p(r|n), respectively). With increasing adaptation, the detectability of the feature monotonically decreased for all trials (Figure **3-4**B; black). However, when the trials were parsed such that 'burst trials' corresponded to trials where the response to the feature resulted in burst firing and 'tonic trials' corresponded to trials where the response to the feature resulted in tonic firing, it was evident that burst trials remained highly detectable regardless of the adaptation condition (Figure **3-4**B; red). However, the high detectability of burst trials had a limited effect on the overall detectability (Figure **3-4**B; black) due to the reduction in the absolute number of burst trials with increasing noise amplitudes Figure 3-2C).

Furthermore, the ability of an ideal observer to discriminate between two different stimulus features ($A_F$ = 2, 16°) was quantified. As described above, the response distribution for each feature amplitude was estimated from the spiking activity of the thalamic neuron (Figure **3-4**C; left). A response threshold was identified using a maximum

likelihood framework such that an observer would infer which stimulus was presented by selecting the stimulus for which the likelihood $p(r|f_i)$ is maximized. Discrimination performance was quantified using a performance matrix whereby the accuracy of the observer is compared to the correct stimulus classification (Figure **3-4**C; right). Given that the ideal observer was discriminating between two feature amplitudes, operating at chance corresponds to a correct identification probability of 0.5. The discriminability was maximized across all trials at an intermediate level of adaptation (Figure **3-4**D; black). However, the discrimination performance for only burst trials (Figure **3-4**D; red) remained lower than the discrimination performance across all trials or only tonic trials (Figure **3-4**D; black and grey, respectively) consistent with the view that bursting is better for strong activation than for descriptive signaling (Sherman, 2001a).

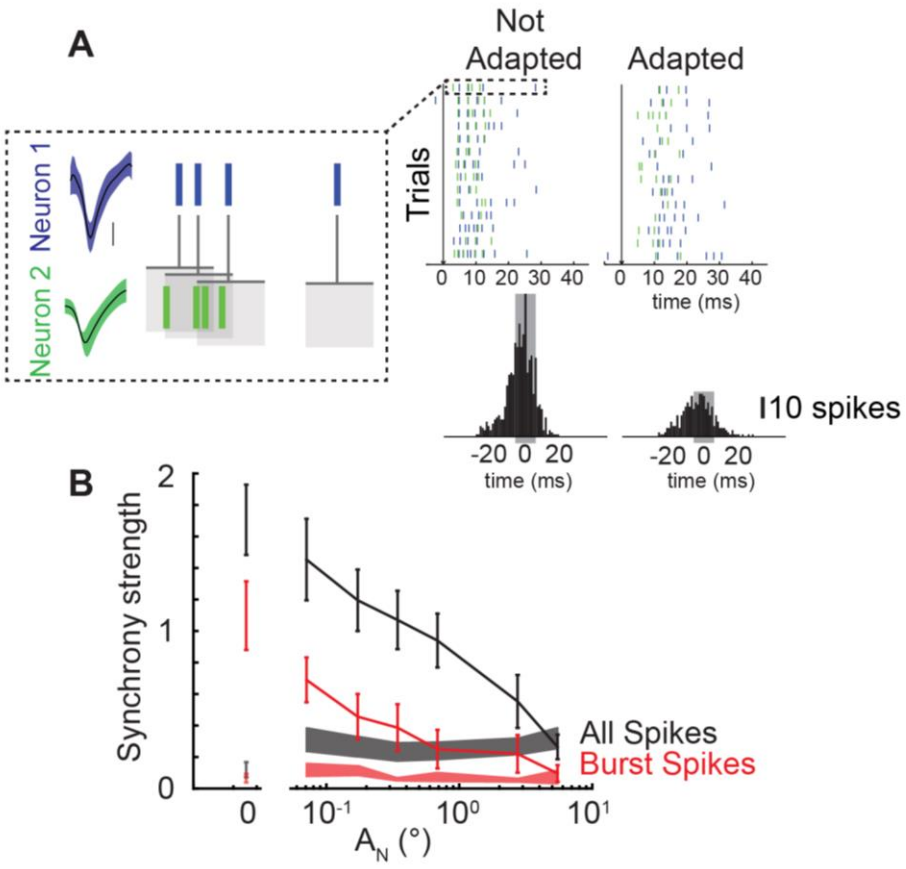

**Figure 3-5: Adapting sensory noise modulates synchrony of thalamic bursting.** A. Example neuron pair response to feature (t = 0 ms, black arrow) presented in an Adapted and Not Adapted condition ($A_N$ = [0,0.3433]°, $A_F$ = 16° ). Scale bar: 100 µV. One example trial is shown in the dotted box whereby the spike times from Neuron 2 were rearranged relative to Neuron 1 to build the cross correlogram shown beneath the two noise stimulus conditions. Synchrony strength was defined as the number of spikes within a 10 ms window of the cross-correlogram (gray shading) normalized by the number of spikes from each neuron. B. Synchrony of all feature-evoked spikes (black) and feature-evoked burst spikes (red) across adapting stimulus amplitude (n = 12 pairs; mean ± SEM). The synchrony of noise-evoked spikes across cells is shown as shaded bars (black: all noise-evoked spikes, red: all burst-evoked spikes; mean ± SEM). Spontaneous synchrony is shown as a shaded bar at $A_N$ = 0.

### 3.3.5 Thalamic synchrony and bursting

Cortical neurons are particularly sensitive to the timing of spiking inputs within and across cells due to weak thalamocortical synapses paired with the narrow cortical integration window, mediated by the disynaptic feedforward inhibition (Gabernet et al., 2005). Synchronous firing across thalamic neurons has been identified as a mechanism to overcome the weak synaptic strength of thalamocortical connections to send strong suprathreshold inputs to cortex (Bruno and Sakmann, 2006). To assess the effects of increasing degrees of adaptation on population synchronization and bursting, we used a multi-electrode drive to simultaneously record from pairs of thalamic neurons with two electrodes residing within the same barreloid. Electrodes were independently controlled and latencies in response to single whisker stimuli were tested to ensure proper localization ($A_F$ = 16°, FSL = 6.6 ± 0.6 ms, $R_F$ = 3.37 ± 0.2 spikes, n = 12 pairs of neurons; all data from synchronously recorded neurons (n = 24) are also included in single unit responses presented in Figure 3-2 & Figure **3-4**). In an example pair of neurons, a feature presented without adaptation elicits a large number of spikes with a short latency as was observed for individual neuron recordings (Figure 5A; Not Adapted condition). To assess synchronous firing between these two neurons, we used correlation analysis to quantify the spiking

activity of Neuron 2 relatively to Neuron 1 (Figure 5A; dotted box). The cross-correlogram in the Not Adapted condition revealed a higher level of synchrony, or more synchronous spikes within a ±5 ms window, than the cross-correlogram in the Adapted condition (Figure 3-5A; grey shaded region of cross correlogram). Increasing levels of adaptation also led to a reduction in the number of spikes that were elicited in response to a sensory feature. To account for the reduction in overall spike count, the synchrony strength, quantified as the number of near-synchronous spikes within a ±5 ms window, was normalized by the number of spikes from each of the neurons (see Methods), thus providing a normalized measure of the number of near synchronous spikes evoked by the stimulus.

Increasing levels of adapting noise amplitude (and thus degrees of adaptation) led to a continuous decrease in the synchrony strength between pairs of simultaneously recorded thalamic neurons (Figure 3-5B; black, n = 12 pairs). When only the synchrony of burst firing was considered, there was a similar reduction in feature-evoked burst spike synchrony with increasing noise amplitudes (Figure 3-5B; red line, n = 12 pairs), suggesting that adaptation modulates both burst firing within a single neuron and synchronous burst firing across pairs of neurons. Furthermore, the spontaneous synchrony for both total spiking activity and burst spiking alone in the absence of sensory stimulation was low relative to feature evoked synchrony (Figure 3-5B; shaded lines at $A_N$=0). The lack of spontaneous synchronous firing and synchronous burst firing further underscores the importance of sensory drive in synchronizing bursting activity in the thalamus. The synchrony in response to the noise stimulus was also relatively low and invariant to the amplitude of the noise (Figure 3-5B; shaded lines) demonstrating that thalamic neurons are not always synchronized.

## 3.4 Discussion

Although thalamic bursting was originally identified in sleeping animals as a proposed mechanism to decouple thalamocortical activity from the peripheral world (Steriade et al., 1993), recent evidence suggests that thalamic bursting plays a fundamental role in sensory processing and is evoked by naturally induced firing patterns (Wang et al., 2007). Significant work in the visual pathway has explored the role of thalamic bursting in information transmission where it has been hypothesized that thalamic state, as quantified by the intrinsic membrane potential of the thalamic neurons, is responsible for switching the encoding, or "gating", mechanism of the thalamus from a burst to a tonic firing mode (Sherman, 1996). However, in natural sensing conditions, organisms are faced with a continuous stream of sensory stimuli with relevant information embedded intermittently rather than a simple presence or absence of relevant sensory information. Here, we have shown that the state of the thalamus is continuously modulated by ongoing sensory activity allowing graded transitions between synchronous bursting and asynchronous tonic firing regimes. Although present at lower rates than observed in the anesthetized state, previous studies from both the visual (Bezdudnaya et al., 2006; Guido and Weyand, 1995) and somatosensory (Swadlow and Gusev, 2001) pathways have demonstrated the presence of thalamic bursting in awake, attentive states, suggesting a potential role for burst modulation in sensory perception. However, further studies are needed to further elucidate this in the context of behavior.

Although the precise role of sensory adaptation is still debated, it is largely accepted that adaptation serves a beneficial purpose as opposed to just fatigue (Wark et al., 2007). Adaptive gain control has been proposed as one mechanism to promote efficient coding by adjusting the operating range for inputs based on recent stimulus history (Fairhall et al., 2001; Maravall et al., 2007). Our results suggest that sensory adaptation goes beyond a change in operating points for the neurons by providing a relevant mechanism for fundamentally shifting sensory-evoked bursting activity along a continuum of values based

entirely on the subthreshold activity of the thalamic neurons, resulting in dramatic changes in feature selectivity. Simple gain scaling will be further amplified by the nonlinear response properties of thalamic neurons as they transition between varying states of the burst/tonic continuum.

The ideal observer analysis of thalamic spiking activity demonstrates the functional effect of adaptation on detectability loss but discriminability gain, consistent with prior electrophysiological and behavioral studies (Ollerenshaw et al., 2014; Q. Wang et al., 2010; Zheng et al., 2015). When parsing the trials by the presence or absence of a feature-evoked burst, the detectability of burst responses remained high regardless of adaptation condition, as suggested by the view of burst spikes as sending a strong signal to cortex (Guido et al., 1995). However the transmission of a thalamic spike downstream is entirely dependent on the thalamocortical synapse. The long period of hyperpolarization, required to de-inactivate the T-type calcium channels and prepare them to open, plays an additional role in information transmission by permitting the depressing thalamocortical synapse to recover from previous spiking activity (Swadlow and Gusev, 2001). Furthermore, the high frequency burst of spiking becomes a strong driving input to a cortical neuron that will integrate thalamic spiking activity within a short window, known as the cortical window of integration (Q. Wang et al., 2010). While the size of this window is dependent on prior thalamic activity and is relatively short for Not Adapted probes, the cortical integration window in barrel cortex extends to approximately 10 ms in duration after repetitive stimulation (Gabernet et al., 2005). The importance of not only burst firing within a single neuron, but synchronous burst firing across neurons, is further underscored by the fact that cortical neurons are integrating spiking information from many thalamic neurons simultaneously within this cortical window of integration (Bruno and Sakmann, 2006).

Importantly, we have shown that synchronous firing across neurons is stimulus driven. In the absence of sensory stimulation, high levels of synchronous firing have been associated with the anesthetized or sleeping state (Steriade et al., 1993). However, our

results show that neither burst nor tonic spiking was spontaneously synchronous across neurons in the fentanyl-anesthetized rat, consistent with findings from the awake rabbit (Swadlow and Gusev, 2001). Instead, we found that synchronous bursting was only elicited by strong sensory stimulation, suggesting that this pattern of activity is reserved for sensory-driven responses.

While it is likely that several biophysical mechanisms underlie the adaptation effects seen extracellularly, we specifically investigated net depolarization effects as a mechanism to modulate bursting activity. Although the thalamus receives strong driver inputs from the peripheral whisker sensors via the brainstem, the majority of the synapses on thalamic neurons originate in cortex (Varela, 2014). In addition, recent evidence has shown that direct corticothalamic feedback onto VPm neurons can lead to a sustained depolarization of the baseline membrane potential (Crandall et al., 2015b; McCormick and von Krosigk, 1992; Mease et al., 2014). As such, depolarization via corticothalamic feedback is a strong candidate mechanism for cortical control of thalamic state. However, the net depolarization induced by optogenetic currents alone was insufficient to explain the reduction in the evoked sensory feature response. We hypothesize that adaptation is acting through multiple mechanisms, including subthalamic changes, to modulate the thalamic encoding. The reduced sensory drive/synaptic input could be due to adaptation effects in subthalamic processing such as depression of the trigemino-thalamic synapse (Deschênes et al., 2003). While our modeling results suggest that a net depolarization and reduced neural drive presents one possible explanation for our findings, there are likely multiple other mechanisms by which adaptation is modulating thalamic encoding. In particular, the adapting stimulus presented a noisy context surrounding the embedded feature that likely evokes significant changes in synaptic background activity. Evidence from in vitro recordings suggests that the synaptic noise, also potentially mediated by corticothalamic feedback, will significantly change the level of bursting in thalamic neurons (Wolfart et al., 2005). In the awake behaving animal, there will also be significant alterations to

thalamic encoding due to neuromodulatory inputs as well as behavioral state fluctuations (Castro-alamancos and Gulati, 2014; Niell and Stryker, 2010) which further highlights the abundance of neural mechanisms to alter thalamic state.

In the visual pathway, sensory-evoked bursting activity in the thalamus has been proposed to be well suited for detecting change in the visual scene (Lesica et al., 2006; Lesica and Stanley, 2004; Wang et al., 2007). Paired with results from the somatosensory pathway presented here, the effect of burst/tonic firing on information encoding appears consistent between the sensory modalities such that bursts are highly detectable while tonic firing maintains a more linear input-output function. Furthermore, sensory encoding in both the visual and somatosensory pathways is extremely precise (Butts et al., 2007; Petersen et al., 2008) suggesting an important role for temporal coding in both pathways. However, the temporal dynamics of feature selectivity of thalamic neurons in the somatosensory pathway are significantly faster than those in the visual pathway (full width of half maximum of the temporal receptive field of approximately 3.5 ms vs 20 ms, respectively) (Lesica et al., 2007; Petersen et al., 2008) and somatosensory detection tasks support near instantaneous encoding rather than sensory integration (Waiblinger et al., 2015a, 2015b) suggesting that bursting in the somatosensory pathway may be critical for rapid touch encoding. There are also some differences in the anatomical connectivity of these two sensory pathways. Within thalamus, both visual and somatosensory thalamic relay nuclei receive inhibitory input from the reticular nucleus, but the visual thalamus also incorporates inhibitory input from interneurons. The reticular thalamus provides a strong level of inhibitory tone (Halassa et al., 2014; Pinault, 2004) while interneurons within visual thalamus are hypothesized to play a role in shaping feature selectivity in the pathway (Butts et al., 2011). The absence or presence of inhibitory interneurons could play an important role in determining both the temporal dynamics of the feature selectivity and the burst response properties of the excitatory thalamocortical neurons in these sensory pathways (Alitto et al., 2005; Denning and Reinagel, 2005; Lesica and Stanley, 2004).

Beyond the primary sensory pathway, the processing of somatosensory information is also influenced by motor signals during active touch (Hentschke et al., 2006). While all stimuli in this study were presented passively, previous studies with passive whisker stimulation embedded in active whisking conditions have shown a dependency of the evoked cortical response on the whisking state of the animal (Crochet and Petersen, 2006; Fanselow and Nicolelis, 1999). Furthermore, exploratory whisker behavior can involve complex spatiotemporal patterns at the whisker pad due to multiple whiskers repeatedly contacting an object (Sachdev et al., 2001). The passive single whisker stimulation paradigm used here, which did not incorporate motor control or complex spatiotemporal whisker patterns, provided a simplified paradigm to systematically characterize the relationship between sensory adaptation and thalamic state. However we would hypothesize that additional sensorimotor cortical and sub-cortical circuits, as well as the complex dynamics of the sensory stimulation, play a fundamental role in shaping the processing of somatosensory information at multiple levels of the pathway. While the potential role of motor feedback on processing in the somatosensory cortex has been identified (Ferezou et al., 2007; Zagha et al., 2013), the implications for subcortical processing remain unknown.

Ultimately our results link ongoing sensory stimulation with continuous modulations in thalamic state, as evidenced by the synchronous bursting activity. Adaptive alterations to the firing patterns in thalamus have profound implications for thalamic feature selectivity (Lesica et al., 2006), thalamocortical efficacy (Swadlow and Gusev, 2001), and functional encoding properties (Q. Wang et al., 2010). The ability of sensory adaptation to shift thalamic firing patterns along a continuum of patterns opens up a dynamic interplay between the incoming sensory information and the demands on the system that allows for flexible encoding. Although the adaptive state modulation shown here could be mediated by corticothalamic feedback from primary somatosensory cortex providing a sustained depolarizing drive to thalamic neurons, additional work is required

to understand how different mechanisms, such as adaptation, active sensing, and neuromodulatory inputs, interact in the context of state-dependent encoding. Taken together, the deeply interconnected thalamocortical loop could be performing significant processing in a non-feedforward manner with modulating inputs from multiple brain regions.

# CHAPTER 4 THALAMIC STATE CONTROL OF CORTICAL DYNAMICS

*This chapter was originally published as an article in* Journal of Neurophysiology *and is presented with only minor stylistic changes* [3]

Sensory stimulation drives complex interactions across neural circuits as information is encoded and then transmitted from one brain region to the next. In the highly interconnected thalamocortical circuit, these complex interactions elicit repeatable neural dynamics in response to temporal patterns of stimuli that provide insight into the circuit properties that generated them. Here, using a combination of in-vivo voltage sensitive dye (VSD) imaging of cortex, single unit recording in thalamus, and optogenetics to manipulate thalamic state in the rodent vibrissa pathway, we probed the thalamocortical circuit with simple temporal patterns of stimuli delivered either to the whiskers on the face (sensory stimulation) or to the thalamus directly via electrical or optogenetic inputs (artificial stimulation). VSD imaging of cortex in response to whisker stimulation revealed classical suppressive dynamics, while artificial stimulation of thalamus produced an additional facilitation dynamic in cortex not observed with sensory stimulation. Thalamic neurons showed enhanced bursting activity in response to artificial stimulation, suggesting that bursting dynamics may underlie the facilitation mechanism we observed in cortex. To test this experimentally, we directly depolarized the thalamus using optogenetic modulation of the firing activity to shift from a burst to a tonic mode. In the optogenetically depolarized thalamic state, the cortical facilitation dynamic was completely abolished. Taken together, the results obtained here from simple probes suggest that thalamic state, and ultimately

---

[3] Whitmire CJ, Millard DM, Stanley GB. Thalamic state control of cortical paired-pulse dynamic. Journal of Neurophysiology (2016). DOI: 10.1152/jn.00415.2016

thalamic bursting, may play a key role in shaping more complex stimulus-evoked dynamics in the thalamocortical pathway.

## 4.1 Introduction

Sensory pathways are strongly influenced by the interplay between excitation and inhibition that carves out complex neural dynamics. Stimulus-evoked dynamics are highly sensitive to both timing of patterns of sensory stimulation on slower timescales of hundreds of milliseconds and to timing of synaptic inputs on faster timescales of tens of milliseconds. However, due to the complexity of the neural circuitry, the relevant mechanisms are still unclear. Nonlinear dynamics in the thalamocortical circuit have been investigated in vision and audition (Hawken et al., 1990; Kilgard and Merzenich, 1998), but are particularly well-studied in the rodent vibrissa system (Boloori et al., 2010; Boloori and Stanley, 2006; Castro-Alamancos and Connors, 1996a; Civillico and Contreras, 2005; Higley and Contreras, 2007; Simons, 1985). Paradoxically, the nonlinear dynamics of the circuit have been characterized as both suppressive and facilitative in a range of experimental conditions due to complexities in the temporal interactions between excitatory and inhibitory network dynamics (Ego-Stengel et al., 2005; Webber and Stanley, 2006, 2004). However, because previous studies used only peripheral sensory stimulation of the whiskers to study the dynamics of the pathway, it has not yet been possible to disambiguate dynamics due to pre-thalamic effects from those established in the thalamocortical circuit.

Due to unique cellular and circuit properties, the thalamus is ideally positioned to dynamically gate and/or modulate information transmission to cortex (Crick, 1984). Specifically, the thalamus operates in two distinct firing modes: tonic firing and burst firing (Sherman, 2001a). Switching between these two states occurs regularly in concert with shifts in arousal (Fanselow et al., 2001; Llinas and Steriade, 2006; Ramcharan et al., 2000), attention (McAlonan et al., 2008), or sensory drive (Whitmire et al., 2016), and is linked through these mechanisms to the desynchronized thalamocortical state (Crochet and

Petersen, 2006; Poulet and Petersen, 2008). Through the use of optogenetics, recent work has demonstrated that the artificial hyperpolarization or depolarization of the thalamus is sufficient to drive cortex into the synchronized (Halassa et al., 2011) or desynchronized (Poulet et al., 2012) states. And yet, the effect of thalamic state on the propagation of stimulus-evoked activity to downstream structures remains poorly understood.

Here using simple stimulus probes, we experimentally investigated the thalamocortical circuit of the rodent vibrissa pathway in response to whisker, electrical, and optogenetic inputs using voltage sensitive dye (VSD) imaging to record the spatiotemporal stimulus-evoked cortical activity. Specifically, the VSD imaging targeted subthreshold activity in the supragranular layers of cortex (layer 2/3), reflecting suprathreshold input from cortical layer 4 (Wang et al., 2012; Zheng et al., 2015). Consistent with previous literature, we found that simple whisker deflections primarily produced suppression for all stimulus intensities. In contrast, artificial thalamic stimuli elicited significant cortical facilitation. We hypothesized that this facilitation could be due to the bursting dynamics between the thalamocortical projection nucleus (VPm) and the inhibitory reticular nucleus (nRT) of the thalamus. To determine the effect of thalamic state, or thalamic polarization levels, on the facilitation, we used direct optogenetic control of thalamic depolarization to shift the thalamic firing patterns from burst to tonic encoding. The removal of bursting through optogenetic modulation of thalamic state eliminated the cortical facilitation elicited by sub-threshold thalamic microstimulation, such that the dynamics were purely suppressive and therefore more similar to those of actual sensory stimuli. Taken together, we suggest that the interplay between excitation and inhibition in the thalamocortical circuit, in concert with burst/tonic state regulation in thalamus, shapes the signaling in the pathway and may serve to enhance specific temporal patterns of sensory inputs.

## 4.2 Methods

### 4.2.1 Experimental Preparation

All procedures were approved by the Institutional Animal Care and Use Committee at the Georgia Institute of Technology, and were in agreement with guidelines established by the National Institutes of Health. Eighteen female adult albino rats (220-350g; Sprague Dawley, Charles River Laboratories, Wilmington, MA) were used in the study. Briefly, female albino rats were sedated with 2% vaporized isoflurane and anesthetized with sodium pentobarbital (50 mg/kg, i.p., initial dose); supplemental doses were given as needed to maintain a surgical level of anesthesia, confirmed by measurements of heart rate, respiration and eyelid/pedal reflexes to averse stimuli (toe or tail pinch). Importantly, only physiological measurements were used to maintain the anesthesia level. Simultaneous electrophysiological measurements of cortical activity were not performed within this study. Therefore, there are no electrical measures of cortical state such as local field potential to quantify the anesthesia depth from a neurological perspective. In all experiments, body temperature was maintained at 37° C by a servo-controlled heating blanket (FHC, Bowdoinham, ME). After initial anesthesia, the animal was mounted on a stereotactic device (Kopf Instruments, Tujunga, CA) in preparation for the surgery and subsequent recordings. Atropine (0.5 mg/kg, s.c.) was injected and lidocaine was administered subdermally to the scalp. After the initial midline incision on the head, tissue and skin were resected, and connective tissue was carefully removed. A craniotomy was made on the left hemisphere over the barrel cortex (stereotactic coordinates: 1.0-4.0 mm caudal to the bregma, and 3.5-7.0 mm lateral to the midline) and over the ventroposterior medial nucleus (VPm) of the thalamus (2.0-4.0 mm caudal, 2.0-3.5mm lateral to the midline (Paxinos and Watson, 1998)). A dam was constructed with dental acrylic around the craniotomy over the barrel cortex to contain the voltage sensitive dye solution

(RH1691, 1.5mg/ml, Optical Imaging Ltd, Rehovot, Israel) for staining. Mineral oil was periodically applied to the cortical surface over VPm to keep the brain moist. After the recording session, the animal was euthanized with an overdose of sodium pentobarbital.

A separate batch of experiments (N = 5 of 18 animals) was performed recording only the electrophysiological response of single neurons in the ventroposteromedial (VPm) nucleus of the thalamus to optogenetic stimulation in the thalamus. These surgical procedures were performed as described above, but differed in the anesthetic used during recording (fentanyl-cocktail anesthesia; fentanyl [5 μg/kg], midazolam [2 mg/kg], and dexmedetomidine [150 μg/kg]).

### 4.2.2 VSD Imaging

Voltage sensitive dye imaging was achieved by using a high speed, low noise camera coupled with a tandem lens (MiCAM 2, SciMedia, Tokyo, Japan). After the craniotomy over the barrel cortex, the dura mater was allowed to dry for 15 minutes (Lippert et al., 2007). The cortex was stained with a solution of dye RH1691 (1.5mg/mL; Optical Imaging) for two hours, during which the dye solution was circulated every 5 minutes to prevent the cerebral spinal fluid from impeding the staining. After staining, saline was applied generously to wash off the dye residue. The dam was then filled with saline and a glass cover slide was placed on top of the dam to prevent the saline from vaporizing. The dye was excited by a 150W halogen lamp filtered to pass wavelengths only in the 615-645nm band. In all experiments, a 1.0x magnification lens was used as the objective lens in conjunction with a 0.63x condenser lens to provide 1.6x magnification (48 pixels/mm). Twenty trials of VSD data were collected for each stimulus and they were averaged offline for the data analysis (see response analysis section below).

### 4.2.3 VSD Imaging

Multiple trials of VSDI data were collected for each stimulus. For each trial, the 40 frames (200ms) collected before the presentation of the stimulus were averaged to calculate

the background fluorescence, against which the activation was measured. For each frame, the background fluorescence was subtracted to produce a differential signal $\Delta F$. Additionally, each frame was divided by the background image to normalize for uneven illumination and staining to produce the signal $\Delta F/F_0$. For presentation purposes only, the individual trials were averaged together and then filtered with a 9x9 pixel (~200x200μm) spatial averaging filter. The anatomical mapping, acquired through cytochrome oxidase histology, was registered with the functional cortical column mapping from VSDI by solving a linear inverse problem, the details of which have been described previously (Wang et al., 2012). Following the functional image registration, the cortical response was discretized, where each signal corresponds to a single functional cortical column. In so doing, the VSDI signal was averaged spatially within the contour of the cortical column.

The cortical response amplitude (R) was quantified as the maximum VSDI signal elicited in response to each stimulus in the paired pulse paradigm, after averaging within a single cortical column, on a trial-by-trial basis. The paired pulse ratio (PPR) was defined as the response to the second stimulus (R2) divided by the sum of the response to the first (R1) and second stimuli (PPR = R2/(R1+R2)). A simple ratio of R2/R1, as has been used previously for electrophysiology data (Jouhanneau et al., 2015), was not used here for imaging data because near-zero changes in the fluorescence in response to the first stimulus would push the ratio towards infinity. In this work, a PPR of 0.5 corresponds to no interaction between the pair of stimuli as they elicited equal responses to the first and second stimuli, assuming the response to the first stimulus had completely decayed before the onset of the response to the second stimulus. A PPR less than 0.5 meant that the response to the second stimulus was smaller than the response to the first (suppression) while a PPR of greater than 0.5 corresponds to a larger response to the second stimulus (facilitation).

The time course of the VSD signal decay was quantified in response to the first stimulus in the pair. Each trial was only characterized if the peak evoked response was

greater than three times the standard deviation of the background fluctuation (as quantified from the 200 millisecond VSD trace prior to stimulus onset). The VSD signal from the peak evoked response to 125 milliseconds afterwards (25 frames) was used to fit a sum of exponentials where:

$$VSD = a_1 e^{-t/\tau_1} + a_2 e^{-t/\tau_2}$$

$\tau_1$ was restricted to be the shorter time constant while $\tau_2$ was the longer time constant.

### 4.2.4 Electrophysiological Recordings

Extracellular recordings in the VPm were obtained by using single tungsten microelectrodes (approximately 1MOhm, 75μm in diameter, FHC, Bowdoinham, ME). The detailed procedure was described previously (Q. Wang et al., 2010). Briefly, after the craniotomy, a tungsten microelectrode was slowly advanced into VPm using a hydraulic micropositioner (Kopf Instruments, Tujunga, CA). During electrode advancement through VPm, individual whiskers were stimulated manually to identify the principal whisker (PW), i.e. the whisker that evokes the strongest response. We aimed to recruit barrel fields in the E and D rows, which are located close to the center of the imaging field in our preparation. Neuronal signals were amplified, band-pass filtered (500-5kHz), digitized at 30 kHz/channel, and collected using a 32, 64, or 96-channel data-acquisition system (Plexon, Inc., Dallas, TX; Blackrock Microsytems, Salt Lake city, UT; and Tucker Davis Technologies, Alachua, FL, respectively). Data were then sorted using WaveClus software (Quiroga et al., 2004). Data were excluded if the neuron was not light sensitive (<1 spike/stimulus at the strongest light intensity) or if the waveform was not sufficiently isolated (as quantified by the waveform signal-to-noise ratio). Waveform SNR was defined as the peak-to-peak voltage of the mean waveform divided by the average standard deviation of the waveform over the full waveform snippet for all recorded waveforms. All cells with a waveform SNR < 3 were excluded from the analysis.

### 4.2.5 Electrophysiological Analysis

Single unit thalamic responses were recorded in response to optogenetic stimulation using a custom optrode consisting of an optical fiber (200 μm diameter; Thorlabs) and an electrode (tungsten microelectrode; FHC) that was lowered into the VPm. The response to the stimulus was quantified as the number of spikes in 20 milliseconds following the onset of the light pulse. Spikes were classified as part of a T-type calcium channel burst if two or more spikes were separated by an interspike interval of 4 milliseconds or less and the first spike in the burst was preceded by at least 100 milliseconds of silence (Lesica et al., 2006; Lu et al., 1992; Reinagel et al., 1999). The burst ratio was defined as the number of burst spikes within the 20 millisecond response window divided by the total number of spikes within the 20 millisecond response window, as described previously (Whitmire et al., 2016). The first spike latency was defined as the first spike following stimulus onset. Any latencies greater than 5 milliseconds were excluded from the trial average as this indicated the lack of a light evoked response.

### 4.2.6 Thalamic Microstimulation

After the principal whisker was identified, the thalamic electrode was used to deliver single electrical current pulses to evoke cortical responses in the somatosensory pathway. The electrical stimuli were created using a digital stimulus generator (Model: DS8000, WPI Inc., Sarasota, Florida) and delivered using a digital linear stimulus isolator (Model: DLS 100, WPI Inc., Sarasota, Florida) acting in current source mode. All individual electrical stimuli were charge balanced, cathode-leading, symmetric biphasic current pulses of 200 microseconds duration per phase. A paired pulse stimulus paradigm was used, where two stimuli with the same current amplitude were delivered separated by an inter-stimulus interval. Current amplitudes (30-150 μA) and inter-stimulus intervals (50, 100, 150, 200, 250, 500 milliseconds) were varied. Current amplitudes were chosen to span the full range of cortical activation from no response to maximal cortical excitation.

### 4.2.7 Whisker Stimulation

Sensory stimulation was applied through computer controlled whisker deflections. Whiskers were trimmed at approximately 12mm from the face, and were inserted into a glass pipette fixed to the end of a calibrated multi-layered piezoelectric bimorph bending actuator (range of motion, 1 mm; bandwidth, 200 Hz; Physik Instrumente (PI), Auburn, MA) positioned 10 mm from the vibrissa pad. Vibrissae were always deflected in the rostral-caudal plane. Punctate deflections consisted of exponential rising and falling phases (99% rise time, 5 ms; 99% fall time, 5 ms) were used as sensory stimuli (Boloori et al., 2010; Q. Wang et al., 2010). A paired pulse stimulus paradigm was used, where two whisker stimuli with the same velocity were delivered separated by a specified inter-stimulus interval. Velocities (75-1200°/s) and inter-stimulus intervals (50, 100, 150, 200, 250, 500 milliseconds) were varied. Whisker velocities were chosen to span the full range of cortical activation from no response to maximal cortical excitation.

### 4.2.8 Optogenetic Expression

A subset of animals (N = 7) underwent an initial surgery for the injection of a viral vector (UNC Vector Core, Chapel Hill, NC) to induce expression of either channelrhodopsin (AAV-CaMKIIa-hChR2(H134R)-mCherry) or the stabilized step function opsin (AAV-CaMKIIa-hChR2(C128S/D156A)-mCherry). The viral injection (1μL) was delivered at a rate of 0.2μL/min in the ventral postero-medial (VPm) thalamus according to coordinates described above. Given the dense structure of thalamus, expression was restricted to excitatory neurons using the CaMKIIa promoter (Aravanis et al., 2007) to prevent opsin expression in the nearby reticular thalamus (nRT). However due to the close proximity of posteromedial thalamus (POm), it is possible that both VPm and POm expressed opsins. Viral expression was verified experimentally in all animals through light-responsive electrophysiological recordings, and using histology in animals not used for experimentation. A single experimental animal was perfused after recording for

histological analysis and is included in Figure 5. Although this animal and our histology only animals (data not shown) demonstrate strong opsin expression within the thalamus, we are not able to differentiate between VPm and POm expression within each of the experimental animals presented here.

### 4.2.9 Optogenetic Stimulation

Depolarizing opsins were used in two distinct ways: first, to drive the pathway using pairs of light pulses and second, to modulate the pathway using low amplitude ongoing light stimulation. For both driving and modulating neural activity, light emitting diodes (LEDs) were used to excite the ChR2 and SSFO in vivo. An "optrode" was positioned in the VPM thalamus, with the fiber optic directly attached to the LED to minimize light loss. A 465nm LED was used for animals expressing ChR2. When driving the pathway, the same paired stimulus design implemented for sensory and electrical stimulation was used for optical stimulation. Two five-millisecond pulses of light at varying intensity (47-139 $mW/mm^2$) were administered with a 150 millisecond inter-stimulus interval. Light intensities were chosen to span the full range of cortical activation from no response to maximal cortical excitation. The 150 millisecond inter-stimulus interval was chosen because it most reliably activated the facilitation described for the electrical stimulation. In the thalamic electrophysiology experiments, a 470 nm LED and commercial LED driver were used (Thorlabs Inc., Newton, New Jersey).

When modulating the pathway, both ChR2 and SSFO were used. Because ChR2 quickly closed when the light was removed (Mattis et al., 2012), when using this opsin the light was delivered continuously to maintain the long timescale depolarization involved in this study. A custom current source was used to drive the LED (Newman et al., 2015). For animals expressing the SSFO, a 465nm LED (LED Engin Inc, San Jose, CA) was used in combination with a 590nm LED (LED Engin Inc, San Jose, CA) through a wavelength combiner (Doric Lenses Inc, Quebec, Canada). The SSFO channel has a long closing time,

such that the channel remains open long past the duration of the light stimulus, so brief pulses of light (~5-50ms) from the 465nm LED were used to open the channel over long timescales. To close the channel, 15 seconds of yellow light from the 590nm LED was delivered through the fiber optic. SSFO and ChR2 were activated in conjunction with electrical stimulation (paired pulse design as described above) in VPm to assess the effects of thalamic state on cortical activation.

### 4.2.10 Statistical Analysis

The statistical analyses performed in this manuscript were implemented using multi-way ANOVA (factors included animal, stimulus condition, and stimulus number). For the paired pulse ratio (PPR), an assumption of normality is violated by the data bounds of 0 and 1 which would limit the accuracy of the ANOVA. To overcome this limitation, the PPR data was transformed from bounded data ([0,1]) to unbounded data ([-∞,∞]) using a logit function and statistical significance was assessed with respect to the first stimulus condition. All statistical tests of partially bounded data, such as spike counts, were performed on the original data without any transformation.

## 4.3 Results

### 4.3.1 Artificial stimulation of thalamus isolates dynamics of thalamocortical processing

In this work, we experimentally investigated the simple dynamics of the thalamocortical circuit of the rodent vibrissa somatosensory system (Figure 4-1A). Specifically, we utilized paired-pulse inputs (Figure 4-1B), where the spatiotemporal cortical activation was measured in response to temporally spaced pairs of whisker, electrical, and optogenetic inputs using voltage sensitive dye imaging (VSDI) (Figure 4-1C). In a subset of experiments, thalamic state was modulated optically in conjunction with microstimulation of thalamus to investigate the role of thalamic state on information

transmission (Figure 4-1B, bottom). The temporal component of the cortical response was extracted from the full spatiotemporal images by computing the mean activity within a specific barrel in each frame (Figure 4-1C, top; region of interest outlined in black) and the response was computed as the maximum amplitude of the evoked response in a window following stimulus presentation relative to baseline (Figure 4-1C, Optical Stimulation, R1, R2). The dynamics of the cortical response were classified as suppressive when the response to the first stimulus was larger than the response to the second (Figure 1, Sensory Stimulation, 1200°/s) and facilitative when the response to the first stimulus was smaller than the response to the second (Figure 4-1, Electrical Stimulation, 40μA). Furthermore, while whisker stimulation will activate each stage of the sensory pathway, the artificial stimulation through electrical and optogenetic means will circumvent pre-thalamic processing by directly activating the thalamocortical relay neurons, providing a mechanism to separate the dynamics of the thalamocortical circuit from the processing that occurs from the periphery to thalamus (Figure 4-1A; see discussion for additional information about artificial stimulation of thalamus).

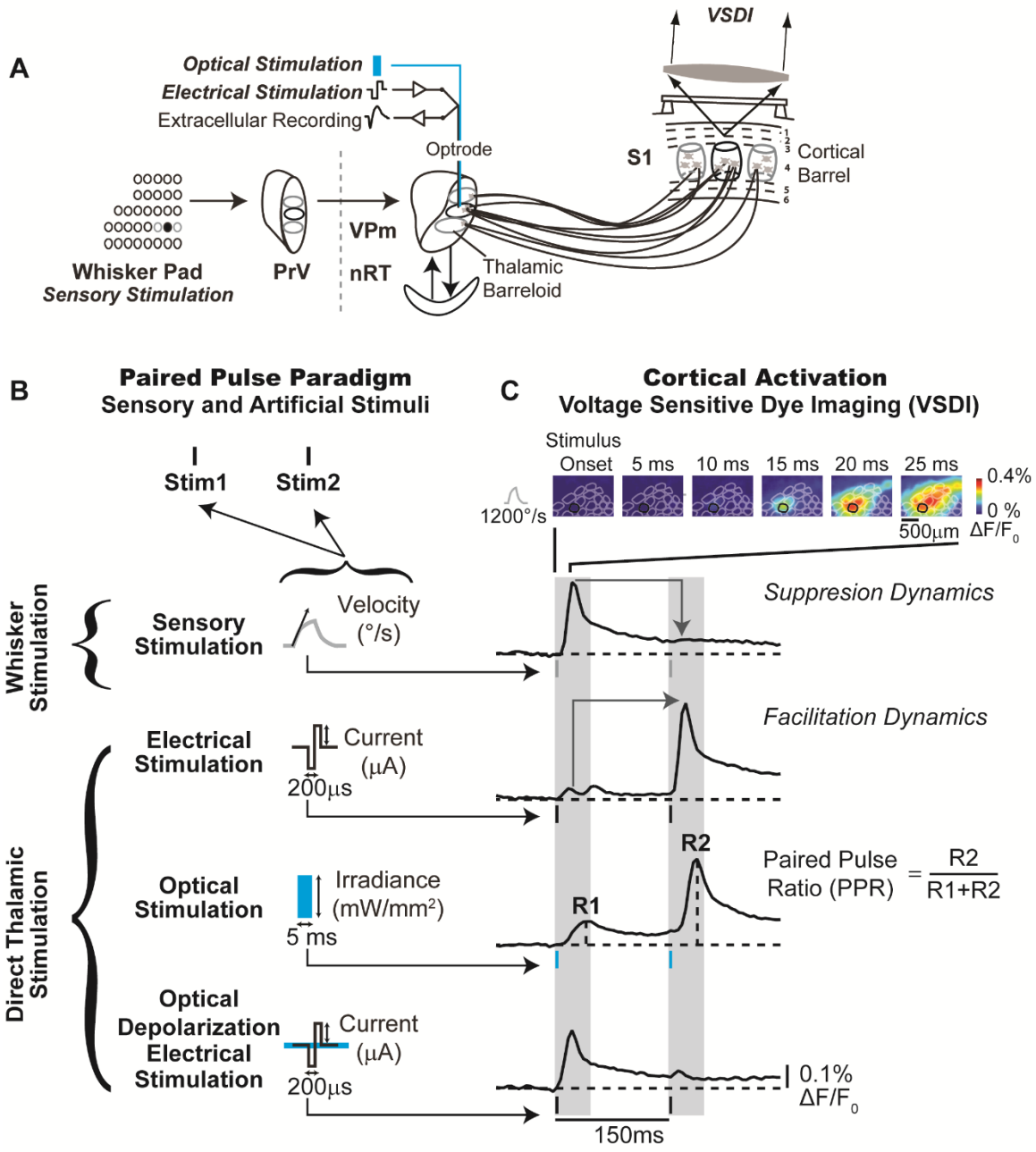


**Figure 4-1: Quantification of thalamocortical dynamics using natural and artificial paired pulse paradigm.** A. Schematic of the feedforward lemniscal circuit of the rat whisker pathway. The optrode was positioned in the ventral posteromedial (VPm) nucleus of the thalamus for optical and electrical stimulation. B. The paired pulse paradigm consists of two temporally spaced stimuli administered at the whisker (sensory stimulus) or directly to the thalamus (electrical and optical stimulation). C. Voltage sensitive dye imaging (VSDI) of the barrel cortex (S1BC) recorded the cortical activation (top). The activity within a barrel/region-of-interest is averaged together to quantify the temporal

response to a stimulus (black traces). Trial-averaged examples of the cortical response are depicted in response to pairs of whisker (1200°/s), electrical (40 μA), optical (90 $mW/mm^2$), and electrical in the presence of optical depolarization (60 μA) stimuli.

### 4.3.2 Sensory stimulation elicits primarily suppression dynamics

Temporal patterns of sensory input are known to produce nonlinear responses even in the early sensory pathways (Chung et al., 2002; Ganmor et al., 2010). Significant work from the thalamocortical circuit of the rodent whisker system, using pairs or triplets of individual whisker deflections to map out the dynamics of neurons in the primary somatosensory cortex, has principally detailed paired-pulse suppression, where the response to the second stimulus is suppressed due to the presence of a previous stimulus occurring immediately prior (Boloori et al., 2010; Boloori and Stanley, 2006; Castro-Alamancos and Connors, 1996a; Simons, 1985; Webber and Stanley, 2006, 2004), which can lead to more complex dynamics in response to more rich patterns of inputs. Here, in agreement with these studies, we used pairs of whisker stimuli at varying inter-stimulus intervals with fixed stimulus intensities (Figure 4-2A, top; velocity = 150, 1200 °/s) and varying velocities with a fixed inter-stimulus interval (Figure 4-2 B, top; ISI = 150 ms) to directly probe the second order dynamics of the system. Figure 4-2A shows an example of the temporal response in cortex, averaged across trials, to pairs of whisker deflections at low (left) and high (right) angular velocities. When the whisker stimulus was weak, the response to the second stimulus was approximately equal in strength to the response to the first stimulus, except at the 50 ms inter-stimulus interval (Figure 4-2A left), indicating a very short duration for the dynamic interactions between the responses to the deflections in the sequence. However, when the whisker stimulus was strong, the cortical response exhibited profound paired pulse suppression (Figure 4-2A right) such that the response to the second stimulus was strongly suppressed relative to the first. This suggests an activity dependent modulation of the dynamics, consistent with previous reports in the barrel cortex

(Boloori et al., 2010). To quantify the strength of the suppression as a function of stimulus intensities, we analyzed single trials of the VSDI signal for the fixed 150ms inter-stimulus interval across velocities (Figure 4-2B, top). The response to each stimulus was defined as the peak cortical response in the window following stimulus onset relative to the baseline activity level prior to any stimulation. Note that the cortical activity after the first stimulus may not have returned to baseline before the onset of the second stimulus (see Figure 4-4). Rather than making any assumptions about the interaction between the ongoing cortical activity and the second stimulus-evoked response, we used absolute maximum fluorescence values. The dynamics of the evoked response were quantified using a paired pulse ratio (Figure 4-1B; PPR = R2/(R2+R1), see methods for additional details). With this metric, a value greater than 0.5 is indicative of facilitation dynamics and a value less than 0.5 is indicative of suppression dynamics. The paired pulse ratio is less than 0.5 for stronger whisker velocities, indicative of stronger paired pulse suppression with stronger stimuli (Figure 2B, bottom, n = 4 animals; two-way ANOVA, * indicates $p<0.05$).

On a single trial basis, the peak response to the second stimulus was plotted relative to the peak response to the first stimulus (Figure 4-2C). Each data point is the peak cortical response to a single presentation of the paired pulse stimulus, with the color indicating the velocity of the whisker deflections. As the velocity of the whisker deflections increased, the response to the first stimulus also increased. However, for all velocities, the response to the second stimulus was suppressed relative to the first for the majority of trials, as most of the data points fell below the unity line (Figure 4-2C, black). These trends are consistent across four experiments, where the data from each experiment has been normalized (Figure 4-2C). A few trials at low velocity showed strong responses to the second stimulus, with no response to the first, but this occurred at low probability. This is consistent with the response to the second stimulus being dependent on the first, and responding probabilistically in the same manner as the first response (Gollnick et al., 2016). We can estimate the amount of suppression or facilitation on each trial by computing the distance

from the unity line for each trial (Figure 4-2C; diagonal histogram). This depiction shows that the lower stimulus intensities show very little dynamic interaction (blue data, Figure 2C histogram), but as the intensity of the whisker stimulus increases, the intensity of the suppression also increases (orange data, Figure 4-2C histogram). Again, the majority of trials lie in bins below the unity line, indicating a prevalence of paired pulse suppression amongst the cortical population in response to pairs of whisker deflections.

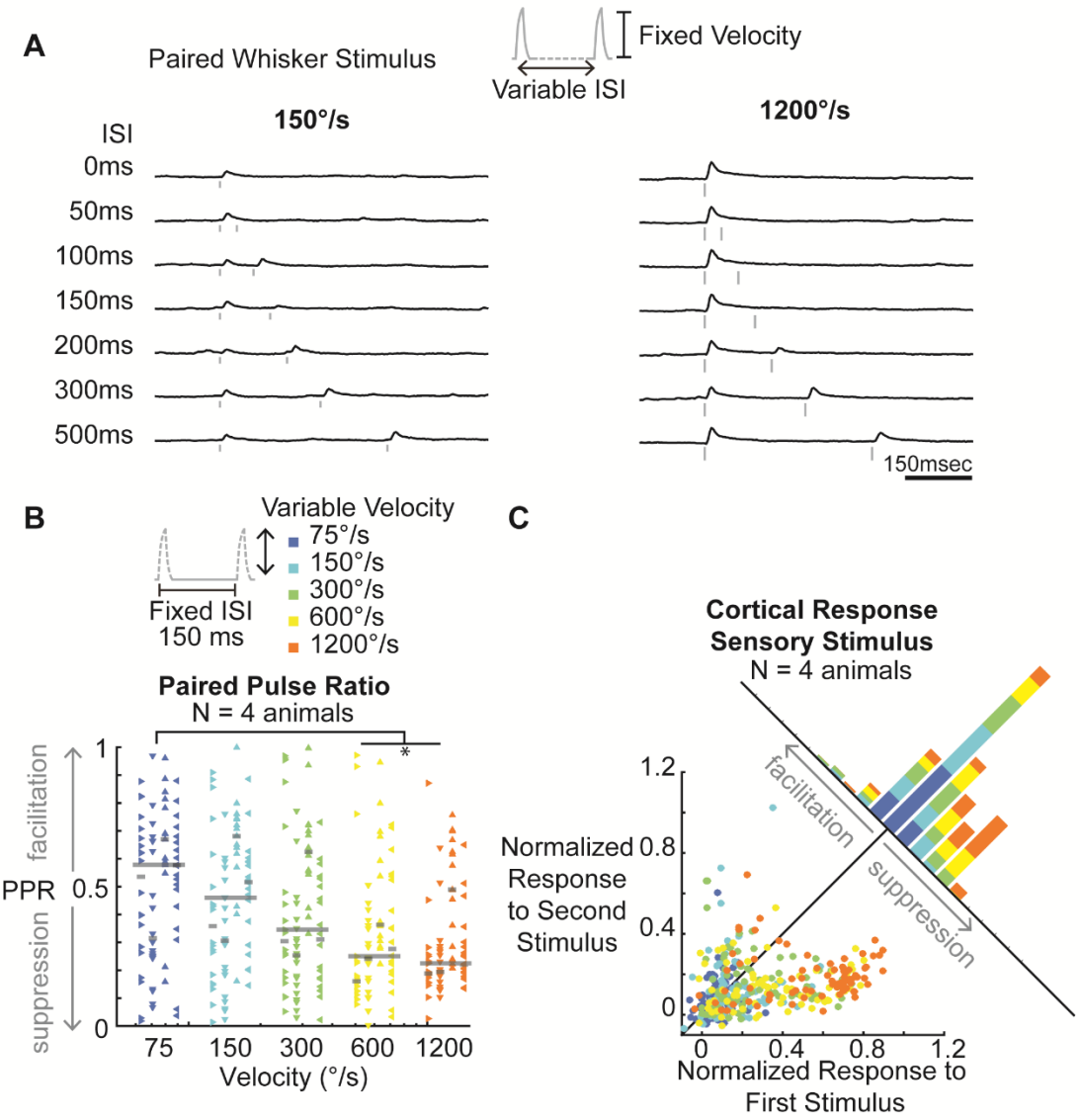


**Figure 4-2: Sensory evoked cortical responses elicit different paired-pulse dynamics.** A. Cortical response to pairs of weak (150°/s) whisker stimuli (left). The response to the second stimulus was suppressed only for the 50ms inter-stimulus interval. Cortical

response to pairs of high velocity (1200 °/s) whisker deflections at varying inter-stimulus interval (right). The response to the second stimulus was suppressed relative to the first, with the suppression relaxing for longer inter-stimulus intervals. B. With the interstimulus interval (ISI) fixed at 150 ms, the velocity of the stimuli was varied systematically (top). The paired pulse ratio (PPR) is plotted as a function of stimulus intensity, represented by the color. Each trial across experiments (N = 4 animals, each denoted by a vertical line of points) is plotted as a dot with the median of the distribution indicated by the horizontal black bars (animal median shown as well as population median). For each condition, * indicated statistical significance relative to first stimulus condition (two-way ANOVA; factors: animal, stimulus condition; $p < 0.05$). P-values for each stimulus condition [150, 300, 600, 1200°/s] relative to the first stimulus condition (75°/s) are p = [0.8727, 0.2698, 3.73e-4, 3.99e-5]. C. The normalized response to the first and second stimulus are plotted for all single trials across all whisker deflection velocities at the 150ms inter-stimulus interval for all experiments (n = 4 animals). Along the diagonal, a histogram represents the distance of each trial from the unity line (black). Data below the unity line is indicative of suppressive dynamics while data above the unity line is indicative of facilitation dynamics.

### 4.3.3 Artificial stimulation elicits facilitative dynamics

Within the paired pulse paradigm, we also recorded the cortical response to pairs of thalamic microstimulation pulses to disentangle thalamic and pre-thalamic contributions to the cortical paired pulse dynamics. As shown for whisker stimulation, Figure 3A shows an example of the temporal response in cortex, averaged across trials, to pairs of thalamic microstimuli at low and high current amplitude with varying interstimulus intervals. While the high current stimuli exhibited paired pulse suppression (Figure 4-3A right) similar to high velocity whisker deflections (Figure 4-2A right), the low current stimuli produced a dramatically different nonlinear response (Figure 4-3A left). For inter-stimulus intervals of 100-200ms, the response to the second stimulus was strongly facilitated even though the first stimulus was sub-threshold and produced little to no cortical response. Similar to the sensory stimulation, the paired pulse ratio is approximately 0.5 for low current amplitudes and is significantly reduced at high current amplitudes. However, in contrast to the whisker

stimuli, the paired pulse ratio shows significant facilitation at intermediate current levels (Figure 4-3B; n=4 animals, two-way ANOVA, * indicates $p<0.05$).

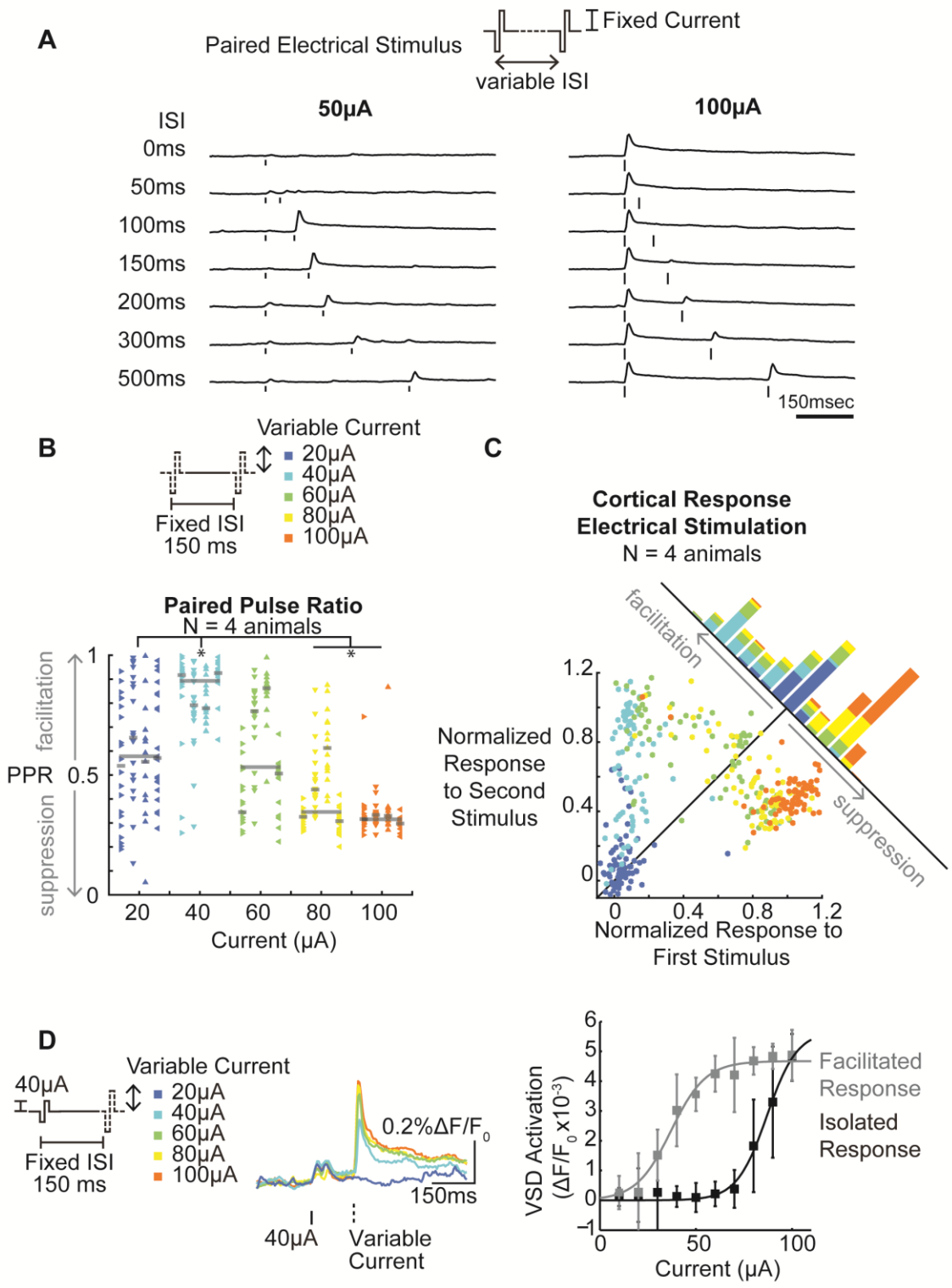


**Figure 4-3: Artificially evoked cortical responses elicit different paired-pulse dynamics.** A. Cortical response to pairs of weak (50 µA) electrical stimuli (left). The response to the second stimulus was facilitated relative to the first, but only for the 100-

200ms inter-stimulus intervals. Cortical response to pairs of strong (100μA) electrical stimuli at varying inter-stimulus interval was purely suppressive (right). The response to the second stimulus was suppressed relative to the first, with the suppression relaxing for longer inter-stimulus intervals. B. With the interstimulus interval (ISI) fixed at 150 ms, the amplitude of the current was varied systematically (top). The paired pulse ratio (PPR) is plotted as a function of stimulus intensity, represented by the color. Each trial across experiments (N = 4 animals, each denoted by a vertical line of points) is plotted as a dot with the median of the distribution indicated by the horizontal black bars (animal median shown as well as population median). For each condition, * indicated statistical significance relative to first stimulus condition (two-way ANOVA; factors: animal, stimulus condition; $p < 0.05$). P-values for each stimulus condition [40, 60, 80. 100 μA] relative to the first stimulus condition (20 μA) are p = [9.92e-9, 0.9992, 1.08e-7, 9.92e-9]. C. The normalized response to the first and second stimulus are plotted for all single trials across all current amplitudes at the 150ms inter-stimulus interval for all experiments (n = 4 animals). Along the diagonal, a histogram represents the distance of each trial from the unity line (black). Data below the unity line is indicative of suppressive dynamics while data above the unity line is indicative of facilitation dynamics. Note the significant number of trials classified as facilitative. D. In a separate experiment (N = 1 animal), the first stimulus was held fixed at a facilitating current amplitude (60 μA) while the second stimulus was allowed to vary in amplitude. The evoked response to the second variable amplitude stimulus (right, Facilitated Response) was greater than the response to the same current amplitude presented in isolation (left, Isolated Response). Values shown are mean +/- SEM (10 trials per condition).

The facilitation and suppression were consistent across trials for sub- and supra-threshold stimuli, respectively. The normalized response to the second stimulus is plotted relative to the normalized response to the first for single trials and varying current amplitude for the 150ms inter-stimulus interval on a trial by trial basis across experiments (Figure 4-3C, n = 4 animals; same as shown for Figure 4-2C). For the lowest current intensity (dark blue), there was no response to either stimulus presentation. At a slightly higher current intensity (light blue), the response to the second stimulus was strongly facilitated for each trial, leading to a cluster of points in the upper left quadrant of Figure 4-3C. Importantly, the clustering in the upper left quadrant of the axes distinguished the

reliable facilitation of electrical stimulation from the lack of facilitative nonlinear dynamics for sub-threshold whisker inputs in Figure 4-2C. At the highest current intensities (yellow and orange), the response to the second stimulus was consistently suppressed relative to the first, leading to a cluster in the lower right quadrant. At threshold stimulus intensity (green), the response to the first stimulus varied significantly on a trial-to-trial basis, as shown previously (Millard et al., 2015). This transition from facilitative to suppressive dynamics with increasing stimulus amplitudes is further emphasized by visualizing the distance from the unity line as a function of stimulus intensity (Figure 4-3C; diagonal inset). The consistency of the pattern across animals established the distinct bimodality of the cortical nonlinear dynamics in response to thalamic microstimulation (Millard et al., 2013) as compared to sensory stimuli (data from Figure 4-2 and Figure 4-3 were recorded from the same experimental preparation, N=4 animals total).

Finally, to further isolate the cause of the facilitative effects for intermediate current amplitudes, another experiment was conducted where the amplitude of the first pulse was fixed at a facilitative value (60 μA) and the amplitude of the second pulse was allowed to vary (Figure 4-3D left, N = 1 experiment). Across trials, the response to a given current amplitude preceded by a 60 μA stimulus was compared to the response to the same current amplitude presented in isolation (Isolated Response; Figure 4-3D left). Across all intermediate stimulus intensities, the 60 μA stimulus provided 150 milliseconds before the test stimulus led to an enhanced, or facilitated, response (Facilitated Response, Figure 4-3D right).

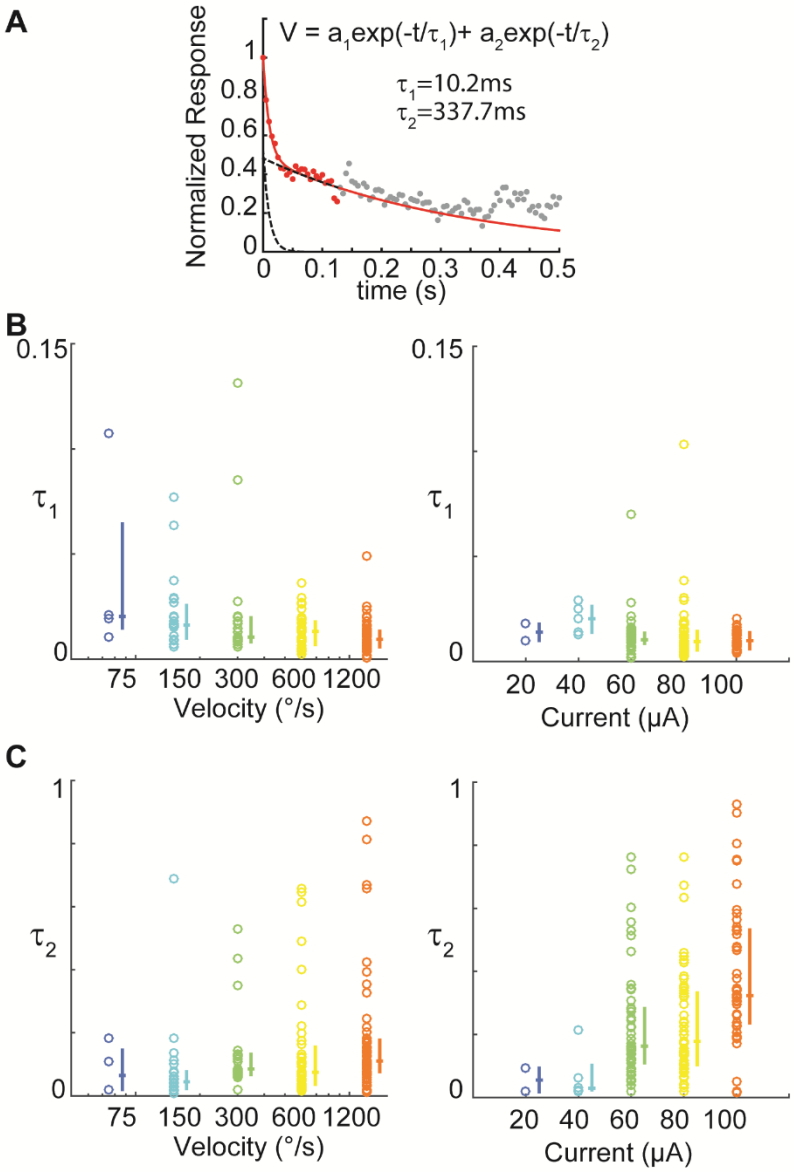


**Figure 4-4: Temporal dynamics of the decay of cortical activation following stimulation can last hundreds of milliseconds.** A. The decay from the peak response was well approximated by the sum of two exponentials (equation, left). In this example ($\tau_1$= 10.2 ms, $\tau_2$= 337.7 ms), the data points used to fit the curve are shown in red while the ongoing response is shown in grey (left; full curve fit shown as solid red line, individual exponentials plotted as dotted lines). B. Across experiments, $\tau_1$was defined as the shorter time constant. Median $\tau_1$ values are [20.3, 16.2, 10.5, 13.1, 9.3] milliseconds for increasing whisker stimulus amplitudes and [14.0, 20.4, 10.1, 9.5, 10.0] milliseconds for increasing current stimulus amplitudes. C. Across experiments, $\tau_2$ was defined as the longer time constant. Median $\tau_2$ values are [64.5, 44.6, 85.2, 74.6, 110.3] milliseconds for increasing

whisker stimulus amplitudes and [55.3, 29.4, 162.8, 177.6, 323.2] milliseconds for increasing current stimulus amplitudes.

Importantly, the cortical response to both artificial and sensory stimuli measured using VSDI can persist for hundreds of milliseconds. To quantify this, we fit a sum of exponential equation to the decay of the evoked response to the first stimulus (Figure 4-4A). Across conditions, the rapid decay time constant ($\tau_1$) was on the order of 10-15 milliseconds (Figure 4-4B; Median $\tau_1$ values are [20.3, 16.2, 10.5, 13.1, 9.3] milliseconds for increasing whisker stimulus amplitudes and [14.0, 20.4, 10.1, 9.5, 10.0] milliseconds for increasing current stimulus amplitudes.). However the slow decay time constant ($\tau_2$) was an order of magnitude larger, reaching 110 milliseconds for the largest whisker velocity and 320 milliseconds for the largest current amplitude (Figure 4-4C; Median $\tau_2$ values are [64.5, 44.6, 85.2, 74.6, 110.3] milliseconds for increasing whisker stimulus amplitudes and [55.3, 29.4, 162.8, 177.6, 323.2] milliseconds for increasing current stimulus amplitudes.). Therefore, it was often the case that the fluorescence signal had not yet returned to baseline when the second stimulus arrived 150 milliseconds after the first. Importantly, the prolonged fluorescence trace is not likely due to temporal artifacts from the dye. Instead, evidence from simultaneously recorded VSDI of cortex with individual intracellular recordings from L2/3 has shown a strong correlation between the VSD signal and the subthreshold voltage fluctuations (Petersen et al., 2003a). This provides strong evidence that the prolonged VSD signal is representative of the underlying neural activity rather than sensor artifacts.

If one assumes that the cortical responses to the first and second stimulus add linearly, then we could subtract the measured cortical response to a single stimulus from the paired pulse response to isolate the amplitude of the response to the second stimulus from the ongoing response to the first pulse. However, subtraction of the estimated response to the first stimulation would only further enhance the suppression dynamic by reducing the quantified response to the second pulse and would have no impact on the

facilitation dynamic due to the near-zero response to the first pulse in facilitation conditions. Rather than assuming linear superposition of the ongoing cortical activity and the stimulus-evoked response, we defined the response to the second stimulus as the maximum of the absolute amplitude of the trace without attempting to correct for ongoing cortical activity in response to the first stimulus to avoid unnecessarily biasing the data.

### 4.3.4 Thalamic bursting activity as a mechanism underlying facilitation dynamics

In a separate set of experiments (N=5 animals), we performed an identical analysis for optogenetic stimulation of the thalamus as opposed to electrical stimulation and found a similar bimodality in the nonlinear dynamics that was seen for thalamic microstimulation (Figure 4-5A; example of opsin expression within thalamus). As shown for one example, the cortical response to increasing light intensities demonstrated both facilitation and suppression dynamics (Figure 4-5B). In Figure 4-5C, the response to the second stimulus is plotted relative to the response to the first stimulus for each trial across stimulus intensities. Similar to the thalamic microstimulation results described in Figure 3, three clusters are apparent in this representation of the data. At very low stimulus intensities, there was no response to either of the two stimuli. At intermediate stimulus intensities, the majority of trials exhibited facilitation, forming a cluster in the upper left quadrant of the axes. At the highest stimulus intensities, the cortical response to the second stimulus was suppressed relative to the response to the first, forming a cluster in the lower right quadrant of the axes (Figure 4-5C, N = 5 animals).

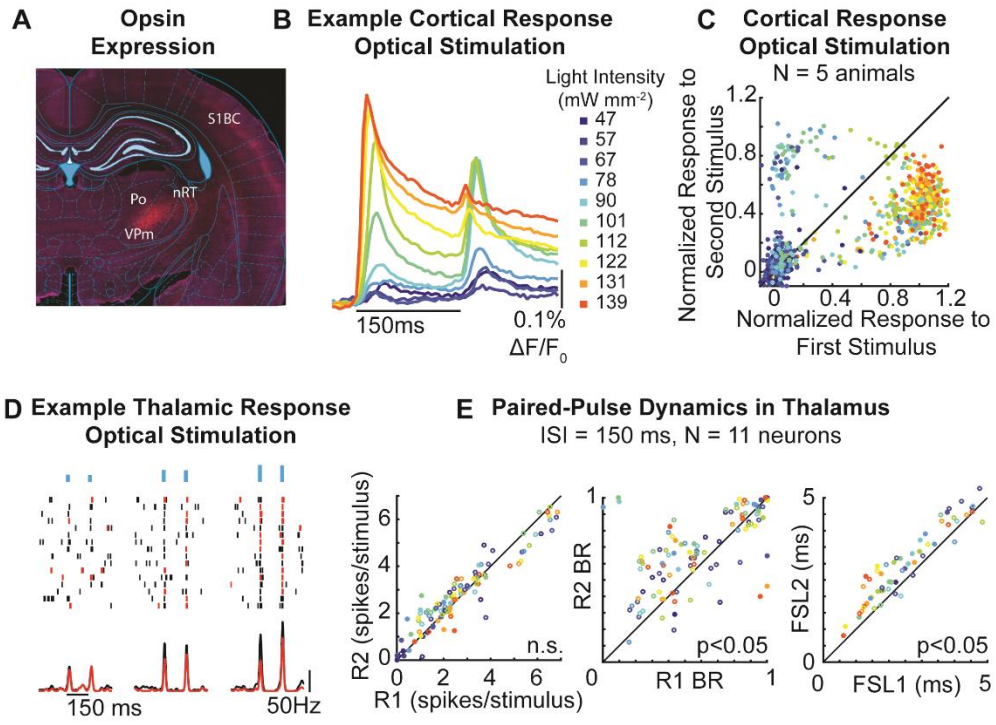


**Figure 4-5: Optogenetic stimulation of the thalamus also exhibits bimodal nonlinear dynamics.** A. Example histological image of opsin spread within thalamus (VPm: Ventral posteromedial thalamus, PO: Posterior thalamus, nRT: reticular nucleus of the thalamus, S1BC: barrel cortex). B. Example of the cortical response, averaged within a single cortical column, to increasing stimulus intensities (ISI = 150 ms). C. The response of the second stimulus is plotted against the response of the first stimulus for single trials of varying light intensity. Points above the unity line (black) were facilitated, while points below the unity line were suppressed (N = 5 animals). The responses were normalized, for each animal, relative to the mean response for the strongest light intensity during that experiment. Optogenetic stimulation exhibited a mixture of facilitation and suppression, with the facilitation less reliable on a trial-to-trial basis. D. Rastergram and peristimulus time histogram for an example single-unit VPM cell in response to paired optogenetic stimuli of increasing intensity. Within the rastergram, red spikes belong to an identified burst. E. Across neurons (n = 11 neurons), the overall evoked response, defined as the average number of spikes elicited within 20ms of stimulus onset, was not different for the first and second stimulus (left; p=0.47, three-way ANOVA; factors: animal, stimulus condition, stimulus number), but the burst activity was higher in response to the second stimulus (middle; p=2.79e-4, three-way ANOVA; factors: animal, stimulus condition, stimulus number). The first spike latency was also higher in response to the second pulse compared

to the first (right; p=0.001, three-way ANOVA; factors: animal, stimulus condition, stimulus number). Note that 8 of 11 neurons were collected using a different anesthesia. These data points are indicated as the open circles while neurons collected using the same anesthesia as the imaging experiments are filled circles.

Importantly, optogenetic stimulation of thalamus can be used in conjunction with electrophysiological recordings in thalamus because it does not introduce the same electrical artifact caused by thalamic microstimulation. In our paired pulse paradigm, the direct optical activation of thalamic neurons is transmitted downstream to produce the cortical dynamics measured using optical techniques. Therefore, we have direct access to the input to the cortical circuit with the ability to record from the thalamic neurons that are being stimulated and can begin to investigate the source of the facilitation/suppression dynamics measured in cortex. It is possible that similar facilitation/suppression dynamics are present in the spiking activity of thalamic neurons and that these thalamic dynamics are simply inherited at the level of cortex as the information is transmitted downstream. However it is also possible that the dynamics of the thalamic spiking activity are dissimilar to those seen in cortex such that the cortical dynamics are instead generated by integrating across thalamic inputs. Using extracellular recordings in thalamus, we quantified the dynamics of the thalamic spiking response to attempt to identify the source of the facilitation/suppression dynamics seen cortically.

For an example neuron, the evoked spiking activity in response to the light increases with increasing light intensity (Figure 4-5D). This example neuron was driven by the same paired optogenetic stimulus used in Figure 4-5B, consisting of two five millisecond pulses of light at varying light intensity, separated by a 150 millisecond inter-stimulus interval. Putative T-type calcium channel bursts, shown in red (Figure 4-5D), were classified as any set of spikes where the first spike is preceded by 100 milliseconds of silence or more and every subsequent spike in the burst is separated by an interspike interval that is less than 4 milliseconds (Lu et al., 1992; Reinagel et al., 1999). In response

to a weak light input, the cell responded occasionally to the stimulation. In response to the intermediate light intensity (middle), the cell responded reliably across trials, but with an approximately equal number of burst spikes in response to either pulse (red spikes in the raster plot belong to a burst). In response to a higher light intensity, the bursting response to the second stimulus was facilitated relative to the first stimulus. Across neurons, the number of thalamic spikes evoked in response to the second stimulus was plotted against the number of thalamic spikes elicited in response to the first stimulus for varying light intensity (Figure 4-5E, left, N = 11 neurons). In contrast to the cortical results, no strong suppression or facilitation of the evoked thalamic spike count in response to the optical stimulus occurred, as all data points were approximately on the unity line (Figure 4-5E, left, black diagonal line; n = 11 neurons, p=0.47, three-way ANOVA). However, when plotting the burst ratio, defined as the number of burst spikes divided by the total number of spikes, of the evoked response to the first pulse versus the evoked response to the second pulse, there is a facilitation of the bursting dynamic (Figure 4-5E, middle; n = 11 neurons, p=2.79e-4, three-way ANOVA). Furthermore, the first spike latency in response to the second stimulus was longer than for the first stimulus, consistent with the slow calcium dynamics underlying a burst response that increases latency (Figure 4-5E, right; n = 11 neurons, p=0.001, three-way ANOVA). Given that the absolute number of spikes did not exhibit strong interactions between the first and second stimulus, but the bursting activity was reliably enhanced in response to the second stimulus, we suggest that thalamic bursting dynamics induced by the paired pulse paradigm could underlie the facilitation dynamics in cortex. Specifically, we hypothesize that the interactions between VPm and nRT will enhance bursting at inter-stimulus intervals on the order of 100 - 150 milliseconds (see Discussion). Note that there was no strong suppression dynamic in the thalamic neurons. We propose that, at least in part, the cortical suppression dynamic is due to rapid synaptic depression (see Discussion).

### 4.3.5 Modulation of thalamic state eliminates facilitation dynamic

To directly test the role of thalamic bursting on cortical facilitation dynamics, we transitioned from using optogenetics to drive the thalamic neurons (Figure 4-5) to using the optogenetics in a more subtle way to modulate the state of the thalamus (Figure 4-6). Thalamic state is believed to play a critical role in the nonlinear dynamics of the cortical response (Sherman, 2001a). Previous work in the rodent vibrissa system has shown that optogenetic depolarization of the thalamus is sufficient to shift thalamic firing modes from burst to tonic (Whitmire et al., 2016) as well as cortical state from synchronized to desynchronized (Poulet et al., 2012). Here, we experimentally depolarized the state of the thalamus optogenetically to shift the firing mode while quantifying the role of thalamic state on the generation of the cortical facilitation dynamic in response to thalamic microstimulation.

Under anesthesia, the VPM neurons were principally in the burst firing mode where the neuron fires classically defined bursts of spikes in response to a stimulus (Figure 4-6A, left). Using the same experimental setup as before, an optical fiber attached to an electrode was used to deliver a constant amount of light to chronically depolarize the thalamic neurons and move them into the tonic firing mode (Figure 4-6B, left). The optically depolarized state led to increased firing rates and decreased bursting relative to the baseline condition, as described previously (Whitmire et al., 2016). To illustrate the difference in firing statistics between these two modes, we analyzed the inter-spike interval distributions. For each spike, the time since the previous spike (previous ISI) and the time until the next spike (next ISI) are plotted against each other to investigate temporal patterns in the spiking data. Within these axes, the red boxes indicate a classically defined T-type calcium channel burst, where the box in the lower right corner signifies the start of a burst with a long (>100ms) previous ISI followed a short (<4ms) ISI, and the box in the lower left corner contains any subsequent spikes in the burst. The final spike in the burst will lie along the left axis. In the burst firing mode, a large portion of the spikes (52% in this example) are

classified as part of a burst (Figure 4-6A, right). The tonic firing mode, however, has a much smaller proportion of spikes classified as burst spikes, and instead the majority of the spikes lie in a cloud along the diagonal of the axes (Figure 4-6B, right, 3% in this example).

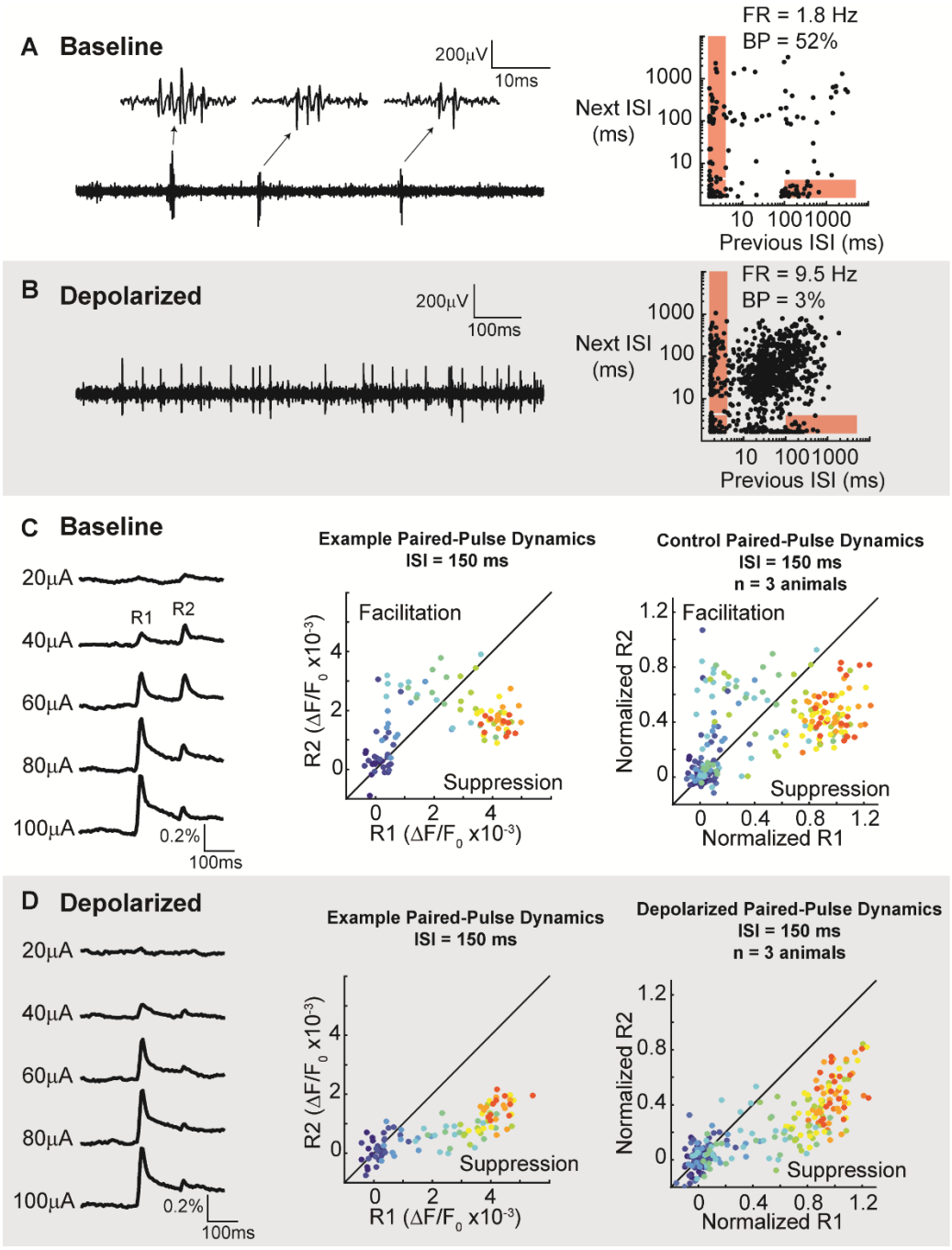


**Figure 4-6: Depolarization of the thalamus eliminates thalamic bursting and cortical paired-pulse facilitation.** A. Under anesthesia, thalamic neurons spontaneously burst,

firing multiple action potentials in quick succession (left). For each spike, the interspike interval to the previous spike is plotted against the interspike interval to the next spike. The red boxes outline spikes that could make up a burst. In the anesthetized state, the proportion of spikes that make up bursts is 52% (right). B. When depolarized through optogenetic manipulation, the thalamic neurons switch to a tonic firing mode (left) and the majority of spikes occur in tonic firing, and very few (3%) occur during bursts (right). C. Example of the mean cortical response, as measured through VSDI, to pairs of thalamic microstimuli with increasing strength (inter stimulus interval is 150 ms). As described earlier, facilitation occurs at sub-threshold currents whereas suppression characterizes supra-threshold currents in the control state (middle), and this is consistent across animals (right, n = 3 animals). D. When the thalamus is depolarized, there is no longer facilitation in the evoked cortical response (left). In an example recording with thalamic depolarization, the cortical response undergoes paired-pulse suppression for all current intensities (middle), and this is consistent across animals (right, n = 3 animals). The data are normalized with respect to the maximum response amplitude within that experiment.

Using depolarizing opsins, we controlled the relative depolarization of the thalamus to directly investigate the effect of thalamic state on neural activity propagation in the thalamocortical circuit. Voltage sensitive dye imaging was used to record the cortical response to thalamic microstimulation in the baseline anesthetized state (Baseline) and the optogenetically depolarized state (Depolarized). Consistent with our earlier data (Figure 4-3C), the cortical response to thalamic microstimulation in the baseline anesthetized state (Baseline) exhibited bimodal nonlinear dynamics where intermediate current amplitudes elicited facilitation dynamics while strong current amplitudes elicited profound suppression (Figure 4-6C).

If the cortical facilitation dynamic were caused by thalamic bursting, then the optogenetic depolarization of the thalamus, which prevents burst firing by inactivating the T-type calcium channels and preventing activation of the h-current at hyperpolarized potentials, would also prevent the cortical facilitation. Indeed, this was the case. Figure 4-6D presents the matched experiment to Figure 4-6C, but under optogenetic depolarization (Depolarized state). In this case, regardless of the stimulus intensity or

response amplitude, the response to the second stimulus was suppressed relative to the response to the first. This occurred reliably across trials and experiments, as the overwhelming majority of data points fell below the unity line (Figure 4-6D, center and right). Importantly, the response to the first stimulus was similar in both the control and the depolarization condition ($p>0.05$, Wilcoxon rank sum test) and therefore only the response to the second stimulus was affected. By manipulating the state of the thalamus, and therefore the associated bursting activity, the nonlinear propagation of neural activity within the thalamocortical circuit shifted from a facilitative dynamic in the anesthetized control condition to a suppressive dynamic in the depolarized tonic thalamic state condition.

## 4.4 Discussion

Across nearly all sensory modalities, the thalamus is a common stage of processing that links the peripheral sensory world to the cortex. Before reaching the thalamus, sensory information is transduced at the receptor and processed by a diverse set of pre-thalamic circuits. For example, in the visual system, a significant amount of processing occurs at the periphery where photons are transduced into electrical signals (Schnapf et al., 1990) before a network of excitatory and inhibitory interactions in the retina shape information flow to the visual thalamus (Laughlin, 1987). In the somatosensory pathway, the pre-thalamic processing is arguably less complex where mechanical deformations at the whisker follicle are transduced by sensory neurons (Lottem and Azouz, 2011) that synapse directly in the brainstem before the sensory information is transmitted to the thalamus (Diamond et al., 2008b). The first order neurons in the vibrissa pathway encode an incredibly precise representation of the relevant features of the whisker movement (Bale et al., 2015; Jones et al., 2004) that is transformed by the highly ordered brainstem circuitry (Sakurai et al., 2013). Although not historically viewed as such, the transformation from the brainstem to thalamus actually represents a significant stage of sensory processing (Sosnik et al., 2001).

Therefore, observations of thalamic and cortical activity are always confounded by pre-thalamic dynamics, making it difficult to establish what happens where. Here, we used a range of experimental tools and compared response properties across different conditions in the intact circuit in-vivo, to ultimately disentangle the simplest aspects of these observed dynamics.

### 4.4.1 The role of thalamic firing modes in thalamocortical information transmission

It has long been hypothesized that the distinct firing modes of thalamus, known as burst and tonic firing modes, present a mechanism to differentially transmit information to cortex. While the transition between firing modes, or thalamic states, can be achieved through a variety of natural and artificial mechanisms, the impact on information transmission remains speculative. Prior to the development of optogenetic tools, the primary method to control thalamocortical state was through the activation of the natural neuromodulatory arousal mechanisms in the brain (M. A. Castro-Alamancos, 2002; Goard and Dan, 2009; Llinas and Steriade, 2006). However, with the advent of optogenetics, it has become possible to quickly and easily shift the thalamocortical state locally and bidirectionally. Activating the reticular thalamus, or hyperpolarizing the thalamocortical projection nuclei of the thalamus, increases both bursting activity in the thalamus and spindle generation in the local field potential in cortex (Halassa et al., 2011). On the other hand, direct depolarization of the thalamus causes the transition from burst to tonic firing rate (Whitmire et al., 2016), producing the classically described desynchronized state (Poulet et al., 2012). Yet, in neither case has the effect on the propagation of stimulus-evoked activity been quantified. Here, we directly tested the role of thalamic state in the propagation of neural activity in response to thalamic microstimulation during the tonic and burst firing modes of the thalamus.

In the burst firing mode (i.e. the baseline anesthetized state), thalamic microstimulation activated bimodal nonlinear cortical dynamics with facilitation of sub-

threshold inputs and suppression of supra-threshold inputs in the cortical response. Artificial stimulation of the thalamus causes extreme precision of the thalamic spiking output relative to whisker driven activity (Millard et al., 2015). When considered across a population of thalamic neurons, the extreme synchrony induced by artificial stimuli enhances the strength of both the feedforward input to cortex and the input to the feedback pathway with the thalamic reticular nucleus (nRT), which is the only known source of inhibition to the VPm (Pinault, 2004). We propose that this strong synchronous activation of the thalamic reticular nucleus will elicit a robust inhibitory feedback response to the VPm neurons. In the context of the paired-pulse stimulus, this nRT-mediated inhibition will strongly hyperpolarize the VPm neurons shortly after the first stimulus, which will prime the T-type calcium channels to open. The hyperpolarizing input from nRT will also activate h-currents which will depolarize the neurons and prepare the thalamus to burst (Lüthi and McCormick, 1998). When the second stimulus arrives 100-150 milliseconds later, after the inhibition has decayed, the current pulse will provide the necessary depolarizing input to elicit a strong bursting response in the thalamic projection neurons. The facilitation of bursting in response to the second stimulus could therefore underlie the facilitation dynamic seen in cortex. Recent biophysical modeling of the thalamocortical circuit also suggests that feedback from nRT could provide a mechanism for facilitated thalamocortical activation due to low-threshold bursting for stimuli arriving at approximately 10 Hz (Willis et al., 2015). We directly tested the role of bursting in the facilitation dynamic by optogenetically depolarizing the thalamus to reduce thalamic bursting, as we have done previously (Whitmire et al., 2016). As predicted, the cortical facilitation dynamics were eliminated in the depolarized thalamus condition. By directly depolarizing the VPm neurons, we propose that we were able to counteract the stimulus-evoked inhibition from nRT, preventing both the activation of h-current and the opening of the T-type calcium channels in response to the second stimulus. This is consistent with previous work showing a reduction in the paired pulse facilitation of the cortical response

to thalamic microstimulation during natural transitions of an awake animal between quiescent and active states (Castro-Alamancos and Connors, 1996b), which would presumably lead to a shift in thalamic state.

Importantly, a shift in thalamic state leads to a shift in the overall amount of thalamic spiking activity. In the tonic mode, the increased firing activity will likely cause any thalamocortical synapses to be in a more depressed state and therefore could play a role in the elimination of the facilitation dynamic in the transition from burst to tonic firing. While we could not control for the overall firing rates in the two thalamic firing modes, we did perform an experiment to test the role of the synapse state in the generation of the facilitation dynamic (Figure 4-3D). In this paradigm, the cortical response to thalamic microstimulation was compared between current pulses presented in isolation and those preceded by a facilitating current pulse amplitude (60μA). When presented in isolation, the thalamus should be in the Baseline anesthetized condition (burst firing mode) such that the thalamocortical synapses are not pre-depressed. The cortical response to the facilitating current pulse is minimal, but still could potentially impact the thalamocortical synapses leading to a synaptically depressed state. However, when presented 150 milliseconds after the facilitating current pulse, the evoked cortical response was facilitated across current amplitudes. Given that the thalamocortical synapses were either in similar or slightly depressed states relative to the stimulus isolation condition, this result suggests that the facilitation dynamic cannot be attributed to short term depression dynamics. Furthermore, when using optogenetics to modulate the state of the thalamus, the light stimulus began at least 200 milliseconds prior to the onset of the first electrical stimulus in the paired stimulus train. As such, the thalamic neurons should have been optically depolarized, and the synapses sufficiently depressed, at the time of the first stimulus presentation. However, a comparison of the evoked cortical response to the first electrical stimulus in the Baseline and Depolarized condition found no difference. This suggests that it is the dynamics of this temporal pattern of stimuli that elicits the facilitation dynamic. While the state of the

synapse at the time of stimulus arrival will certainly play a critical role in whether or how that information is transmitted, and likely underlies the paired-pulse suppression dynamics presented here, it cannot explain the facilitation dynamic.

### 4.4.2 Alternative mechanisms that could underlie the cortical facilitation dynamic elicited by artificial thalamic stimulation

While we explicitly tested modulations to thalamic bursting as a mechanism to explain the facilitation dynamics described here, there are at least three alternative candidate mechanisms through which the artificial stimuli could have recruited the additional nonlinear dynamics: 1) simultaneous activation of axons from the postero-medial (POm) nucleus in the thalamus, which has been associated with the thalamocortical augmenting response (Castro-Alamancos and Connors, 1996b), 2) non-specific circuit excitation through artificial stimulation, or 3) preferential activation of class II, facilitating synapses that extend directly from VPm to layer 2/3 cells (Viaene et al., 2011).

The thalamocortical augmenting response was originally described more than 70 years ago (Dempsey and Morison, 1943), but has more recently been studied in the rodent whisker system (Castro-Alamancos and Connors, 1996b). The augmenting response is characterized by progressive facilitation of the cortical response to thalamic microstimulation for interstimulus intervals between 50 and 200 milliseconds, and has been shown to occur in the awake animal (Castro-Alamancos and Connors, 1996b). The exact mechanism of the augmenting response is disputed, however, with some pointing to cortical mechanism, while others propose the dynamics are thalamic in origin. Principally, though, the augmenting response is believed to be a product of bursting thalamocortical recipient cells within layer 5 of cortex. In the rodent vibrissa system, this has primarily been considered through stimulation of the POm nucleus, which projects to layer 5 of cortex as a part of the paralemniscal pathway, whereas VPm primarily projects to layer 4 (although recent evidence has also demonstrated direct projections from VPm to layer 5

(Constantinople and Bruno, 2013)). Due to the close proximity of POm and VPm, it is possible that thalamic microstimulation recruited the augmenting response by activating POm axons passing through/near VPm. However, given the observation of facilitated bursting in the VPm units, facilitation caused by optogenetic stimuli (which are believed to stimulate axons to a lesser extent), and the elimination of facilitation induced by electrical stimulation with modulation of thalamic state (which would not directly impact the region of tissue activated by electrical stimulation), the classical augmenting response likely was not the primary mechanism of the facilitation.

Although commonly used, electrical stimulation is nonspecific in its excitation such that antidromic activation is possible. In the context of the facilitation dynamic explored here, antidromic stimulation of cholinergic axons projecting to thalamus could play an important role by subsequently providing cholinergic activation to cortex. Cholinergic activation has been shown to increase firing rates in the VPm nucleus of the thalamus which shifts the cortex into a desychronized state (Hirata and Castro-Alamancos, 2010). At the level of cortex, continuous optogenetic activation of the basal forebrain led to an increase in both the spontaneous and stimulus evoked firing rate (Pinto et al., 2013). Furthermore, in conjunction with sensory stimulation, cholinergic activation of cortex has been shown to facilitate the responsiveness to sensory inputs (Metherate and Ashe, 1993). However, in contrast to the prolonged cholinergic activation used in these prior studies, our electrical stimulation of thalamus provided brief (400 μs) stimuli that would limit the temporal duration of any potential effects of cholinergic axon activation. Furthermore, as described above, with optogenetics, the activation is restricted to neurons expressing the opsin (and therefore will not activate the nearby terminals). Therefore the similarity in the evoked response for both electrical and optical stimulation suggests that antidromic activation of brain regions projecting to thalamus by electrical stimulation, such as cholinergic neurons in the basal forebrain and brainstem, likely do not play a significant role in the dynamics described here.

Direct synaptic connections from VPm to layer 2/3 have recently been reported with facilitation properties such that 10Hz stimuli delivered to VPm in vitro elicited facilitation of the post synaptic potential in the layer 2/3 neurons (Viaene et al., 2011). This was in contrast to the synaptic response in layer 4 neurons, which demonstrated suppression. While this may have played a role in the cortical facilitation dynamic, the elimination of facilitation with increased thalamic firing rates in VPm during optogenetic depolarization suggest that facilitating synapses in L2/3 alone are insufficient to explain the observed trends. As such, we propose that thalamic bursting coupled between the VPm and nRT thalamic nuclei is the fundamental mechanism underlying the paired pulse facilitation dynamic seen for artificial stimuli.

### 4.4.3 Differential circuit activation by sensory and artificial stimulation

The profound facilitation dynamics in cortex in response to this paired pulse paradigm were primarily recruited by direct stimulation of the thalamic neurons. In building a comparison between the sensory stimulation and the artificial stimulation, we have recently published a fairly extensive analysis of the evoked cortical response (Millard et al., 2015). We found that both sensory and artificial stimuli can elicit a full range of cortical response amplitudes, but that they vary in the variability of the evoked cortical response. To identify a potential cause for this difference in variability trend, we directly compared the thalamic response to a single optical stimulus and a single whisker stimulus. We found that the optogenetic activation of the thalamic neurons led to a highly precise spiking response, which we modeled as a potential factor underlying the variability trends seen cortically. In this work, we hypothesized that synchronous activation of the thalamic neurons by the optogenetic activation (and likely the electrical stimulation) provided a strong input to the reticular thalamus (nRT), which facilitated bursting in response to the second stimulus, whereas the effects of whisker stimulation were confounded by pre-thalamic processing. Pre-thalamic processing represents an important stage of encoding in

the whisker pathway that is not activated by direct thalamic stimulation. While some individual trials showed facilitation, whisker stimulation primarily led to suppression dynamics in the cortical response. However, the dynamics of the whisker to barreloid response are difficult to separate from the thalamocortical dynamics we sought to quantify here, leading to uncertainty about the source of the suppression dynamic seen for sensory stimulation. A particularly relevant candidate mechanism is depression at the trigeminothalamic synapse (Deschênes et al., 2003) such that the synaptic drive in thalamus in response to the second sensory stimulus would be lower than the synaptic drive in response to the first sensory stimulus leading to suppression dynamics before the signal even reaches thalamus. Importantly, synaptic depression is particularly salient in the anesthetized animal where spontaneous firing rates are considerably lower than in the awake animal (Borst, 2010; Reinhold et al., 2015). We propose that the response to each whisker stimulus in the paired pulse train likely elicits different responses at the level of the thalamus due, at least in part, to the synaptic depression dynamics that cannot be decoupled from the thalamocortical processing. Direct stimulation of the thalamic neurons using artificial stimulation techniques allowed us to override any potentially suppressive dynamics that occur in pre-thalamic processing to focus on the dynamics established in the thalamocortical processing. In this restricted paradigm, we were able to recruit profound facilitation dynamics. However, the 150 millisecond interstimulus interval that demonstrated cortical facilitation in response to artificial thalamic activation here has also been identified as relevant from extracellular recordings from cortical layer 4 in response to time varying pairs of whisker stimuli (Boloori et al., 2010; Boloori and Stanley, 2006; Webber and Stanley, 2004). Rather than simply showing a monotonic recovery from suppression in the cortical spiking activity with increasing duration between the first and the second whisker stimulus, the equivalent measures of paired pulse ratio in these studies had a local maximum at stimulus intervals of 100-150 milliseconds for different whisker deflection directions (Webber and Stanley, 2004) and different stimulus velocities (Boloori

et al., 2010). These results suggest that the temporal spacing of stimulus patterns is critical in shaping the neural dynamics of the sensory pathway and that this 100-150 millisecond interstimulus interval is critical for sensory information transmission. When the sensory stimulus pattern is expanded to include a third whisker stimulus, the cortical response can demonstrate facilitated spiking as the dynamics interact to drive a "suppression of suppression" (Boloori and Stanley, 2006; Webber and Stanley, 2006). When extended to even more complex patterns of stimulation, this can create fairly complex, yet reliable response patterns. While the pre-thalamic processing may restrict the intensity of the facilitation dynamic seen cortically in response to two whisker stimuli, these complex interactions across more naturalistic stimuli could provide a mechanism to facilitate information that arrives to thalamus at a frequency of approximately 10 Hz. In the vibrissa pathway, this stimulus frequency becomes very relevant where active sensing is achieved through sweeping whisking motions at 5-15 Hz (Berg and Kleinfeld, 2003).

In probing neural circuits, simple paired-pulse paradigms have built the foundation for our understanding of more complex sensory evoked cortical dynamics (Simons, 1985). Here, using a combination of optogenetic thalamic state modulation and electrical paired-pulse stimulation of thalamus, we have identified the bursting dynamics of the thalamic circuitry as a potential mechanism to facilitate information transfer to cortex. While these thalamic state transitions are not entirely understood, it is evident that thalamic state transitions can occur rapidly as a function of both sensory input and neuromodulatory influences. Combined with the continuous nature of arriving sensory inputs, the rapid state transitions may selectively facilitate the transmission of information related to particular patterns of sensory inputs over this timescale. The simple dynamic interaction identified here must be expanded to incorporate the temporal interactions across stimuli that capture the interplay between excitatory and inhibitory circuitry as the patterns of stimuli become increasingly complex (Boloori et al., 2010). When combined with the state dependence of the neural dynamics, temporal patterns of stimulation are capable of eliciting diverse

cortical responses, which are ultimately the likely substrate upon which sensory percepts are built.

# CHAPTER 5 STATE-DEPENDENT FEATURE SELECTIVITY

## 5.1 Introduction

Sensory information in the thalamocortical pathway is represented by precise temporal patterns of neural activity. In the thalamus, neurons are capable of firing in two distinct patterns known as burst and tonic firing. It has been hypothesized that these two firing modes represent a fundamental ability of the thalamus to gate information flow to cortex (Sherman, 2001b). The burst mode is classically described as providing a strong signal to cortex that is not representative of specific stimulus information but instead signals a change in stimulus statistics while the tonic mode is described as relaying detailed sensory information (Sherman, 2001a, 2001b). Our results from CHAPTER 3 are consistent with this view for punctate whisker stimuli that are distinct from ongoing stimulus statistics (Whitmire et al., 2016). However, the relationship between burst and tonic firing in representing temporal stimulus response properties during ongoing sensory stimulation remains unknown. Furthermore, for a cortical neuron interpreting these two patterns of neural firing, the information about the same stimulus could be represented with two different temporal patterns of spiking inputs. The state dependent processing of the thalamus could therefore impact the representation of sensory information in the thalamocortical circuit through alterations to the temporal spiking patterns.

Here, we quantify the role of thalamic state transitions on temporal feature selectivity in the thalamocortical circuit of the rodent whisker pathway. The spatiotemporal tuning of neurons in the rodent vibrissa thalamocortical circuit make this an ideal model system to pursue questions of state-dependent encoding. The whisker pathway has obvious spatial tuning both anatomically (Woolsey and Van der Loos, 1970) and functionally (Brecht and Sakmann, 2002; Ramirez et al., 2014) as well as temporal feature selectivity (Estebanez et al., 2012; Petersen et al., 2008). In this study, we assessed the temporal feature selectivity using traditional reverse correlation techniques. First, we found that

feature selectivity in thalamic units (VPm) and cortical fast spiking units (FSU) was very similar. Then, we found that bursts in the thalamus do not have clear feature selectivity as computed from the spike triggered average and that this leads to a degradation of the recovered linear filter in primary somatosensory cortex (S1). Furthermore, the shift to a burst state in thalamus actually leads to a reduced stimulus sensitivity as quantified by the nonlinearity. This is in contrast to what we might have expected for burst spikes, but is consistent with the burst state being a poor representation of the precise sensory information. Taken together, these results suggest an interesting relationship between tonic spikes that are faithfully representing the stimulus and burst spikes that are also representative of the stimulus but at a lower temporal precision.

## 5.2 Methods

### 5.2.1 Acute Surgery

All procedures were approved by the Georgia Institute of Technology Institutional Animal Care and Use Committee and were in agreement with guidelines established by the National Institutes of Health. Female albino rats (Sprague-Dawley, 250-300g) were used for these experiments. Animals were initially anesthetized using 4-5% isoflurane and maintained at 2-3% until the tail vein was inserted. The anesthesia was then switched to a fentanyl cocktail (fentanyl (5 µg/kg), midazolam (2 mg/kg), dexmedetomidine (150 µg/kg)) continuously administered intravenously using a drug pump throughout the duration of the experiment. Anesthesia depth was monitored by heart rate, respiratory rate, and toe pinch reflex. Body temperature was maintained using a feedback controlled heating pad (FHC, Inc.). The animal was secured in a stereotaxic device (Kopf Instruments) using penetrating ear bars on a vibration isolation table in an electromagnetically shielded surgery suite. A craniotomy was performed (2-4 mm caudal to bregma, 1.5-3.5 mm lateral to the midline) to permit access to the left ventral posteromedial nucleus (VPm) of thalamus. In a subset of animals, a second craniotomy was performed (1-3 mm caudal to

bregma, 4.5-6 mm lateral to the midline) to permit access to the left primary somatosensory cortex (S1). The craniotomy was filled with saline to prevent drying of the cortex. At the termination of the experiment, the animal was euthanized with an overdose of sodium pentobarbital (euthasol, 0.5 mL at 390 mg/mL). All optogenetically transfected animals were perfused and their brains were imaged for verification of opsin location and cortical probe location (in the subset of cortical experiments).

### 5.2.2 Electrophysiology

Tungsten microelectrodes were lowered into the brain (depth: 4.5-6 mm) using either a hydraulic micropositioner (Kopf) or a motorized micropositioner (Luigs-Neumann) to record extracellularly from VPm neurons. Recordings were made using a 32 channel Plexon data acquisition system (Plexon, Inc.) or a 64-channel TDT data acquisition system (Tucker Davis Technologies). Multielectrode probes (A1x32-10mm-50-177, NeuroNexus) were lowered perpendicular to S1 (45° relative to vertical; depth: 2 mm). Importantly, units were analyzed thus far without respect to the spatial location of the unit. Cortical units were only subdivided based on the shape of the waveform. The topographic location of the electrode was identified through manual stimulation of the whisker pad. Upon identification of a whisker sensitive single unit, the primary whisker was threaded into the galvo motor to permit stimulation of a single whisker.

### 5.2.3 Sensory Stimulus

Mechanical whisker stimulation was delivered using a precisely controlled galvo motor (Cambridge Technologies). The galvo motor was controlled using custom software (Matlab, Mathworks) to provide millisecond precision. The mechanical stimulus applied to the whisker in the rostral-caudal direction consisted of sensory white noise (low pass filtered at 200 Hz due to mechanical limitations of the galvo motor, standard deviation of the noise was 0.172°). The correlation in the sensory white noise stimulus limits the temporal resolution of the recovered linear filters. Multiple white noise stimuli were

administered across the reported dataset. Each included a repeated stimulus segment (frozen white noise) and multiple novel stimuli (unfrozen white noise). In the subset of optogenetics experiments, an additional consisted of sensory white noise stimulation during hyperpolarizing light administration.

### 5.2.4 Viral injection surgeries

All surgical procedures followed sterile protocol. Animals were initially anesthetized using 4-5% isoflurane and were maintained at 2-3%. A small craniotomy was made above VPm (3 mm lateral, 3 mm caudal to bregma). A 10 µL syringe (Neuros Syringe, Hamilton, Inc) filled with the virus (rAAV5-CamKIIa-Jaws-KGC-GFP-ER2 or rAAV5-CamKIIa-eNpHR3.0-EYFP, UNC Viral Vector Core Services) was lowered to depth of 5.2 mm before injecting 1 µL of virus at a rate of 0.2 µL/min (iSi system, Stoelting). The syringe remained in place for five minutes after the injection was complete to allow the virus to diffuse. After the syringe was removed, the hole in the skull was filled with bone wax and the skin was closed using wound clips. The animal was given buprenorphine for pain management (0.03 mg/kg). Animals were monitored daily following injection surgery. Wound clips were removed at 10-13 days post-surgery. Further experimentation resumed following full recovery and full opsin expression. Opsin expression was fully realized at 2-3 weeks post-surgery.

### 5.2.5 Optical Stimulation

Optical manipulation was administered with a controlled pulse of light through a custom optrode consisting of an optical fiber (200µm diameter; Thorlabs) and an electrode (Tungsten microelectrode; FHC) that was lowered into the VPm. Upon identifying a whisker sensitive cell, light sensitivity was assessed by the post-inhibitory rebound spiking response using a train of 250 millisecond Hz light pulses ($\lambda$ = 590 or 617nm for Halorhodopsin and Jaws, respectively). The optical & whisker stimulus consisted of the

white noise stimulus described above embedded in continuous light waveforms (50 mW/mm2).

### 5.2.6 Awake Electrophysiology

All experimental and surgical procedures were carried out in accordance with standards of the Society of Neuroscience and the German Law for the Protection of Animals. Awake electrophysiological recordings were obtained from two female albino rats (Sprague-Dawley). The basic procedures for head-cap surgery, habituation to head-fixation, and behavioral training followed previously published methods (Schwarz et al., 2010). Electrophysiological recordings were obtained while the rats were performing a detection of change task (Waiblinger et al., 2015a).

### 5.2.7 Data Acquisition

Data was recorded on multiple electrophysiology systems including Plexon and Tucker Davis Technologies data acquisition systems. Spike sorting for single channel recordings was performed online and validated offline using Waveclus (Quiroga et al., 2004). Spike sorting for multichannel electrodes was performed offline using the KlustaKwik software suite (Rossant et al., 2015). Unit quality was assessed based on the waveform of the SNR (peak-to-peak voltage of the mean waveform divided by the average standard deviation of the noise across the waveform snippet) and the fraction of spikes occurring within the refractory period. Cortical units were subdivided into regular spiking units (RSU) and fast spiking units (FSU) based on the temporally trough-to-peak delay (Bartho et al., 2004). Units with a trough-to-peak delay of less than 0.5μs were classified as FSUs while units with a trough-to-peak delay greater than 0.5μs were classified as RSUs.

### 5.2.8 Data Analysis

5.2.8.1 Spike triggered analysis

Feature selectivity was estimated for each recorded unit using traditional reverse correlation techniques to recover the spike triggered average (STA) (Schwartz et al., 2006).

$$STA = \frac{1}{N}\sum_{j}\vec{s}(t_j)$$

Where N is the number of spikes and $\vec{s}$ is the stimulus segment immediately prior to each spike (spike-triggered ensemble, STE). The burst-triggered average was computed using only the spike times from the first spike in each burst. The baseline/hyperpolarized condition triggered averages were computed from all spikes in a given stimulus condition. To make comparisons across the population of recorded neurons, a principal component analysis was performed across all recovered spike triggered averages. The two principle components that explained the majority of the variance in the spike triggered averages across the population of recovered spike triggered averages are plotted in the chapter figures.

The non-linearity ($P(spike|\vec{s})$) was estimated as the ratio of the probability of spike-trigged stimuli ($P(\vec{s}|spike)$) to the probability of any stimulus segment in the stimulus ($P(\vec{s})$) multiplied by the mean firing rate of the neuron($P(spike)$) (Schwartz et al., 2006).

$$P(spike|\vec{s}) = \frac{P(\vec{s}|spike) * P(spike)}{P(\vec{s})}$$

5.2.8.2 Temporal precision in the STA

Unlike punctate stimuli that have a distinct onset, the neural response to continuous sensory white noise is ongoing without any clear 'events'. Instead of using a first-spike latency method that would be appropriate for distinct sensory events, we developed a method to compute the precision of the spiking activity relative to the average response (STA). The

spike triggered ensemble (STE) is an array of stimulus segments for each spike while the spike triggered average (STE) is simply the average over all spikes. Here, we computed the correlation between the STA with each individual STE stimulus segment and extracted the peak correlation value and the peak correlation temporal lag. The peak correlation value identifies how similar an single instantiation of the stimulus segment is to the spike triggered average while the temporal lag describes how precisely that neuron is firing. A delta function distribution for the temporal lag would describe an infinitely precise neuron. As the width of the temporal lag distribution increase, the jitter in the neural response is increasing which suggests reduced precision in the noise-evoked stimulus response.

5.2.8.3 Cortical state classification

Cortical synchronized/desynchronized state was classified as the ratio of the power in the local field potential (LFP) in the 2-5 Hz band divided by the total power in the 2-50 Hz band (Saleem et al., 2010). Cortical up/down state was classified from the continuous local field potential (LFP) recording on a deep probe electrode contact (Saleem et al., 2010). Briefly, the LFP was filtered into multiple low frequency bands (<2Hz, 2-4Hz) and a state variable (sLFP) was estimated based on the phase of the oscillations (Figure 1-1). Each state transition was required to be at least 100 milliseconds in duration in order to remain classified to prevent artificially fast state switching due to spurious classifications. Importantly, the up/down state classification did not address all data points as typically approximately 1/3 of the data remained unclassified. In the example trace shown, the up, down, and unclassified time points are depicted as red, blue, and black, respectively. The inability to classify every time period does lead to some uncertainty in the exact transition times to an up or a down state.

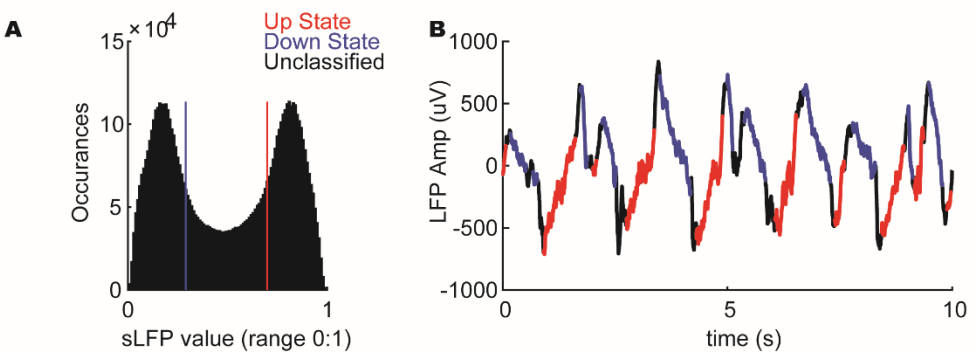


**Figure 5-1: Example classification of cortical state.** A. Distribution of sLFP (state variable) across all time points. Thresholds for classifying up and down states are shown in red and blue respectively. B. Example LFP trace with pseudo-colored state classifications (up: red, down: blue).

5.2.8.4 Burst classification

All thalamic spikes were classified as burst or tonic spikes by the classical bursting definition of two or more spikes with an interspike interval of less than four milliseconds with the first spike preceded by 100 milliseconds of silence (Reinagel et al., 1999). Burst ratio was quantified as the total number of burst spikes divided by the total number of spikes.

5.2.8.5 Spiking metrics

The spiking properties of each unit was analyzed using four metrics. The ISI ratio is defined as the total occurrences of interspike intervals (ISI) less than 15 milliseconds normalized by the total number of spikes from a given unit. The coefficient of variation is defined as standard deviation of the ISI divided by the mean ISI. The fano factor is defined as the standard deviation of the firing rate across trials in 8 millisecond bins divided by the mean firing rate across trials. The peak correlation is defined as the maximum correlation between two peristimulus time histograms (PSTH) computed from non-overlapping trials from the same unit.

## 5.3 Results

### 5.3.1 Thalamocortical States are linked during sensory stimulation

State-dependent activity in the brain is often described in terms of the cortical state. However, as we have discussed here, the thalamus is also capable of operating in distinct states and these thalamic state transitions could directly impact information transmission in the thalamocortical circuit. Experimentally, we measured the effect of spontaneous thalamic state transitions on encoding properties in the lemniscal thalamic nucleus of the rodent vibrissa pathway, the ventral posteromedial nucleus (VPm) simply by separating the firing modes into burst and tonic firing. However, classification of the thalamic state is more difficult on a single trial basis because thalamic LFP does not provide the same frequency signatures of state as are seen in cortical LFP. Ideally, we would like to estimate the probability of firing burst spikes or tonic spikes on a population level using the subthreshold membrane potential oscillations across thalamic neurons. However, there are practical limitations to implementing this experimental paradigm. Instead, we chose to pursue optogenetic modulation of the thalamic activity to bias the membrane potential towards the burst state during white noise stimulation. Previous work has shown that adaptive, or ongoing, sensory stimulation likely depolarizes cortical (Ramirez et al., 2014) and thalamic (Whitmire et al., 2016) neurons such that the evoked response to a white noise stimulus will evoke a more tonic spiking response in thalamus. Therefore, we used optogenetic hyperpolarization of the thalamic neurons to bias the noise-evoked spiking patterns towards burst firing (Figure 5-2A,E).

In a second set of experiments, cortical activity was recorded extracellularly while the state of the thalamus was manipulated optogenetically (Figure 5-2A). In this example histological image, both the tract of the cortical probe, which was inserted perpendicular to the cortical surface, and the opsin expression in the thalamic terminals of the cortical barrel can be visualized (Figure 5-2B). The thalamic state biased data allows for direct

comparisons between the thalamic 'baseline' condition (no optogenetic manipulation) and the thalamic 'hyperpolarized' condition (optogenetic hyperpolarization) on the evoked cortical response.

Although there is some understanding of thalamocortical oscillations in the context of sleep, we wanted to quantify how thalamic and cortical state co-vary during ongoing sensory stimulation. The state of the cortex is typically segmented into two distinct states knows as synchronized and desynchronized states with further classification of the synchronized state as up/down states (Saleem et al., 2010). The thalamus also operates in two distinct firing mode states known as the burst and tonic state (Sherman, 2001b). Importantly, the thalamus and cortex do not act independently. Instead, there is an interaction between state transitions in these two highly interconnected regions of the brain (Figure 5-2C).

To investigate the link between thalamic and cortical state, we first classified cortical state as synchronized or desynchronized using a ratio of low power frequency content in the LFP normalized by the total power content (power ratio, PR). The distribution of power ratios was unimodal and biased towards high PR (majority of the power was found in the low frequency band) suggesting that the recordings exhibited primarily synchronized dynamics (data not shown). This might be expected given that all cortical recordings were performed in the anesthetized animal where cortical activity is more synchronized than in the awake brain. Within the synchronized state, the membrane potentials of cortical cells are fluctuating between a hyperpolarized and a depolarized state, known as down and up states respectively. The state of the cortex at the time of stimulus presentation will directly impact the evoked neural response (Petersen et al., 2003b) In the absence of intracellular recordings, the state of the cortex can be estimated from the phase of the low frequency oscillations in the local field potential (Saleem et al., 2010). Therefore, we further classified the cortical LFP into up and down states (see methods). We then aligned the neural activity to the onset of the state transitions (either to an upstate

or to a downstate) and analyzed the average activity. The onset of the state transition was defined by the time when the state classifier identified an up or down state. The data presented here was collected during ongoing sensory white noise stimulation. The cortical LFP exhibited a clear negative peak at the onset of the up state, which was accompanied by an increase in cortical and thalamic firing (Figure 5-2D, red). The increase in both thalamic and cortical firing shows that the state of the cortex is correlated with the firing properties in thalamus. At the onset of the down state, there was a peak in the cortical LFP and a corresponding reduction in the cortical and thalamic firing activity (Figure 5-2D, blue). Interestingly, this also manifested as an increase in the thalamic bursting activity at the time of transition to a downstate (Figure 5-2D, bottom). The relationship between burst firing and the cortical state demonstrates how thalamic and cortical states may interact at the transitions between them. As a caveat here, the state transition times here were estimated from the phase of the local field potential. Therefore, it is likely that there is significant jitter in the true onset of an up or down state. However, despite this temporal jitter, up/down state transitions affect thalamic and cortical firing properties, suggesting that the effect size would be even larger with a more precise estimate of cortical state transition times.

Although the relationship between cortical membrane potential and cortical state has been well established (Petersen et al., 2003b; Sachdev et al., 2004), the correlation between subthreshold oscillations across thalamus and cortex or even within thalamus but across thalamic state transitions remains unclear. As discussed earlier, there are technical difficulties in estimating the state of the thalamus from a single extracellular recording. Therefore, we chose to bias the state of the thalamus using optogenetic manipulation. At the onset of the hyperpolarizing light, the thalamic neurons show a reduction in firing activity and an increase in bursting after approximately 200 milliseconds (Figure 5-2E, left) while the offset of the light evokes strong post-inhibitory rebound spiking (Figure 5-2E, right). This is consistent with what we expect to see from thalamic neurons due to

their bursting characteristics. In cortex, the onset of thalamic hyperpolarization during sensory stimulation leads to a transient increase in the probability of a down state while the offset of the thalamic hyperpolarization (and strong post-inhibitory rebound spiking in thalamus) causes a large increase in both cortical firing and the probability of being in a cortical upstate. This is consistent with the correlations between increases in thalamic firing at the start of an up state and decreases in thalamic firing at the start of a down state. While this bidirectional effect demonstrates the correlation between thalamic and cortical states and firing properties, it cannot establish causality for state transitions between the two structures. However, with causal manipulation of the thalamic state, we can begin to identify the properties of neural coding that can be attributed to the firing mode of the thalamus.

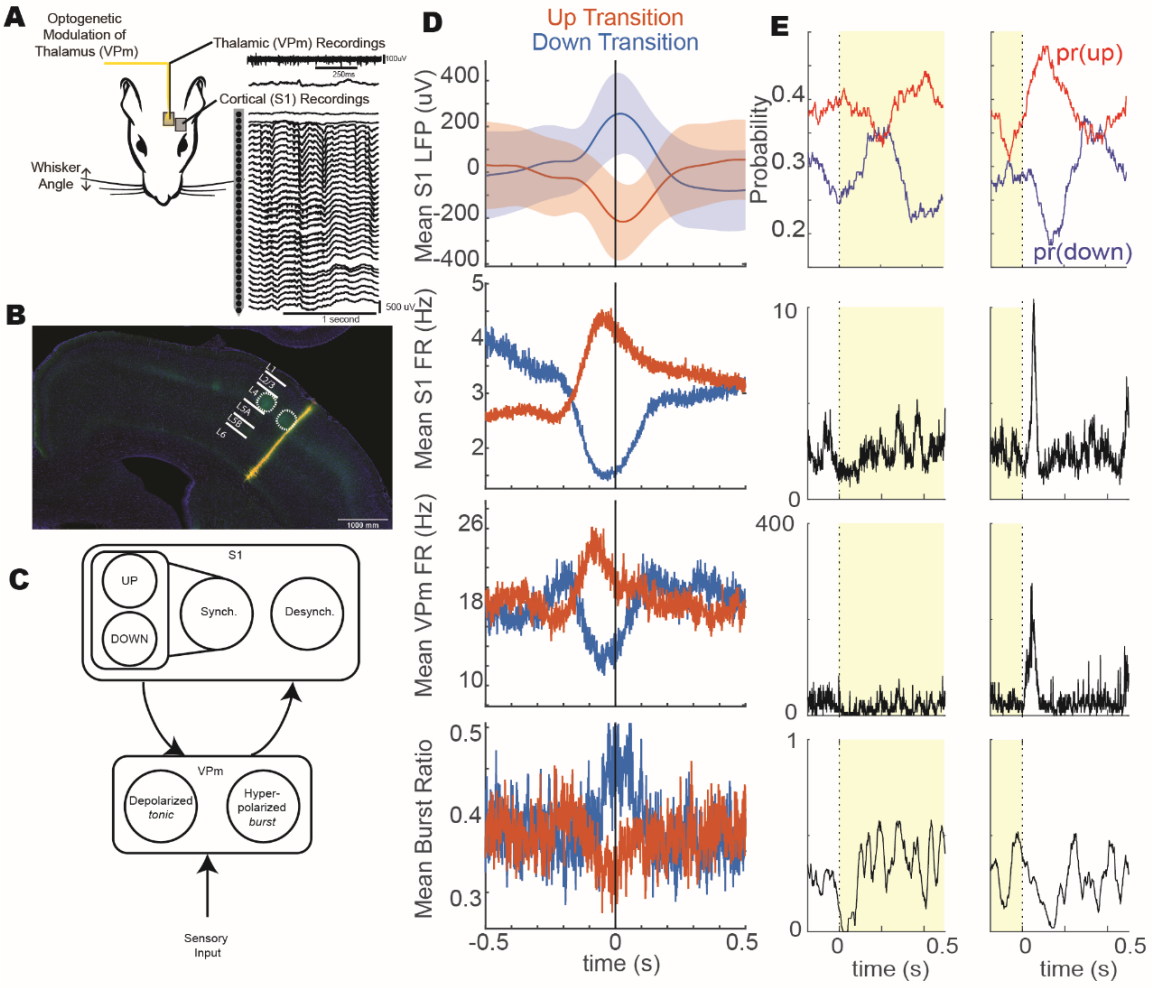

**Figure 5-2: Cortical and thalamic state transitions are linked.** A. Cortical probe recordings (A1x32-6mm-50-177) during thalamic state manipulation. Sensory stimulation applied with a galvo motor (Gaussian distributed white noise, LPF at 200 Hz). In a subset of animals transfected with Jaws, light modulation was applied via an optic fiber ($\lambda$ = 617nm). B. Example histology slice showing probe (DiI; yellow) and opsin expression in the terminals in S1 (green) in a 100µm brain slice stained with DAPI (blue). C. Thalamocortical schematic of state interactions. D. Mean Cortical LFP (n = 8 experiments), Mean S1 FR (n = 504 units), Mean VPm FR (n = 3 units) & Mean VPm BR (n = 3 units) triggered on cortical state transitions. All three thalamic units were collected simultaneously with the cortical probe recordings in topographically aligned barreloids. E. Mean Cortical LFP (n = 8 experiments), Mean S1 FR (n = 504 units), Mean VPm FR (n = 11 units) & Mean VPm BR (n = 11 units) triggered on thalamic state transitions imposed optogenetically.

### 5.3.2 Optogenetically imposed thalamic state manipulations

Given the observed relationships between state transitions in thalamus and cortex, this naturally begs the question as to whether this affects feature selectivity and what the relationship between feature selectivity in thalamus and cortex are. We first attack this through controlled manipulation of thalamic state. Before exploring the impact of optogenetic state manipulation of encoding, we first confirmed that optogenetically hyperpolarizing the thalamus is capable of changing the thalamic firing mode. For an example neuron, the evoked response to a frozen white noise segment is shown as a rastor plot across trials with the corresponding PSTH in each condition (Figure 5-3A). Burst spikes are pseudo-colored red. In the hyperpolarized condition (left), there is a much higher proportion of burst firing than in the baseline (not optogenetically manipulated, right) condition. The change in the spiking patterns can be visualized by looking at the inter-spike intervals (Figure 5-3B). In this plot, each dot represents a single spike that is plotted as a function of the time since the neuron last spiked (ISI pre) and the time until the next spike occurs (ISI post). In this plot, clustering along the axes is indicative of burst firing (grey boxes) while clustering along the diagonal is indicative of tonic firing. In the baseline

condition, there is some bursting activity but the response is primarily tonic while in the hyperpolarized condition, there is significant bursting activity. If we visualize the PSTH from these two conditions, the same points in the noise are driving firing activity in this neuron just with different firing patterns (Figure 5-3C). Across neurons, we can analyze the spiking properties for burst/tonic spikes and for hyperpolarized/baseline conditions. We first used a simple ISI ratio (number of spikes with an ISI less than 15 milliseconds divided by the total number of spikes) to quantify how 'bursty' the firing patterns were. When the thalamic spikes were classified as burst spikes, almost by definition the ISI ratio was higher (Figure 5-3D, ISI ratio left, $p<0.05$). Interestingly, there was a similar increase in burstiness in the cortical activity when the thalamus was hyperpolarized (Figure 5-3D, ISI ratio right, $p<0.05$). The variability of the spiking patterns, as assessed using the coefficient of variation and the fano factor, was also higher for burst spikes than tonic spikes and for thalamic neurons in the hyperpolarized relative to baseline condition (data not shown, $p<0.05$ Wilcoxon signed rank test). This increase in variability with a hyperpolarized thalamic state did not extend to cortical neurons (data not shown, p = n.s. Wilcoxon signed rank test). Finally, the reliability of the noise evoked response was measured as the peak correlation between the peristimulus time histogram for one half of the trials and the peristimulus time histogram for the second half of the trials. The tonic spikes had a significantly higher peak correlation than the burst spikes and correspondingly the baseline condition had a higher peak correlation than the hyperpolarized condition (Figure 5-3D, Peak Correlation, $p<0.05$). Taken together, these spiking statistics show that hyperpolarizing the thalamus leads to higher variability in the spiking patterns, as would be expected for the burst firing mode, as well as reduced reliability in encoding frozen white noise segments. This is consistent with the view that tonic spikes reliably transmit information about the sensory stimulus while bursts in this context seem to be more variable.

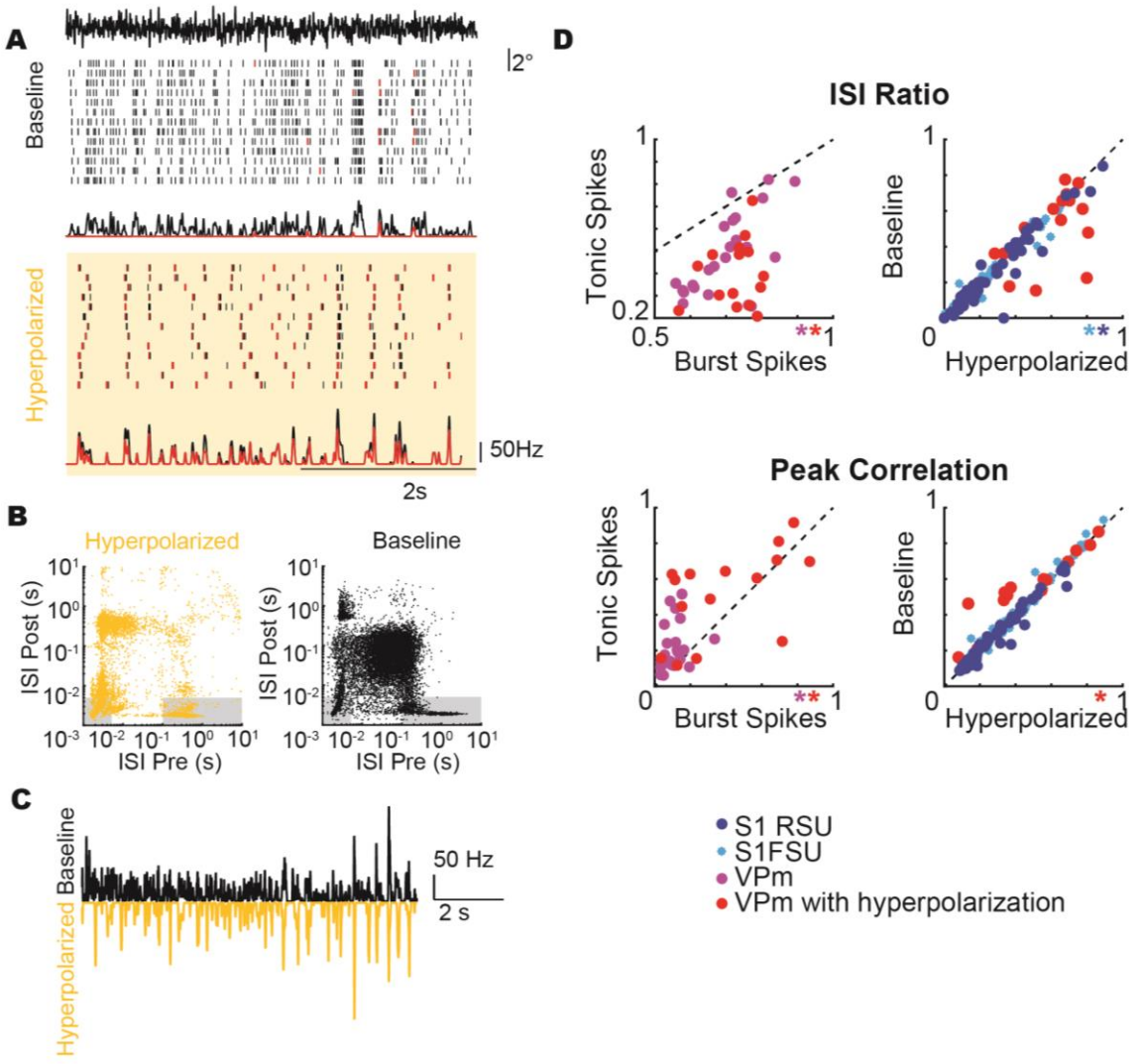


**Figure 5-3: Optogenetically imposed shifts in thalamic state.** A. Using a hyperpolarizing opsin, we are able to hyperpolarize the thalamus and shift the firing mode to a more burst encoding scheme. In this example neuron, we can view the spiking patterns in response to sensory white noise in the absence (baseline) or presence (hyperpolarized) of optogenetic stimulation (denoted by yellow coloring). Bursts are colored red in both the rastor plot and the PSTH. B. When viewing the ISI distribution plots for this example neuron, there is a clear change in the firing patterns such that the hyperpolarized condition shows increased firing within the 'burst' zones (indicated by grey boxes) while the baseline condition shows a majority of spiking outside of the 'burst' zones. C. We can also directly compare the PSTH of this example response to repeated white noise segments for the two conditions from an individual neuron. Note that the features that elicit reliable firing in the baseline condition also elicit reliable responses in the hyperpolarized condition. D. Spiking

statistics as a function of the burst/tonic or optogenetic state manipulation. Asterisks denote statistical significance ($p<0.05$, Wilcoxon signed-rank test).

### 5.3.3 Thalamic feature selectivity as a function of thalamic state

While spiking metrics give an overall idea of the patterns of elicited spiking, feature selectivity provides an estimate of the encoding properties of an individual neuron. Here we quantified the temporal feature selectivity of the thalamic neurons by stimulating with sensory white noise on a single whisker and using traditional spike triggered averaging. Briefly, the stimulus segments immediately prior to the spike time are extracted (Figure 5-4 top). Overlaying the spike triggering stimulus segments begins to show similarities in the stimulus immediately prior to spike time onset (Figure 5-4 bottom). The spike triggered average, shown in red, shows some structure in the ~15 milliseconds prior to spike time, but is otherwise nonsignificant for longer time delays (as indicated by the flat line extending backwards in time). Importantly, the galvo motor used for providing precise whisker stimulation can only reliably provide frequency content up to approximately 200 Hz. Therefore, there will be a correlation in the recovered filters on the timescale of a few milliseconds that places a limit on the temporal resolution of the recovered spike triggered averages.

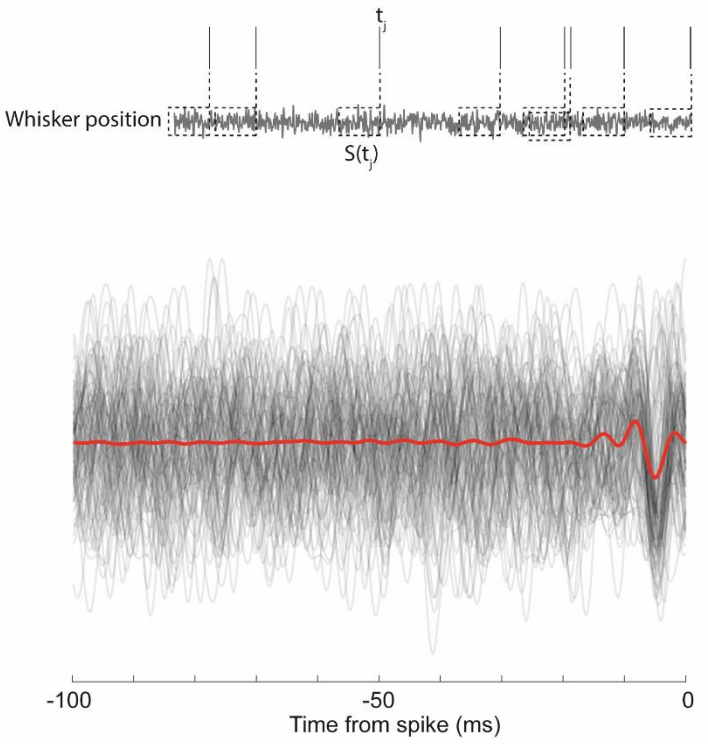


**Figure 5-4: Visualizing the spike triggered average.** A stimulus segment (s) is extracted for the time period immediately prior to each spike. This is referred to as the spike-triggered ensemble (top). Overlaying the spike triggered stimulus segments (transparent black) for all spikes (n = 100 segments for visualization purposes) shows commonalities in the stimulus segment that immediately precedes a spike (spike triggered average shown in red).

For an example unit (Figure 5-5A, black), the recovered filter (spike triggered average) is approximately 15 milliseconds in duration and has a multimodal shape. In this pathway, this filter shape is equivalent to a deflection of a single whisker in the rostral-caudal direction. In order to make comparisons across all of the recorded thalamic neurons, we performed a principal component analysis on the set of estimated spike triggered averages (Estebanez et al., 2012). The first two principle components for the full thalamic data set (Figure 5-5A, red, blue, n = 37 units) account for most of the variance across units. This suggests that the linear filters are very similar across neurons. This is consistent with prior findings from the rodent whisker thalamus (Petersen et al., 2008). Using this technique, we can quantify changes in the feature selectivity as a function of the thalamic firing mode

(Figure 5-5B). When the spike triggered average is computed from only the tonic spikes, the feature selectivity matches that of all the all spikes condition (Figure 5-5B grey).

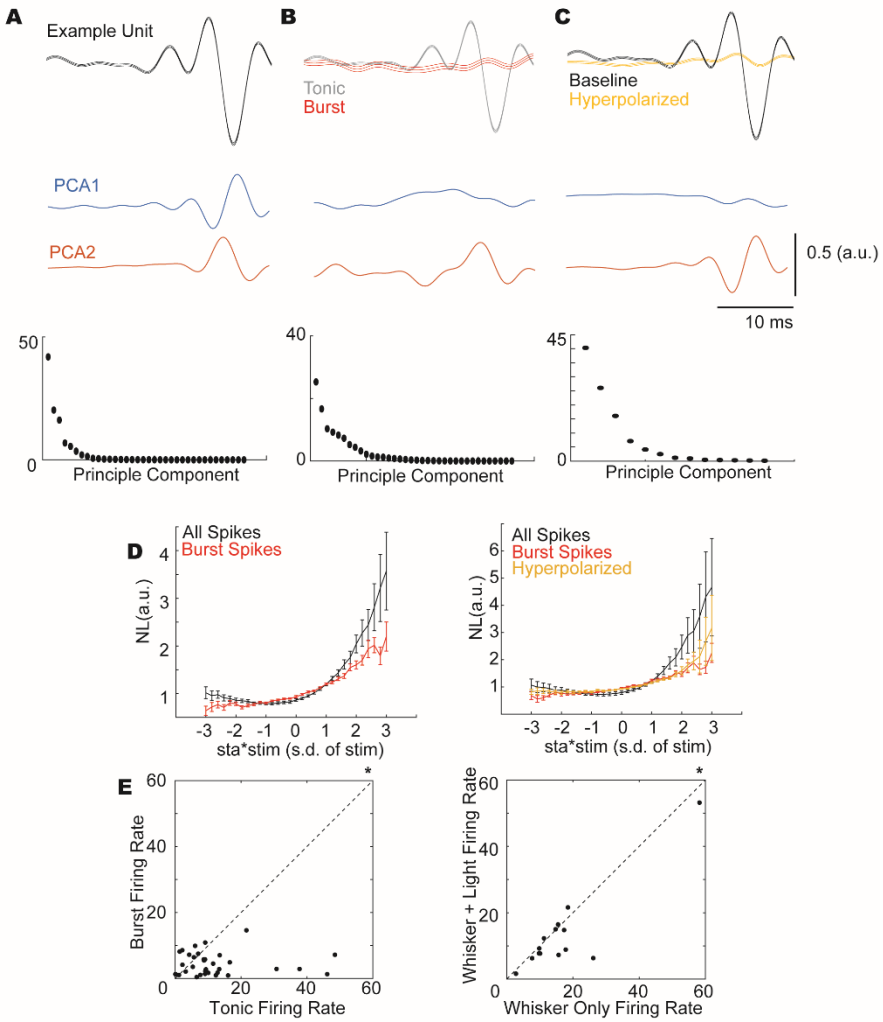


**Figure 5-5: Thalamic Feature Selectivity.** An example unit shows clear feature selectivity as indicated by the amplitude of the spike triggered average. Across units (n = 37 units), a principal component analysis of the recovered filters shows commonality. B. When spikes are parsed by burst/tonic, the tonic feature retains the feature selectivity while the bursting feature selectivity is abolished. This is evident across units by viewing the PCA of the recovered filters (n = 37 units). C. In a subset of neurons expressing hyperpolarizing opsin, we could shift the firing mode of the thalamus and found the same shift in feature selectivity as seen for burst spikes. D. The nonlinearities for these conditions shows a reduced stimulus sensitivity for burst spikes/hyperpolarized condition. E. Bursting conditions also show lower firing rates on average.

However, when the spike triggered average is computed from the first spike in the burst, there is no obvious feature selectivity (Figure 5-5B, example unit). Similarly, when

we compute the spike triggered average for the hyperpolarized condition, there is a complete loss of feature selectivity in this example neuron (Figure 5-5C, example unit). Importantly, this unit showed similar peaks in the noise-evoked response in the hyperpolarized condition relative to the baseline condition suggesting at least some similarity in the tuning properties (Figure 5-3A). However, there is also significant variability in the spike timing in the hyperpolarized condition. The short temporal spike triggered average could be completely lost not due to a lack of tuning in the burst mode, but instead due to increased temporal jitter in the burst condition. We can repeat the same principal component analysis of the recovered burst triggered averages and the hyperpolarized condition spike triggered averages and show that the first principle component does not depict any obvious feature selectivity while some of the filter is maintained in the second principle component. This could suggest that the burst state is not representing sensory information with the same level of temporal precision as the tonic state, consistent with the overall reliability spiking metric in Figure 5-3.

Quantifying across trial precision for punctate stimuli is typically achieved by taking the variability of the first spike latency, but this is a more difficult task when looking at precision across ongoing stimulus segments. Here, we computed the correlation between the recovered spike triggered average (computed from all spikes) and every spike triggered stimulus segment to quantify the peak correlation value as well as the lag of the associated peak correlation (see methods, Figure 5-6A). If every spike was elicited with infinite precision to a single stimulus dimension, we would expect to recover a delta function distribution of peak correlation lags centered at lag zero. However, with increasing jitter in the spiking mechanism relative to the stimulus, this distribution will widen, indicating a greater variability in the precision of the spiking patterns. For this example neuron, the tonic spiking shows clear clustering around lag zero (Figure 5-6B, left) while the burst spiking has lost that temporal precision (Figure 5-6B, middle). The loss of temporal precision is also evident in the optogenetically hyperpolarized condition (Figure 5-6A,

right). While this is only a single example neuron, it does begin to indicate that the burst spiking patterns may introduce increased jitter into the noise evoked response, which could be impacting the ability to recover the linear filter.

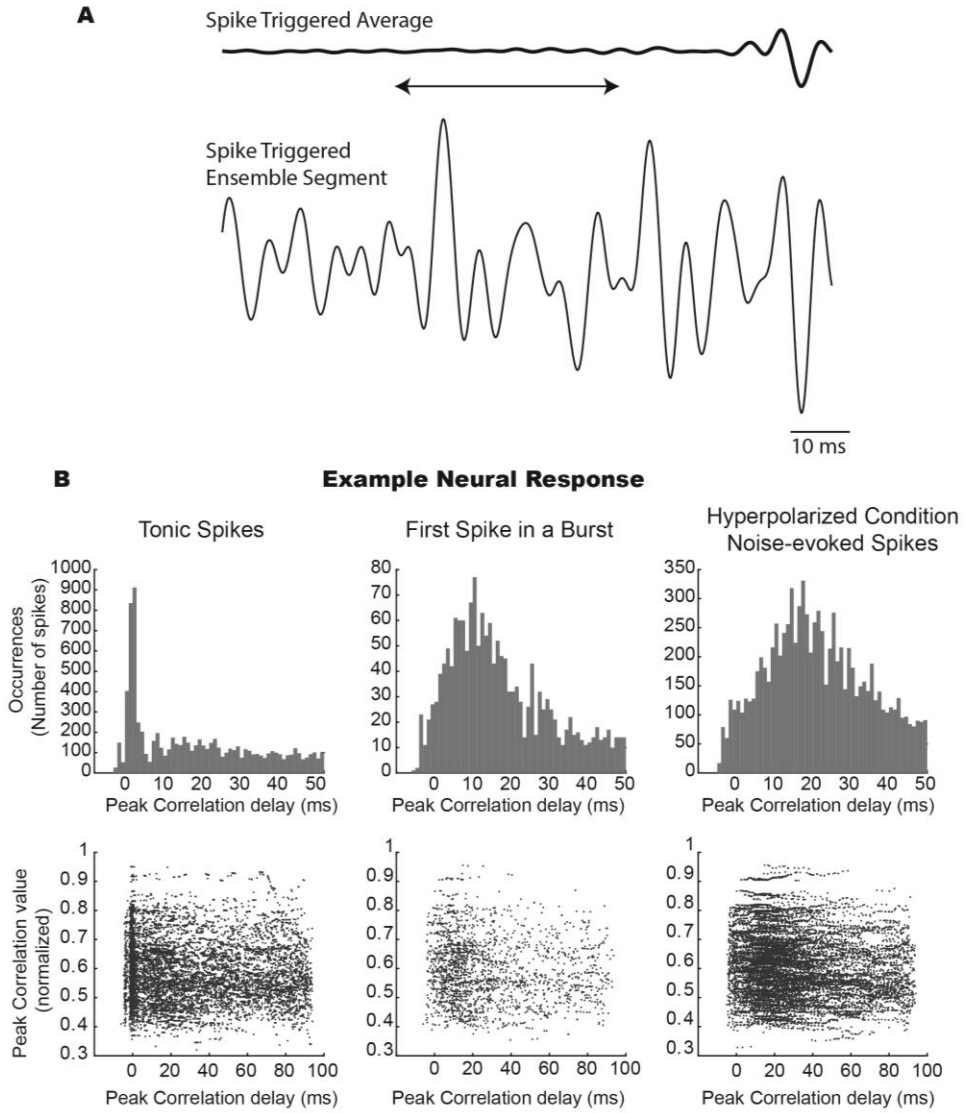


**Figure 5-6: Example spike triggered ensemble shows spiking precision for tonic spikes relative to burst spikes.** A. We performed a simple correlation between the estimated spike triggered average and each spike triggered stimulus segment. B. The peak correlation delay shows greater temporal precision for tonic spikes than burst spikes as evidenced by the distribution of peak correlation delays.

Using the recovered linear filter, we can also estimate the spiking nonlinearity of each neuron. Across the population, there is a high sensitivity (or steeper slope) for all

spikes relative to just burst spikes as well as for the baseline condition relative to the hyperpolarized condition (Figure 5-5D). Note that the units here are arbitrary as this is only a ratio of two probability distributions (see methods). The scaling of this non-linearity into units of firing rate is achieved by multiplying the nonlinearity by the average firing rate. Here, there is also a higher gain for tonic spikes as quantified by the mean firing rate (Figure 5-5E). This is in contrast to what we might expect based on theories of burst spikes providing a higher gain than tonic spikes (Sherman, 2001a; Swadlow and Gusev, 2001; Swadlow et al., 2002). However it may simply be reflective of the differences in the stimulus evoked properties of the burst and tonic spikes such that an LN model is most informative for tonic spiking patterns.

In a subset of experiments, thalamic spiking activity was recorded from the awake behaving animal during continuous white noise stimulation. However, there were differences in the frequency content of the sensory white noise provided in the anesthetized and awake conditions (white noise frequency cut off of 200 Hz and 100 Hz, respectively). To attempt to make comparisons between the datasets, we performed post hoc filtering of the anesthetized recordings to reduce the high frequency contributions to the recovered filters. When the frequency content of the sensory stimulus was matched between the anesthetized and awake recordings, the principle components showed very similar shapes (Figure 5-7) suggesting that the basic properties of feature selectivity are not fundamentally altered by anesthesia. However, that is not to say that the awake and anesthetized brain are spending the same amount of time in each brain state or even in the exact same brain states. There are important comparisons that can be made for the recovered feature selectivity, but future work would need to address how state-dependence impacts neural coding in the awake brain.

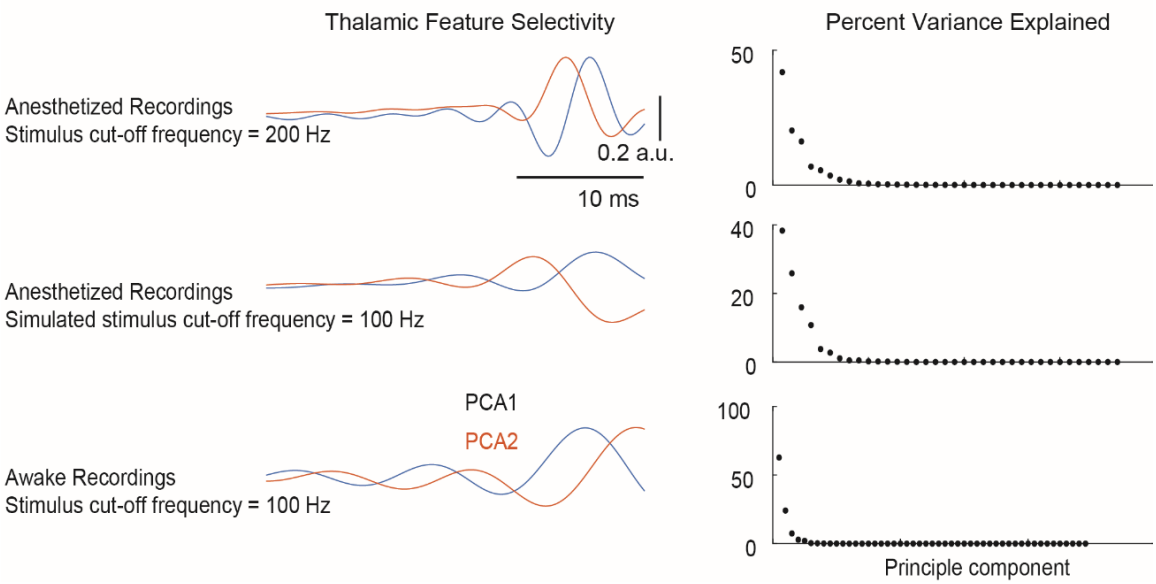


**Figure 5-7: Feature selectivity in the awake and the anesthetized thalamus.** A. There were differences in the stimulus statistics such that the sensory white noise applied in the anesthetized condition had a cutoff frequency of 200 Hz while the awake recordings had a stimulus cut off frequency of 100 Hz. In order to account for the effects of stimulus properties, we low pass filtered the anesthetized filters to match the frequency content of the awake filters. This posthoc analysis shows a general agreement between the filter shape in the anesthetized and the awake rat whisker thalamus.

### 5.3.4 Cortical feature selectivity as a function of thalamic state

The feature selectivity estimated using a spike triggered analysis estimates the transformation from the sensory stimulus to the spiking patterns in that specific region of the brain. However, in reality, the feature selectivity of a given region is entirely determined by the spiking patterns of the presynaptic inputs. Therefore, the changes in thalamic firing modes can directly impact the encoding in cortex. Here, we analyzed the feature selectivity in the cortex as a function of the optogenetically manipulated state in thalamus (hyperpolarized/baseline).

First, we classified units as fast spiking or regular spiking based on the shape of the spiking waveform (see methods) and computed the spike triggered average. The units were then functionally classified as having a significant linear filter if the duration of time the STA exceeded the confidence intervals was greater than 5 milliseconds (n = 85/213 FSU,

63/291 RSU). Note that the probability of demonstrating a measurable STA was markedly higher for FSUs than RSUs even though there were fewer FSUs recorded. Example spike triggered averages as well as the principle components show greater similarity between FSU filters than RSU filters (Figure 5-8A). Furthermore, this is not simply due to differences in the spike rates between FSUs and RSUs. While FSUs spike more frequently than RSUs, removal of portions of the FSU spikes does not abolish the recovered spike triggered averages for FSUs (Figure 5-9B).

Then, we analyzed the feature selectivity as a function of the thalamic state manipulation (baseline/hyperpolarized). When the thalamus is hyperpolarized, this also impacts the cortical feature selectivity (Figure 5-8B) such that the amplitude of the STA is reduced. This sort of reduction in the STA amplitude could be due to a blurring of the thalamic spikes (as you might expect from a bursting neuron) and is consistent in examples from both FSUs and RSUs. However, the commonality in the feature space is still present only in FSUs. We also compared the effects of the thalamic hyperpolarization on the spiking nonlinearity and found a similar effect to what was seen in thalamus such that the hyperpolarized thalamic condition led to a reduction in the cortical gain.

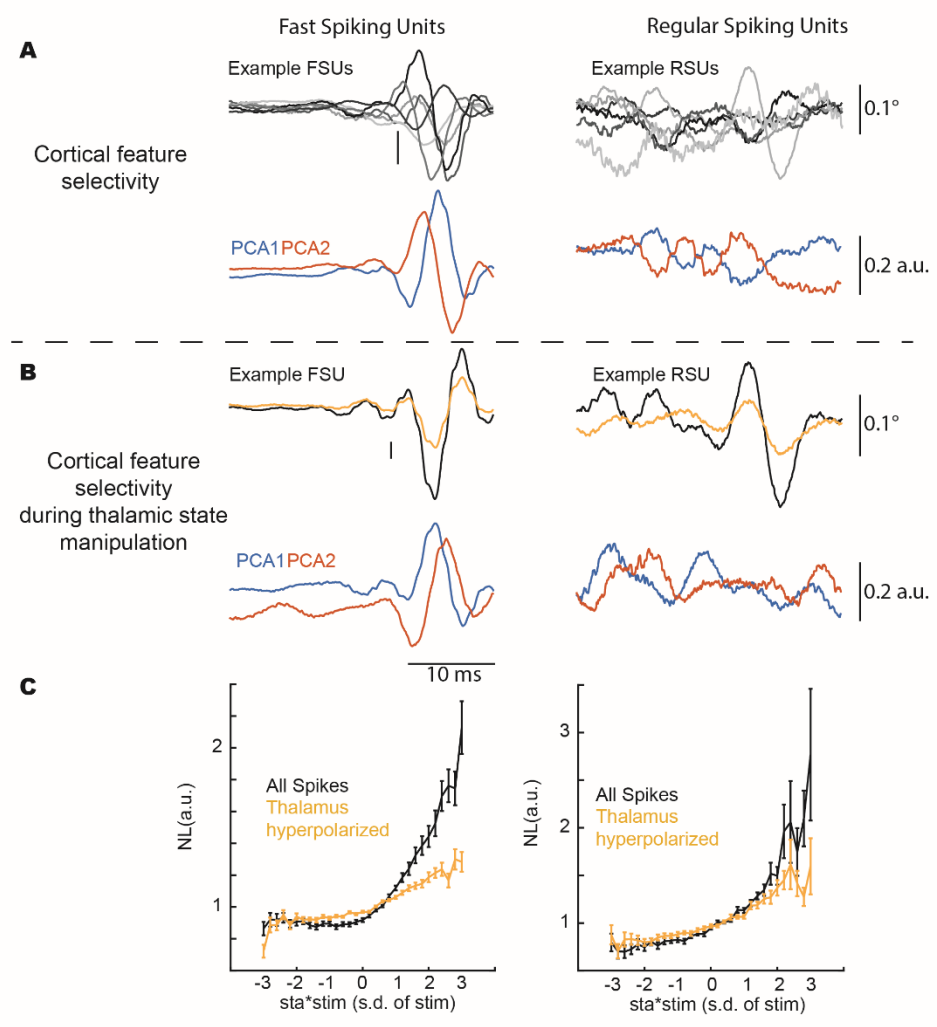


**Figure 5-8 Impact of thalamic firing mode on cortical feature selectivity.** A. Fast spiking units (n = 85 units) have more similar and pronounced feature selective than regular spiking units (n = 63 units). B. When hyperpolarizing the thalamus, the amplitude of the spike triggered average is reduced for both FSU and RSU (example, top), but the general shape of the recovered filters is unchanged. C. Similar to what is seen in thalamus, there is a reduction in the spiking nonlinearity with the presence of thalamic hyperpolarization.

### 5.3.5 Comparison of thalamic and cortical feature selectivity

Identifying the common subspace for the recovered linear filters allows for direct comparison of the thalamic and cortical STA (Figure 5-9A). As described above, the RSUs did not show a clear common feature space. However, the first two principle components

of the STA space for FSUs looked like a time shifted version of the VPm feature selectivity (delay of 1.6 milliseconds).

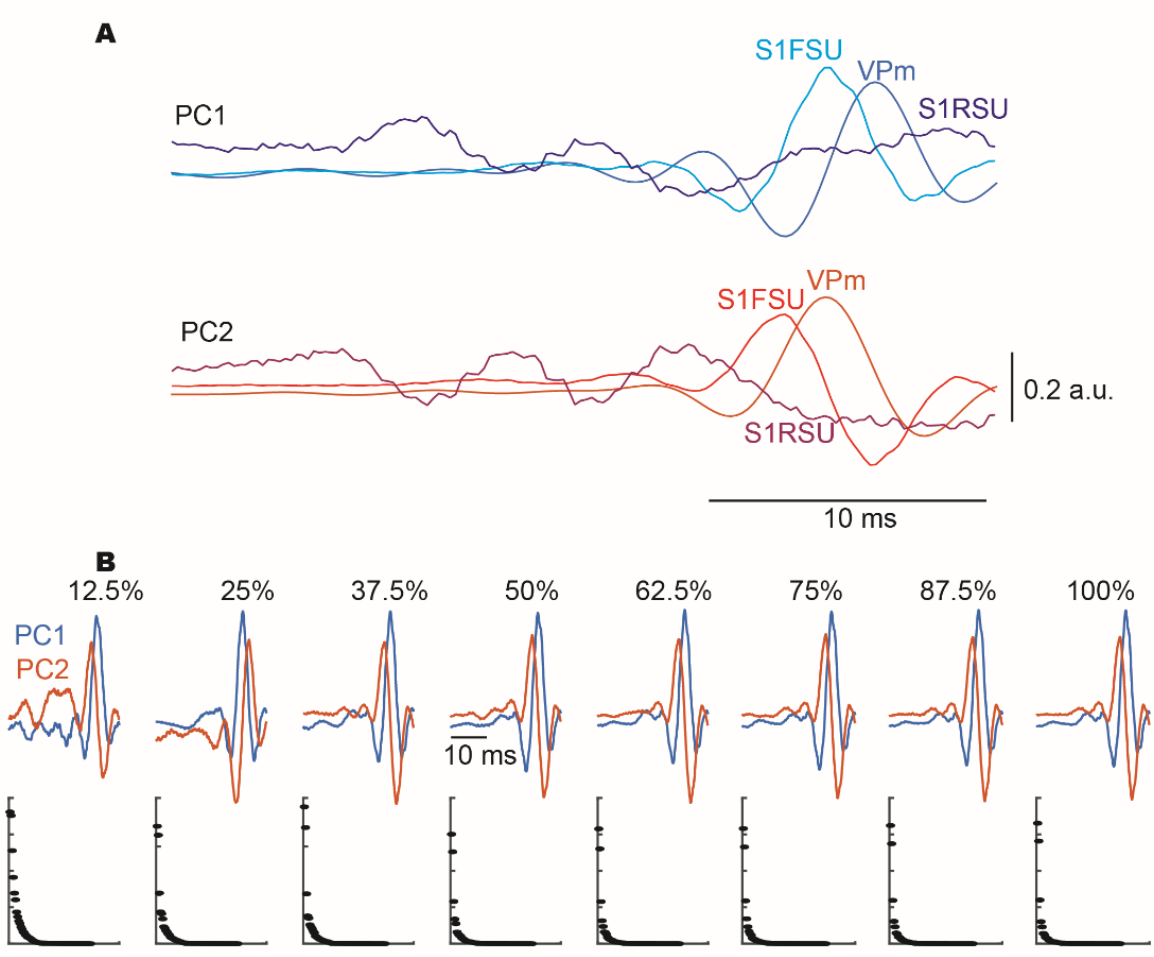


**Figure 5-9 Comparison of feature selectivity across thalamus and cortex.** A. A comparison of the feature selectivity across units shows a close alignment between VPm units and FSUs where the feature selectivity has a similar shape but with a short time delay (PC1 delay: 1.6 ms, PC2 delay: 1.65 ms). B. It is also the case that FSUs have higher firing rates than RSUs. To control for this effect, we threw out a proportion of the FSU spikes (from 12.5% to 87.5% of spikes) and repeated this analysis. Even with a fraction of the number of spikes, FSUs still show prominent feature selectivity.

## 5.4 Discussion

The thalamic processing of incoming sensory signals is capable of driving activity in two fundamentally distinct states – the burst state and the tonic state. However, how the

thalamic firing modes impact precise encoding properties such as feature selectivity remain unknown. In this work, we used optogenetic manipulation of thalamic state to quantify the effects of thalamic firing mode on stimulus encoding properties in the thalamocortical circuit of the rat vibrissa pathway. In agreement with previous hypotheses, the tonic spiking activity reliably encoded sensory information and the burst spiking activity did not. However, in contrast to previous studies, the thalamic burst spiking did not present a higher gain within the linear-nonlinear model framework pursued here.

### 5.4.1 Thalamocortical state interactions

Interactions between thalamocortical state has primarily been investigated in the context of ongoing oscillations during sleep. In fact, the firing mode of the thalamus was originally linked to the waking state of an animal such that a burst firing mode was indicative of a sleeping state while a tonic firing mode was indicative of an alert state (Steriade et al., 1993). Importantly, the view of burst firing has expanded since these seminal studies demonstrated their prominent role in sleep.

First, there is significant evidence for thalamic bursting in the awake animal across multiple experimental paradigms (Ramcharan et al., 2000; Swadlow and Gusev, 2001; Whitmire et al., 2016) as well as stimulus evoked bursting that can be replicated across trials (Lesica and Stanley, 2004; Wang et al., 2007). This shows that bursting activity is not just an indicator of state, but it is also repeatably evoked by the sensory stimulation and is present in the awake animal.

Second, the connectivity required for the coordinated thalamocortical state oscillations present in the sleeping brain is also evident in the waking brain. The transitions between states likely occurs along a continuum and during anesthesia, we are restricted to a subspace of that brain state map. This work is certainly not presented without limitations. However, we expect that the discoveries made within this restricted regime can be extrapolated across the states of wakefulness. Furthermore, there is evidence that

optogenetically driving the thalamus can shift the state of the cortex (Poulet et al., 2012; Wimmer et al., 2015) and that optogenetically activating the corticothalamic feedback projections can shift the state of the thalamus (Mease et al., 2014). These studies show that the infrastructure is in place for the thalamus to influence cortical state and for the cortex to influence thalamic state. The question now becomes how is this occurring naturally in the brain. Future work should be aimed at trying to decouple state in these brain regions in order to understand the circuit dynamics.

### 5.4.2 Thalamocortical feature selectivity

While feature selectivity can be linked directly to the sensory organ in the periphery, neurons beyond the periphery only receive input from other neurons. Ultimately it is synaptic connectivity that gives rise to the feature selectivity of any given neuron, but our ability to reliably estimate the role of any given feedback region in shaping the feature selectivity of its postsynaptic target is limited by our experimental techniques. Multiple studies performed in vitro have investigated the effects of local connectivity on feature selectivity using simultaneous whole cell recordings (Harris and Mrsic-Flogel, 2013; Ko et al., 2013, 2011). However, the loss of long range connectivity in slice experiments limits our ability to assess functional connectivity of the intact circuitry. Using a combination of optogenetic stimulation and electrophysiological recording techniques, I have performed a series of experiments to alter only the state of the thalamus (as estimated from the baseline polarization level) and quantify the effects on encoding in the thalamocortical circuit. Using this technique, we have precise control of the firing mode in thalamus without altering any processing occurring from the whisker to thalamus enabling us to decouple the changes in thalamic firing mode on cortex from any changes occurring in subthalamic processing. It seems that the burst mode does not reliably transmit sensory information on the millisecond precision timescale. This can be manipulated in thalamus and visualized in

the cortical units. However, it also seems that the burst mode is capable of activating cortex and inducing more burst like firing patterns in cortex.

Without any manipulation, we see a commonality in the feature selectivity for fast spike units and thalamic neurons that is not prevalent for regular spiking units. This could represent a framework for differential encoding of feedforward whisker information based on cortical cell type. Measurements of synaptic efficacy from *in vitro* slice experiments have found that thalamic synapses onto fast spike units are stronger than those onto regular spiking units (Gil et al., 1999). This might suggest that the inhibitory neurons are tasked with reliably encoding passive whisker position information while the excitatory neurons represent a different component of the sensory stimulus. Future work should address the feature selectivity of the pathway using more naturalistic sensory stimuli or even active sensing conditions.

### 5.4.3 Temporal precision

Through analysis of the spike timing precision, we found that the burst firing mode experienced increased temporal jitter relative to the tonic firing regime. There are multiple mechanisms that could underlie the reduced temporal precision in the burst firing mode including variability in the time to reach threshold, the slow dynamics of the calcium depolarization, as well as changes in the integration properties of the thalamic neurons. Burst firing is defined by prolonged hyperpolarization that would push the thalamic membrane potential farther from the spiking threshold. Any incoming depolarizing sensory stimuli would then have to induce a greater depolarization to cause the neuron to reach spiking threshold which could induce greater variability in the time from stimulus drive onset to spiking output compared to the tonic firing regime where the cell could be operating much closer to spiking threshold. Furthermore, burst spikes ride on top of a slow calcium wave of depolarization. The slow nature of this current could also underlie some of the timing variability seen for burst spikes. Another interesting, but untested idea could

be that the thalamic units are actually integrating the incoming information differently such that the burst mode could be integrating sensory drive over a longer time window, which could lead to increased stimulus-evoked jitter. Each of these mechanisms suggests that the T-type calcium current that underlies thalamic bursting could be introducing temporal variability into the firing patterns of the thalamic neurons. This is consistent with the view that bursts are not representing detailed stimulus information and with the results shown here. Instead, it is possible that the mechanisms of thalamic bursting only become temporally precise for strong sensory signals, as we have shown previously (CHAPTER 3 ), and tonic spikes are responsible for encoding ongoing or continuous sensory information.

### 5.4.4 Summary

Ultimately, this work provides a comprehensive examination of thalamic state-dependent feature selectivity in the thalamocortical circuit of the rat vibrissa pathway. Consistent with the hypothesis that tonic spikes are destined to faithfully relay sensory information, we did find that the feature selectivity in thalamic units was best estimated using the tonic spiking whereas burst spiking did not demonstrate clear feature selectivity. Furthermore, the change in firing modes in thalamus affected the encoding properties in cortex such that the cortical feature selectivity was diminished during the thalamic hyperpolarization condition. We propose that the loss of feature selectivity, as assessed using spike triggered techniques, is not due to a true loss of stimulus selectivity but instead is due to changes in the precision of the temporal spiking in burst firing modes. This creates an interesting dynamic about the timescales of precision in neural coding and the impact on representing temporal patterns of sensory stimulation.

# CHAPTER 6 CONCLUSIONS AND FUTURE DIRECTIONS

## 6.1 Conclusions

Each component of this thesis quantifies the impact of thalamic firing mode on encoding in the thalamocortical circuit. Ultimately, however, each of these components breaks down to a single concept: timing. The brain is a highly organized system with circuits that exemplify convergence and divergence configurations. When information is conveyed across brain structures, it is strongly shaped by the convergence and divergence properties of the circuitry such that multiple temporally coordinated inputs are required to activate a brain region. The temporal and spatial integration properties of neural circuits are much more complex than simple linear summation models might suggest, making the temporal interactions between spikes even more important. From the perspective of a downstream cortical neuron, tonic spikes and burst spikes differ only in the timing between them. However, this thesis articulates how these two firing modes can differ on multiple timescales from milliseconds with respect to jitter, synchrony, and feature selectivity to hundreds of milliseconds with respect to circuit dynamics and state transitions.

### 6.1.1 Timescales of thalamic firing mode

Burst firing in the thalamus is mediated through t-type calcium channels such that a prolonged hyperpolarization will de-inactivate these channels to prepare them to open upon the arrival of a depolarizing input. Activation of this low threshold current provides a slow wave depolarization on top of which the burst spikes ride (Perez-Reyes, 2003). Therefore, the burst spikes are initiated by a distinct mechanism from ongoing tonic spiking. However, a cortical neuron interpreting thalamic spiking does not receive information about the subthreshold membrane potential of the thalamic neuron. Instead, the cortical neuron receives only information about thalamic spiking through the thalamocortical synapse. The thalamocortical synapse is particularly sensitive to the timing of thalamic spiking because it is a depressing synapse (Gil et al., 1999, 1997). Bursts

generated by the t-type calcium channel mechanism are particularly advantageous for this type of synapse because they require a prolonged period of silence to deinactivate the bursting mechanism and therefore provide sufficient time for the thalamocortical synapse to recover from prior spiking activity. Furthermore, there is also evidence that tonic spikes with a time-matched silence period to bursts show similar synaptic efficacy increases relative to ongoing tonic spiking that occurs without a silence period (Swadlow and Gusev, 2001). This suggests that the real distinctions between burst and tonic firing from the perspective of downstream neurons is the timing of the spikes.

### 6.1.2 Timing across multiple scales

#### 6.1.2.1 Thalamic precision and synchrony

In primary sensory pathways, spike timing has been shown to be critical for sensory information representation and transmission (Stanley, 2013). In response to punctate whisker stimuli, the relevant timescale for encoding ranges from the primary afferents which show microsecond-scale precision (Bale et al., 2015) to the thalamic and cortical neurons which show millisecond-scale precision (Gabernet et al., 2005; Millard et al., 2015) to downstream interpretation of spiking responses which show integration over tens of milliseconds. However, the relevant time scales for encoding are also flexible as a function of the sensory stimulus. In the visual pathway, the precision of the thalamic spike trains can adjust based on the frequency content of the input to maintain an accurate representation of the stimulus (Butts et al., 2011). The synchrony of spiking across thalamic units is also variable as a function of the statistics of the sensory stimulus (Q. Wang et al., 2010).

##### *6.1.2.1.1 Cortical Integration Window*

In the thalamocortical circuit, the timescale of milliseconds to tens of milliseconds has been identified as particularly relevant in the context of the cortical integration window.

The anatomical connectivity from thalamus to cortex is defined by disynaptic feedforward inhibition such that an excitatory drive from thalamus onto an excitatory neuron will be followed by a feedforward inhibitory input on that same excitatory neuron. This leads to a brief period of excitability that has been referred to as the cortical integration window (Gabernet et al., 2005). Furthermore, the thalamocortical synapses are fairly weak suggesting that coordinated activity across neurons is critical to driving cortical neurons to fire (Bruno and Sakmann, 2006). To effectively excite a cortical neuron, the thalamic inputs must be synchronous within the cortical integration window. This can be achieved by packing multiple spikes from the same neuron (burst), single spikes across multiple neurons (synchrony), or multiple spikes across multiple neurons (synchronous bursting) into the window of opportunity. In CHAPTER 3 we explored each of these concepts in the context of a sensory adaptation paradigm.

*6.1.2.1.2 Spiking timing precision in the thalamus*

Sensory adaptation is often defined as the reduced amplitude of an evoked response with repetitive or ongoing stimulation. However, adaptation does not simply reduce spiking activity, it is also involved in shifting the temporal response properties of the circuitry. In CHAPTER 3 we demonstrate how adaptation reduces the temporal precision of an evoked response for a single neuron across trials and reduces the synchrony of thalamic firing across pairs of neurons. Thalamic spiking activity must be coordinated, or synchronous across neurons to effectively drive cortex. The reduction in thalamic spike timing precision with sensory adaptation is paired with an elongation the cortical integration window thereby affecting the optimal levels of spike timing precision (Gabernet et al., 2005).

*6.1.2.1.3 Shifts in thalamic state*

Adaptation also had an effect of the firing mode, or state, of the thalamus. Increasing levels of adaptation shifted the thalamus into a more tonic firing regime. In Chapter 3, we tested the hypothesis that the adaptive shift in firing mode was due to a tonic

depolarization of the thalamic neurons. Again, while this subthreshold depolarization would not be transmitted to cortex, the impact that the subthreshold depolarization has on the bursting activity of the thalamus and therefore the temporal pattern of spiking would be transmitted. Therefore, adaptation provided another mechanism to shift the timing of thalamic spiking through inactivation of the t-type calcium channels – reduction in the bursting activity. Using an ideal observer analysis based on spike counts, we showed that burst responses remained detectable but were less discriminable due to the more stereotyped all-or-none response properties (Whitmire et al., 2016).

#### 6.1.2.2 Temporal Feature Selectivity

The ability of tonic spikes to encode information in a more graded manner with a narrow window of cortical excitability, as shown through an ideal observer analysis of the discriminability of the tonic spiking activity, led me to ask how tonic spikes would represent more detailed information about the sensory stimulus. To address this, we quantified the feature selectivity of the thalamocortical pathway in response to ongoing sensory stimulation. The recovered spike triggered average, or kernels, represent some integration properties of the pathway. For example, in the whisker pathway, temporal kernels are approximately 10-15 milliseconds in duration (CHAPTER 5 ). This suggests that the integration window for sensory drive for an individual neuron is restricted to tens of milliseconds in duration. Therefore, in order to recover a linear filter for an individual neuron, you must have stimulus driven spikes that are precise on this timescale of tens of milliseconds. Furthermore, the shape of the recovered filter provides information about which components of the sensory stimulus the neuron is sensitive to. For example, a biphasic filter would suggest that a neuron is sensitive to a change in the stimulus dimension. Therefore, the recovered feature selectivity provides a window into the temporal stimulus processing properties of a sensory pathway.

The feature selectivity can be estimated from tonic spiking activity in both the thalamus and the cortex. However, through manipulation of the thalamic state, we have shown that the burst firing mode does not maintain this precise stimulus locking that is evident for tonic firing. Instead, bursts tend to have greater jitter in the noise-evoked responses leading to reduced trial to trial repeatability. Therefore, the reliability of burst firing is lower than tonic firing, consistent with the view that tonic spikes are important for faithfully relaying sensory information while burst spikes provide a strong albeit less informative signal. However, it should be noted that there is a distinct difference between variability across trials and variability across neurons. The increased jitter in the bursting responses across trials does not eliminate the possibility that the jitter relative to the stimulus is coordinated across thalamic neurons such that the across neurons on a single trial jitter is small. Future work should investigate coordination across thalamic units to quantify the effects of synchrony on a trial-by-trial basis relative to the jitter across trials.

#### 6.1.2.3 Circuit dynamics

While the lemniscal thalamus is the primary focus of this thesis, it is embedded within a dynamic and complex circuit. Within the thalamus, the VPm is densely interconnected with the nearby inhibitory nRT. Both nuclei are capable of bursting dynamics and their reciprocal connectivity could be responsible for rhythmic bursting activity (Willis et al., 2015). While only VPm projects to S1, both VPm and nRT receive direct projections from S1 (Crandall et al., 2015a). Within this reticulo-thalamo-cortical circuit, there are intrinsic properties that might permit enhanced information propagation that is dependent on the relative timing of activation. In CHAPTER 4 we found that direct stimulation of the thalamus at a fixed interval of 150 milliseconds could facilitate the cortical activation. We further tested the role of thalamic bursting in this facilitation by depolarizing the thalamic neurons to inactivate the t-type calcium channels. Through this thalamic state manipulation, we were able to abolish the facilitation seen for direct

activation of VPm (Whitmire et al., 2017). These results suggest that timing of inputs on the order of 100-150 milliseconds could represent the resonant frequency of this circuit for enhancing information transmission in the TC circuit which is dependent on the bursting dynamics in the thalamus.

### 6.1.3 Thalamic state across time scales

Thalamic activity, and ultimately cortical processing, is strongly affected by fluctuating subthreshold membrane potential levels in the thalamus, or the thalamic state. It has long been posited that hyperpolarizing the thalamus will lead to a 'burst' firing mode while depolarizing the thalamus will lead to a 'tonic' firing mode. Although we have some knowledge of the firing modes induced by thalamic state, we do not have a clear understanding of how these firing modes affect the transmission of sensory information. Through this thesis, firing properties as a function of thalamic state have shown changes in the timing of encoding ranging from milliseconds (temporal precision) to tens of milliseconds (feature selectivity) to hundreds of milliseconds (paired pulse dynamics). This presents a more nuanced view of how bursting activity can impact encoding not just in the patterns of spiking activity, but also in terms of network dynamics and ultimately cortical activation.

## 6.2 Experimental limitations

The work described in this thesis are not presented without limitations. While I believe the experimental methodology employed provided an excellent preparation in which to explore precise questions of neural coding, there were a number of experimental design decisions that should be outlined as caveats for the presented work. Specifically, the experimental limitations include the nearly exclusive use of an anesthetized preparation, the choice of the rodent vibrissa pathway as a model system, the restricted stimulation paradigm, and the extracellular recording technique.

### 6.2.1 Anesthetized preparation

Although the anesthetized preparation provides a controlled environment for precise dissection of neural function, it is absolutely a restricted state within the continuum range of brain states. The primary focus of this thesis revolved around the state of the thalamus and how modulating the state impacts encoding. While this is discussed in detail in earlier chapters (see 3.4, 4.4.1), bursting does play a role in sensory encoding in the awake brain, albeit to a lesser extent than in the anesthetized brain. We were able to replicate some of these findings in the awake, behaving animal (collaboration with Christian Waiblinger and Cornelius Schwarz), but there is still a lot of work to do in terms of pushing all of these findings into an awake experimental preparation. I would predict that the findings presented in this thesis are relevant in the awake animal, but they do not represent the whole story. Expanding the experimental paradigm to view sensory encoding across states of wakefulness will likely expand the view of how thalamocortical states interact and drive the encoding properties of the pathway.

### 6.2.2 Rodent vibrissa pathway as a model system

The rodent vibrissa pathway provides an excellent model system for exploring questions of sensory coding (see 1.2), but it also is not a direct homolog of human sensory processing. However, I would argue that the exact sensory system studied is not critical to the questions of state and encoding presented here. Instead, the vibrissa pathway is a convenient model system for studying sensory encoding in the thalamocortical circuit which is conserved across nearly all sensory pathways. The commonality in this thalamocortical circuit motif could suggest canonical neural computations such that findings from the rodent vibrissa pathway could be translated into other sensations.

### 6.2.3 Restricted stimulus paradigm

Similar to the experimental decision to use the rodent vibrissa pathway as a model system, the use of a restricted single whisker stimulation paradigm has its own limitations.

In naturalistic sensing, it is unlikely that a single whisker would be stimulated due to the close proximity of all of the whiskers along the whisker pad. Studying the neural response to naturalistic stimuli is incredibly important for learning about the pathway, but I would argue that the presentation of computationally convenient stimuli (such as sensory white noise) also plays an important role in characterizing the response properties of the pathway. Similar to human touch, the vibrissa sensation is also an active process with sweeping motions of the whisker interacting with external objects. The internally generated component of active sensing could not be studied within the context of this anesthetized preparation, but future work could be aimed at identifying more naturalistic sensing scenarios. Importantly, the objective of this thesis was not to study the intricacies of whisker encoding but instead to try to identify common principles of neural processing in the thalamocortical circuit. The vibrissa pathway is organized into discrete clusters of neural tissue that are sensitive to a primary whisker. This discretized topographic map provides an ideal system for studying information transmission across topographically aligned circuits. I think it would be excellent to see this work expanded into more complex sensory paradigms to look at things such as cross-whisker effects and multi-whisker patterns of activation, but this was simply not achievable within the purview of this thesis.

### 6.2.4 Extracellular recording techniques

Extracellular recordings provide high temporal resolution views of the spiking activity of the neurons. What we cannot see from this recording technique is the subthreshold membrane potential. In the context of burst/tonic firing, subthreshold techniques would be particularly advantageous for identifying putative T-type calcium channel bursts. However, this is incredibly technically difficult to achieve *in vivo* in deep brain structure such as the thalamus. Therefore, we used an interspike interval metric to classify each spike as part of a burst or not (see 3.2.2.3). Although this is not the ground truth identification of bursting activity, it is a restrictive measure meant to identify bursting

activity from an ongoing spike train. As technology continues to develop, I hope this work can be expanded upon in the intact circuitry using a subthreshold membrane potential recording technique in the thalamus.

## 6.3 Future scientific directions

I think the idea that thalamic state, as defined by the bursting activity in the circuit, could manipulate neural activity across multiple time scales is an exciting proposal for outlining future work. I would split the future directions for this work into two projects. The first explores the direct relationship between thalamic and cortical state to investigate how coupled these two notions are. The second systematically investigates each of the inputs to the VPm to identify how each circuit component modulates or controls the state of the thalamus and therefore its encoding properties. Finally, I would also like to just briefly discuss some other research directions that extend beyond coding in the thalamocortical circuit.

### 6.3.1 Thalamocortical state interactions

In CHAPTER 5 we began to identify a relationship between the transition in cortical up-down state and the bursting activity in the thalamus. While there has been evidence that increasing thalamic activity leads to an up state transition (Poulet et al., 2012), there has been very little investigation into exactly how coupled thalamic and cortical states are. One technical hurdle to address here is exactly how to quantify thalamic state. Although we have primarily referred to thalamic state as the relative amount of bursting activity throughout this thesis, it is worth noting that this may only be one of the relevant dimensions of the 'state' of the thalamus. The thalamic state may also be defined by the overall level of activation (firing rate), the coordination across neurons (synchrony), or the coupling between the excitatory (VPm) and inhibitory (nRT) nuclei of the thalamus. I think a critical next step is to expand upon this and perform a systematic characterization of the thalamic firing properties to properly define the state. In cortex, this sort of state

classification is well-established, but always continuing to update. Cortical state is typically classified based on the local field potential and/or the subthreshold membrane potential, both of which are not incredibly viable options for the thalamus. I believe that by performing a circuit level analysis of the thalamic firing properties across behavioral states, we will be able to identify the relevant dimensions to classify state. At the lowest level, I would suggest using multielectrode probes to study coordinated activity across multiple thalamic units simultaneously. Upon identifying a suitable candidate method for classifying thalamic state across time, I think we need to first perform a correlative analysis of the relationship with cortical states. Then, I would propose using optogenetics to causally manipulate the state of the thalamus, the cortex, or both to decouple extrinsic factors that could affect state transitions from the direct thalamocortical interactions. The state of a given brain region at the time of sensory input can fundamentally affect the encoding of that particular stimulus. This project could form the basis for understanding the intrinsic properties of the thalamocortical state (ideally across different states) and build a framework for spontaneous interactions in this circuit.

### 6.3.2 Network control of thalamic state

We believe that the corticothalamic feedback (S1), thalamo-reticular feedback (nRT), and neuromodulatory inputs play a major role in the maintenance of thalamic state. Investigating the impact of each of these brain regions on the thalamic processing will develop a circuit level view of state-dependent encoding in this sensory pathway. I have outlined a few experimental directions below for each circuit component I would address.

#### 6.3.2.1 Thalamo-reticular Interactions

As described throughout this thesis, t-type calcium channel bursting requires a prolonged hyperpolarization. A silence period could be induced by a lack of excitatory drive or a direct inhibitory input. The only known inhibitory input to the VPm is from nRT (Pinault, 2004). Furthermore, significant evidence from the cortex suggests that the

inhibitory inputs are so strong that they can almost completely control the firing activity levels of their excitatory targets (Reinhold et al., 2015). The nRT has been a historically difficult nucleus to study due to its sheet-like structure that is thin and distributed (Halassa and Acsády, 2016). However, recent advances in transgenic mouse lines have made it possible to genetically target nRT. These technological advances have made it possible to actually interact with the nRT component of this thalamic circuit and study how this nucleus can control information encoding and transfer in the VPm. I think this is a particularly critical circuit to study and could provide answers such as how these two regions are coupled spontaneously and during evoked behavior (and whether they can act independently) and how their intrinsic dynamics impact information transmission.

6.3.2.2 Cortico-thalamic Interactions

The role of cortical feedback in shaping thalamic processing has become an increasingly popular question with the advent of a transgenic mouse line that specifically targets the L6CT neurons. Some of the preliminary studies in this direction have shown that activating the corticothalamic feedback pathway can actually depolarize the thalamic neurons and therefore shift them from a burst to a tonic firing mode (Crandall et al., 2015a; Mease et al., 2014). This presents a really interesting effect where the cortex can directly impact the firing mode of the region from which it receives direct input. I think the next really critical question to investigate here is – when are the L6CT neurons active? What drives their firing and therefore what is their role in normal sensory function? I think the way to investigate this is to use the transgenic mouse line to specifically tag L6CT neurons for identification in cortical recordings. Realistically, the next step will be to provide mice with a rich sensory environment or behavioral task and perform a systematic analysis of the feature selectivity. Work from L6CT neurons in vision has shown that they have extremely precise feature selectivity, as measured from their subthreshold membrane potential, but with low firing rates (or no firing at all) (Vélez-Fort et al., 2014).

Furthermore, as an added layer of complexity, activation of L6CT actually inhibits cortical activity across the layers (Bortone et al., 2014; Olsen et al., 2012; Vélez-Fort and Margrie, 2012). Therefore, studying the role of the L6CT neurons presents an opportunity to look at a single class of neurons that can have a marked effect on both thalamic and cortical circuits. I would predict that the dual structure innervation of this neuron subclass suggests it is critical in coordinating activity across the two structures.

#### 6.3.2.3 Neuromodulatory Interactions

The final circuit component that I would suggest for exploration in the context of thalamic processing are the neuromodulatory inputs. Neuromodulators play a significant role in shaping neural activation throughout the brain especially the thalamocortical circuit (Bezdudnaya and Castro-Alamancos, 2014; Castro-alamancos and Gulati, 2014). Measuring the level of a neuromodulator within a brain region is incredibly difficult given our current experimental techniques, making exploration via experimental manipulations the more desirable route. Going after this problem will require careful experimental considerations for whether the neuromodulator should be directly applied via microinfusion or indirectly released through optogenetic activation of the neuromodulatory pathways. Given the diffuse projection patterns of neuromodulatory pathways, it is possible that they present another mechanism for coordinating activity patterns across brain regions. Regardless of the mechanism of application, I think questions of how to decouple the effects of neuromodulatory inputs in a given region from other circuit level effects could provide an alternative view of how processing should work normally and perhaps develop a framework for outlining how failures in the neuromodulatory pathways could underlie neurological disorders.

### 6.3.3 From spikes to action

Within the framework of the proposed experiments, the major question becomes how do the changes in temporal properties affect behavioral performance. We could first

consider a simple behavioral task where an animal is trained to detect a sensory stimulus. Even within this simple behavioral paradigm, there are a lot of different nuclei involved in transforming a sensory stimulus into a motor output. However, if we continue to focus on the thalamocortical circuitry, we could ask how thalamic state impacts the perception of punctate whisker stimuli. Replicating the experimental thalamic state manipulations, we might predict that hyperpolarizing the thalamus to elicit a burst state would improve behavioral performance on a detection task while impairing the animal's ability to perform a discrimination task. Providing a direct link between state manipulation and behavioral performance would build an exciting view of how changing spike timing properties can drive changes in animal behavior.

Understanding how each component of the neural circuitry is involved in gating thalamic information traveling to cortex provides a thalamic-centric view of neural processing. While this is a perspective I have held for most of this thesis, the neural circuitry is incredibly interconnected and complicated such that focusing on any given nucleus will likely preclude us from building a comprehensive understanding of neural function. Instead, the real test of our understanding of neural coding will come from a more global perspective where we try to understand the relationships between nuclei and how information is exchanged to produce behavior. And given the importance of state in neural processing, we really want to be looking across structures simultaneously and ideally in an awake animal providing a behavioral readout. I would really love to push in this direction to build an understanding of distributed representations of information not just within a single neuron or a small population of neurons, but across circuits.

## REFERENCES


Abbott, L.F., Varela, J.A., Sen, K., Nelson, S.B., 1997. Synaptic Depression and Cortical Gain Control. Science (80-. ). 275, 221–224. doi:10.1126/science.275.5297.221

Abeles, M., 1982. Role of the cortical neuron: integrator or coincidence detector? Isr. J. Med. Sci. 18, 83–92. doi:10.1016/S0166-2236(96)80019-1

Adams, N., Lozsadi, D.A., Guillery, R.W., 1997. Complexities in the thalamocortical and corticothalamic pathways. Eur. J. Neurosci. 9, 204–209.

Ahissar, E., Sosnik, R., Haidarliu, S., 2000. Transformation from temporal to rate coding in a somatosensory thalamocortical pathway. Nature 406, 302–6. doi:10.1038/35018568

Alitto, H.J., Weyand, T., Usrey, W.M., 2005. Distinct Properties of Stimulus-Evoked Bursts in the Lateral Geniculate Nucleus. J. Neurosci. 25, 514–523. doi:10.1523/JNEUROSCI.3369-04.2005

Allman, J., Miezin, F., McGuinness, E., 1985. Stimulus specific responses from beyond the classical receptive field : Neurophysiological Mechanisms for Local-Global Comparisons in Visual Neurons. Annu. Rev. Neurosci. 8, 407–430.

Anderson, J., Lampl, I., Reichova, I., Carandini, M., Ferster, D., 2000. Stimulus dependence of two-state fluctuations of membrane potential in cat visual cortex. Nat. Neurosci. 3, 617–21. doi:10.1038/75797

Anderson, L.A., Christianson, G.B., Linden, J.F., 2009. Stimulus-specific adaptation occurs in the auditory thalamus. J. Neurosci. 29, 7359–7363. doi:10.1523/jneurosci.0793-09.2009

Anstis, S., Verstraten, F.A.J., Mather, G., 1998. The Motion Aftereffect. Trends Cogn. Sci. 2, 111–117.

Antunes, F.M., Nelken, I., Covey, E., Malmierca, M.S., 2010. Stimulus-Specific Adaptation in the Auditory Thalamus of the Anesthetized Rat. PLoS One 5, e14071. doi:10.1371/journal.pone.0014071

Arabzadeh, E., Zorzin, E., Diamond, M.E., 2005. Neuronal encoding of texture in the whisker sensory pathway. PLoS Biol. 3, e17. doi:10.1371/journal.pbio.0030017

Aravanis, A.M., Wang, L.-P., Zhang, F., Meltzer, L.A., Mogri, M.Z., Schneider, M.B., Deisseroth, K., 2007. An optical neural interface: in vivo control of rodent motor cortex with integrated fiberoptic and optogenetic technology. J. Neural Eng. 4, S143–S156. doi:10.1088/1741-2560/4/3/S02

Ayala, Y. a., Malmierca, M.S., 2015. Cholinergic Modulation of Stimulus-Specific Adaptation in the Inferior Colliculus. J. Neurosci. 35, 12261–12272. doi:10.1523/JNEUROSCI.0909-15.2015

Azevedo, F.A.C., Carvalho, L.R.B., Grinberg, L.T., Farfel, J.M., Ferretti, R.E.L., Leite, R.E.P., Filho, W.J., Lent, R., Herculano-Houzel, S., 2009. Equal numbers of neuronal and nonneuronal cells make the human brain an isometrically scaled-up primate brain. J. Comp. Neurol. 513, 532–541. doi:10.1002/cne.21974

Azouz, R., Gray, C.M., 2000. Dynamic spike threshold reveals a mechanism for synaptic coincidence detection in cortical neurons in vivo. Proc. Natl. Acad. Sci. U. S. A. 97, 8110–8115. doi:10.1073/pnas.130200797

Bale, M.R., Campagner, D., Erskine, A., Petersen, R.S., 2015. Microsecond-Scale Timing Precision in Rodent Trigeminal Primary Afferents. J. Neurosci. 35, 5935–5940. doi:10.1523/JNEUROSCI.3876-14.2015

Barlow, H., 1961. Possible principles underlying the transformation of sensory messages. Sens. Commun.

Bartho, P., Hirase, H., Zugaro, M., Harris, K.D., Zu-, M., Harris, K.D., 2004. Characterization of Neocortical Principal Cells and Interneurons by Network Interactions and Extracellular Features 600–608.

Baylis, G.C., Rolls, E.T., 1987. Responses of neurons in the inferior temporal cortex in short term and serial recognition memory tasks. Exp. Brain Res. 65, 614–22. doi:10.1007/BF00235984

Beierlein, M., Gibson, J.R., Connors, B.W., 2003. Two dynamically distinct inhibitory networks in layer 4 of the neocortex. J. Neurophysiol. 90, 2987–3000. doi:10.1152/jn.00283.2003

Benda, J., Herz, A.V.M., 2003. A universal model for spike-frequency adaptation. Neural Comput. 15, 2523–2564. doi:10.1162/089976603322385063

Benucci, A., Saleem, A.B., Carandini, M., 2013. Adaptation maintains population homeostasis in primary visual cortex. Nat Neurosci 16, 724–729. doi:10.1038/nn.3382

Berg, R.W., Kleinfeld, D., 2003. Rhythmic whisking by rat: retraction as well as protraction of the vibrissae is under active muscular control. J. Neurophysiol. 89, 104–17. doi:10.1152/jn.00600.2002

Bezdudnaya, T., Cano, M., Bereshpolova, Y., Stoelzel, C.R., Alonso, J.-M., Swadlow, H.A., 2006. Thalamic burst mode and inattention in the awake LGNd. Neuron 49, 421–432. doi:10.1016/j.neuron.2006.01.010

Bezdudnaya, T., Castro-Alamancos, M.A., 2014. Neuromodulation of whisking related neural activity in superior colliculus. J. Neurosci. 34, 7683–95. doi:10.1523/JNEUROSCI.0444-14.2014

Bhattacharjee, A., Kaczmarek, L.K., 2005. For K+ channels, Na+ is the new Ca2+. Trends Neurosci. 28, 422–428. doi:10.1016/j.tins.2005.06.003

Bissière, S., Humeau, Y., Lüthi, A., 2003. Dopamine gates LTP induction in lateral amygdala by suppressing feedforward inhibition. Nat. Neurosci. 6, 587–592. doi:10.1038/nn1058

Blakemore, C., Campbell, F.W., 1969a. On the existence of neurones in the human visual system selectively sensitive to the orientation and size of retinal images. J. Physiol. 203, 237–260. doi:10.1113/jphysiol.1969.sp008862

Blakemore, C., Campbell, R.W., 1969b. Adaptation to spatial stimuli. J. Physiol. - London 200, 11–13. doi:10.1016/S0140-6736(00)96392-X

Blitz, D.M., Regehr, W.G., 2005. Timing and specificity of feed-forward inhibition within the LGN. Neuron 45, 917–928. doi:10.1016/j.neuron.2005.01.033

Boloori, A.-R., Jenks, R. a, Desbordes, G., Stanley, G.B., 2010. Encoding and decoding cortical representations of tactile features in the vibrissa system. J. Neurosci. 30, 9990–10005. doi:10.1523/JNEUROSCI.0807-10.2010

Boloori, A.-R., Stanley, G.B., 2006. The dynamics of spatiotemporal response integration in the somatosensory cortex of the vibrissa system. J. Neurosci. 26, 3767–82. doi:10.1523/JNEUROSCI.4056-05.2006

Bonin, V., Mante, V., Carandini, M., 2005. The Suppressive Field of Neurons in Lateral Geniculate Nucleus. J. Neurosci. 25, 10844–10856. doi:10.1523/JNEUROSCI.3562-05.2005

Borst, J.G.G., 2010. The low synaptic release probability in vivo. Trends Neurosci. 33, 259–266. doi:10.1016/j.tins.2010.03.003

Bortone, D.S., Olsen, S.R., Scanziani, M., 2014. Translaminar inhibitory cells recruited by layer 6 corticothalamic neurons suppress visual cortex. Neuron 82, 474–485. doi:10.1016/j.neuron.2014.02.021

Boudreau, C.E., Ferster, D., 2005. Short-term depression in thalamocortical synapses of cat primary visual cortex. J. Neurosci. 25, 7179–7190. doi:10.1523/JNEUROSCI.1445-05.2005

Brecht, M., Sakmann, B., 2002. Whisker maps of neuronal subclasses of the rat ventral posterior medial thalamus, identified by whole-cell voltage recording and morphological reconstruction. J. Physiol. 495–515. doi:10.1013/jphysiol.2001.012334

Bruno, R.M., 2011. Synchrony in sensation. Curr. Opin. Neurobiol. 21, 701–8. doi:10.1016/j.conb.2011.06.003

Bruno, R.M., Sakmann, B., 2006. Cortex is driven by weak but synchronously active thalamocortical synapses. Science 312, 1622–7. doi:10.1126/science.1124593

Buonomano, D. V., Maass, W., 2009. State-dependent computations: spatiotemporal processing in cortical networks. Nat. Rev. Neurosci. 10, 113–125. doi:10.1038/nrn2558

Buonomano, D. V., Merzenich, M.M., 1998. Cortical plasticity: from synapses to maps. Annu. Rev. Neurosci. 21, 149–186. doi:10.1146/annurev.neuro.21.1.149

Butler, A.B., 2008. Evolution of the thalamus: a morphological and functional review. Thalamus Relat. Syst. 4, 35–58. doi:10.1017/S1472928808000356

Butts, D.A., Weng, C., Jin, J., Alonso, J., Paninski, L., 2011. Temporal Precision in the Visual Pathway through the Interplay of Excitation and Stimulus-Driven Suppression. J. Neurosci. 31, 11313–11327. doi:10.1523/JNEUROSCI.0434-11.2011

Butts, D. a, Weng, C., Jin, J., Yeh, C.-I., Lesica, N.A., Alonso, J.-M., Stanley, G.B., 2007. Temporal precision in the neural code and the timescales of natural vision. Nature 449, 92–96. doi:10.1038/nature06105

Buzsáki, G., 1984. Feed-forward inhibition in the hippocampal formation. Prog. Neurobiol. 22, 131–153. doi:10.1016/0301-0082(84)90023-6

Carandini, M., Heeger, D., 2012. Normalization as a canonical neural computation. doi:10.1038/nrn3136

Carandini, M., Heeger, D.J.D., 2012. Normalization as a canonical neural computation. Nat. Rev. Neurosci. 13, 51–62. doi:10.1038/nrn3136

Castro-Alamancos, M.A., 2002. Different temporal processing of sensory inputs in the rat thalamus during quiescent and information processing states in vivo. J. Neurophysiol. 567–578. doi:10.1013/jphysiol.2001.013283

Castro-alamancos, M.A., Gulati, T., 2014. Neuromodulators Produce Distinct Activated States in Neocortex. J. Neurosci. 34, 12353–12367. doi:10.1523/JNEUROSCI.1858-14.2014

Castro-Alamancos, M. a, 2004a. Dynamics of sensory thalamocortical synaptic networks during information processing states. Prog. Neurobiol. 74, 213–47. doi:10.1016/j.pneurobio.2004.09.002

Castro-Alamancos, M. a, 2004b. Absence of rapid sensory adaptation in neocortex during information processing states. Neuron 41, 455–64.

Castro-Alamancos, M. a, 2002. Role of thalamocortical sensory suppression during arousal: focusing sensory inputs in neocortex. J. Neurosci. 22, 9651–5.

Castro-Alamancos, M. a, Connors, B.W., 1996a. Cellular mechanisms of the augmenting response: short-term plasticity in a thalamocortical pathway. J. Neurosci. 16, 7742–7756.

Castro-Alamancos, M. a, Connors, B.W., 1996b. Spatiotemporal properties of short-term plasticity sensorimotor thalamocortical pathways of the rat. J. Neurosci. 16, 2767–79.

Castro-Alamancos, M. a, Oldford, E., 2002. Cortical sensory suppression during arousal is due to the activity-dependent depression of thalamocortical synapses. J. Physiol. 541, 319–331. doi:10.1113/jphysiol.2002.016857

Cavanaugh, J.R., Bair, W., Movshon, J.A., Li, G., Yao, Z., Wang, Z., Yuan, N., Talebi, V., Tan, J., Zhou, Y., Baker, C.L., Snyder, A.C., Morais, M.J., Kohn, A., Smith, M.A., Cavanaugh, J.R., Bair, W., Movshon, J.A., 2002. Nature and Interaction of Signals From the Receptive Field Center and Surround in Macaque V1 Neurons. J. Neurophysiol. 88, 2530–2546. doi:10.1152/jn.00692.2001

Chance, F.S., Abbott, L.F., 2001. Input-specific adaptation in complex cells through synaptic depression. Neurocomputing 38–40, 141–146. doi:10.1016/S0925-2312(01)00550-1

Chance, F.S., Nelson, S.B., Abbott, L.F., 1998. Synaptic depression and the temporal response characteristics of V1 cells. J. Neurosci. 18, 4785–4799.

Chen, I.-W., Helmchen, F., Lutcke, H., 2015. Specific Early and Late Oddball-Evoked Responses in Excitatory and Inhibitory Neurons of Mouse Auditory Cortex. J. Neurosci. 35, 12560–12573. doi:10.1523/JNEUROSCI.2240-15.2015

Chung, S., Li, X., Nelson, S.B., Street, S., 2002. Short-term depression at thalamocortical synapses contributes to rapid adaptation of cortical sensory responses in vivo. Neuron 34, 437–46.

Civillico, E.F., Contreras, D., 2005. Comparison of responses to electrical stimulation and whisker deflection using two different voltage-sensitive dyes in mouse barrel cortex in vivo. J. Membr. Biol. 208, 171–82. doi:10.1007/s00232-005-0828-6

Clifford, C.W.G., Webster, M.A., Stanley, G.B., Stocker, A. a, Kohn, A., Sharpee, T.O., Schwartz, O., 2007. Visual adaptation: neural, psychological and computational aspects. Vision Res. 47, 3125–31. doi:10.1016/j.visres.2007.08.023

Cohen-Kashi Malina, K., Jubran, M., Katz, Y., Lampl, I., 2013. Imbalance between excitation and inhibition in the somatosensory cortex produces postadaptation facilitation. J. Neurosci. 33, 8463–71. doi:10.1523/JNEUROSCI.4845-12.2013

Constanti, A., Brown, D.A., 1981. M-currents in voltage-clamped mammalian sympathetic neurones. Neurosci. Lett. 24, 289–294.

Constantinople, C.M., Bruno, R.M., 2013. Deep Cortical Layers Are Activated Directly by Thalamus. Science (80-. ). 340, 1591–1594. doi:10.1126/science.1236425

Crandall, S.R., Cruikshank, S.J., Connors, B.W., 2015a. A Corticothalamic Switch: Controlling the Thalamus with Dynamic Synapses. Neuron 86, 1–15. doi:10.1016/j.neuron.2015.03.040

Crandall, S.R., Cruikshank, S.J., Connors, B.W., Crandall, S.R., Cruikshank, S.J., Connors, B.W., 2015b. A Corticothalamic Switch: Controlling the Thalamus with Dynamic Synapses. Neuron 86, 1–15. doi:10.1016/j.neuron.2015.03.040

Crick, F., 1984. Function of the thalamic reticular complex: The searchlight hypothesis.

Proc. Natl. Acad. Sci. U. S. A. 81, 4586–4590.
Crochet, S., Petersen, C.C.H., 2006. Correlating whisker behavior with membrane potential in barrel cortex of awake mice. Nat. Neurosci. 9, 608–10. doi:10.1038/nn1690
Cruikshank, S.J., Lewis, T.J., Connors, B.W., 2007. Synaptic basis for intense thalamocortical activation of feedforward inhibitory cells in neocortex. Nat. Neurosci. 10, 462–8. doi:10.1038/nn1861
Cruikshank, S.J., Urabe, H., Nurmikko, A. V., Connors, B.W., 2010. Pathway-Specific Feedforward Circuits between Thalamus and Neocortex Revealed by Selective Optical Stimulation of Axons. Neuron 65, 230–245. doi:10.1016/j.neuron.2009.12.025
Dayan, P., Abbott, L.F., 2001. Chapter 04. Information Theory, in: Computational and Mathematical Modeling of Neural Systems. pp. 123–50.
de Boer, E., Kuyper, P., 1968. Triggered correlation. IEEE Trans. Biomed. Eng. 15, 169–179. doi:10.1109/TBME.1968.4502561
Dean, I., Harper, N.S., McAlpine, D., 2005. Neural population coding of sound level adapts to stimulus statistics. Nat. Neurosci. 8, 1684–1689. doi:10.1038/nn1541
Debanne, D., Shulz, D.E., Fregnac, Y., 1998. Activity-dependent regulation of "on" and "off" responses in cat visual cortical receptive fields. J Physiol 508, 523–48. doi:DOI 10.1111/j.1469-7793.1998.00523.x
Dempsey, E.W., Morison, R.S., 1943. The Electrical Activity of a Thalamocortical Relay System. Am. J. Physiol. 138, 283–296.
Denning, K.S., Reinagel, P., 2005. Visual Control of Burst Priming in the Anesthetized Lateral Geniculate Nucleus. J. Neurosci. 25, 3531–3538. doi:10.1523/JNEUROSCI.4417-04.2005
Desbordes, G., Jin, J., Weng, C., Lesica, N.A., Stanley, G.B., Alonso, J., 2008. Timing precision in population coding of natural scenes in the early visual system. PLoS Biol. 6, e324. doi:10.1371/journal.pbio.0060324
Deschênes, M., Hu, B., 1990. Electrophysiology and pharmacology of the corticothalamic input to lateral thalamic nuclei: An intracellular study in the cat. Eur. J. Neurosci. 2, 140–152. doi:10.1111/j.1460-9568.1990.tb00406.x
Deschênes, M., Timofeeva, E., Lavallée, P., 2003. The relay of high-frequency sensory signals in the Whisker-to-barreloid pathway. J. Neurosci. 23, 6778–87.
Dhruv, N.T., Carandini, M., 2014. Cascaded Effects of Spatial Adaptation in the Early Visual System. Neuron 81, 529–535. doi:10.1016/j.neuron.2013.11.025
Diamond, M.E., von Heimendahl, M., Knutsen, P.M., Kleinfeld, D., Ahissar, E., 2008a. "Where"and'what'in the whisker sensorimotor system. Nat. Rev. … 9, 601–12. doi:10.1038/nrn2411
Diamond, M.E., von Heimendahl, M., Knutsen, P.M., Kleinfeld, D., Ahissar, E., 2008b. "Where" and "what" in the whisker sensorimotor system. Nat. Rev. Neurosci. 9, 601–12. doi:10.1038/nrn2411
Díaz-Quesada, M., Maravall, M., 2008. Intrinsic mechanisms for adaptive gain rescaling in barrel cortex. J. Neurosci. 28, 696–710. doi:10.1523/JNEUROSCI.4931-07.2008
DiCarlo, J.J., 2001. Sensory System Organization. eLS. doi:10.1038/npg.els.0000076
Dragoi, V., Rivadulla, C., Sur, M., 2001. Foci of orientation plasticity in visual cortex. Nature 411, 80–86. doi:10.1038/35075070

Dragoi, V., Sharma, J., Sur, M., 2000. Adaptation-induced plasticity of orientation tuning in adult visual cortex. Neuron 28, 287–298. doi:10.1016/S0896-6273(00)00103-3

Duque, D., Malmierca, M.S., 2014. Stimulus-specific adaptation in the inferior colliculus of the mouse: anesthesia and spontaneous activity effects. Brain Struct. Funct. 3385–3398. doi:10.1007/s00429-014-0862-1

Duque, D., Wang, X., Nieto-Diego, J., Krumbholz, K., Malmierca, M.S., 2016. Neurons in the inferior colliculus of the rat show stimulus-specific adaptation for frequency, but not for intensity. Sci. Rep. 6, 24114. doi:10.1038/srep24114

Ebara, S., Kumamoto, K., Matsuura, T., Mazurkiewicz, J.E., Rice, F.L., 2002. Similarities and differences in the innervation of mystacial vibrissal follicle-sinus complexes in the rat and cat: a confocal microscopic study. J. Comp. Neurol. 449, 103–19. doi:10.1002/cne.10277

Eggermont, J.J., 1991. Rate and synchronization measures of periodicity coding in cat primary auditory cortex. Hear. Res. 56, 153–167. doi:10.1016/0378-5955(91)90165-6

Eggermont, J.J., Johannesma, P.I.M., Aertsen, A.M.H., 1983. Reverse correlation methods in auditory research. Q. Rev. Biophys. 16, 341–414. doi:10.1017/S0033583500005126

Ego-Stengel, V., Mello e Souza, T., Jacob, V., Shulz, D.E., 2005. Spatiotemporal characteristics of neuronal sensory integration in the barrel cortex of the rat. J. Neurophysiol. 93, 1450–67. doi:10.1152/jn.00912.2004

Escera, C., Malmierca, M.S., 2014. The auditory novelty system: an attempt to integrate human and animal research. Psychophysiology 51, 111–23. doi:10.1111/psyp.12156

Estebanez, L., Boustani, S. El, Destexhe, A., Shulz, D.E., De, N., Scientifique, R., Terrasse, D., Médicale, R., National, C., Recherche, D., El Boustani, S., Destexhe, A., Shulz, D.E., 2012. Correlated input reveals coexisting coding schemes in a sensory cortex. Nat. Neurosci. 15, 1–14. doi:10.1038/nn.3258

Eytan, D., Brenner, N., Marom, S., 2003. Selective adaptation in networks of cortical neurons. J. Neurosci. 23, 9349–9356. doi:23/28/9349 [pii]

Fairhall, A.L., Lewen, G.D., Bialek, W., de Ruyter Van Steveninck, R.R., 2001. Efficiency and ambiguity in an adaptive neural code. Nature 412, 787–92. doi:10.1038/35090500

Fanselow, E.E., Nicolelis, M.A.L., 1999. Behavioral modulation of tactile responses in the rat somatosensory system. J. Neurosci. 19, 7603–16.

Fanselow, E.E., Sameshima, K., Baccala, L. a, Nicolelis, M.A.L., 2001. Thalamic bursting in rats during different awake behavioral states. Proc. Natl. Acad. Sci. U. S. A. 98, 15330–5. doi:10.1073/pnas.261273898

Farley, B.J., Quirk, M.C., Doherty, J.J., Christian, E.P., 2010. Stimulus-specific adaptation in auditory cortex is an NMDA-independent process distinct from the sensory novelty encoded by the mismatch negativity. J Neurosci 30, 16475–16484. doi:10.1523/JNEUROSCI.2793-10.2010

Feldmeyer, D., Brecht, M., Helmchen, F., Petersen, C.C.H., Poulet, J.F.A., Staiger, J.F., Luhmann, H.J., Schwarz, C., 2013. Barrel cortex function. Prog. Neurobiol. 103, 3–27. doi:10.1016/j.pneurobio.2012.11.002

Felsen, G., Shen, Y.S., Yao, H., Spor, G., Li, C., Dan, Y., 2002. Dynamic modification of cortical orientation tuning mediated by recurrent connections. Neuron 36, 945–954. doi:10.1016/S0896-6273(02)01011-5

Ferezou, I., Haiss, F., Gentet, L.J., Aronoff, R., Weber, B., Petersen, C.C.H., 2007. Spatiotemporal dynamics of cortical sensorimotor integration in behaving mice. Neuron 56, 907–23. doi:10.1016/j.neuron.2007.10.007

Finch, D.M., Tan, A.M., Isokawa-Akesson, M., 1988. Feedforward inhibition of the rat entorhinal cortex and subicular complex. J. Neurosci. 8, 2213–2226.

Fleidervish, I.A., Friedman, A., Gutnick, M.J., 1996. Slow inactivation of Na+ current and slow cumulative spike adaptation in mouse and guinea-pig neocortical neurones in slices. J. Physiol. 493, 83–97. doi:10.1113/jphysiol.1996.sp021366

Forsythe, I.D., 2002. Auditory Processing. eLS.

Fox, C.J., Barton, J.J.S., 2007. What is adapted in face adaptation? The neural representations of expression in the human visual system. Brain Res. 1127, 80–89. doi:10.1016/j.brainres.2006.09.104

Fritz, J.B., Shamma, S.A., Elhilali, M., Klein, D., 2003. Rapid task-related plasticity of spectrotemporal receptive fields in primary auditory cortex. Nat. Neurosci. 6, 1216–23. doi:10.1038/nn1141

Froemke, R.C., Dan, Y., 2002. Spike-timing-dependent synaptic modification induced by natural spike trains. Nature 416, 433–8. doi:10.1038/416433a

Gabernet, L., Jadhav, S.P., Feldman, D.E., Carandini, M., Scanziani, M., 2005. Somatosensory integration controlled by dynamic thalamocortical feed-forward inhibition. Neuron 48, 315–27. doi:10.1016/j.neuron.2005.09.022

Ganmor, E., Katz, Y., Lampl, I., 2010. Intensity-dependent adaptation of cortical and thalamic neurons is controlled by brainstem circuits of the sensory pathway. Neuron 66, 273–86. doi:10.1016/j.neuron.2010.03.032

Garabedian, C.E., Jones, S.R., Merzenich, M.M., Dale, A., Moore, C.I., Garabedian, C.E., Jones, S.R., Merzenich, M.M., Dale, A., Moore, C.I., 2003. Band-Pass Response Properties of Rat SI Neurons. J. Neurophysiol. 1379–1391. doi:10.1152/jn.01158.2002

Gardner, E.P., 2010. Touch. Encycl. Life Sci. 1–12. doi:10.1002/9780470015902.a0000219.pub2

Georgeson, M.A., Harris, M.G., 1984. Spatial selectivity of contrast adaptation: Models and data. Vision Res. 24, 729–741. doi:10.1016/0042-6989(84)90214-1

Gil, Z., Connors, B.W., Amitai, Y., 1999. Efficacy of thalamocortical and intracortical synaptic connections: quanta, innervation, and reliability. Neuron 23, 385–97.

Gil, Z., Connors, B.W., Amitai, Y., 1997. Differential regulation of neocortical synapses by neuromodulators and activity. Neuron 19, 679–686. doi:10.1016/S0896-6273(00)80380-3

Gilbert, C.D., 1998. Adult cortical dynamics. Physiol. Rev. 78, 467–485.

Gjorgjieva, J., Mease, R.A., Moody, W.J., Fairhall, A.L., 2014. Intrinsic Neuronal Properties Switch the Mode of Information Transmission in Networks. PLoS Comput. Biol. 10. doi:10.1371/journal.pcbi.1003962

Goard, M., Dan, Y., 2009. Basal forebrain activation enhances cortical coding of natural scenes. Nat. Neurosci. 12, 1444–9. doi:10.1038/nn.2402

Goble, A.K., Hollins, M., 1994. Vibrotactile enhances frequency discrimination. J. Acoust. Soc. Am. 96, 771–780. doi:10.1121/1.410314

Goble, A.K., Hollins, M., 1993. Vibrotactile adaptation enhances amplitude discrimination. J. Acoust. Soc. Am. 96, 771–780.

Goldman, M.S., Nelson, S.B., Abbott, L.F., 1999. Decorrelation of spike trains by synaptic depression. Neurocomputing 26–27, 147–153. doi:10.1016/S0925-2312(99)00068-5
Gollnick, C.A., Millard, D.C., Ortiz, A.D., Bellamkonda, R. V, Stanley, G.B., 2016. Response reliability observed with voltage-sensitive dye imaging of cortical later 2/3: The Probability of Activation Hypothesis. J. Neurophysiol. jn.00547.2015-. doi:10.1152/ajpheart.00896.2013
Goodwin, A.W., 2005. Somatosensory Systems. eLS 1–8. doi:10.1038/npg.els.0004082
Greenlee, M.W., Heitger, F., 1988. The functional role of contrast adaptation. Vision Res. 28, 791–797. doi:10.1016/0042-6989(88)90026-0
Grimm, S., Escera, C., 2012. Auditory deviance detection revisited: Evidence for a hierarchical novelty system. Int. J. Psychophysiol. 85, 88–92. doi:10.1016/j.ijpsycho.2011.05.012
Grosenick, L., Marshel, J.H., Deisseroth, K., 2015. Closed-Loop and Activity-Guided Optogenetic Control. Neuron 86, 106–139. doi:10.1016/j.neuron.2015.03.034
Guido, W., Lu, S.M., Vaughan, J.W., Godwin, D.W., Sherman, S.M., 1995. Receiver operating characteristic (ROC) analysis of neurons in the cat's lateral geniculate nucleus during tonic and burst response mode. Vis. Neurosci. 12, 723–741. doi:10.1017/S0952523800008993
Guido, W., Weyand, T., 1995. Burst responses in thalamic relay cells of the awake behaving cat. J. Neurophysiol. 74, 1782–1786.
Gutnisky, D.A., Dragoi, V., 2008. Adaptive coding of visual information in neural populations. Nature 452, 220–224. doi:10.1038/nature06563
Haas, J.S., Greenwald, C.M., Pereda, A.E., 2016. Activity-dependent plasticity of electrical synapses: increasing evidence for its presence and functional roles in the mammalian brain. BMC Cell Biol. 17, 14. doi:10.1186/s12860-016-0090-z
Haider, B., Duque, A., Hasenstaub, A.R., Yu, Y., McCormick, D.A., 2007. Enhancement of visual responsiveness by spontaneous local network activity in vivo. J. Neurophysiol. 97, 4186–202. doi:10.1152/jn.01114.2006
Haider, B., Krause, M.R., Duque, A., Yu, Y., Touryan, J., Mazer, J.A., McCormick, D.A., 2010. Synaptic and Network Mechanisms of Sparse and Reliable Visual Cortical Activity during Nonclassical Receptive Field Stimulation. Neuron 65, 107–121. doi:10.1016/j.neuron.2009.12.005
Haider, B., McCormick, D.A., 2009. Rapid Neocortical Dynamics: Cellular and Network Mechanisms. Neuron 62, 171–189. doi:10.1016/j.neuron.2009.04.008
Halassa, M.M., Acsády, L., 2016. Thalamic inhibition: Diverse sources, diverse scales. Tins In press, 1–14. doi:10.1016/j.tins.2016.08.001
Halassa, M.M., Chen, Z., Wimmer, R.D., Brunetti, P.M., Zhao, S., Zikopoulos, B., Wang, F., Brown, E.N., Wilson, M.A., 2014. State-Dependent Architecture of Thalamic Reticular Subnetworks. Cell 158, 808–821. doi:10.1016/j.cell.2014.06.025
Halassa, M.M.M., Siegle, J.H., Ritt, J.T., Ting, J.T., Feng, G., Moore, C.I., 2011. Selective optical drive of thalamic reticular nucleus generates thalamic bursts and cortical spindles. Nat. Neurosci. 14, 1118–20. doi:10.1038/nn.2880
Harris, K.D., Mrsic-Flogel, T.D., 2013. Cortical connectivity and sensory coding. Nature 503, 51–8. doi:10.1038/nature12654
Harris, K.D., Shepherd, G.M.G., 2015. The neocortical circuit: themes and variations. Nat. Neurosci. 18, 170–181. doi:10.1038/nn.3917

Hart, A., Sengupta, P., 2001. Sensory Transduction Mechanisms. Encycl. Life Sci. 1–8.
Hartings, J. a, Temereanca, S., Simons, D.J., 2003. Processing of periodic whisker deflections by neurons in the ventroposterior medial and thalamic reticular nuclei. J. Neurophysiol. 90, 3087–3094. doi:10.1152/jn.00469.2003
Häusser, M., Spruston, N., Stuart, G.J., Hausser, M., 2015. Diversity and Dynamics Signaling of Dendritic Signalling. Science (80-. ). 290, 739–744. doi:10.1126/science.290.5492.739
Hawken, M.J., Shapley, R.M., Grosof, D.H., 1990. Temporal-frequency selectivity in monkey visual cortex. Vis. Neurosci. 13, 477–492. doi:10.1017/S0952523800008154
Heeger, D.J., 1992. Normalization of cell responses in cat striate cortex. Vis. Neurosci. 9, 181–197.
Heiss, J.E., Katz, Y., Ganmor, E., Lampl, I., 2008. Shift in the balance between excitation and inhibition during sensory adaptation of S1 neurons. J. Neurosci. 28, 13320–30. doi:10.1523/JNEUROSCI.2646-08.2008
Hentschke, H., Haiss, F., Schwarz, C., 2006. Central signals rapidly switch tactile processing in rat barrel cortex during whisker movements. Cereb. cortex 16, 1142–56. doi:10.1093/cercor/bhj056
Henze, D.A., Buzsáki, G., 2001. Action potential threshold of hippocampal pyramidal cells in vivo is increased by recent spiking activity. Neuroscience 105, 121–130. doi:10.1016/S0306-4522(01)00167-1
Hershenhoren, I., Taaseh, N., Antunes, F.M., Nelken, I., 2014. Intracellular Correlates of Stimulus-Specific Adaptation. J. Neurosci. 34, 3303–3319. doi:10.1523/JNEUROSCI.2166-13.2014
Higley, M.J., Contreras, D., 2007. Frequency adaptation modulates spatial integration of sensory responses in the rat whisker system. J. Neurophysiol. 97, 3819–3824. doi:10.1152/jn.00098.2007
Higley, M.J., Contreras, D., 2006. Balanced excitation and inhibition determine spike timing during frequency adaptation. J. Neurosci. 26, 448–457. doi:10.1523/JNEUROSCI.3506-05.2006
Hirata, A., Castro-Alamancos, M. a, 2010. Neocortex network activation and deactivation states controlled by the thalamus. J. Neurophysiol. 103, 1147–1157. doi:10.1152/jn.00955.2009
Hofman, M.A., 2014. Evolution of the human brain: when bigger is better. Front. Neuroanat. 8, 15. doi:10.3389/fnana.2014.00015
Hofman, M.A., 1985. Size and shape of the cerebral cortex in mammals: I. The Cortical Surface. Brain Behav. Evol. 27, 28–40. doi:10.1017/CBO9781107415324.004
Hooser, S.D. Van, 2005. Visual System. Encycl. Life Sci. 1–8. doi:10.1038/npg.els.0000230
Huang, C.G., Zhang, Z.D., Chacron, M.J., 2016. Temporal decorrelation by SK channels enables efficient neural coding and perception of natural stimuli. Nat. Commun. 7, 11353. doi:10.1038/ncomms11353
Hubel, D., Wiesel, T., 1962. Receptive fields, binocular interaction and functional architecture in the cat's visual cortex. J. Physiol. 160, 106–154.
Hubel, D., Wiesel, T., 1959. Receptive fields of single neurones in the cat's striate cortex. J. Physiol. 574–591.
Isaacson, J.S., Scanziani, M., 2011. How inhibition shapes cortical activity. Neuron 72,

231–243. doi:10.1016/j.neuron.2011.09.027
Jin, D.Z., Dragoi, V., Sur, M., Seung, H.S., 2005. Tilt aftereffect and adaptation-induced changes in orientation tuning in visual cortex. J. Neurophysiol. 94, 4038–4050. doi:10.1152/jn.00571.2004
Johansson, R.S., Vallbo, A.B., 1979a. Detection of tactile stimuli. Thresholds of afferent units related to psychophysical thresholds in the human hand. J. Physiol. 297, 405–22. doi:0022-3751/79/6320-0181
Johansson, R.S., Vallbo, a. B., 1983. Tactile sensory coding in the glabrous skin of the human hand. Trends Neurosci. 6, 27–32. doi:10.1016/0166-2236(83)90011-5
Johansson, R.S., Vallbo, a B., 1979b. Tactile Sensibility in the Human Hand: Relative and Absolute Densities of Four Types of Mechanoreceptive Units in Glabrous Skin 283–300.
Jones, E.G., 2002. Thalamic circuitry and thalamocortical synchrony. Philos. Trans. R. Soc. B Biol. Sci. 357, 1659–1673. doi:10.1098/rstb.2002.1168
Jones, H.E., Grieve, K.L., Wang, W., Sillito, a M., 2001. Surround suppression in primate V1. J. Neurophysiol. 86, 2011–2028.
Jones, L.M., Depireux, D.A., Simons, D.J., Keller, A., 2004. Robust Temporal Coding in the Trigeminal System. Science (80-. ). 304, 1986–1989. doi:10.1126/science.1097779
Jouhanneau, J.-S., Kremkow, J., Dorrn, A.L., Poulet, J.F.A., 2015. In Vivo Monosynaptic Excitatory Transmission between Layer 2 Cortical Pyramidal Neurons. Cell Rep. 2098–2106. doi:10.1016/j.celrep.2015.11.011
Jubran, M., Mohar, B., Lampl, I., 2016. The transformation of adaptation specificity to whisker identity from brainstem to thalamus. Front. Syst. Neurosci. doi:10.3389/fnsys.2016.00056
Jung, H.Y., Mickus, T., Spruston, N., 1997. Prolonged sodium channel inactivation contributes to dendritic action potential attenuation in hippocampal pyramidal neurons. J. Neurosci. 17, 6639–6646.
Kaliukhovich, X.D.A., Vogels, R., 2016. Divisive Normalization Predicts Adaptation-Induced Response Changes in Macaque Inferior Temporal Cortex. J. Neurosci. 36, 6116–6128. doi:10.1523/JNEUROSCI.2011-15.2016
Karmarkar, U.R., Dan, Y., 2006. Experience-Dependent Plasticity in Adult Visual Cortex. Neuron 52, 577–585. doi:10.1016/j.neuron.2006.11.001
Khatri, V., Hartings, J. a, Simons, D.J., 2004. Adaptation in thalamic barreloid and cortical barrel neurons to periodic whisker deflections varying in frequency and velocity. J. Neurophysiol. 92, 3244–54. doi:10.1152/jn.00257.2004
Khouri, L., Nelken, I., 2015. Detecting the unexpected. Curr. Opin. Neurobiol. 35, 142–147. doi:10.1016/j.conb.2015.08.003
Kilgard, M.P., Merzenich, M.M., 1998. Plasticity of temporal information processing in the primary auditory cortex. Nat. Neurosci. 1, 727–731. doi:10.1038/3729
King, J.L., Lowe, M.P., Stover, K.R., Wong, A.A., Crowder, N.A., 2016. Adaptive Processes in Thalamus and Cortex Revealed by Silencing of Primary Visual Cortex during Contrast Adaptation. Curr. Biol. 26, 1–6. doi:10.1016/j.cub.2016.03.018
Ko, H., Cossell, L., Baragli, C., Antolik, J., Clopath, C., Hofer, S.B., Mrsic-Flogel, T.D., 2013. The emergence of functional microcircuits in visual cortex. Nature 496, 96–100. doi:10.1038/nature12015

Ko, H., Hofer, S.B., Pichler, B., Buchanan, K. a, Sjöström, P.J., Mrsic-Flogel, T.D., 2011. Functional specificity of local synaptic connections in neocortical networks. Nature 473, 87–91. doi:10.1038/nature09880

Kohn, A., 2007. Visual adaptation: physiology, mechanisms, and functional benefits. J. Neurophysiol. 97, 3155–3164. doi:10.1152/jn.00086.2007

La Camera, G., Rauch, A., Thurbon, D., Lu, H., Senn, W., Fusi, S., 2006. Multiple Time Scales of Temporal Response in Pyramidal and Fast Spiking Cortical Neurons. J. Neurophysiol. 96, 3448–3464. doi:10.1152/jn.00453.2006.

Ladenbauer, J., Augustin, M., Shiau, L., Obermayer, K., 2012. Impact of adaptation currents on synchronization of coupled exponential integrate-and-fire neurons. PLoS Comput. Biol. 8, e1002478. doi:10.1371/journal.pcbi.1002478

Lancaster, B., Nicoll, R. a, 1987. Properties of two calcium-activated hyperpolarizations in rat hippocampal neurones. J. Physiol. 389, 187–203.

Landisman, C.E., Connors, B.W., 2007. VPM and PoM nuclei of the rat somatosensory thalamus: intrinsic neuronal properties and corticothalamic feedback. Cereb. Cortex 17, 2853–65. doi:10.1093/cercor/bhm025

Laughlin, S.B., 1987. Form and function in retinal processing. Trends Neurosci. 10, 478–483. doi:10.1016/0166-2236(87)90104-4

Laughlin, S.B., Hardie, R.C., 1978. Common strategies for light adaptation in the peripheral visual systems of fly and dragonfly. J. Comp. Physiol. ??? A 128, 319–340. doi:10.1007/BF00657606

Lee, C.J., Whitsel, B.L., 1992. Mechanisms underlying somatosensory cortical dynamics: I. In vivo studies. Cereb. Cortex 2, 81–106.

Lesica, N.A., Jin, J., Weng, C., Yeh, C.-I., Butts, D. a, Stanley, G.B., Alonso, J.-M., 2007. Adaptation to stimulus contrast and correlations during natural visual stimulation. Neuron 55, 479–91. doi:10.1016/j.neuron.2007.07.013

Lesica, N.A., Stanley, G.B., 2006. Decoupling functional mechanisms of adaptive encoding. Network 17, 43–60. doi:10.1080/09548980500328409

Lesica, N.A., Stanley, G.B., 2005. An LGN inspired detect/transmit framework for high fidelity relay of visual information with limited bandwidth. Lect. Notes Comput. Sci. (including Subser. Lect. Notes Artif. Intell. Lect. Notes Bioinformatics) 3704 LNCS, 177–186. doi:10.1007/11565123_18

Lesica, N.A., Stanley, G.B., 2004. Encoding of natural scene movies by tonic and burst spikes in the lateral geniculate nucleus. J. Neurosci. 24, 10731–40. doi:10.1523/JNEUROSCI.3059-04.2004

Lesica, N.A., Weng, C., Jin, J., Yeh, C.-I., Alonso, J.-M., Stanley, G.B., 2006. Dynamic encoding of natural luminance sequences by LGN bursts. PLoS Biol. 4, e209. doi:10.1371/journal.pbio.0040209

Levinson, E., Sekular, R., 1976. Adaptation Alters Perceived Direction of Motion. Vision Res. 16, 779–781.

Lippert, M.T., Takagaki, K., Xu, W., Huang, X., Wu, J.-Y., 2007. Methods for voltage-sensitive dye imaging of rat cortical activity with high signal-to-noise ratio. J. Neurophysiol. 98, 502–12. doi:10.1152/jn.01169.2006

Llinas, R., Steriade, M., 2006. Bursting of Thalamic Neurons and States of Vigilance. J. Neurohysiology 95, 3297–3308. doi:10.1152/jn.00166.2006.

Lottem, E., Azouz, R., 2011. A unifying framework underlying mechanotransduction in

the somatosensory system. J. Neurosci. 31, 8520–32. doi:10.1523/JNEUROSCI.6695-10.2011
Lottem, E., Azouz, R., 2008. Dynamic translation of surface coarseness into whisker vibrations. J. Neurophysiol. 100, 2852–65. doi:10.1152/jn.90302.2008
Louie, K., Khaw, M.W., Glimcher, P.W., 2013. Normalization is a general neural mechanism for context-dependent decision making. Proc. Natl. Acad. Sci. Unites States Am. 110, 6139–44. doi:10.1073/pnas.1217854110
Lu, S., Guido, W., Sherman, S.M., 1992. Effects of Membrane Voltage on Receptive Field Properties of Lateral Geniculate Neurons in the Cat: Contributions of the Low-Threshold Ca^ 2^+ Conductance. J. Neurophysiol. 68.
Lundstrom, B.N., Fairhall, A.L., Maravall, M., 2010. Multiple timescale encoding of slowly varying whisker stimulus envelope in cortical and thalamic neurons in vivo. J. Neurosci. 30, 5071–7. doi:10.1523/JNEUROSCI.2193-09.2010
Lundstrom, B.N., Higgs, M.H., Spain, W.J., Fairhall, A.L., 2008. Fractional differentiation by neocortical pyramidal neurons. Nat. Neurosci. 11, 1335–1342. doi:10.1038/nn.2212
Luo, L., Callaway, E., Svoboda, K., 2008. Genetic Dissection of Neural Circuits. Neuron 57, 634–660. doi:10.1016/j.neuron.2008.01.002.Genetic
Lüthi, A., McCormick, D.A., 1998. H-current: Properties of a neuronal and network pacemaker. Neuron 21, 9–12. doi:10.1016/S0896-6273(00)80509-7
MacDonald, J., McGurk, H., 1978. Visual influences on speech perception processes. Percept. Psychophys. 24, 253–257. doi:10.3758/BF03206096
Malmierca, M.S., 2015. The cortical modulation of stimulus-specific adaptation in the auditory midbrain and thalamus: a potential neuronal correlate for predictive coding. Front. Syst. Neurosci. 9, 1–14. doi:10.3389/fnsys.2015.00019
Malmierca, M.S., Cristaudo, S., Pérez-González, D., Covey, E., 2009. Stimulus-specific adaptation in the inferior colliculus of the anesthetized rat. J. Neurosci. 29, 5483–5493. doi:10.1523/JNEUROSCI.4153-08.2009
Mancini, F., Bauleo, A., Cole, J., Lui, F., Porro, C.A., Haggard, P., Iannetti, G.D., 2014. Whole-body mapping of spatial acuity for pain and touch. Ann. Neurol. 75, 917–924. doi:10.1002/ana.24179
Mante, V., Frazor, R. a, Bonin, V., Geisler, W.S., Carandini, M., 2005. Independence of luminance and contrast in natural scenes and in the early visual system. Nat. Neurosci. 8, 1690–7. doi:10.1038/nn1556
Maravall, M., Alenda, A., Bale, M.R., Petersen, R.S., 2013. Transformation of adaptation and gain rescaling along the whisker sensory pathway. PLoS One 8. doi:10.1371/journal.pone.0082418
Maravall, M., Petersen, R.S., Fairhall, A.L., Arabzadeh, E., Diamond, M.E., 2007. Shifts in coding properties and maintenance of information transmission during adaptation in barrel cortex. PLoS Biol. 5, e19. doi:10.1371/journal.pbio.0050019
Mattis, J., Tye, K.M., Ferenczi, E.A., Ramakrishnan, C., Shea, D.J.O., Prakash, R., Gunaydin, L. a, Hyun, M., Fenno, L.E., Gradinaru, V., Yizhar, O., Deisseroth, K., O'Shea, D.J., Prakash, R., Gunaydin, L. a, Hyun, M., Fenno, L.E., Gradinaru, V., Yizhar, O., Deisseroth, K., 2012. Principles for applying optogenetic tools derived from direct comparative analysis of microbial opsins. Nat. Methods 9, 159–72. doi:10.1038/nmeth.1808

McAlonan, K., Cavanaugh, J., Wurtz, R.H., 2008. Guarding the gateway to cortex with attention in visual thalamus. Nature 456, 391–4. doi:10.1038/nature07382

McCormick, D.A., McGinley, M.J., Salkoff, D.B., 2015. Brain state dependent activity in the cortex and thalamus. Curr. Opin. Neurobiol. 31, 133–140. doi:10.1016/j.conb.2014.10.003

McCormick, D.A., von Krosigk, M., 1992. Corticothalamic activation modulates thalamic firing through glutamate "metabotropic" receptors. Proc. Natl. Acad. Sci. U. S. A. 89, 2774–2778. doi:10.1073/pnas.89.7.2774

McGurk, H., Macdonald, J., 1976. Hearing lips and seeing voices. Nature 264, 691–811. doi:10.1038/264746a0

Mease, R. a, Famulare, M., Gjorgjieva, J., Moody, W.J., Fairhall, A.L., 2013. Emergence of adaptive computation by single neurons in the developing cortex. J. Neurosci. 33, 12154–70. doi:10.1523/JNEUROSCI.3263-12.2013

Mease, R. a, Krieger, P., Groh, A., 2014. Cortical control of adaptation and sensory relay mode in the thalamus. Proc. Natl. Acad. Sci. U. S. A. 111, 6798–803. doi:10.1073/pnas.1318665111

Mensi, S., Naud, R., Pozzorini, C., Avermann, M., Carl, C., Petersen, H., Gerstner, W., Petersen, C.C.H., 2012. Parameter extraction and classification of three cortical neuron types reveals two distinct adaptation mechanisms. J. Neurophysiol. 1756–1775. doi:10.1152/jn.00408.2011

Metherate, R., Ashe, J.H., 1993. Nucleus basalis stimulation facilitates thalamocortical synaptic transmission in the rat auditory cortex. Synapse 14, 132–143. doi:10.1002/syn.890140206

Mill, R., Coath, M., Wennekers, T., Denham, S.L., 2011. A Neurocomputational Model of Stimulus-Specific Adaptation to Oddball and Markov Sequences. PLoS Comput. Biol. 7, e1002117. doi:10.1371/journal.pcbi.1002117

Millard, D.C., Wang, Q., Gollnick, C.A., Stanley, G.B., 2013. System identification of the nonlinear dynamics in the thalamocortical circuit in response to patterned thalamic microstimulation in vivo. J. Neural Eng. 10, 66011. doi:10.1088/1741-2560/10/6/066011

Millard, D.C., Whitmire, C.J., Gollnick, C.A., Rozell, C.J., Stanley, G.B., 2015. Electrical and Optical Activation of Mesoscale Neural Circuits with Implications for Coding. J. Neurosci. 35, 15702–15715. doi:10.1523/JNEUROSCI.5045-14.2015

Miller, E.K., Gochin, P.M., Gross, C.G., 1991. Habituation-like decrease in the responses of neurons in inferior temporal cortex of the macaque. Vis. Neurosci.

Miller, K.D., 2016. Canonical computations of cerebral cortex. Curr. Opin. Neurobiol. 37, 75–84. doi:10.1016/j.conb.2016.01.008

Miller, K.D., Pinto, D.J., Simons, D.J., 2001. Processing in layer 4 of the neocortical circuit: New insights from visual and somatosensory cortex. Curr. Opin. Neurobiol. 11, 488–497. doi:10.1016/S0959-4388(00)00239-7

Montemurro, M. a, Panzeri, S., Maravall, M., Alenda, A., Bale, M.R., Brambilla, M., Petersen, R.S., 2007. Role of precise spike timing in coding of dynamic vibrissa stimuli in somatosensory thalamus. J. Neurophysiol. 98, 1871–82. doi:10.1152/jn.00593.2007

Moore, C.I., 2004. Frequency-dependent processing in the vibrissa sensory system. J. Neurophysiol. 91, 2390–9. doi:10.1152/jn.00925.2003

Moore, C.I., Carlen, M., Knoblich, U., Cardin, J.A., 2010. Neocortical Interneurons: From Diversity, Strength. Cell 142, 189–193. doi:10.1016/j.cell.2010.07.005
Moore, C.I., Nelson, S.B., Sur, M., 1999. Dynamics of neuronal processing in rat somatosensory cortex. Trends Neurosci. 22, 513–20.
Mountcastle, V.B., 1997. The columnar organization of the neocortex. Brain 120, 701–722. doi:10.1093/brain/120.4.701
Mountcastle, V.B., 1957. Modality and topographic properties of single neurons of cat's somatic sensory cortex. J. Neurophysiol. 20, 408–34.
Mrsic-Flogel, T.D., Hübener, M., 2002. Visual cortex: Suppression by depression? Curr. Biol. 12, 547–549. doi:10.1016/S0960-9822(02)01049-7
Mukherjee, P., Kaplan, E., 1995. Dynamics of neurons in the cat lateral geniculate nucleus: in vivo electrophysiology and computational modeling. J. Neurophysiol. 74, 1222–1243.
Musall, S., von der Behrens, W., Mayrhofer, J.M., Weber, B., Helmchen, F., Haiss, F., 2014. Tactile frequency discrimination is enhanced by circumventing neocortical adaptation. Nat. Neurosci. 17. doi:10.1038/nn.3821
Natan, R.G., Briguglio, J.J., Mwilambwe-Tshilobo, L., Jones, S.I., Aizenberg, M., Goldberg, E.M., Geffen, M.N., 2015. Complementary control of sensory adaptation by two types of cortical interneurons. Elife 4, 1–27. doi:10.7554/eLife.09868
Newman, J.P., Fong, M., Millard, D.C., Whitmire, C.J., Stanley, G.B., Potter, S.M., 2015. Optogenetic feedback control of neural activity. Elife 1–24. doi:10.7554/eLife.07192
Niell, C.M., Stryker, M.P., 2010. Modulation of visual responses by behavioral state in mouse visual cortex. Neuron 65, 472–9. doi:10.1016/j.neuron.2010.01.033
O'Connor, D.H., Clack, N.G., Huber, D., Komiyama, T., Myers, E.W., Svoboda, K., 2010. Vibrissa-based object localization in head-fixed mice. J. Neurosci. 30, 1947–67. doi:10.1523/JNEUROSCI.3762-09.2010
Ohshiro, T., Angelaki, D.E., DeAngelis, G.C., 2011. A normalization model of multisensory integration. Nat. Neurosci. 14, 775–82. doi:10.1038/nn.2815
Ollerenshaw, D.R., Zheng, H.J.V. V, Millard, D.C., Wang, Q., Stanley, G.B., 2014. The adaptive trade-off between detection and discrimination in cortical representations and behavior. Neuron 81, 1152–1164. doi:10.1016/j.neuron.2014.01.025
Olsen, S.R., Bhandawat, V., Wilson, R.I., 2010. Divisive normalization in olfactory population codes. Neuron 66, 287–299. doi:10.1016/j.neuron.2010.04.009
Olsen, S.R., Bortone, D.S., Adesnik, H., Scanziani, M., 2012. Gain control by layer six in cortical circuits of vision. Nature 483, 47–52. doi:10.1038/nature10835
Pachitariu, X.M., Lyamzin, D.R., Sahani, M., Lesica, N.A., Pachitariu, M., Lyamzin, D.R., Sahani, M., Lesica, N.A., 2015. State-dependent population coding in primary auditory cortex. J. Neurosci. 35, 2058–73. doi:10.1523/JNEUROSCI.3318-14.2015
Pala, A., Petersen, C.C.H., 2015. In Vivo Measurement of Cell-Type-Specific Synaptic Connectivity and Synaptic Transmission in Layer 2/3 Mouse Barrel Cortex. Neuron 85, 68–75. doi:10.1016/j.neuron.2014.11.025
Patterson, C.A., Wissig, S.C., Kohn, A., 2013. Distinct Effects of Brief and Prolonged Adaptation on Orientation Tuning in Primary Visual Cortex. J. Neurosci. 33, 532–543. doi:10.1523/JNEUROSCI.3345-12.2013
Patterson, C. a, Wissig, S.C., Kohn, A., 2014. Adaptation disrupts motion integration in the primate dorsal stream. Neuron 81, 674–86. doi:10.1016/j.neuron.2013.11.022

Paxinos, G., Watson, C., 1998. The Rat Brain in Stereotaxic Coordinates. Academic Press.
Pérez-González, D., Malmierca, M.S., 2014. Adaptation in the auditory system: an overview. Front. Integr. Neurosci. 8, 19. doi:10.3389/fnint.2014.00019
Perez-Reyes, E., 2003. Molecular physiology of low-voltage-activated t-type calcium channels. Physiol. Rev. 83, 117–161. doi:10.1152/physrev.00018.2002
Petersen, C.C.H., 2007. The functional organization of the barrel cortex. Neuron 56, 339–55. doi:10.1016/j.neuron.2007.09.017
Petersen, C.C.H., Grinvald, A., Sakmann, B., 2003a. Spatiotemporal dynamics of sensory responses in layer 2/3 of rat barrel cortex measured in vivo by voltage-sensitive dye imaging combined with whole-cell voltage recordings and neuron reconstructions. J. Neurosci. 23, 1298–309.
Petersen, C.C.H., Hahn, T.T.G., Mehta, M., Grinvald, A., Sakmann, B., 2003b. Interaction of sensory responses with spontaneous depolarization in layer 2/3 barrel cortex. Proc. Natl. Acad. Sci. U. S. A. 100, 13638–43. doi:10.1073/pnas.2235811100
Petersen, R.S., Brambilla, M., Bale, M.R., Alenda, A., Panzeri, S., Montemurro, M. a, Maravall, M., 2008. Diverse and temporally precise kinetic feature selectivity in the VPm thalamic nucleus. Neuron 60, 890–903. doi:10.1016/j.neuron.2008.09.041
Pillow, J.W., Simoncelli, E.P., 2006. Dimensionality reduction in neural models: an information-theoretic generalization of spike-triggered average and covariance analysis. J. Vis. 6, 414–28. doi:10.1167/6.4.9
Pinault, D., 2004. The thalamic reticular nucleus: structure, function and concept., Brain research. Brain research reviews. doi:10.1016/j.brainresrev.2004.04.008
Pinto, L., Goard, M.J., Estandian, D., Xu, M., Kwan, A.C., Lee, S.-H., Harrison, T.C., Feng, G., Dan, Y., 2013. Fast modulation of visual perception by basal forebrain cholinergic neurons. Nat. Neurosci. 16, 1857–1863. doi:10.1038/nn.3552
Pouille, F., Scanziani, M., 2001. Enforcement of temporal fidelity in pyramidal cells by somatic feed-forward inhibition. Science 293, 1159–1163. doi:10.1126/science.1060342
Poulet, J.F.A., Fernandez, L.M.J., Crochet, S., Petersen, C.C.H., 2012. Thalamic control of cortical states. Nat. Neurosci. 15, 370–2. doi:10.1038/nn.3035
Poulet, J.F.A., Petersen, C.C.H., 2008. Internal brain state regulates membrane potential synchrony in barrel cortex of behaving mice. Nature 454, 881–5. doi:10.1038/nature07150
Pozzorini, C., Naud, R., Mensi, S., Gerstner, W., 2013. Temporal whitening by power-law adaptation in neocortical neurons. Nat. Neurosci. 16, 942–948. doi:10.1038/nn.3431
Prothero, J., Sundsten, J., 1984. Folding of the cerebral cortex in mammals: a scaling model. Brain Behav. Evol. 24, 152–167. doi:10.1017/CBO9781107415324.004
Quiroga, R.Q., Nadasdy, Z., Ben-Shaul, Y., 2004. Unsupervised spike detection and sorting with wavelets and superparamagnetic clustering. Neural Comput. 16, 1661–1687. doi:10.1162/089976604774201631
Ramcharan, E.J., Gnadt, J.W., Sherman, S.M., 2000. Burst and tonic firing in thalamic cells of unanesthetized, behaving monkeys. Vis. Neurosci. 17, 55–62. doi:10.1017/S0952523800171056
Ramirez, A., Pnevmatikakis, E., Merel, J., Paninski, L., Miller, K.D., Bruno, R.M., 2014. The spatiotemporal receptive fields of barrel cortex neurons revealed by reverse correlation of synaptic input. Nat. Neurosci. 17, 866–875.

Regehr, W.G., 2012. Short-term presynaptic plasticity. Cold Spring Harb. Perspect. Biol. 4, a005702. doi:10.1101/cshperspect.a005702

Reinagel, P., Godwin, D., Sherman, S.M., Koch, C., 1999. Encoding of visual information by LGN bursts. J. Neurophysiol. 2558–2569.

Reinhold, K., Lien, A.D., Scanziani, M., 2015. Distinct recurrent versus afferent dynamics in cortical visual processing. Nat. Neurosci. 18. doi:10.1038/nn.4153

Reyes, A., Lujan, R., Rozov, A., Burnashev, N., Somogyi, P., Sakmann, B., 1998. Target-cell-specific facilitation and depression in neocortical circuits. Nat. Neurosci. 1, 279–285. doi:10.1038/1092

Reynolds, J.H., Heeger, D.J., 2009. The normalization model of attention. Neuron 61, 168–85. doi:10.1016/j.neuron.2009.01.002

Richardson, B.D., Hancock, K.E., Caspary, D.M., 2013. Stimulus-Specific Adaptation in Auditory Thalamus of Young and Aged Awake Rats. J. Neurophysiol. doi:10.1152/jn.00403.2013

Ringo, J.L., 1996. Stimulus specific adaptation in inferior temporal and medial temporal cortex of the monkey. Behav. Brain Res. 76, 191–197. doi:10.1016/0166-4328(95)00197-2

Ritt, J.T., Andermann, M.L., Moore, C.I., 2008. Embodied information processing: vibrissa mechanics and texture features shape micromotions in actively sensing rats. Neuron 57, 599–613. doi:10.1016/j.neuron.2007.12.024

Rossant, C., Kadir, S.N., Goodman, D.F.M., Schulman, J., Belluscio, M., Buzsáki, G., Harris, K.D., Hunter, M.L.D., Saleem, A.B., Grosmark, A., Denfield, G.H., Ecker, A.S.S., Tolias, A.S., Solomon, S.G., Carandini, M., Belluscio, M., Denfield, G.H., Ecker, A.S.S., Tolias, A.S., Solomon, S.G., Buzsáki, G., Carandini, M., Harris, K.D., 2015. Spike sorting for large, dense electrode arrays. Nat. Neurosci. 15198. doi:10.1038/nn.4268

Sachdev, R.N., Sellien, H., Ebner, F.F., 2001. Temporal organization of multi-whisker contact in rats. Somatosens. Mot. Res. 18, 91–100. doi:10.1080/135578501012006192

Sachdev, R.N.S., Ebner, F.F., Wilson, C.J., 2004. Effect of subthreshold up and down states on the whisker-evoked response in somatosensory cortex. J. Neurophysiol. 92, 3511–3521. doi:10.1152/jn.00347.2004

Sakurai, K., Akiyama, M., Cai, B., Scott, A., Han, B.X., Takatoh, J., Sigrist, M., Arber, S., Wang, F., 2013. The Organization of Submodality-Specific Touch Afferent Inputs in the Vibrissa Column. Cell Rep. 5, 87–98. doi:10.1016/j.celrep.2013.08.051

Saleem, A.B., Chadderton, P., Apergis-Schoute, J., Harris, K.D., Schultz, S.R., 2010. Methods for predicting cortical UP and DOWN states from the phase of deep layer local field potentials. J. Comput. Neurosci. 29, 49–62. doi:10.1007/s10827-010-0228-5

Sanchez-Vives, M. V, Nowak, L.G., McCormick, D.A., 2000. Cellular mechanisms of long-lasting adaptation in visual cortical neurons in vitro. J. Neurosci. 20, 4286–4299. doi:20/11/4286 [pii]

Sathian, K., Zangaladze, A., 1996. Tactile spatial acuity at the human fingertip and lip: bilateral symmetry and interdigit variability. Neurology 46, 1464–1466. doi:10.1212/WNL.46.5.1464

Sato, T.K., Haider, B., Häusser, M., Carandini, M., 2016. An excitatory basis for divisive

normalization in visual cortex. Nat. Neurosci. 19, 2–7. doi:10.1038/nn.4249
Sawamura, H., Orban, G.A., Vogels, R., 2006. Selectivity of Neuronal Adaptation Does Not Match Response Selectivity: A Single-Cell Study of the fMRI Adaptation Paradigm. Neuron 49, 307–318. doi:10.1016/j.neuron.2005.11.028
Schmahmann, J.D., 2003. Vascular syndromes of the thalamus. Stroke 34, 2264–2278. doi:10.1161/01.STR.0000087786.38997.9E
Schnapf, J.L., Nunn, B.J., Meister, M., Baylor, D.A., 1990. Visual transduction in cones of the monkey Macaca fascicularis. J. Physiol. 427, 681–713. doi:10.1038/299726a0
Schwartz, O., Pillow, J.W., Rust, N.C., Simoncelli, E.P., 2006. Spike-triggered neural characterization. J. Vis. 6, 484–507. doi:10.1167/6.4.13
Schwarz, C., Hentschke, H., Butovas, S., Haiss, F., Stüttgen, M.C., Gerdjikov, T. V, Bergner, C.G., Waiblinger, C., 2010. The head-fixed behaving rat--procedures and pitfalls. Somatosens. Mot. Res. 27, 131–48. doi:10.3109/08990220.2010.513111
Scott, T.R., 2007. Taste: Central Processing. eLS. doi:10.1002/9780470015902.a0020288
Sekuler, R., Ganz, L., 1963. Aftereffect of Seen Motion with a Stabilized Retinal Image. Science (80-. ). 139, 419–419. doi:10.1126/science.139.3553.419
Sen, K., Jorge-Rivera, J.C., Marder, E., Abbott, L.F., 1996. Decoding synapses. J. Neurosci. 16, 6307–18.
Sengpiel, F., Bonhoeffer, T., 2002. Orientation specificity of contrast adaptation in visual cortical pinwheel centres and iso-orientation domains. Eur. J. Neurosci. 15, 876–886. doi:10.1046/j.1460-9568.2002.01912.x
Seriès, P., Stocker, A. a, Simoncelli, E.P.P., 2009. Is the homunculus "aware" of sensory adaptation? Neural Comput. 21, 3271–3304. doi:10.1162/neco.2009.09-08-869
Shapley, R.M., Victor, J.D., 1979. The contrast gain control of the cat retina. Vision Res. 19, 431–434. doi:10.1016/0042-6989(79)90109-3
Sharpee, T.O., Sugihara, H., Kurgansky, A. V, Rebrik, S.P., Stryker, M.P., Miller, K.D., 2006. Adaptive filtering enhances information transmission in visual cortex. Nature 439, 936–942. doi:10.1038/nature04519
Sherman, S.M., 2001a. A wake-up call from the thalamus. Nat. Neurosci. 4, 344–6. doi:10.1038/85973
Sherman, S.M., 2001b. Tonic and burst firing: Dual modes of thalamocortical relay. Trends Neurosci. 24, 122–126. doi:10.1016/S0166-2236(00)01714-8
Sherman, S.M., 1996. Dual response modes in lateral geniculate neurons: mechanisms and functions. Vis. Neurosci. 13, 205–213. doi:10.1017/S0952523800007446
Sherman, S.M., Guillery, R.W., 2002. The role of the thalamus in the flow of information to the cortex. Philos. Trans. R. Soc. Lond. B. Biol. Sci. 357, 1695–708. doi:10.1098/rstb.2002.1161
Sherman, S.M., Guillery, R.W., 1998. On the actions that one nerve cell can have on another : Distinguishing "' drivers'" from "' modulators.'" Proc. Natl. Acad. Sci. 95, 7121–7126.
Sherman, S.M., Guillery, R.W., 1996. Functional Organization of Thalamocortical Relays. J. Neurophysiol. 76.
Sherman, S.M., Koch, C., 1986. The control of retinogeniculate transmission in the mammalian lateral geniculate nucleus. Exp. Brain Res. 1–20.
Sheth, B.R., Moore, C.I., Sur, M., 1998. Temporal modulation of spatial borders in rat barrel cortex. J. Neurophysiol. 79, 464–470.

Shipp, S., 2007. Structure and function of the cerebral cortex. Curr. Biol. 17, R443–R449. doi:10.1016/j.cub.2007.03.044
Silver, R.A., 2010. Neuronal arithmetic. Nat. Rev. Neurosci. 11, 474–489. doi:10.1038/nrn2864
Simoncelli, E.P., Paninski, L., Pillow, J.W., Schwartz, O., 2004. Characterization of neural responses with stochastic stimuli. New Cogn. Neurosci.
Simons, D.J., 1985. Temporal and spatial integration in the rat SI vibrissa cortex. J. Neurophysiol. 54, 615–35.
Simons, S.B., Tannan, V., Chiu, J., Favorov, O. V, Whitsel, B.L., Tommerdahl, M.A., 2005. Amplitude-dependency of response of SI cortex to flutter stimulation. BMC Neurosci. 6, 43. doi:10.1186/1471-2202-6-43
Solomon, S.G., Peirce, J.W., Dhruv, N.T., Lennie, P., 2004. Profound contrast adaptation early in the visual pathway. Neuron 42, 155–162. doi:10.1016/S0896-6273(04)00178-3
Sosnik, R., Haidarliu, S., Ahissar, E., 2001. Temporal Frequency of Whisker Movement . I . Representations in Brain Stem and Thalamus. Am. Physiol. Soc. 339–353.
Stanley, G.B., 2013. Reading and writing the neural code. Nat. Publ. Gr. 16, 259–263. doi:10.1038/nn.3330
Stanley, G.B., 2002. Adaptive spatiotemporal receptive field estimation in the visual pathway. Neural Comput. 14, 2925–2946. doi:10.1162/089976602760805340
Steriade, M., McCormick, D.A., Sejnowski, T.J., 1993. Thalamocortical oscillations in the sleeping and aroused brain. Science 262, 679–685. doi:10.1126/science.8235588
Stevens, C.F., Wang, Y., 1995. Facilitation and depression at single central synapses. Neuron 14, 795–802. doi:10.1016/0896-6273(95)90223-6
Stoelzel, C.R., Huff, J.M., Bereshpolova, Y., Zhuang, J., Hei, X., Alonso, J.-M., Swadlow, H. a, 2015. Hour-long adaptation in the awake early visual system. J. Neurophysiol. jn.00116.2015. doi:10.1152/jn.00116.2015
Strobach, T., Carbon, C.C., 2013. Face adaptation effects: Reviewing the impact of adapting information, time, and transfer. Front. Psychol. 4, 1–12. doi:10.3389/fpsyg.2013.00318
Stüttgen, M.C., Rüter, J., Schwarz, C., 2006. Two psychophysical channels of whisker deflection in rats align with two neuronal classes of primary afferents. J. Neurosci. 26, 7933–41. doi:10.1523/JNEUROSCI.1864-06.2006
Suga, N., Ma, X., 2003. Multiparametric corticofugal modulation and plasticity in the auditory system. Nat. Rev. Neurosci. 4, 783–794. doi:10.1038/nrn1222
Suzuki, S., Rogawski, M.A., 1989. T-type calcium channels mediate the transition between tonic and phasic firing in thalamic neurons. Proc. Natl. Acad. Sci. U. S. A. 86, 7228–7232. doi:10.1073/pnas.86.18.7228
Swadlow, H.A., Gusev, A.G., 2001. The impact of "bursting" thalamic impulses at a neocortical synapse. Nat. Neurosci. 4, 402–8. doi:10.1038/86054
Swadlow, H. a, Gusev, A.G., Bezdudnaya, T., 2002. Activation of a cortical column by a thalamocortical impulse. J. Neurosci. 22, 7766–73.
Taaseh, N., Yaron, A., Nelken, I., 2011. Stimulus-Specific Adaptation and Deviance Detection in the Rat Auditory Cortex. PLoS One 6, e23369. doi:10.1371/journal.pone.0023369
Tannan, V., Whitsel, B.L., Tommerdahl, M.A., 2006. Vibrotactile adaptation enhances

spatial localization. Brain Res. 1102, 109–16. doi:10.1016/j.brainres.2006.05.037
Temereanca, S., Brown, E.N.N., Simons, D.J., 2008. Rapid changes in thalamic firing synchrony during repetitive whisker stimulation. J. Neurosci. 28, 11153–64. doi:10.1523/JNEUROSCI.1586-08.2008
Theunissen, F.E., Sen, K., Doupe, A.J.J., 2000. Spectral-temporal receptive fields of nonlinear auditory neurons obtained using natural sounds. J. Neurosci. 20, 2315–2331.
Tiesinga, P., Fellous, J.M., Sejnowski, T.J., 2008. Regulation of spike timing in visual cortical circuits. Nat Rev Neurosci 9, 97–107. doi:10.1038/nrn2315
Toib, a, Lyakhov, V., Marom, S., 1998. Interaction between duration of activity and time course of recovery from slow inactivation in mammalian brain Na+ channels. J. Neurosci. 18, 1893–903.
Tommerdahl, M.A., Favorov, O., Whitsel, B.L., 2002. Optical imaging of intrinsic signals in somatosensory cortex. Behav. Brain Res. 135, 83–91.
Tommerdahl, M.A., Hollins, M., 2005. Human vibrotactile frequency discriminative capacity after adaptation to 25 Hz or 200 Hz stimulation Human vibrotactile frequency discriminative capacity after adaptation to 25 Hz or 200 Hz stimulation. doi:10.1016/j.brainres.2005.04.031
Ulanovsky, N., Las, L., Nelken, I., 2003. Processing of low-probability sounds by cortical neurons. Nat. Neurosci. 6, 391–398. doi:10.1038/nn1032
Van Der Werf, Y.D., Witter, M.P., Uylings, H.B.M., Jolles, J., 2000. Neuropsychology of infarctions in the thalamus: A review. Neuropsychologia 38, 613–627. doi:10.1016/S0028-3932(99)00104-9
Varela, C., 2014. Thalamic neuromodulation and its implications for executive networks. Front. Neural Circuits 8, 1–22. doi:10.3389/fncir.2014.00069
Vélez-Fort, M., Margrie, T.W., 2012. Cortical Circuits: Layer 6 Is a Gain Changer. Curr. Biol. 22, R411–R413. doi:10.1016/j.cub.2012.03.055
Vélez-Fort, M., Rousseau, C. V., Niedworok, C.J., Wickersham, I.R., Rancz, E.A., Brown, A.P.Y., Strom, M., Margrie, T.W., 2014. The Stimulus Selectivity and Connectivity of Layer Six Principal Cells Reveals Cortical Microcircuits Underlying Visual Processing. Neuron 83, 1431–1443. doi:10.1016/j.neuron.2014.08.001
Viaene, A.N., Petrof, I., Sherman, S.M., 2011. Synaptic properties of thalamic input to layers 2/3 and 4 of primary somatosensory and auditory cortices. J. Neurophysiol. 105, 279–292. doi:10.1152/jn.00747.2010
Vierck, C.J., Jones, M.B., 1970. Influences of low and high frequency oscillation upon spatio-tactile resolution. Physiol. Behav. 5, 1431–5.
Vinje, W.E., Gallant, J.L., 2002. Natural stimulation of the nonclassical receptive field increases information transmission efficiency in V1. J. Neurosci. 22, 2904–2915. doi:20026216
von Békésy, G., 1957. Neural volleys and the similarity between some sensations produced by tones and by skin vibrations. J. Acoust. Soc. Am.
von der Behrens, W., Bauerle, P., Kossl, M., Gaese, B.H., 2009. Correlating Stimulus-Specific Adaptation of Cortical Neurons and Local Field Potentials in the Awake Rat. J. Neurosci. 29, 13837–13849. doi:10.1523/JNEUROSCI.3475-09.2009
Waiblinger, C., Brugger, D., Schwarz, C., 2015a. Vibrotactile discrimination in the rat whisker system is based on neuronal coding of kinematic parameters. Cereb. Cortex.

doi:10.1093/cercor/bht305
Waiblinger, C., Brugger, D., Whitmire, C.J., Stanley, G.B., Schwarz, C., 2015b. Support for the slip hypothesis from whisker-related tactile perception in a noisy environment. Front. Integr. Neurosci. 9, 1–11. doi:10.3389/fnint.2015.00053
Wang, H.-P., Spencer, D., Fellous, J.-M., Sejnowski, T.J., 2010. Synchrony of thalamocortical inputs maximizes cortical reliability. Science (80-. ). 328, 106–109. doi:10.1126/science.1183108
Wang, Q., Millard, D.C., Zheng, H.J.V. V, Stanley, G.B., 2012. Voltage-sensitive dye imaging reveals improved topographic activation of cortex in response to manipulation of thalamic microstimulation parameters. J. Neural Eng. 9, 26008. doi:10.1088/1741-2560/9/2/026008
Wang, Q., Webber, R.M., Stanley, G.B., 2010. Thalamic synchrony and the adaptive gating of information flow to cortex. Nat. Neurosci. 13, 1534–41. doi:10.1038/nn.2670
Wang, X., Wei, Y., Vaingankar, V., Wang, Q., Koepsell, K., Sommer, F.T., Hirsch, J. a., 2007. Feedforward Excitation and Inhibition Evoke Dual Modes of Firing in the Cat's Visual Thalamus during Naturalistic Viewing. Neuron 55, 465–478. doi:10.1016/j.neuron.2007.06.039
Wark, B., Lundstrom, B.N., Fairhall, A.L., 2007. Sensory adaptation. Curr. Opin. Neurobiol. 17, 423–9. doi:10.1016/j.conb.2007.07.001
Webber, R.M., Stanley, G.B., 2006. Transient and steady-state dynamics of cortical adaptation. J. Neurophysiol. 95, 2923–2932. doi:10.1152/jn.01188.2005.
Webber, R.M., Stanley, G.B., 2004. Nonlinear encoding of tactile patterns in the barrel cortex. J. Neurophysiol. 91, 2010–22. doi:10.1152/jn.00906.2003
Webster, M.A., Kaping, D., Mizokami, Y., Duhamel, P., 2004. Adaptation to natural facial categories. Nature 428, 557–561. doi:10.1038/nature02361.1.
Webster, M.A., MacLeod, D.I. a, 2011. Visual adaptation and face perception. Philos. Trans. R. Soc. B Biol. Sci. 366, 1702–1725. doi:10.1098/rstb.2010.0360
Wehr, M., Zador, A.M., 2003. Balanced inhibition underlies tuning and sharpens spike timing in auditory cortex. Nature 426, 442–6. doi:10.1038/nature02116
Whitmire, C.J., Millard, D.C., Stanley, G.B., 2017. Thalamic state control of cortical paired-pulse dynamics. J. Neurophysiol. 117, jn.00415.2016. doi:10.1152/jn.00415.2016
Whitmire, C.J., Stanley, G.B., 2016. Rapid Sensory Adaptation Redux : A Circuit Perspective. Neuron 92, 298–315. doi:10.1016/j.neuron.2016.09.046
Whitmire, C.J., Waiblinger, C., Schwarz, C., Stanley, G.B., 2016. Information Coding through Adaptive Gating of Synchronized Thalamic Bursting. CellReports 14, 1–13. doi:10.1016/j.celrep.2015.12.068
Wilent, W.B., Contreras, D., 2005a. Stimulus-Dependent Changes in Spike Threshold Enhance Feature Selectivity in Rat Barrel Cortex Neurons. J. Neurosci. 25, 2983–2991. doi:10.1523/JNEUROSCI.4906-04.2005
Wilent, W.B., Contreras, D., 2005b. Dynamics of excitation and inhibition underlying stimulus selectivity in rat somatosensory cortex. Nat. Neurosci. 8, 1364–70. doi:10.1038/nn1545
Willis, A.M., Slater, B.J., Gribkova, E., Llano, D.A., 2015. Open-loop organization of thalamic reticular nucleus and dorsal thalamus: A computational model. J. Neurophysiol. jn.00926.2014. doi:10.1152/jn.00926.2014

Wilson, D.A., Chapuis, J., Wesson, D.W., 2010. Olfaction. Encycl. Life Sci. doi:10.1002/9780470015902.a0000077.pub2

Wimmer, R.D., Schmitt, L.I., Davidson, T.J., Nakajima, M., Deisseroth, K., Halassa, M.M., 2015. Thalamic control of sensory selection in divided attention. Nature. doi:10.1038/nature15398

Wohlgemuth, A., 1911. On the after-effect of seen movement. Br. J. Psychol. Monogr. Suppl. 1, 1–117.

Wolfart, J., Debay, D., Le Masson, G., Destexhe, A., Bal, T., 2005. Synaptic background activity controls spike transfer from thalamus to cortex. Nat. Neurosci. 8, 1760–7. doi:10.1038/nn1591

Wolfe, J., Hill, D.N., Pahlavan, S., Drew, P.J., Kleinfeld, D., Feldman, D.E., 2008. Texture coding in the rat whisker system: slip-stick versus differential resonance. PLoS Biol. 6, e215. doi:10.1371/journal.pbio.0060215

Woolsey, T. a, Van der Loos, H., 1970. The structural organization of layer IV in the somatosensory region (SI) of mouse cerebral cortex. Brain Res. 17, 205–242.

Wu, G.K., Li, P., Tao, H.W., Zhang, L.I., 2006. Nonmonotonic Synaptic Excitation and Imbalanced Inhibition Underlying Cortical Intensity Tuning. Neuron 52, 705–715. doi:10.1016/j.neuron.2006.10.009

Yaron, A., Hershenhoren, I., Nelken, I., 2012. Sensitivity to Complex Statistical Regularities in Rat Auditory Cortex. Neuron 76, 603–615. doi:10.1016/j.neuron.2012.08.025

Zagha, E., Casale, A.E., Sachdev, R.N.S., McGinley, M.J., McCormick, D.A., 2013. Motor cortex feedback influences sensory processing by modulating network state. Neuron 79, 567–78. doi:10.1016/j.neuron.2013.06.008

Zagha, E., McCormick, D.A., 2014. Neural control of brain state. Curr. Opin. Neurobiol. 29, 178–186. doi:10.1016/j.conb.2014.09.010

Zavitz, E., Yu, H.-H., Row, E.G., Rosa, Marcello, G.P., Price, Nicholas, S.C., 2016. Rapid Adaptation Induces Persistent Biases in Population Codes. J Neurosci 36, 4579–4590. doi:10.1523/JNEUROSCI.4563-15.2016

Zheng, H.J.V., Wang, Q., Stanley, G.B., 2015. Adaptive Shaping of Cortical Response Selectivity in the Vibrissa Pathway. J. Neurophysiol. 113, 3850–3865. doi:10.1152/jn.00978.2014

Zucker, R.S., Regehr, W.G., 2002. Short-term synaptic plasticity. Annu. Rev. Physiol. 64, 355–405. doi:10.1146/annurev.physiol.64.092501.114547